Heinrich Heine
Universität Düsseldorf

OSMAC and Co-Culture Approaches for Diversifying Secondary Metabolites from Endophytic Fungi

Inaugural-Dissertation

zur Erlangung des Doktorgrades
der Mathematisch-Naturwissenschaftlichen Fakultät
der Heinrich-Heine-Universität Düsseldorf

vorgelegt von

Mariam Moussa

aus Castrop-Rauxel

Düsseldorf, Jan 2020

aus dem Institut für Pharmazeutische Biologie und Biotechnologie
der Heinrich-Heine-Universität Düsseldorf

Gedruckt mit der Genehmigung der
Mathematisch-Naturwissenschaftlichen Fakultät der
Heinrich-Heine-Universität Düsseldorf

Berichterstatter:

1. Prof. Dr. Dr. h.c. Peter Proksch

2. Prof. Dr. Matthias Kassack

Tag der mündlichen Prüfung:

بِسْمِ اللَّهِ الرَّحْمَنِ الرَّحِيم

Erklärung

Hiermit erkläre ich ehrenwörtlich, dass ich die vorliegende Dissertation mit dem Titel „OSMAC and Co-Culture Approaches for Diversifying Secondary Metabolites from Endophytic Fungi“ selbst angefertigt habe. Außer den angegebenen Quellen und Hilfsmitteln wurden keine weiteren verwendet. Diese Dissertation wurde weder in gleicher noch in abgewandelter Form in einem anderen Prüfungsverfahren vorgelegt.

Düsseldorf, den 15.01.2020

Mariam Moussa

Abstract

The present thesis focuses on the subject about obtaining new secondary metabolites from endophytic fungi by employing various culture methods, such as the OSMAC approach and co-cultivation, in order to induce silent biogenetic gene clusters. Dramatic shifts in the metabolic pattern of the microorganisms that were subject of this study were detected using these methods. The structures of the isolated new and known compounds were elucidated by ESIMS, HRESIMS and 1D and 2D NMR spectroscopy. In case of chiral compounds their absolute configurations were determined by their optical rotation in comparison to the literature, ECD measurements and calculations, and rotation barrier calculations. Obtained compounds were subjected to bioassays for evaluating their antibiotic and cytotoxic profiles.

In summary, 29 natural products were isolated from axenic fermentations of *Stemphylium globuliferum* and mixed fermentations of *Fusarium tricinctum*. From these isolated metabolites, eight compounds proved to be new metabolites.

This thesis contains three manuscripts which were either already published or submitted for publication:

1. *Tetrahydroanthraquinone derivatives from the mangrove-derived endophytic fungus Stemphylium globuliferum*

The endophytic fungus *Stemphylium globuliferum* was isolated from the mangrove plant *Avicennia marina* and cultivated on white beans medium. From the crude extract two new tetrahydroanthraquinone monomers, altersolanol Q and 10-methylaltersolanol Q, and one new anthranoid dimer, alterporriol X, have been isolated. Additionally, thirteen known compounds of same structural characteristics were isolated and identified. The absolute configuration of the new compounds was determined by TDDFT-ECD calculations and by comparison of measured ECD

with the literature. The new compounds were tested against the mouse lymphoma cellline L5178Y. Since they are inactive, this finding can contribute to the structure-bioactivity relationship of active known compounds like altersolanol A, also obtained from this extract.

2. *Co-culture of the fungus Fusarium tricinctum with Streptomyces lividans induces production of cryptic naphthoquinone dimers*

The endophytic fungus *Fusarium tricinctum* was isolated from the plant *Aristolochia paucinervis*. In order to enhance the production of secondary metabolites, the fungus was subjected to a co-culturing experiment with the soil bacterium *Streptomyces lividans*. The dramatic shift in the metabolic profile of the co-culture, compared to the axenic cultures, indicated the induction of cryptic compounds. The isolation process resulted in the identification of four new naphthoquinone dimers, fusatricinones A, B, C and D with an additional derivative of the bioactive lateropyrone, dihydrolateropyrone. The co-culture also caused an up to 12-fold upregulation of constitutively present bioactive compounds, like lateropyrone, the enniatins and the lipopeptide fusaristatin A. Furthermore, the co-culture induced the production of known cryptic compounds. The structures of the new compounds were elucidated by using 1D and 2D NMR and HRESIMS. The absolute configuration of dihydrolateropyrone was unambiguously determined by TDDFT-ECD. The new compounds were subjected to bioassays evaluating the cytotoxic and antibiotic activity, showing no activity.

3. *Co-culture of the bacterium Pseudomonas aeruginosa with the fungus Fusarium tricinctum induces bacterial antifungal and quorum sensing signalling molecules*

The co-culture of the fungus *F. tricinctum* with the viable human pathogenic bacterium *Pseudomonas aeruginosa* triggered the activation of silent bacterial biosynthetic gene clusters. The bacterial reaction was seen on a macroscopic level through distance inhibition of the fungus

and dark greenish growth of the bacterial colonies. The accumulation of cryptic pseudomonad metabolites was detected via HPLC analysis. The antifungal compounds phenazine-1-carboxylic acid (PCA) and phenazine-1-carboxylic amide (PCN), along with the quorum sensing metabolite 2-heptyl-4-hydroxy-quinolone (HHQ), which are of bacterial origin, were induced during co-cultivation with *F. tricinctum*. In contrast to other co-culture experiments employing *F. tricinctum*, such as the co-culture of the fungus with *S. lividans*, no fungal reaction in terms of metabolite induction was observed during co-cultivation of *F. tricinctum* with *P. aeruginosa*.

Zusammenfassung

Die vorliegende Arbeit beschäftigt sich mit dem Thema der Gewinnung neuer Sekundärmetabolite aus endophytischen Pilzen durch Anwendung verschiedener Kultivierungsmethoden, wie der Kultivierungsansatz nach OSMAC und die Co-Kultivierung, mit dem Ziel ruhende biogenetische Genabschnitte zu aktivieren. Es wurden hierbei auffällige Veränderungen im metabolischen Profil der Mikroorganismen, die Gegenstand dieser Arbeit sind, detektiert. Die Strukturaufklärung der isolierten neuen und bekannten Substanzen wurde mittels ESIMS, HRESIMS, 1D und 2D NMR Spektroskopie durchgeführt. Im Falle von chiralen Substanzen wurde deren absolute Stereochemie durch Vergleich der optischen Rotation mit der Literatur, ECD-Messungen und -Berechnungen, sowie mittels Berechnungen der Rotationsbarrieren bestimmt. Die erhaltenen Substanzen wurden mittels Biotests bezüglich deren antibiotischen und zytotoxischen Profile evaluiert.

Zusammengefasst wurden in dieser Arbeit 29 Naturprodukte aus axenischer Fermentation von *Stemphylium globuliferum* und gemischten Fermentationen von *Fusarium tricinctum* isoliert. Von diesen Sekundärmetaboliten konnten acht Substanzen als neue Metabolite beschrieben werden. Die vorliegende Arbeit beinhaltet drei Manuskripte, welche bereits publiziert oder für Publikationszwecke eingereicht wurden:

1. *Tetrahydroanthrachinonderivate aus dem mangroven endophytischen Pilz Stemphylium globuliferum*

Der endophytische Pilz *Stemphylium globuliferum* wurde aus der mangroven Pflanze *Avicennia marina* isoliert und auf weißen Bohnen kultiviert. Zwei neue Monomere vom Tetrahydroanthrachinontyp, Altersolanol Q und 10-methylaltersolanol Q, und ein neues Anthranoiddimer, Alterporriol X, wurden aus dem Rohextrakt isoliert. Zusätzlich wurden dreizehn bekannte Substanzen, welche strukturelle Ähnlichkeiten aufweisen, isoliert und identifiziert. Die

absolute Konfiguration der neuen Substanzen wurde mittels TDDFT-ECD Berechnungen und durch Literaturvergleich von gemessenen ECD Spektren bestimmt. Die neuen Substanzen wurden gegen die murine Lymphoma Zellline L5178Y getestet. Diese zeigten keine Aktivität. Und im Vergleich zu strukturähnlichen aktiven Substanzen, wie Altersolanol A, welche ebenfalls aus diesem Extrakt gewonnen wurden, kann dieses Ergebnis zur Klärung des Struktur-Bioaktivitätsverhältnisses herangezogen werden.

2. *Co-Kultur des Pilzes Fusarium tricinctum mit Streptomyces lividans induziert die Produktion kryptischer Naphthochinondimere*

Der endophytische Pilz *Fusarium tricinctum* wurde aus der Pflanze *Aristolochia paucinervis* isoliert. Um die Produktion von Sekundärmetaboliten zu erhöhen, wurde der Pilz in einem Experiment mit dem Bodenbakterium *Streptomyces lividans* co-kultiviert. Die auffällige Veränderung im metabolischen Profil der Co-Kultur im Vergleich zu den axenischen Kulturen wies auf eine Induktion kryptischer Substanzen hin. Chromatographische Auftrennung führte zur Identifizierung von vier neuen Naphthochinondimeren, nämlich Fusatricinone A, B, C and D, und zusätzlich einem Derivat des bioaktiven Lateropyrons, dem Dihydrolateropyron. Durch die Co-Kultur wurde ebenfalls eine bis zu 12-facher verstärkten Produktion der standardmäßig vorhandenen bioaktiven Substanzen erzielt, wie Lateropyron, die Enniatine und das Lipopeptid Fusaristatin A. Ebenfalls hat die Co-Kultivierung die Produktion kryptischer bekannter Substanzen erzielt. Die Strukturen der neuen Substanzen wurden mithilfe von 1D und 2D NMR und HRESIMS aufgeklärt. Die absolute Konfiguration des Dihydrolateropyrons wurde durch TDDFT-ECD bestimmt. Die neuen Substanzen wurden mittels Biotests hinsichtlich der zytotoxischen und antibiotischen Eigenschaften charakterisiert, und zeigten dabei keine Aktivitäten.

3. *Co-Kultur des Bakteriums Pseudomonas aeruginosa mit dem Pilz Fusarium tricinctum induziert bakterielle antipilz und quorum sensing Signalmoleküle*

Die Co-Kultivierung des Pilzes *F. tricinctum* mit lebenden humanpathogenen Bakterien, *Pseudomonas aeruginosa*, führte zur Aktivierung von ruhenden biosynthetischer Genabschnitte des Bakteriums. Die Reaktion des Bakteriums konnte makroskopisch durch Distanzinhibition des Pilzes und tief grüner Verfärbung der Bakterienkolonien festgestellt werden. Die Anhäufung kryptischer Pseudomonaden-Metabolite wurde mittels HPLC Analyse detektiert. Die antimykotischen Substanzen Phenazin-1-carboxylsäure (PCA) und Phenazin-1-carboxylamid (PCN), zusammen mit dem quorum sensing Metabolit 2-Heptyl-4-hydroxychinolon (HHQ), welche bakteriellen Ursprungs sind, wurden während der Co-Kultivierung mit *F. tricinctum* induziert. Im Gegensatz zu anderen Co-Kultivierungsexperimenten mit *F. tricinctum*, wie die Co-Kultur des Pilzes mit *S. lividans*, zeigte sich während der Co-Kultivierung von *F. tricinctum* mit *P. aeruginosa*, im Hinblick auf metabolischer Induktion, keine Reaktion des Pilzes.

Index

1 General Introduction

1.1 Natural products in drug discovery - a historical overview

Human history is closely connected to the development of health care systems throughout each era of civilization. Earliest evidences are scripts, describing the usage of natural products (NPs), found in Mesopotamia (in cuneiform on clay tablets, 2600 BC) or Egypt ("*Ebers Papyrus*", 1600 BC). Traditional medicine, such as the Indian Ayurveda system ("*Susruta Samhita*", 1000 BC) and the Chinese Medicine ("*Nei Ching*", 1300 BC), evolved over millennia and are still applied until today (Chintalapally and Rao, 2016). A milestone towards drug discovery were the investigations of pharmacists and physicians starting from the eighteenth century. They administered herbals to themselves or to patients. The aim was to publish these results. James Lind set up the first clinical trial, Anton von Störck conducted animal tests for finding safe doses of traditionally used medicine (Sneader, 2005) and William Withering´s investigation on foxglove (Digitalis) led to the discovery of the small molecule digoxin and thus resulted in the elucidation of the heart-disease mechanism (Rishton, 2008). Morphine was isolated from opium by Friedrich Serturner and Joseph Buchner obtained the alcoholic *β*-glucoside salicin from willow bark (Rishton, 2008; Doyle, 2014). The latter discovery describes the use of natural compounds as lead drugs, since the acetylation of salicylic acid yields the prodrug Aspirin®, which inhibits cyclooxygenase (COX) by acetylation and was developed by Felix Hoffmann in 1897 (Kuhnert, 2000). Alexander Fleming´s famous observation of antibacterial activity and identification of penicillin from mould opened the door for not only studying bacterial infections and antibiotics, but also established fungi as potential producers of biologically active secondary metabolites (Rishton, 2008; Aly *et al.*, 2010).

1.2 Fungi as potential producers of drugs and drug leads

The discovery of bioactive secondary metabolites from fungi dates back to over 50 years, as exemplified by the *β*-lactam antibiotics. Nevertheless, only a small part of the fungal metabolic diversity has been investigated by researchers up to date (Aly *et al.*, 2011a).

1.2.1 Fungal NPs in the treatment of infections

The beforementioned discovery of penicillin shifted the focus of researchers to fungi as potent producers of NPs for the treatment of life-threatening diseases (Strobel *et al.*, 2004). Collaborating American and British scientists engaged in excessive studies during war time. Ultimately the structure of penicillin was elucidated, which includes the *β*-lactam thiazolidine core. A crucial acylation step yielded penicillin G from its precursor penicillin V, thus giving a general synthesis scheme for obtaining natural and NP-derived penicillins (Sheehan *et al.*, 1959). The mode of action of penicillin-derivatives has been extensively studied in detail and is as follows: they target the bacterial cell wall synthesis by inhibiting its final step of cross-linking peptidoglycans, essentially by inhibiting penicillin-binding proteins (Sauvage *et al*., 2008; Shi *et al*., 2011). It is worthy to mention that they are able to substitute amino acids in their active domain to create resistance towards *β*-lactam antibiotics (Spratt and Cromie, 1988). Despite the occurrence of resistance, *β*-lactams have the highest ranking in usage for the treatment of infections (Blumenthal *et al.*, 2018).

When further looking into their biosynthesis in filamentous fungi, researchers found that penicillins share the same first three steps, which include isopenicillin N (IPN) as precursor, with cephalosporins. IPN is built from the intermediate *δ*(L-α-aminoadipyl)-L-cysteinyl-D-valine (LLD-ACV). The cyclization step to IPN and further phenylacylation leads to penicillin G. Whereas, penicillin is only produced in filamentous fungi, namely *Aspergillus nidulans* and

Penicillium chrysogenum, cephalosporins are NPs that are known from both fungi and bacteria, respectively (Brakhage, 1998; Brakhage *et al*., 2004). Cephalosporins are another type of penicillins. The first step towards the discovery of cephalosporin was the isolation and purification of the fungus *Cephalosporium acremonium* from sea water samples. Isolation of its "antibiotic principle" led to the ability of *in vitro* testing against bacterial strains of *Staphylococci*, *Streptococci*, *Bacillus anthracis*, *Salmonella typhi*, *Vibrio cholerae*, *Yersinia pestis* and *Brucella melitensis*. The studies went further by describing *in vivo* clinical trials with fungal liquid cultures or liquid extracts to treat patients. After causing serious side effects, these results pointed out the necessity of purifying the antibiotic NPs (Brotzu, 1948). The first purification and structure elucidation of cephalosporin N was described in 1953 as a new type of penicillin (Abraham *et al.*, 1953). The structure revealed a ring expansion and this discovery was followed by the characterization of cephalosporin C in 1955 (Newton and Abraham, 1956). Both compounds are produced by numerous *Cephalosporium* species. This led to the investigation of a series of semisynthetic compounds, like ceftolozane (Newman *et al.*, 2000; Waller *et al.*, 2018). Cephalosporins are used as broad-spectrum antibiotics in the treatment of penicillin resistant bacteria. They showed less susceptibility towards *beta*-lactamases than the penicillins, causing less allergic reactions than the latter. Their side effects, which include epileptical- seizure in patients, are drawing researchers' attention to their effect on $GABA_a$ receptors and synaptic transmission *in vivo* (Ribeiro *et al.*, 2018; Amakhin *et al*., 2018). Fusidic acid, another fungal antibiotic, resembles the structure of cephalosporin P1. This NP represents a steroid-like compound, produced by the parasitic fungus *Fusidium coccineum*. It showed significant activity against penicillin- and methicillin-resistant *Staphylococcus aureus* (Godtfredsen *et al.*, 1962; Crosbie, 1963). It inhibits the protein synthesis at the ribosome-dependant GTPase activity of the G-factor.

Simultaneously, the interruption of functional binding of aminoacyl-sRNA to the ribosomal A site results in the inhibition of polypeptide synthesis (Tanaka *et al.*, 1968; Cundliffe, 1972). Fusidic acid shows synergistic effect in combination with *β*-lactam antibiotics when treating *Staphylococci* caused endocarditis (Penman, 1962; Taylor and Bloor, 1962; Whitby, 1999). Further, it has the ability of penetrating infection sites, e.g. the aqueous eyeball without causing loss of visual acuity (Chadwick and Jackson, 1969). Other more promising antibiotics were not able to reach this part of the human body (Williamson *et al.*, 1970). The prevented relapse of infections, during a fusidic acid treatment, demonstrates the efficacy of the treatment with this agent (Kanski, 1974).

The discovery and structure determination of griseofulvin proved the ability of fungi to produce antifungal NPs. It was isolated from the mould *Penicillium griseofulvum* in 1938 (Oxford *et al.*, 1939; Grove *et al*., 1952; Newman and Cragg, 2016). Griseofulvin was the first drug applied orally to treat dermatophytes and shows fungistatic activities. The mode of action was determined as inhibiting mitosis by suppressing spindle microtubule dynamics. It binds to tubulin and thus interrupts the microtubule function (Huber and Gottlieb, 1968; Richardson and Warnock, 2003). Due to its accumulation in the lipid and keratin rich areas of the cell wall, it shields new healthy tissue from further fungal infection. This quality makes it selective for the treatment of skin, nails and hair infections (Richardson and Warnock, 2003). Preventing human toxicity by clinical dose adherence makes griseofulvin a safe drug, despite its mitosis inhibition (Panda *et al.*, 2005). Researchers discovered the antifungal cyclic lipopeptides, called echinocandins, in 1974, when echinocandin B (ECB) was isolated from *Aspergillus nidulans* (Benz *et al.*, 1974; Keller-Juslén *et al.*, 1976). After the isolation of ECB, twenty further natural echinocandins from ascomycetes followed. All of them feature a cyclic-hexapeptide structure and target the fungal cell wall by inhibiting the *β*-1,3-glucan synthase (Emri *et al.*, 2013). Structure-activity relationship (SAR)

studies served as a basis to construct semisynthetic analogues. In order to enhance the antifungal potency, the acyl group of the side chain was modified (Debono *et al*., 1995). Cilofungin is one example which was developed from ECB and is clinically applied (Denning, 1997). Their activity was proven against systemic aspergillosis (Pfaller *et al.*, 1998). Another related group was the new antifungal class of pneumocandins, discovered by Merck in 1989 from the fungus *Zalerion arboricola*, indicating their activity against the two pathogens *Pneumocystis carinii* and *Candida* spp. (Schwartz *et al.*, 1989; Denning, 1997). ECB and pneumocandin B served as the lead compounds for the first approved semisynthetic antifungal drugs of the echinocandin-type caspofungin (Cancidas®), micafungin (Mycamine®) and anidulafungin (Eraxis®). They are used in the treatment of invasive candidiasis infections, also targeting the inhibition of β-1,3-glucan synthase of fungi (Butler, 2004; Aly *et al.*, 2011a; Chin *et al.*, 2006). Recent insights into resistance trends of clinically significant *Candida* isolates towards echinocandins, e.g. micafungin, appear increasingly in clinical reports. These reports are rising the awareness of local resistant patterns, aiming at an appropriate empirical treatment strategy (McCarty *et al.*, 2018).

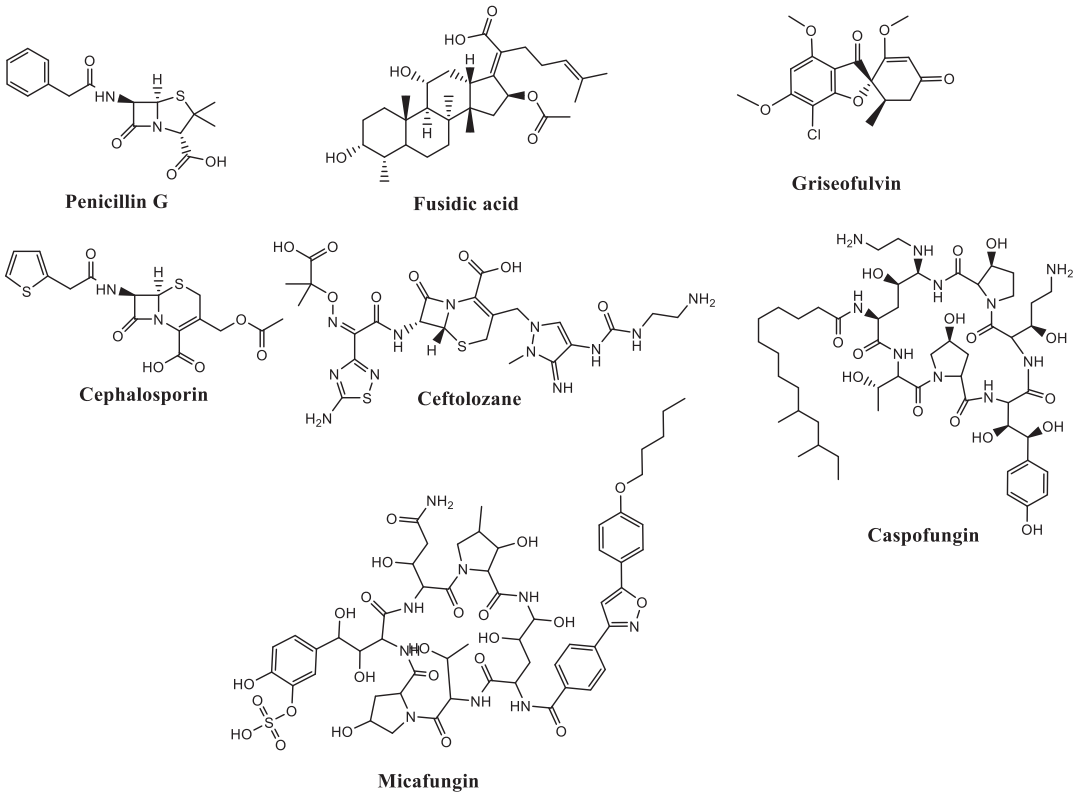

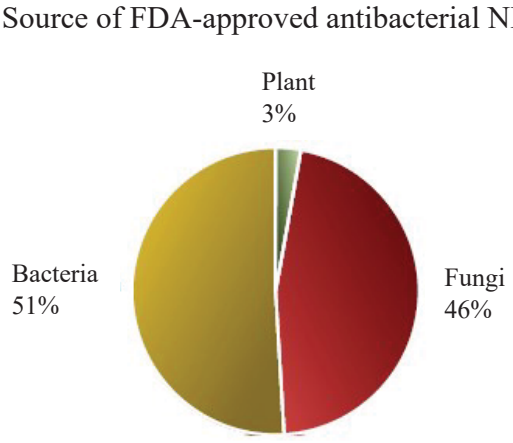

Figure 1.1 Circular chart representing the biological source of FDA-approved antibacterial NPs (Partridge *et al*., 2016)

A recent assessment from 2016 confirms the important role of fungi in serving as sources for FDA-approved therapeutic agents in the treatment of infections. Reviews indicate that more than 69 % of all antibacterial agents originate from NPs, 46 % of which are fungal derivatives (Partridge *et al*., 2016).

1.2.2 Fungal NPs in the treatment of hyperlipidaemia

The so-called statins are cholesterol-lowering agents of fungal origin (Endo *et al.*, 1976). They were discovered firstly in 1976 with the isolation of mevastatin from *Penicillium citrinum*. The discovery of lovastatin (mevinolin) from *Monascus ruber* and *Aspergillus terreus* followed shortly after (Negishi *et al.*, 1986). These NPs were described simultaneously with their mode of action as inhibitors of cholesterogenesis (Buckland, 1989). Lovastatin served as a lead compound for the synthesis of simvastatin and pravastatin. This fact makes them synthetic in nature, nevertheless NP derivatives (Newman *et al.*, 2000). These fungal metabolites target the 3-hydroxy-3-methylglutaryl coenzyme A (HMG CoA) in the mevalonate pathway of cholesterol-biosynthesis (Alberts *et al.*, 1980). This research demonstrated a mechanism of LDL clearance and increased hepatic LDL receptor activity (Alberts, 1988). The results show the positive effects on lower stroke risk, cardiac attacks, sudden cardiac death, retardation of atherosclerosis progression, plaque stabilization and improved endothelial function (Aly *et al.*, 2011a). All naturally occurring statins have the ring-opened lactone-structure in common, resembling mevalonic acid. The NPs served as leads for the synthesis of the synthetic drugs fluvastatin, atorvastatin and cerivastatin (Newman *et al.*, 2000). Recent studies are focusing on the ability of statins to cause tumor-specific apoptosis. Notable was breast cancer shrinkage, due to the significant sensitivity of estrogen receptor-negative subtypes to statin-induced apoptosis (van Leeuwen *et al.*, 2017). Induction of apoptosis

by statins is promoted by degradation of conformational mutant TP53 (mutp53) which shows oncogenic gain-of-function activities (Parrales *et al.*, 2018).

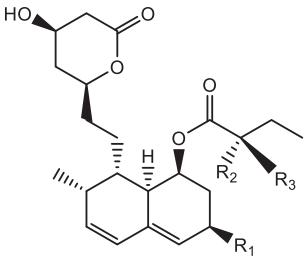

Mevastatin R_1=H, R_2=Me, R_3=H
Lovastatin R_1=Me, R_2= Me, R_3=H
Simvastatin R_1=Me, R_2=Me, R_3=Me

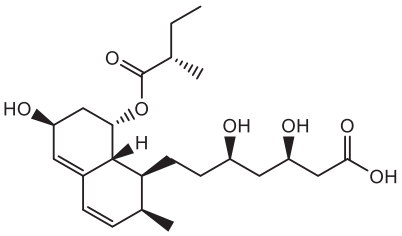

Pravastatin

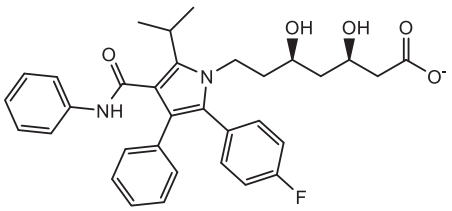

Atorvastatin

1.2.3 Fungal NPs as immunosuppressant agents

The soil fungus *Tolypocladium inflatum* provided the NP cyclosporine A (CsA), thereby introducing a new era of immunosuppressive therapy. Not only did this discovery enable the selective control of the immune response, but also helped in gaining an insight into the principles of the immune system at the molecular level (Shaw, 1989). The immediate spur in transplantation medicine, immune therapy and knowledge of T-cell biochemistry is based on the mode of action of CsA. The drug binds to mitochondrial matrix protein cyclophilin D, which prevents the dephosphorylation of the transcription factor NF-AT (nuclear factor of activated T-cells). As a result, the calcineurin activity is being inhibited and thereby the production of pro-inflammatory mediators downregulated, such as TNF-α or interleukin 2 (Pritchard, 2005; Aly *et al.*, 2011a). Besides the inhibition of calcineurin, the binding of CsA to cyclophilin D also inhibits mitochondrial permeability transition, which regulates necrotic cell death and initiation of apoptogenic signalling. Despite the beforementioned advantages of CsA, it´s usage remains limited and ineffective for the treatment of autoimmune diseases that require chronic management. With the isolation of myriocin from the thermophilic fungus *Myriococcum albomyces*, the first

step was taken towards the discovery of fingolimod (Kluepfel *et al.,* 1972). Myriocin acts as an antibiotic, which was nevertheless too toxic for therapeutic employment. This motivated researchers to conduct SAR studies (Adachi *et al.*, 1995). By simplifying the structure of myriocin, which included removal of the side chain functionalities and elimination of chiral centres, finally a compound exhibiting potent immunosuppressant activity was designed: fingolimod (Brinkmann *et al.*, 2002). Fingolimod shows first-in-class bioavailability when applied orally, targeting the sphingosine-1-phosphate (S1P) receptors, thus becoming the first-line drug for the treatment of multiple sclerosis (MS). Besides this, fingolimod improved the understanding of the biology of the S1P receptors (Brinkmann *et al.*, 2010). By phosphorylation of the drug *in vivo*, fingolimod-phosphate resembles the naturally occurring S1P and can thus bind to the five known subtypes of S1P ($S1P_{1\text{-}5}$). These receptor subtypes are relevant for MS, a disease in which the pathology is defined by the release of autoimmune lymphocytes into the blood. The lymphocytes cross the blood-brain barrier and enter the central nervous system (CNS) causing neurodegeneration. Relapsing inflammation in the CNS causes disability, since S1P receptors are responsible for lymphocyte release that cause neuropathology in the CNS. This explains the success of fingolimod for the treatment of relapsing MS (Chun and Hartung, 2010).

FDA-approved drugs for immunosuppression during renal transplantation are mizoribine, a NP isolated from the mould *Eupenicillium brefeldianum*, and mycophenolate mofetil (MMF), the morphoniloethyl ester prodrug of mycophenolic acid (MPA), obtained from several *Penicillium* species. Mizoribine acts *in vivo* as an antagonistic blocker of IMPDH (inosine-5′-monophosphate dehydrogenase) and GMP (guanosine monophosphate)-synthetase, thereby inhibiting the humoral and cellular immunity. It inhibits lymphocyte antiproliferation selectively by IMPDH inhibition, which aligns with the nucleoside structure of the imidazole class of this compound (Ishikawa,

1999). The formation to MMF increased the oral bioavailability of the NP, which is a selective inhibitor of T- and B-lymphocytes proliferation. It transforms into MPA *in vivo*, which inhibits the IMPDH as well, thus reducing graft rejection (European Mycophenolate Mofetil Cooperative Study Group, 1995; Sollinger, 1995; Allison and Eugui, 2000).

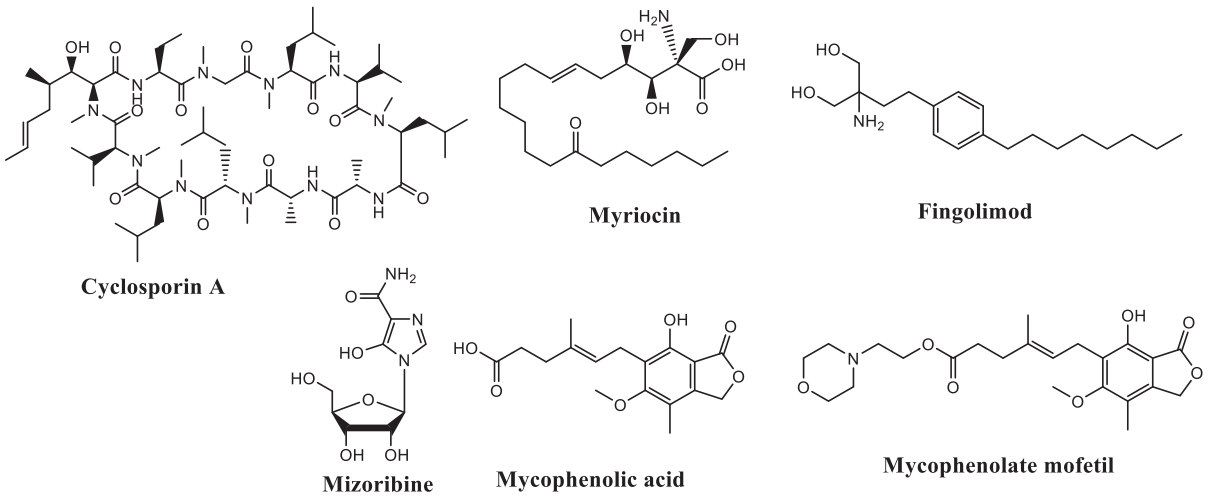

1.2.4 Fungal NPs as anti-proliferative agents

The role of fungi as biological sources to provide anticancer agents was intensely discussed by oncologists after the discovery of paclitaxel (Taxol®) from the bark of *Taxus brevifolia* (Pacific yew) in the late 1960s. The drug is used for the treatment of refractory ovarian and breast cancer (Stull *et al.*, 1995). The restricted amount and uneconomic approach of the plant's bark, being the only source of supply, and following isolation of paclitaxel from endophytic fungi, solved an economic problem (Kingston *et al.*, 1994). Another improved approach of semi-synthesis by finding other plant sources resulted in the production of the drug from the NP baccatin III, which occurs in the English or European yew, *Taxus baccata* (Li *et al*., 2017). The endophytic fungus *Taxomyces andreanae* which is associated with the Pacific yew tree and was isolated from its bark was described as a producer of Taxol® (Stierle *et al.*, 1993). The *de novo* synthesis of taxol by the

endophyte was demonstrated by labelling studies (Stierle *et al.*, 1995). A review published by Zhou *et al.* in 2010 provides a list of more than thirty Taxol®-producing endophytic fungi, e.g. *Fusarium* and *Penicillium* species, with the ultimate aim of a large-scale industrial fermentation of fungi for production of taxol (Zhou *et al.*, 2010). The search for endophytic Taxol® producers still attracts the attention of researchers, who aim at establishing culture conditions suitable for upscaling of the production of this important anticancer drug, e.g. the effect of darkness or co-culture of *Aspergillus terreus* with plant endogenous microbes (Soliman and Raizada, 2018; El-Sayed *et al.*, 2018). The pentacyclic quinolone alkaloid camptothecin was likewise the first encountered NP, isolated from *Camptotheca acuminata*, to be later isolated from another endophytic fungus of the same host plant, named *Entrophospora infrequens* (Chin *et al.*, 2006; Kharwar *et al*., 2011). This NP has already been isolated from several endophytic fungi, e.g. *Fusarium solani*. Camptothecin acts antineoplastic by inhibiting topoisomerase I (TOP1) enzyme selectively. It only binds to the complex which is formed by TOP1 during DNA cleavage, and neither to TOP1 nor DNA separately (Kharwar *et al*., 2011). Due to its physicochemical characteristics, especially the poor solubility that causes severe bladder toxicity, the NP is not used therapeutically (Oberlies and Kroll, 2004). Nevertheless, it gave rise to the water-soluble semisynthetic analogues, irinotecan and topotecan (Cragg and Newman, 2013). The two analogues are being successfully employed for the treatment of both, ovarian and colorectal cancers, respectively (Mathijssen *et al.*, 2002). Further examples of plant compounds also found in fungi include the aryltetralin cyclolignan podophyllotoxin. a precursor for clinically applied anticancer drugs from *Podophyllum peltatum* (Kadkade, 1982; Xia *et al.*, 2000; Eyberger *et al.*, 2006). It also occurs as a secondary metabolite of the endophytic fungus *Phialocephela fortinii* (Eyberger *et al.*, 2006). Structural modification of this NP led to three anticancer drugs, i.e. etoposide, which targets

DNA topoisomerase II (TOP2) (Yu *et al.*, 2017). This molecular target allows the treatment with etoposide against a wide range of cancer, e.g. small cell lung cancer, sarcomas, lymphomas and leukaemias (Hande, 1998; Baldwin and Osheroff, 2005; Montecucco and Biamonti, 2007). Likewise, the Vinca alkaloids vincristine and vinblastine, which are products from *Catharanthus roseus*, were later also reported from the endophytes *Fusarium oxysporum* and *Alternaria* sp. (Aly *et al*., 2011b; Kumar *et al.*, 2013). Vinca alkaloids act as inhibitors of the mitotic spindle function. But due to their non-specific mode of action they also show cytotoxic effects against normal tissues, e.g. human skin and/or lung fibroblasts. In order to reduce systemic toxicity and sensitize the agents' effect towards cancerous cell lines, free radical scavenging antioxidants have been investigated to antagonize the cytotoxicity towards healthy tissue, which are simply plant extracts (Rajabalian, 2008). Both agents interfere with normal microtubule dynamics by binding to tubulin monomers and preventing their polymerization, which leads to metaphase arrest (Liebner, 2015). Another anticancer agent, named plinabulin, was developed from two fungal NPs, the diketopiperazine halimide, isolated from the sponge-associated fungus *Aspergillus* sp., and its 6(*S*)-stereoisomer phenylahistin, obtained from the terrestrial fungus *Aspergillus ustus*, (Kanoh *et al.*, 1997; Fenical *et al.*, 2000; Yamazaki *et al.*, 2010). The anti-microtubule agent plinabulin was found to act as a vascular disrupting agent, which reached the clinical pipeline in phase III combination therapy against lung cancer (NSCLC) (Millward *et al.*, 2012; Cimino *et al.*, 2019). It stands out through its anticancer and additional immune enhancing activity by activating dendrite cells and related T-cells (Blayney *et al.*, 2018).

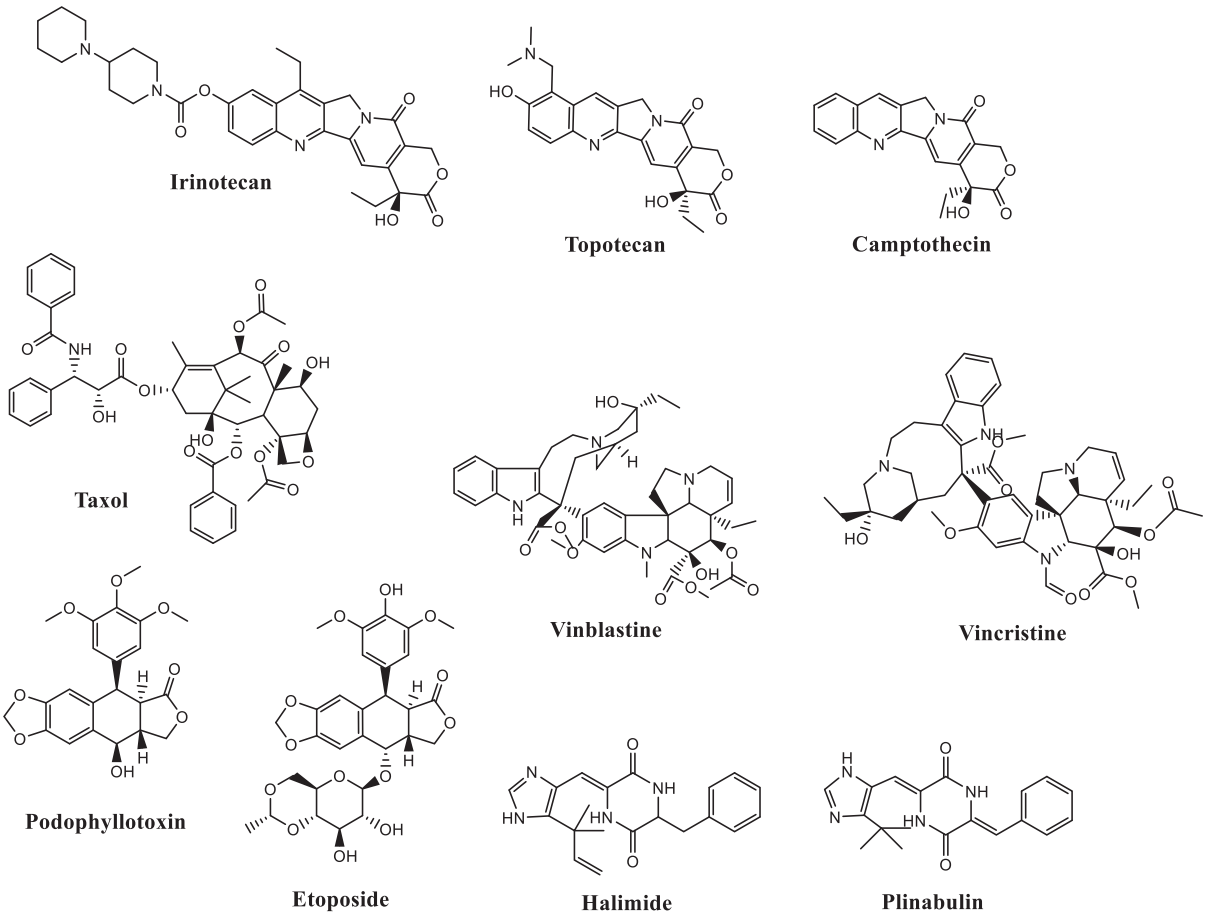

1.3.1 Endophytic fungi

The fact that endophytic fungi are rich sources of novel bioactive phytochemicals has already been discussed in section 1.2.4, where plant anticancer drugs were found to be produced by endophytic fungi isolated from the same host plants, e.g. paclitaxel, camptothecin and podophyllotoxin. (Chandra, 2012; Aly *et al.*, 2013). Investigation of the biosynthetic potential of endophytic fungi and their signal transduction and regulation of biosynthesis of NPs can possibly lead to an economically feasible production of desired secondary metabolites (Weber, 2009; Ashour *et al.*, 2011).

Endophytes are defined as inhabitants of their host plant, without causing virulence, regardless of which plant organ is inhabited (Jalgaonwala *et al.*, 2011). The endophyte-host association balances

the pathogen host antagonism. Both organisms control this balance genetically. The host can benefit from the fungal metabolic response system to a hostile environment by presenting the host with defending chemicals. The latter can be of use for medicine, agriculture or for the chemical industry (Jalgaonwala *et al.*, 2011; Ashour *et al.*, 2011). With special regard to medicinal host plants, reviews on isolated NPs from endophytic fungi, expressing relevant bioactivity, reflect the high metabolic diversity of these microbes. They provide structures like terpenoids, steroids, quinones, phenols, coumarins etc. as new potent anticancer, immunomodulatory, antioxidant, antiparasitic, antiviral, antitubercular, insecticidal etc. compounds (Aly *et al.*, 2010; Kaul *et al.*, 2012; Debbab *et al.*, 2012b; Aly *et al.*, 2013). The fact that the fungal isolates are repeatedly subjects to cycles of sub-culturing often results in downregulation or non-expression of certain gene clusters which are involved in fungal NP production (Aly *et al.*, 2010). Researchers speculate that this is partly due to the lack of host plant signalling molecules that drive the NP-biosynthesis of fungi.

1.3.2 Mangrove-derived fungi

Fungi that are isolated from halotolerant higher plants have proven to be producers of interesting bioactive NPs, exemplified by alternariol. Alternariol showed activity in many bioassays, targeting for example the cancer related protein kinases Aurora A and B. This NP has been isolated from *Alternaria* sp. inhabiting the mangrove plant *Sonneratia alba* (Proksch *et al.*, 2010). Mangrove plants can only be found in subtropical and tropical areas of the intertidal zone. These plants are constantly exposed to stress conditions, since the roots are anchored in salt-water and the aboveground organs have to cope with tropical climate conditions (Proksch *et al.*, 2010). Assessing the chemistry of the isolated fungal endophytes of these types of plants has repeatedly led to new bioactive NPs (Debbab *et al.*, 2013). For example, the fungal endophyte *Bionectria ochroleuca*,

isolated from the mangrove plant *Sonneratia caseolaris*, yielded two new peptides pullularins E and F, which exhibit strong cytotoxicity against murine lymphoma L5178Y cells (Ebrahim *et al.*, 2012). The investigation of the mangrove-derived endophyte *Phomopsis longicolla*, isolated from the same host *S. caseolaris*, provided a new tetrahydroxanthone dimer (12-deacetylphomoxanthone) and two new structurally related monomers (phomo-2,3-dihydrochromone and isomonodictyphenone). Alongside, the fungal mycotoxin phomoxanthone A (PXA) was co-isolated and showed the strongest pro-apoptotic activity. Several cytotoxicity assays were targeting human cancer cell lines, e.g. cisplatin-resistant cells. The loss of activity of PXA up to 100-fold against healthy peripheral blood mononuclear cells, its activation of murine T lymphocytes, NK-cells and macrophages, revealed the dual effect of PXA as an immune system activator and a pro-apoptotic agent (Rönsberg *et al.*, 2013). SAR studies which compared PXA to naturally biosynthesised and semisynthetic derivatives of PXA proved the position of the biaryl linkage and the acetylated substitutions to be essential for the beforementioned bioactivities (Frank *et al.*, 2015). These results attracted researchers' attention to further study the mode of action on a molecular level. Böhler *et al.* discussed the mitochondrial function as the target of PXA. PXA causes the fragmentation of IMM (inner mitochondrial membrane) and disrupts the mitochondrial christae, independant of the fusion mediators DRP1 (dynamin related protein 1) and OPA1 (optic atrophy 1). The response system releases pro-apoptotic factors that initiate the apoptosis. This novel mode of action of PXA might lead to a better understanding of mitochondrial ion homeostasis and membrane dynamics (Böhler *et al.*, 2018).

1.4 Triggering silent biosynthetic pathways

The search for new NPs with the potential of becoming a drug or drug-lead is experiencing a setback with the increasing high rate of re-isolation of known compounds, which is a negative fact

on time and financial resources. This issue arises often, because laboratorial culturing conditions of microbes do not resemble the natural ecological environment of microbes. In nature multiple factors trigger the transcription of microbial gene clusters. This study tackles this current research issue of silenced biosynthetic pathways, by applying techniques that can create a maximising effect on the chemical diversity of fungal NPs (Daletos *et al.*, 2017).

1.4.1 One Strain MAny Compounds (OSMAC) approach

The OSMAC approach is basically defined by the variation of culturing conditions of axenic microbial cultures. Any change of cultivating factor that influences fungal growth and its chemistry, without breaking the sterility of the culture, represents the implementation of the OSMAC approach (Schiewe and Zeeck, 1999; Daletos *et al.*, 2017). Easily accessible parameters of the cultures are for example media composition, culture vessel, aeration, temperature, pH etc. (Bode *et al.*, 2002). This technique elicited accumulation of known NPs, like fusarielin J from *Fusarium tricinctum*, when the fungus was cultivated in juice-supplemented rice media. In addition, the induction of two new NPs, fusarielin K and L was observed (Hemphill *et al.*, 2017). Culturing the endophytic fungus *Aspergillus versicolor* on DMSO-supplemented Wickerham Medium triggered the production of three cryptic known NPs (sterigmatocystin, infectopyrone and versiol), which were neither detectable in the axenic rice culture of the fungus, nor isolated or detectable in the crude extract of the fungus when co-cultured with the bacterium *Bacillus subtilis* (Abdelwahab *et al.*, 2018). These two examples demonstrate the relevance of the OSMAC approach in drug discovery or characterization of fungal metabolic profile patterns, even in comparison with other techniques, like the very useful co-culturing tool. Wang *et al.* demonstrated the usefulness of this approach in their study on the endophyte *Fusarium tricinctum*. The fungus accumulates bioactive depsipeptides, named enniatins, which occur as mixtures of enniatins A, B

and B_1. Culturing the fungus on solid white beans (*Phaseolus vulgaris*) yielded the highest quantity of enniatins A, A_1, B and B_1, after 18 days of fermentation, when compared to other media (Wang *et al.*, 2013a). These hexadepsipeptides were already suggested to be a potential new class of human immunodeficiency virus type-1 (HIV-1) integrase inhibitors (Dornetshuber *et al.*, 2007; Shin *et al.*, 2009). Fusafungine, a combination of enniatins A, B and C, reached the drug market as an antibiotic agent for the treatment of respiratory tract infections, but was finally removed from the market due to the occurrence of allergic reactions in treated patients (German-Fattal, 2001; Hemphill *et al.*, 2017).

1.4.2 Co-cultivation (mixed fermentation)

The scientific counterparts to axenic microbial cultures are the mixed fermentations, also called co-cultures, of two or more different microorganisms together in one culture vessel. The aim is to mimic the natural environment of microbes, with the effect to trigger silent biosynthetic pathways. Due to interspecies crosstalk, competition for nutrients and space, and activating the chemical defence mechanism of the opponents, a dramatic shift in the metabolic pattern can be observed (Bertrand *et al.*, 2014; Daletos *et al.*, 2017).

1.4.2.1 Fungal co-culture

There is no doubt that co-cultivation has already proven to be an important tool for triggering silent biosynthetic pathways. This has been demonstrated in the positive outcome of isolating new NPs, even from exhaustively investigated endophytic fungi, e.g. of *Aspergilli* and *Fusarium* strains (Wang *et al.*, 2013b; Chen *et al.*, 2015; Abdelwahab *et al.*, 2018). This method, for example, caused the induction of new NPs during the co-culture of *Fusarium tricinctum* with *Bacillus subtilis*, thus resulting in a strikingly enhanced accumulation of bioactive metabolites, like the

enniatins (up to 78-fold) (Ola *et al.*, 2013). Taking this procedure further, co-culture can give a deeper insight into the behaviour of one fungal species when co-cultured with viable or autoclaved strains of the same microbe. This experiment was performed by Akone *et al.* and Ancheeva *et al.*, by growing *Chaetomium* sp. together with viable or autoclaved strains of the bacterium *Bacillus subtilis* or the autoclaved human pathogenic bacterium *Pseudomonas aeruginosa*. Accumulation of constitutively present compounds and induction of known cryptic compounds appeared in both experiments. Akone *et al*. used viable or autoclaved strains of the bacterium *Bacillus subtilis* as the bacterial enemy to the fungus and published the isolation of five new NPs, such as a quinolone derivative (quinomeran), polyketides (chorismeron and serkydayn), a shikimic acid derivative (shikimeran A) and a symmetric dimer (bipherin A). Constitutively present compounds occurred in higher amounts, up to 8.3-fold, in the co-cultures. Seven cryptic compounds of the co-cultures included isosulochrin and protocatechuic acid methyl ester (Akone *et al.*, 2016). Ancheeva *et al.* published additional six new NPs, isolated from the co-culture with human pathogenic bacterium *Pseudomonas aeruginosa*. The mixed fermentation introduced a new butenolide analogue (WF-3681) and new shikimic acid derivatives (chaetoisochorismin and shikimeran B). The accumulation of constitutively present compounds scored up to 33-fold, including four of the new butenolide derivatives (chaetobutenolide A, B, C and WF-3681 methyl ester) (Ancheeva *et al.*, 2017). The comparison of both experiments presents the different response system of a fungus towards different microbial enemies, by the accumulation of constitutive, cryptic and new compounds in the set-up co-cultures (Akone *et al.*, 2016; Ancheeva *et al.*, 2017).

1.4.2.2 Bacterial co-culture

Bacterial co-cultures have already proven their place in microbial engineering (Bader *et al.*, 2010; Zhang *et al.*, 2015; Camacho-Zaragoza *et al.*, 2016). Another field of applying microbial co-

culturing is biodegradation: use of bacterial or fungal-bacterial (Boonchan *et al.*, 2000) co-cultures to degrade dissolved organic matter (DOM), i.e. toxic agents that are used in agriculture, recalcitrant xenobiotics into non-pollutant structures (Awasthi *et al.*, 1997; Dangmann *et al.*, 1996)

Nevertheless, a recent aim of applying microbial co-cultures is the activation of silent gene clusters in bacteria to obtain new or even novel microbial secondary metabolites (MSM):

The novel structure of gordonic acid (acyclic polyene polyketide substituted with a β-D-digitoxopyranose) was explored from the bacterial co-culture of *Streptomyces tendae* and *Gordonia* sp. (Park *et al.*, 2017).

A very important compound class for the food industry are the peptides named bacteriocins. Bacteriocins from lactic acid bacteria (LAB) are applied as natural antimicrobial agents which proved to be safe in the use of food preservation (Chanos and Mygind, 2016). Induction of bacteriocins under laboratorial conditions was conducted by microbial co-cultures. Producing bacterial strains were mainly the *Lactobacillus* sp. (Tabasco *et al.*, 2009; Barefoot *et al.*, 1994; Di Cagno *et al.*, 2009; Ge *et al.*, 2014; Maldonado *et al.*, 2004; Rojo-Bezares *et al.*, 2007; Man *et al.*, 2012), but also *Enterococcus*, *Bacillus* and *Leuconostoc* strains (Kos *et al.*, 2011; Benitez *et al.*, 2011). Bacterial inducers of the LAB or non-LAB bacteriocins were inoculated as living cultures, medium heated or autoclaved and vary widely in their genetic profiles whereas the co-culturing of two living species would positively influence the results (Chanos and Mygind, 2016).

Onaka and co-workers reported heterologous gene expression through microbial co-culture. Mycolic acid-containing bacteria (MACB), i.e. *Tsukamurella pulmonis*, and several *Streptomyces* sp. were chosen as competitors. The gene clusters responsible for bioactive compounds, i.e. microbial pigments, staurosporine (antitumor clinical studies phase II) and rebeccamycin (DNA

TOP1 inhibitor) were inserted into *S. lividans*. Several conducted studies showed that MACB induce silent biosynthetic gene clusters, when physical contact is given. This led to the production of i.e. the new arcyriaflavin E, a cytotoxic indolocarbazole alkaloid, the new chojalactones A–C, cytotoxic butanolides, and niizalactams, multicyclic macrolactams (Onaka *et al.*, 2011; Onaka *et al.*, 2015; Hoshino *et al.*, 2015a; Hoshino *et al.*, 2015b; Hoshino *et al.*, 2015c; Hoshino *et al.*, 2019). The MSM named umezawamides, with polycyclic tetramate macrolactam core structure, were obtained as new compounds from the co-culture of the MACB *Tsukamurella pulmonis* and *Umezawaea* sp. These compounds exhibited growth inhibitory activity against *Candida albicans* and anticancer effects against a murine lymphoma cell line (Hoshino *et al.*, 2018).

The co-culture of marine derived bacteria *Rhodococcus* sp. and *Micromonospora* sp. afforded a new glycosylated anthracycline, named keyicin. Studies on *E. coli* revealed that the new discovered NP does not show nucleic acid disruption. Furthermore, it exhibited antibacterial activity against gram-positive bacteria, i.e. MRSA (Adnani *et al.*, 2017). Later conducted studies, which focused on the genome level, identified *Micromonospora* sp. as the producer. The two microbes were set up in a two-chamber assay with an impermeable membrane. The inhibited growth of *Rhodococcus* sp. and the accumulation of keyicin revealed the NPs antibacterial potency and the non-dependant production of the NP on a cell-cell contact. In fact, the production of this cryptic NP is triggered by quorum sensing (QS) molecules from the N-acyl homoserine lactone type. It is discussed that the microbe performs metabolite reuptake (i.e. small molecules of the competitor), which benefits the bacterium and turns it into an advantage that could represent a self-defence mechanism. The underlying basis is that cryptic biogenetic gene clusters are being triggered, in this special case leading to an overexpression of *kyc*, the responsible biosynthetic gene cluster for the production of keyicin (Acharya *et al.*, 2019).

2 Results

The following chapter is a reprint from published projects that were conducted during this promotion.

2.1 Publication I

Title

"*Tetrahydroanthraquinone derivatives from the mangrove-derived endophytic fungus Stemphylium globuliferum*"

Published in: *Tetrahedron Letters*

Impact factor: 2.379

Personal contribution: 75%, first authorship, performing most of the laboratorial work, literature research and manuscript writing

.

Tetrahedron Letters 57 (2016) 4074–4078

Contents lists available at ScienceDirect

Tetrahedron Letters

journal homepage: www.elsevier.com/locate/tetlet

Tetrahydroanthraquinone derivatives from the mangrove-derived endophytic fungus *Stemphylium globuliferum*

Mariam Moussa [a], Weaam Ebrahim [a,b], Mona El-Neketi [b], Attila Mándi [c], Tibor Kurtán [c], Rudolf Hartmann [d], Wenhan Lin [e], Zhen Liu [a,*], Peter Proksch [a,*]

[a] Institute of Pharmaceutical Biology and Biotechnology, Heinrich-Heine-Universität Düsseldorf, Universitätsstrasse 1, 40225 Düsseldorf, Germany
[b] Department of Pharmacognosy, Faculty of Pharmacy, Mansoura University, Mansoura 35516, Egypt
[c] Department of Organic Chemistry, University of Debrecen, Egyetem tér 1, Debrecen 4032, Hungary
[d] Institute of Complex Systems: Strukturbiochemie, Forschungszentrum Juelich, Wilhelm-Johnen-Straße, 52428 Juelich, Germany
[e] State Key Laboratory of Natural and Biomimetic Drugs, Peking University, Beijing 100191, China

ARTICLE INFO

Article history:
Received 30 May 2016
Revised 26 July 2016
Accepted 28 July 2016
Available online 29 July 2016

Keywords:
Stemphylium globuliferum
Tetrahydroanthraquinone
ECD calculations

ABSTRACT

Two new tetrahydroanthraquinone derivatives, altersolanol Q (**1**) and 10-methylaltersolanol Q (**2**), and the new dimer alterporriol X (**3**), together with 13 known analogues were isolated from white bean solid culture media of the endophytic fungus, *Stemphylium globuliferum*, obtained from the Egyptian mangrove plant *Avicennia marina*. The present study resulted in the production of a large diversity of secondary metabolites including new derivatives. Their structures were elucidated using one- and two-dimensional NMR spectroscopy as well as HRESIMS. The absolute configurations of the new compounds **1–3** were determined by TDDFT-ECD calculations or by comparing ECD data with those of known analogues. Compounds **1–3** were tested against the L5178Y mouse lymphoma cell line but proved to be inactive in contrast to some of the known compounds such as altersolanol A (**6**) that were likewise isolated in this study.

Introduction

Mangrove-derived endophytic fungi are considered an important source for bioactive secondary metabolites that could be of potential use as lead compounds for pharmaceutically relevant drugs.[1–3] Endophytic fungi that inhabit mangrove plants are thought to promote adaptation of their host to survive under harsh ecological conditions such as high salt concentration, high temperature, low oxygen concentration due to changing levels of submersion in seawater, or to counter biological stress caused by herbivores and microbial pathogens.[4] This encouraged us to employ the OSMAC (One Strain Many Compounds)[5,6] approach to *Stemphylium globuliferum*, an endophytic fungus isolated from the mangrove plant *Avicennia marina* (Acanthaceae) collected from Hurghada in Egypt, by changing the culture media in order to trigger the stimulation of silent biogenetic gene clusters.[3] Most compounds previously isolated from this endophyte were reported to be anthraquinone or tetrahydroanthraquinone derivatives including homo- and heterodimers, which are known to possess a wide range of biological activities. For example, altersolanol A (**6**), a tetrahydroanthraquinone derivative obtained in this study but also isolated from *Phomopsis juniperovora*,[7] *Dactylaria lutea*,[8] *Alternaria* sp.,[9] and *Stemphylium globuliferum*,[10] is a potent inhibitor of plant respiration, blocking the uptake of essential metabolites required for photosynthesis[11] and also exhibits cytotoxic activity against 34 human cancer cell lines.[12] In the present study, two new tetrahydroanthraquinone derivatives, altersolanol Q (**1**) and 10-methylaltersolanol Q (**2**), one new anthranoid dimer alterporriol X (**3**), as well as 13 known analogues (**4–16**) were isolated (Fig. 1). Their structure elucidation including determination of the absolute configuration as well as biological activities are reported.

Results and discussion

Compound **1** showed UV absorbances at λ_{max} 224, 268 and 334 nm, similar to those of known altersolanol derivatives.[13,14] It exhibited the molecular formula $C_{16}H_{20}O_6$ as established by HRESIMS. The ^{1}H NMR spectrum (Table 1) showed two *meta*-coupling aromatic protons at δ_H 6.98 (d, H-8) and 6.63 (d, H-6), two oxygenated methines at δ_H 4.93 (d, H-10) and 3.43 (dd, H-3), one methoxy group at δ_H 3.78 (s, H_3-12), one singlet methyl group at

* Corresponding authors. Tel.: +49 211 81 14163; fax: +49 211 81 11923.
E-mail addresses: zhenfeizi0@sina.com (Z. Liu), proksch@uni-duesseldorf.de (P. Proksch).

http://dx.doi.org/10.1016/j.tetlet.2016.07.091
0040-4039/

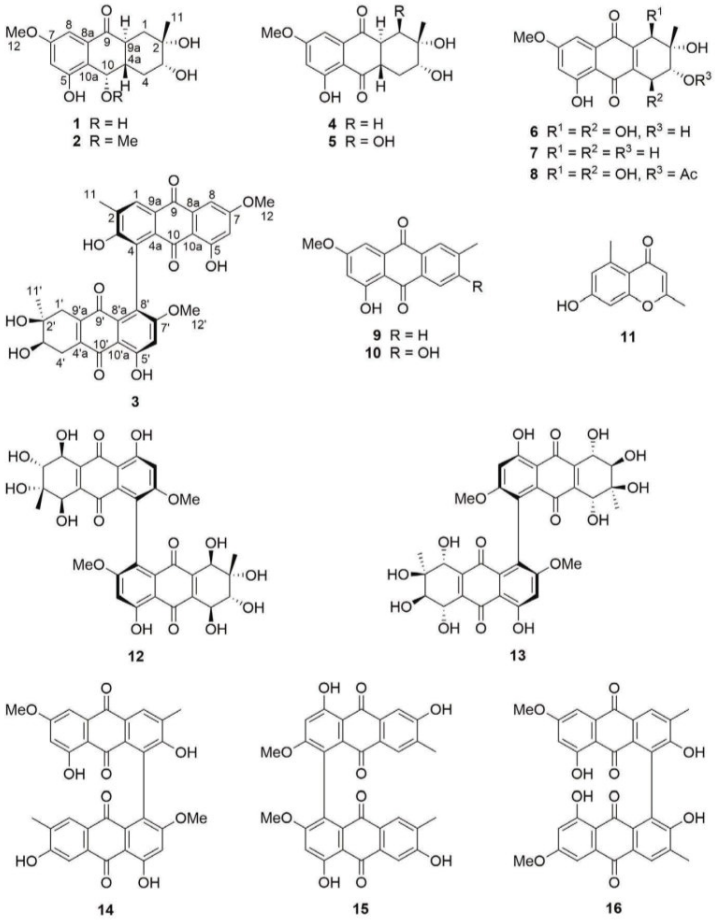

Figure 1. Structures of compounds isolated from *S. globuliferum*.

δ_H 1.31 (s, H_3-11), as well as six aliphatic protons at δ_H 3.05 (td, H-9a), 2.38 (dd, H-1_{eq}), 2.22 (td, H-4_{ax}), 1.93 (tdd, H-4a), 1.71 (ddd, H-4_{eq}) and 1.33 (dd, H-1_{ax}). The planar structure of **1** was elucidated through a detailed analysis of 2D NMR spectra (Fig. 2). The COSY correlations between H_2-1/H-9a, H-9a/H-4a, H-4a/H-10, H-4a/H_2-4 and H_2-4/H-3, together with the HMBC correlations from H_3-11 to C-1, C-2 and C-3 indicated the presence of a cyclohexane ring with a methyl and a hydroxy group attached at C-2, as well as a hydroxy group at C-3. The HMBC correlations from H-6 to C-5, C-7, C-8 and C-10a from H-8 to C-6, C-7, C-8a and C-10a, and from H_3-12 to C-7 established the presence of a 1,2,3,5-tetrasubstituted benzene ring with a hydroxy and a methoxy group attached at C-5

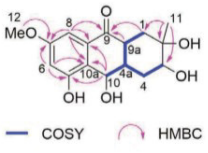

Figure 2. Key COSY, HMBC correlations of compound **1**.

and C-7, respectively. Finally, the HMBC correlations from H_2-1, H-8 and H-9a to C-9 supported the linkage from C-8a to C-9a via the keto carbonyl moiety C-9, and the HMBC correlations from H-10 to C-5, C-8a and C-10a allowed the assignment of the linkage between C-10 and C-10a.

A literature survey indicated that **1** exhibited the same planar structure as altersolanol J,[13] for which the absolute configuration had only been proposed based on biogenetic considerations. However, the small value of $J_{4a,10}$ (2.7 Hz) in **1** in comparison with that of altersolanol J (9.6 Hz) suggested the *cis* orientation of H-4a and H-10 in **1** rather than *trans* orientation in altersolanol J. The relative configuration of the remaining chiral centres was deduced to be the same as that of altersolanol J based on the similar coupling constants and ROESY relationships. The absolute configuration of **1** was determined as 2*S*, 3*R*, 4a*S*, 9a*S* and 10*S* on the ground of the TDDFT-ECD calculation of the related 10-methyl derivative **2** (vide infra).

The molecular formula of **2** was established as $C_{17}H_{22}O_6$ by HRESIMS, indicating an increase of 14 amu in comparison with altersolanol Q (**1**). The UV and NMR spectra of compound **2** resembled those of **1** except for the appearance of an additional methoxy group (δ_C 58.6, δ_H 3.45, CH_3-13) in **2**. The attachment of this

Table 1
NMR data of compounds **1** and **2**[a]

No.	1		2	
	δ_H (J in Hz)	δ_C, type	δ_H (J in Hz)	δ_C, type
1_{ax}	1.33, dd (14.2, 12.2)	39.0, CH_2	1.27, dd (14.2, 12.2)	39.3, CH_2
1_{eq}	2.38, dd (14.2, 4.0)		2.37, dd (14.2, 3.9)	
2		72.1, C		72.1, C
3	3.43, dd (11.8, 4.6)	75.5, CH	3.39, dd (11.8, 4.6)	75.4, CH
4_{eq}	1.71, ddd (12.2, 4.6, 3.5)	33.8, CH_2	1.76, ddd (12.2, 4.6, 3.5)	34.0, CH_2
4_{ax}	2.22, td (12.2, 11.8)		2.23, td (12.2, 11.8)	
4a	1.93, tdd (12.2, 3.5, 2.7)	43.9, CH	1.96, tdd (12.2, 3.5, 2.3)	44.5, CH
5		158.0, C		158.1, C
6	6.63, d (2.5)	108.2, CH	6.63, d (2.5)	107.8, CH
7		161.7, C		161.8, C
8	6.98, d (2.5)	101.8, CH	7.01, d (2.5)	102.8, CH
8a		134.2, C		134.6, C
9		202.2, C		202.2, C
9a	3.05, td (12.2, 4.0)	40.7, CH	3.05, td (12.2, 3.9)	41.3, CH
10	4.93, d (2.7)	64.0, CH	4.60, d (2.3)	73.2, CH
10a		126.0, C		124.4, C
11	1.31, s	27.3, CH_3	1.29, s	27.2, CH_3
12	3.78, s	55.8, CH_3	3.78, s	55.8, CH_3
13			3.45, s	58.6, CH_3

[a] Measured in MeOH-d_4 (^{1}H at 600 MHz and ^{13}C at 150 MHz).

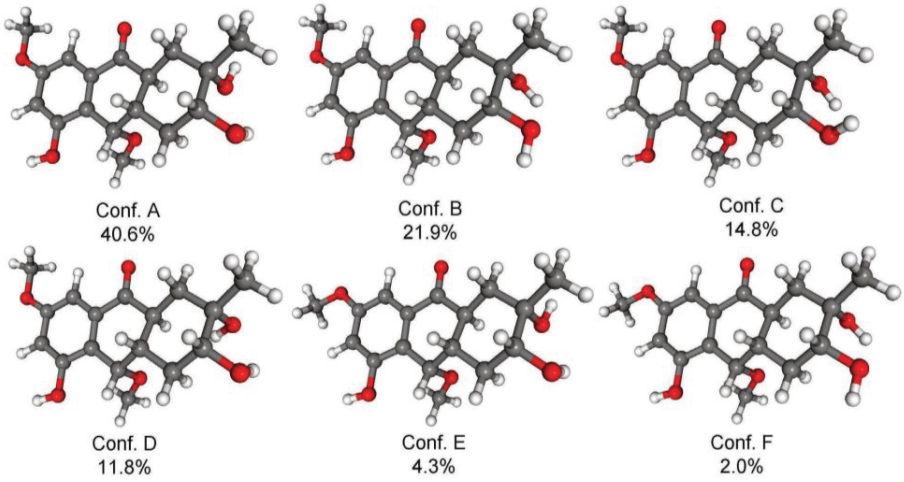

Figure 3. Structure and population of the low-energy B3LYP/6-31G(d) conformers (≥2%) of (2*S*,3*R*,4a*S*,9a*S*,10*S*)-**2**.

methoxy group at C-10 was confirmed by the HMBC correlation from H_3-13 to C-10 along with the obvious downfield shift of C-10 (δ_C 73.2) in **2** compared to the corresponding carbon (δ_C 64.0) in **1**. Thus, compound **2** was determined as 10-methylaltersolanol Q. Its relative configuration was deduced to be the same as **1** due to the similarity of their J values and ROESY correlations.

For the assignment of the absolute configuration of **2**, the solution TDDFT-ECD approach was pursued for the arbitrarily chosen (2*S*,3*R*,4a*S*,9a*S*,10*S*) enantiomer. The initial 20 MMFF conformers were reoptimized at B3LYP/6-31G(d) in vacuo and B97D/TZVP PCM/MeCN levels yielding 6 and 10 low-energy (≥2%) conformers, respectively. In all the computed B3LYP/6-31G(d) conformers, the 10-OMe and 2-OH groups adopted axial orientation (Fig. 3), while the 3-OH was equatorial and the fused cyclohexenone ring of the tetralone chromophore had *M*-helicity ($\omega_{10a,10,4a,9a}$ = −58.0°). The conformers differed only in the orientations of the methoxy group and hydroxyl protons. Similarly to coniothyrinone D,[15] the carbonyl group of **2** could not form an intramolecular hydrogen bond with the phenolic hydroxyl group, which resulted in the separation of the n–π^* [negative Cotton effect (CE) at 350 nm] and π–π^* (positive CE at 312 nm) transitions of the tetralone chromophore in the experimental ECD spectrum. According to the ECD study of coniothyrinone D,[15] the negative n–π^* CE of **2** derives from *M*-helicity of the tetralone chromophore implying (2*S*,3*R*,4a*S*,9a*S*,10*S*) absolute configuration. This assignment was confirmed by ECD calculations of the computed conformers of (2*S*,3*R*,4a*S*,9a*S*,10*S*)-**2** with various functionals and TZVP basis set affording good agreement with the experimental ECD spectrum (Fig. 4). Since all the low-energy conformers gave similar ECD spectra, the absolute configuration of **2** could be unambiguously determined as (2*S*,3*R*,4a*S*,9a*S*,10*S*).

Compound **3** was isolated as orange powder. Its UV spectrum displayed absorption bands at λ_{max} 202, 224, 285 and 400 nm, which were similar to those of alterporriol W.[16] The molecular formula was determined to be $C_{32}H_{26}O_{11}$ by HRESIMS, missing one

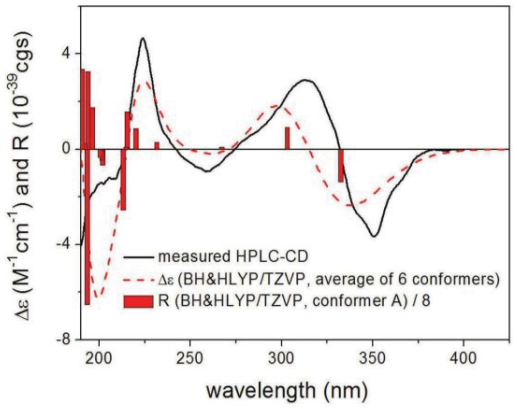

Figure 4. Comparison of the experimental ECD of **2** (black solid) with the Boltzmann-weighted BH&HLYP/TZVP ECD spectra of (2*S*,3*R*,4a*S*,9a*S*,10*S*)-**2** (red dashed) computed for the 6 B3LYP/6-31G(d) in vacuo conformers. Bars represent the computed rotational strength values of the lowest-energy conformer.

Table 2
NMR data of compound **3**[a]

No.	δ_H (*J* in Hz)	δ_C, type	No.	δ_H (*J* in Hz)	δ_C, type
1	8.14, s	130.2, CH	1′	2.51, d (19.2) 2.36, d (19.2)	36.0, CH_2
2		132.0, C	2′		70.2, C
3		159.2, C	3′	3.72, m	71.3, CH
4		n.d.[b]	4′	2.85, m 2.73, m	29.7, CH_2
4a		131.5, C	4′a		144.4, C
5		166.2, C	5′		165.7, C
6	6.66, d (2.6)	106.1, CH	6′	6.87, s	104.3, C
7		166.7, C	7′		165.4, C
8	7.25, d (2.6)	107.0, CH	8′		122.7, C
8a		135.8, C	8′a		125.9, C
9		181.8, C	9′		n.d.
9a		126.0, C	9′a		141.9, C
10		188.8, C	10′		189.4, C
10a		111.5, C	10′a		110.4, C
11	2.41, s	16.9, CH_3	11′	1.19, s	25.0, CH_3
12	3.96, s	56.2, CH_3	12′	3.77, s	56.8, CH_3

[a] Measured in acetone-d_6 (^{1}H at 600 MHz and ^{13}C at 150 MHz).
[b] n.d. = not detected.

oxygen atom compared to alterporriol W. The ^{1}H and ^{13}C NMR data of **3** (Table 2) were closely related to those of alterporriol W,[16] except for the replacement of one oxygenated methine group by a methylene group (δ_C 36.0, δ_H 2.51 and 2.36, CH_2-1′). The HMBC correlations from H_3-11′ (δ_H 1.19, s) to C-2′ (δ_C 70.2), C-3′ (δ_C 71.3) and the methylene CH_2-1′, and in turn from the protons of CH_2-1′ to C-2′, C-3′, C-4′a (δ_C 144.4), C-9′a (δ_C 141.9), indicated that the additional methylene group CH_2-1′ was located at C-1′ in **3**. Thus, compound **3** was elucidated as 1′-dehydroxyalterporriol W, for which the trivial name alterporriol X is proposed. Alterporriol X is a hetero dimer consisting of altersolanol B (**7**) and macrosporin (**10**) subunits which were co-isolated in the present study. This structural assignment was corroborated by interpretation of 2D NMR spectra which were in good agreement with those acquired for altersolanol B and macrosporin, respectively. The absolute configurations at C-2′ and C-3′ in **3** were assumed to be the same as in altersolanol B (**7**) due to their close biogenetic relationship. Due to the 4–8′ biaryl linkage of the anthraquinone-tetrahydroanthraquione dimer, besides the central chirality elements, alterporriol X (**3**) had also axial chirality, which could be determined as (a*R*) on the basis of its similar ECD spectrum to that of the related biaryl natural product alterporriol W having (a*R*) axial chirality.[16]

By comparison of NMR and MS data with the literature, the 13 known compounds were identified as dihydroaltersolanol B (**4**) and C (**5**),[17] altersolanol A (**6**),[18] B (**7**),[19] and N (**8**),[10] 1-hydroxy-3-methoxy-6-methylanthraquinone (**9**),[20] macrosporin (**10**),[21] altechromone A (**11**),[22] alterporriol D (**12**),[18] E (**13**),[18] R (**14**),[9] V (**15**),[23] and W (**16**).[23]

Dihydroaltersolanol C (**5**),[17] altersolanol A (**6**),[17] B (**7**),[17] N (**8**),[10] and alterporriol E (**13**)[17] have been reported to exhibit potent cytotoxicity against L5178Y mouse lymphoma cell line with IC_{50} values in the low micromolar range. However, the new compounds **1–3** showed no significant activity when tested at a dose of 10 μg/mL each.

S. globuliferum is well known for its production of anthraquinone or tetrahydroanthraquinone derivatives including various monomers and dimers. In the present study, fermentation of the titled fungus on solid white bean medium yielded macrosporin (**10**) as an anthraquinone monomer, which gave rise to three anthraquinone homodimers alterporriol R (**14**), V (**15**) and W (**16**), and altersolanol A (**6**) as a tetrahydroanthraquinone monomer, from which two tetrahydroanthraquinone homodimers alterporriol D (**12**) and E (**13**) were detected. In addition, the new heterodimer alterporriol X (**3**) is formed from both macrosporin (**10**) and altersolanol B (**7**) units. *S. globuliferum* was previously cultivated on solid rice medium and yielded tetrahydroanthraquinones, anthraquinones and tetrahydroanthraquinone dimers.[10,17] However, in this study the fermentation of *S. globuliferum* on white beans afforded three new compounds (**1–3**), in addition to some metabolites which were not isolated from the rice culture, including one anthraquinone (**9**), one chromone derivative (**11**) and three anthraquinone dimers (**14–16**), thereby providing evidence for the power of the OSMAC approach.

Acknowledgments

P.P. wants to thank the Manchot Foundation for support. T.K. and A.M. thank the Hungarian National Research Foundation (OTKA K105871) for financial support and the National Information Infrastructure Development Institute (NIIFI 10038) for CPU time.

Supplementary data

Supplementary data (UV, MS and NMR spectra of **1–3** as well as ECD spectrum of **3**) associated with this article can be found, in the online version, at http://dx.doi.org/10.1016/j.tetlet.2016.07.091.

References and notes

1. Aly, A. H.; Debbab, A.; Proksch, P. *Fungal Diversity* **2011**, *50*, 3–19.
2. Debbab, A.; Aly, A. H.; Proksch, P. *Fungal Diversity* **2011**, *49*, 1–12.
3. Elissawy, A. M.; El-Shazly, M.; Ebada, S. S.; Singab, A. B.; Proksch, P. *Mar. Drugs* **2015**, *13*, 1966–1992.
4. Ebrahim, W.; Aly, A. H.; Wray, V.; Proksch, P.; Debbab, A. *Tetrahedron Lett.* **2013**, *54*, 6611–6614.
5. Schiewe, H. J.; Zeeck, A. *J. Antibiot.* **1999**, *52*, 635–642.
6. Bode, H. B.; Bethe, B.; Höfs, R.; Zeeck, A. *ChemBioChem* **2002**, *3*, 619–627.
7. Wheeler, M. M.; Wheeler, D. M. S.; Peterson, G. W. *Phytochemistry* **1975**, *14*, 288–289.
8. Becker, A. M.; Rickards, R. W.; Schmalzl, K. J.; Yick, H. C. *J. Antibiot.* **1978**, *31*, 324–329.
9. Zheng, C.-J.; Shao, C.-L.; Guo, Z.-Y.; Chen, J.-F.; Deng, D.-S.; Yang, K.-L.; Chen, Y.-Y.; Fu, X.-M.; She, Z.-G.; Lin, Y.-C.; Wang, C.-Y. *J. Nat. Prod.* **2012**, *75*, 189–197.
10. Debbab, A.; Aly, A. H.; Edrada-Ebel, R.; Wray, V.; Pretsch, A.; Pescitelli, G.; Kurtan, T.; Proksch, P. *Eur. J. Org. Chem.* **2012**, 1351–1359.
11. Haraguchi, H.; Abo, T.; Fukuda, A.; Okamura, N.; Yagi, A. *Phytochemistry* **1996**, *43*, 989–992.
12. Mishra, P. D.; Verekar, S. A.; Deshmukh, S. K.; Joshi, K. S.; Fiebig, H. H.; Kelter, G. *Lett. Appl. Microbiol.* **2015**, *60*, 387–391.

13. Höller, U.; Gloer, J. B.; Wicklow, D. T. *J. Nat. Prod.* **2002**, *65*, 876–882.
14. Debbab, A.; Aly, A. H.; Edrada-Ebel, R.; Wray, V.; Müller, W. E. G.; Totzke, F.; Zirrgiebel, U.; Schächtele, C.; Kubbutat, M. H. G.; Lin, W. H.; Mosaddak, M.; Hakiki, A.; Proksch, P.; Ebel, R. *J. Nat. Prod.* **2009**, *72*, 626–631.
15. Sun, P.; Huo, J.; Kurtán, T.; Mándi, A.; Antus, S.; Tang, H.; Li, L.; Draeger, S.; Schulz, B.; Krohn, K.; Pan, W.; Yi, Y.; Zhang, W. *Chirality* **2013**, *25*, 141–148.
16. Zhou, X.-M.; Zheng, C.-J.; Chen, G.-Y.; Song, X.-P.; Han, C.-R.; Li, G.-N.; Fu, Y.-H.; Chen, W.-H.; Niu, Z.-G. *J. Nat. Prod.* **2014**, *77*, 2021–2028.
17. Liu, Y.; Marmann, A.; Abdel-Aziz, M. S.; Wang, C. Y.; Müller, W. E. G.; Lin, W. H.; Mándi, A.; Kurtán, T.; Daletos, G.; Proksch, P. *Eur. J. Org. Chem.* **2015**, 2646–2653.
18. Kanamaru, S.; Honma, M.; Murakami, T.; Tsushima, T.; Kudo, S.; Tanaka, K.; Nihei, K.-I.; Nehira, T.; Hashimoto, M. *Chirality* **2012**, *24*, 137–146.
19. Yagi, A.; Okamura, N.; Haraguchi, H.; Abo, T.; Hashimoto, K. *Phytochemistry* **1993**, *33*, 87–91.
20. Boisvert, L.; Brassard, P. *J. Org. Chem.* **1988**, *53*, 4052–4059.
21. Suemitsu, R.; Ueshima, T.; Yamamoto, T.; Yanagawase, S. *Phytochemistry* **1988**, *27*, 3251–3254.
22. Königs, P.; Rinker, B.; Maus, L.; Nieger, M.; Rheinheimer, J.; Waldvogel, S. R. *J. Nat. Prod.* **2010**, *73*, 2064–2066.
23. Chen, B.; Liu, L.; Zhu, X.; Wang, J.; Long, Y.; Jiang, S.; Xu, A.; Lin, Y. *Nat. Prod. Res.* **2015**, *29*, 1212–1216.

2.1a Supplementary data I

Tetrahydroanthraquinone Derivatives from the Mangrove-Derived Endophytic Fungus *Stemphylium globuliferum*

Mariam Moussa[a], Weaam Ebrahim[a,b], Mona El-Neketi[b], Attila Mándi[c], Tibor Kurtán[c], Rudolf Hartmann[d], Wenhan Lin[e], Zhen Liu[a,]*, Peter Proksch[a,]*

[a] *Institute of Pharmaceutical Biology and Biotechnology, Heinrich-Heine-Universität Düsseldorf, Universitätsstrasse 1, 40225 Düsseldorf, Germany*

[b] *Department of Pharmacognosy, Faculty of Pharmacy, Mansoura University, Mansoura 35516, Egypt*

[c] *Department of Organic Chemistry, University of Debrecen, Egyetem tér 1, Debrecen 4032, Hungary*

[d] *Institute of Complex Systems: Strukturbiochemie, Forschungszentrum Juelich, Wilhelm-Johnen-Straße, 52428 Juelich, Germany*

[e] *State Key Laboratory of Natural and Biomimetic Drugs, Peking University, Beijing 100191, China*

*Corresponding authors.

Tel.: +49 211 81 14163; fax: +49 211 81 11923;

e-mail: zhenfeizi0@sina.com (Z. Liu),

proksch@uni-duesseldorf.de (P. Proksch)

Table of Contents

Experimental Section

General Experimental Procedures: Optical rotations were measured with a Perkin-Elmer-241 MC polarimeter. ECD spectra were recorded on a J-810 spectropolarimeter. Solvents were distilled prior to use, and spectral grade solvents were used for spectroscopic measurements. 1D and 2D NMR spectra were recorded with Bruker AVANCE DMX 600 or Bruker ARX 700 NMR spectrometers. Mass spectra were acquired with a Finnigan LCQ Deca mass spectrometer, while HRMSESI spectra were recorded with a FTHRMS-Orbitrap (Thermo-Finnigan) mass spectrometer. HPLC chromatograms were obtained with a Dionex P580 system liked to a photodiode array detector (UVD340S). Routine detection was set at 235, 254, 280, and 340 nm. The analytical column (125 × 4 mm, L × i.d.) was prefilled with Eurosphere-10 C_{18} (Knauer, Germany). Elution was carried out using a gradient of water (adjusted to pH 2 by addition of H_3PO4) and methanol. HPLC separation was carried out using the Lachrom-Merck Hitachi semi-preparative HPLC system (UV detector L-7400; pump L-7100; Eurosphere-100 C_{18}, 300 × 8 mm, Knauer, Germany) at a flow rate of 5.0 mL/min. Column chromatography was conducted using Merck MN Silica gel 60 M (0.04-0.063 mm) and Sephadex LH-20. The isolation progress was monitored with the help of precoated silica gel 60 F254 TLC plates (Merck, Darmstadt, Germany), followed by detection under UV 254 and 365 nm and spraying with anisaldehyde reagent.

Fungal material: The endophytic fungus *Stemphylium globuliferum* was isolated from fresh healthy stems of the mangrove plant *Avicennia marina* (Acanthaceae) adapting standard procedures.[1] The fresh plant was gathered in May 2014 in Hurghada, Egypt. The plant was authenticated by one of the authors (M. E.-N.), and a voucher sample (No. MW140514) was stored in her lab.

Identification of Fungal Culture: The fungus was identified as *S. globuliferum* according to a molecular biological protocol through DNA amplification and sequencing of the ITS region (GenBank accession No. KU140671).[2] A voucher strain (Code AM 1.1) is kept in the Institute

of Pharmaceutical Biology and Biotechnology, Heinrich-Heine University, Düsseldorf, Germany.

Fermentation, Extraction and Isolation: The endophytic fungal strain was cultivated on solid white beans medium prepared by autoclaving 100 g white beans and 100 mL of 3.5% sea salt solution in 1 L Erlenmeyer flask. Fermentation was conducted in 10 flasks for 4 weeks at room temperature under static condition. After the media had been completely covered by the fungus, the flasks were subjected to exhaustive extraction with EtOAc (3 × 500 mL), followed by filtration and subsequent solvent evaporation under reduced pressure. The obtained crude ethyl acetate extract (23.4 g) was fractionated by vacuum liquid chromatography (VLC) on silica gel 60 using a stepwise elution profile of *n*-hexane/EtOAc (100:0 to 0:100) and CH_2Cl_2/MeOH (100:0 to 0:100), where an eluting volume of 1000 mL was used for each step, yielding eighteen fractions (V1–18). Fraction V6 (77.5 mg) was separated on a silica gel column using DCM/MeOH (99:1), to afford seven subfractions (V6Si1–7). Among them, the subfraction V6Si1 was a pure compound **9** (1.5 mg), while the subfraction V6Si3 (40.8 mg) was further purified by semi-preparative HPLC using 60% MeOH/H_2O to give compounds **11** (0.7 mg), **15** (1.9 mg) and **16** (1.5 mg). The VLC fraction V8 (85.9 mg) was refractionated over a Sephadex LH-20 column (100 × 5 cm) using 100% acetone to afford nine subfractions (V8S1–9). The subfraction V8S2 was further purified using semi-preparative RP-HPLC with 60% MeOH/H_2O as mobile phase, to yield compounds **3** (0.4 mg), **4** (0.5 mg), **5** (0.6 mg), **8** (0.8 mg) and **14** (6.3 mg). Fraction V9 (32.5mg) was subjected to semi-preparative RP-HPLC with 55% MeOH/H_2O as eluting system to afford **7** (1.2 mg). Fraction V11 was separated on a Sephadex LH-20 column (80 × 4 cm) using 100% MeOH as an eluting solvent to yield 12 subfractions (V11S1–12). The subfraction V11S7 afforded compound **13** as a pure red precipitate (42.7 mg), whereas, the filtrate was loaded on a Sephadex LH-20 column (100 × 2.5 cm) to afford 7 subfractions (V11S7S1–7). Compound **2** was obtained as a pure precipitate (61.0 mg) from the subfraction V11S7S2. Moreover, the subfraction V11S8 (142.5 mg) was subjected to a

Sephadex LH-20 (100 × 2.5 cm) using 100% acetone to afford 12 subfractions (V11S8S1–12), among which the subfraction V11S8S9 yielded the pure compound **12** (18.7 mg) by precipitation. The subfraction V11S8S2 (43.5 mg) was further purified by semi-preparative RP-HPLC using 50% MeOH/H_2O as mobile phase, to afford compounds **1** (10.5 mg) and **6** (6.7 mg). Fraction V14 afforded compound **10** as a precipitate (17.0 mg).

*Altersolanol Q (**1**)*: brown solid; $[\alpha]_D^{20}$ –3.5 (*c* 0.70, MeOH); UV (MeOH) λ_{max}: 224, 268 and 334 nm; ^{1}H and ^{13}C NMR data see **Table 1**; HRESIMS $[M+Na]^+$ *m/z* 331.1152 (calcd. for $C_{16}H_{20}NaO_6$, 331.1152).

*10-Methoxyaltersolanol Q (**2**)*: brown solid; $[\alpha]_D^{20}$ –4.9 (*c* 0.70, MeOH); UV (MeOH) λ_{max}: 220, 272 and 336 nm; ECD (MeCN, λ [nm] (Δε), $c = 2.33\times10^{-4}$ M): 367sh (–1.18), 350 (–3.66), 340sh (–2.58), 312 (2.90), 283sh (0.58), 258 (–0.92), 224 (4.65), 209sh (–1.24); ^{1}H and ^{13}C NMR data see **Table 1**; HRESIMS $[M+Na]^+$ *m/z* 345.1309 (calcd. for $C_{17}H_{22}NaO_6$, 345.1309).

*Alterporriol X (**3**)*: orange powder; $[\alpha]_D^{20}$ –80.7 (*c* 0.09, MeOH); UV (MeOH) λ_{max}: 202, 224, 285 and 400 nm; ECD (MeCN, λ [nm] (Δε), $c = 8.53\times10^{-5}$ M): 458 (1.25), 386 (–1.50), 324sh (–1.50), 303sh (–2.07), 286 (–4.36), 262 (5.10), 231 (6.12), 217 (–8.15); ^{1}H and ^{13}C NMR data see **Table 2**; HRESIMS $[M+H]^+$ *m/z* 587.1547 (calcd. for $C_{32}H_{27}O_{11}$, 587.1548).

Computational Section: Mixed torsional/low-mode conformational searches were carried out by means of the Macromodel 9.9.223 software[3] using the Merck Molecular Force Field (MMFF) with an implicit solvent model for $CHCl_3$ applying a 21 kJ/mol energy window. Geometry reoptimizations of the resultant conformers [B3LYP/6-31G(d) level *in vacuo* and B97D/TZVP[4,5] with PCM solvent model for MeCN] and TDDFT calculations were performed with Gaussian 09 package[6] using various functionals (B3LYP, BH&HLYP, PBE0) and the TZVP basis set. ECD spectra were generated from the sum of Gaussians[7] with 3000 cm^{-1} half-height width (corresponding to ca. 15 nm at 225 nm), using dipole-velocity-computed rotational strengths. Boltzmann distributions were estimated from the ZPVE-corrected B3LYP/6-31G(d)

energies in the gas-phase calculations and from the B97D/TZVP energies in the PCM model ones. The MOLEKEL[8] software package was used for visualization of the results.

Cytotoxicity Assay: Cytotoxicity was evaluated against the L5178Y mouse lymphoma cell line using the MTT assay as described before.[9] All experiments were carried out in triplicate and repeated three times. Kahalalide F was used as positive control and media with 0.1% DMSO was included as negative control.

References

1. Kjer, J.; Debbab, A.; Aly, A. H.; Proksch, P. *Nat. Protoc.* **2010**, *5,* 479-90.
2. Ebrahim, W.; El-Neketi, M.; Lewald L. I.; Orfali, R. S.; Lin, W. H.; Rehberg, N.; Kalscheuer, R.; Daletos, G.; Proksch, P. *J. Nat. Prod.* **2016**, *79*, 914-922.
3. MacroModel, Schrödinger LLC, **2012**. http://www.schrodinger.com/MacroModel.
4. Grimme, S. *J. Comput. Chem.* **2006**, *27*, 1787−1799.
5. Sun, P.; Xu, D. X.; Mándi, A.; Kurtán, T.; Li, T. J.; Schulz, B.; Zhang, W. *J. Org. Chem.* **2013**, *78*, 7030−7047.
6. Frisch, M. J.; Trucks, G. W.; Schlegel, H. B.; Scuseria, G. E.; Robb, M. A.; Cheeseman, J. R.; Scalmani, G.; Barone, V.; Mennucci, B.; Petersson, G. A.; Nakatsuji, H.; Caricato, M.; Li, X.; Hratchian, H. P.; Izmaylov, A. F.; Bloino, J.; Zheng, G.; Sonnenberg, J. L.; Hada, M.; Ehara, M.; Toyota, K.; Fukuda, R.; Hasegawa, J.; Ishida, M.; Nakajima, T.; Honda, Y.; Kitao, O.; Nakai, H.; Vreven, T.; Montgomery, J. A. Jr.; Peralta, J. E.; Ogliaro, F.; Bearpark, M.; Heyd, J. J.; Brothers, E.; Kudin, K. N.; Staroverov, V. N.; Kobayashi, R.; Normand, J.; Raghavachari, K.; Rendell, A.; Burant, J. C.; Iyengar, S. S.; Tomasi, J.; Cossi, M.; Rega, N.; Millam, J. M.; Klene, M.; Knox, J. E.; Cross, J. B.; Bakken, V.; Adamo, C.; Jaramillo, J.; Gomperts, R.; Stratmann, R. E.; Yazyev, O.; Austin, A. J.; Cammi, R.; Pomelli, C.; Ochterski, J. W.; Martin, R. L.; Morokuma, K.; Zakrzewski, V. G.; Voth, G. A.; Salvador, P.; Dannenberg, J. J.; Dapprich, S.; Daniels, A. D.; Farkas, O.; Foresman, J. B.; Ortiz, J. V.;

Cioslowski, J.; Fox, D. J. Gaussian 09, Revision B.01, **2010**, Gaussian, Inc., Wallingford CT.

7. Stephens, P. J.; Harada, N. *Chirality* **2010**, *22*, 229−233.
8. Varetto, U. MOLEKEL 5.4., **2009**, Swiss National Supercomputing Centre: Manno, Switzerland.
9. Ashour, M.; Edrada, R.; Ebel, R.; Wray, V.; Wätjen, W.; Padmakumar, K.; Müller, W. E. G.; Lin, W. H.; Proksch, P. *J. Nat. Prod.* **2006**, *69,* 1547-1553.

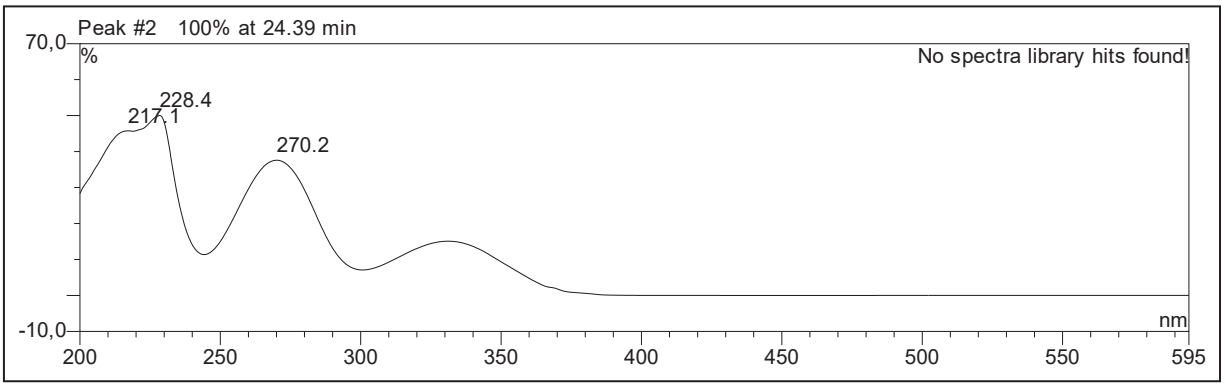

S1. UV spectrum of compound **1**.

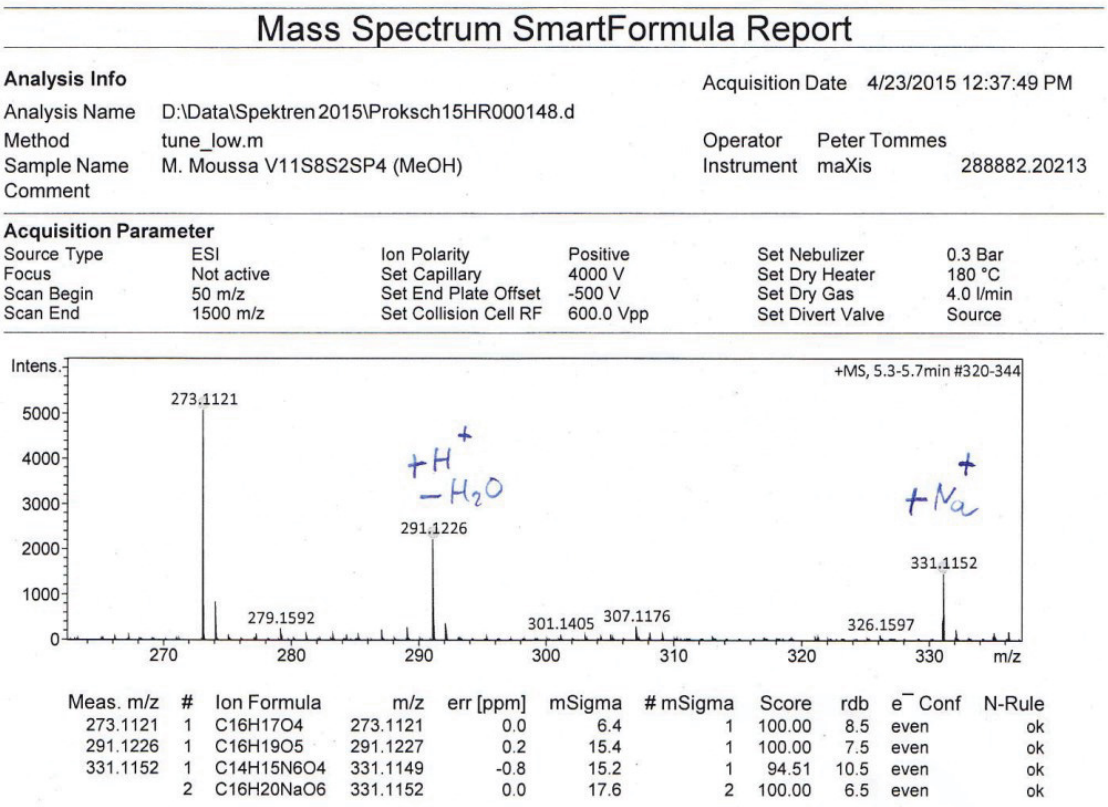

S2. HRESIMS spectrum of compound **1**.

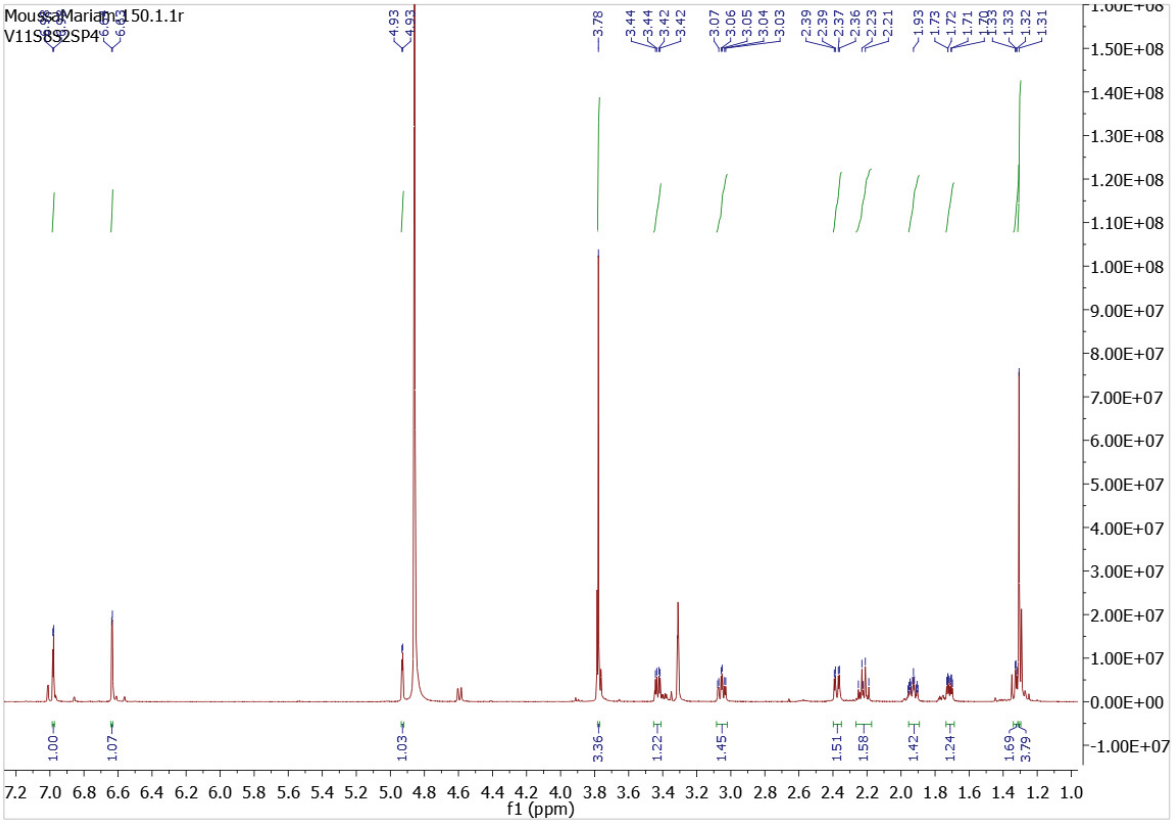

S3.[1]H NMR (600 MHz, MeOD) spectrum compound **1**.

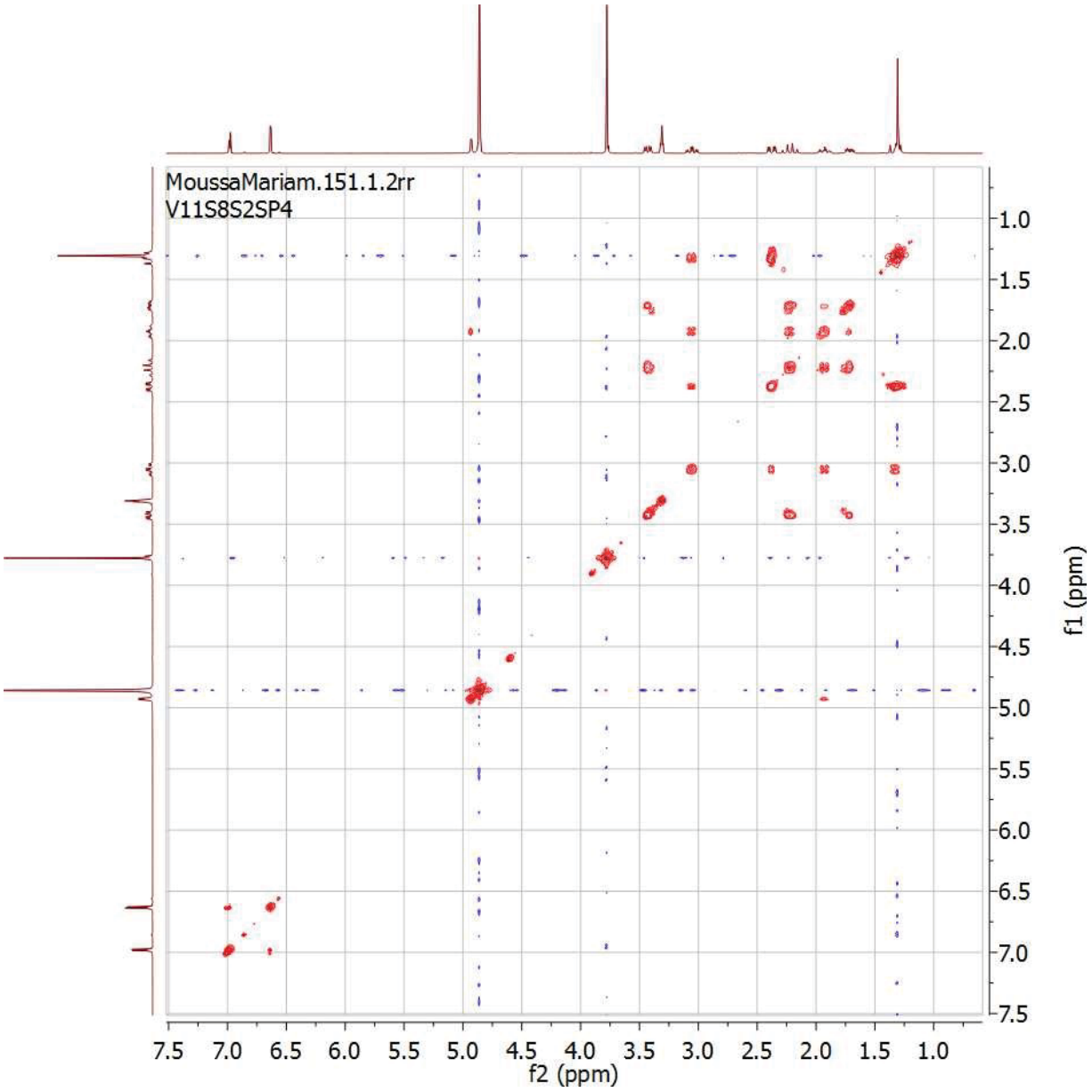

S4. ^{1}H-^{1}H COSY (600 MHz, MeOD) spectrum of compound **1**.

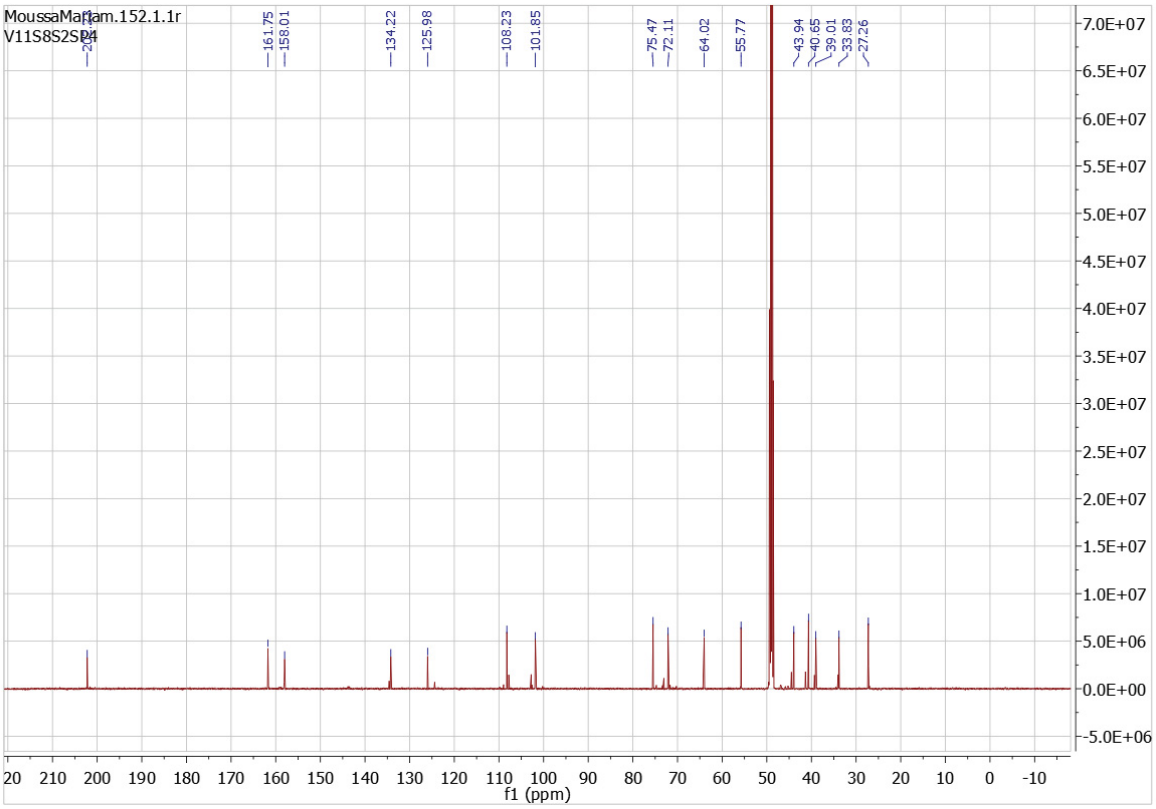

S5. ^{13}C NMR (150 MHz, MeOD) spectrum of compound **1**.

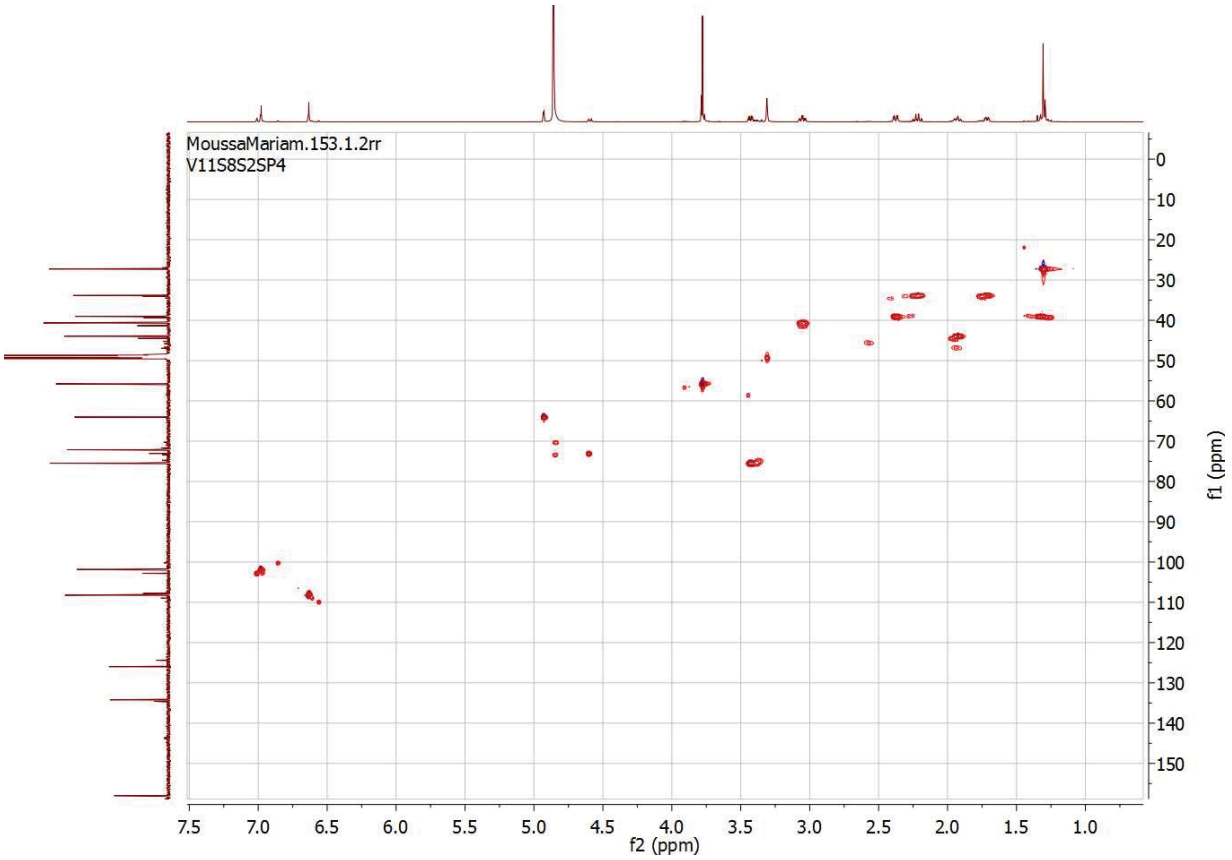

S6. HSQC (600 and 150 MHz, MeOD) spectrum of compound **1**.

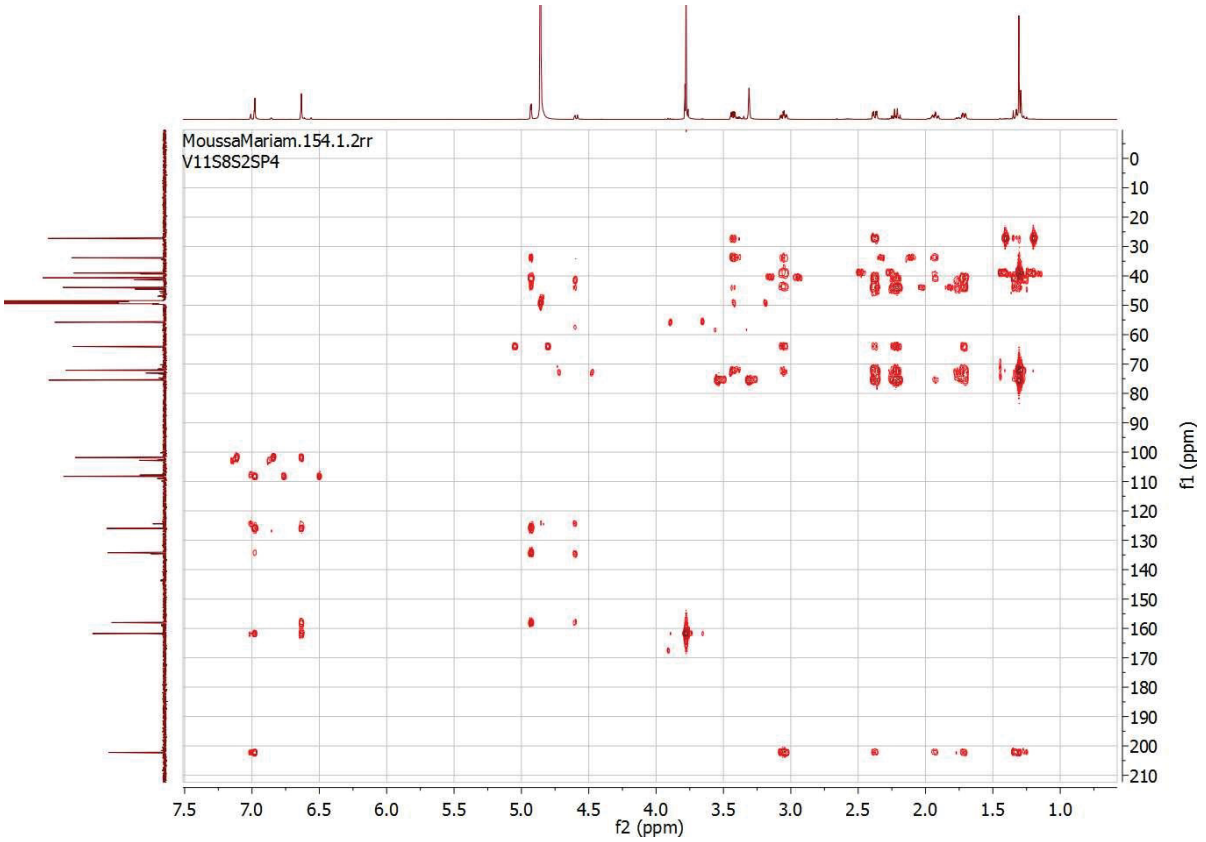

S7. HMBC (600 and 150 MHz, MeOD) spectrum of compound **1**.

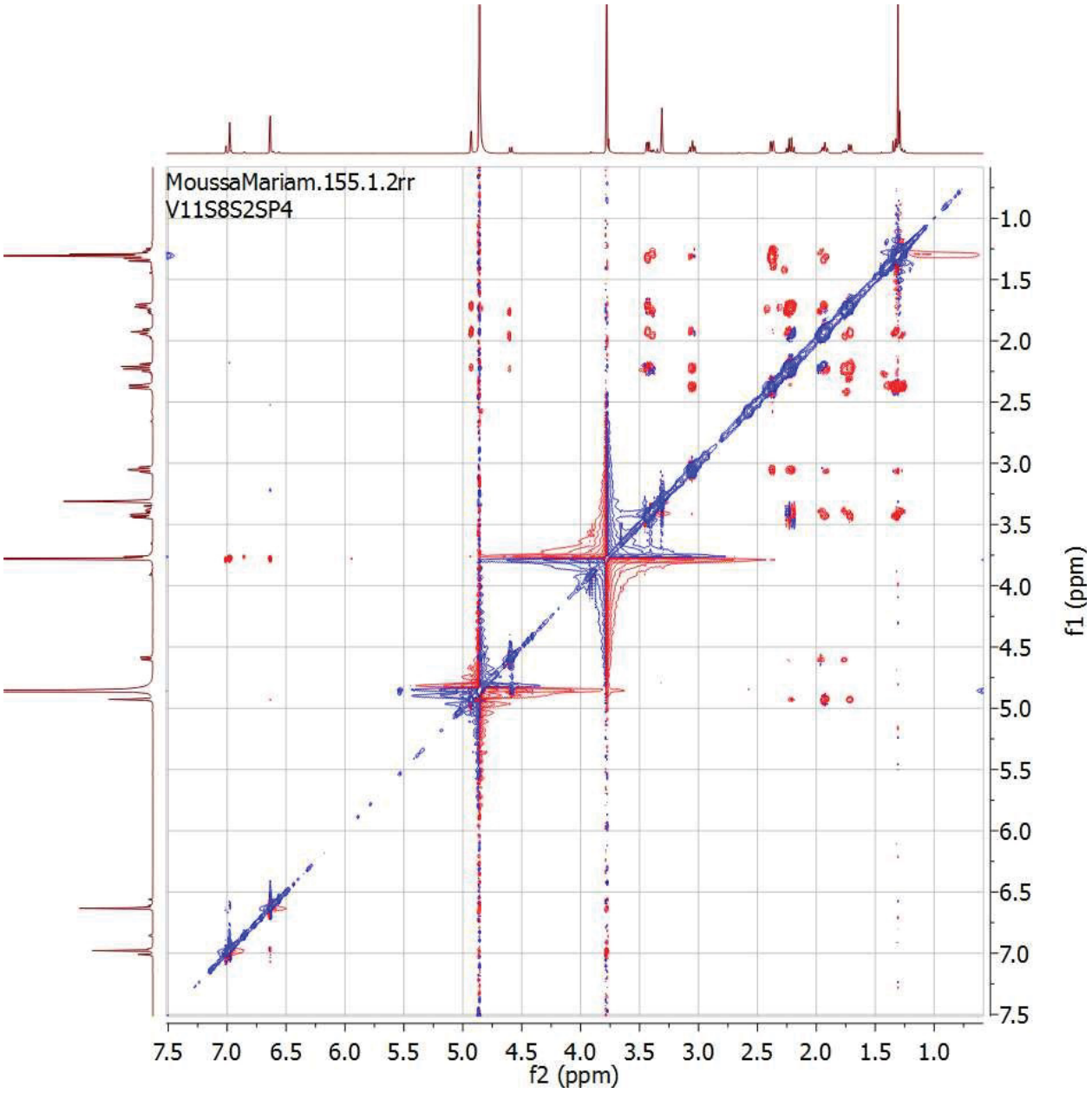

S8. ROESY (600 MHz, MeOD) spectrum of compound **1**.

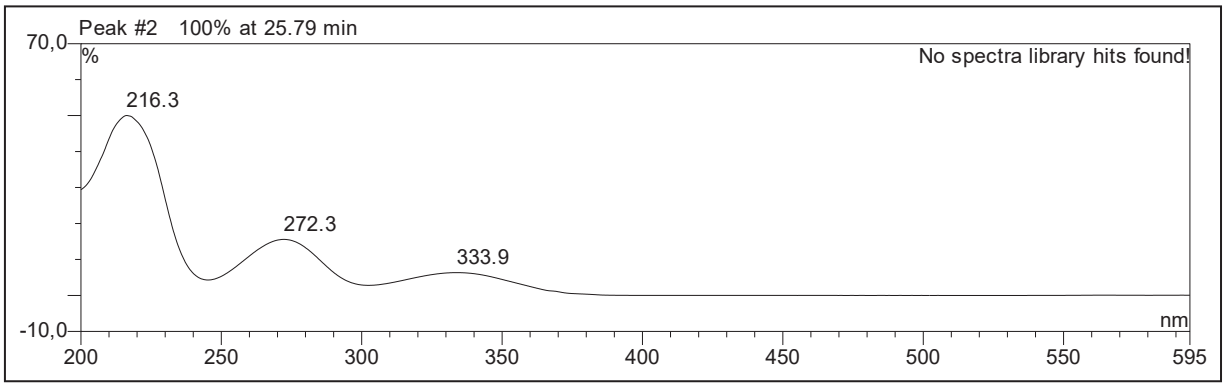

S9. UV spectrum of compound **2**.

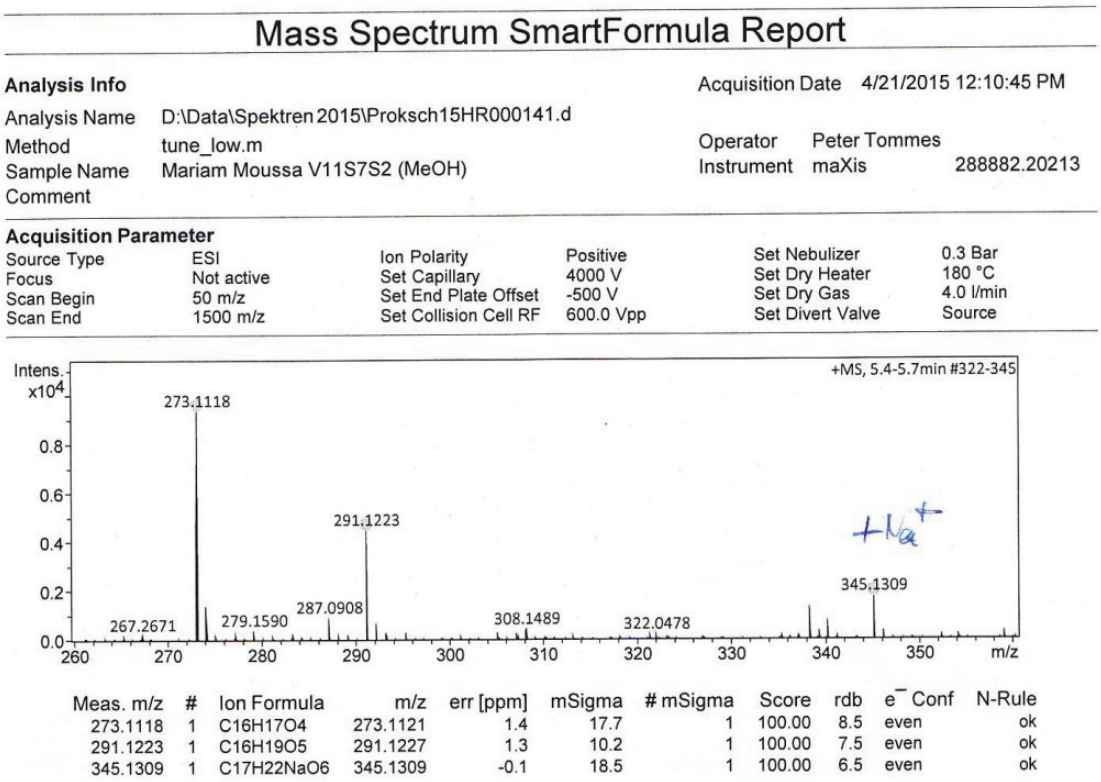

S10. HRESIMS spectrum of compound **2**.

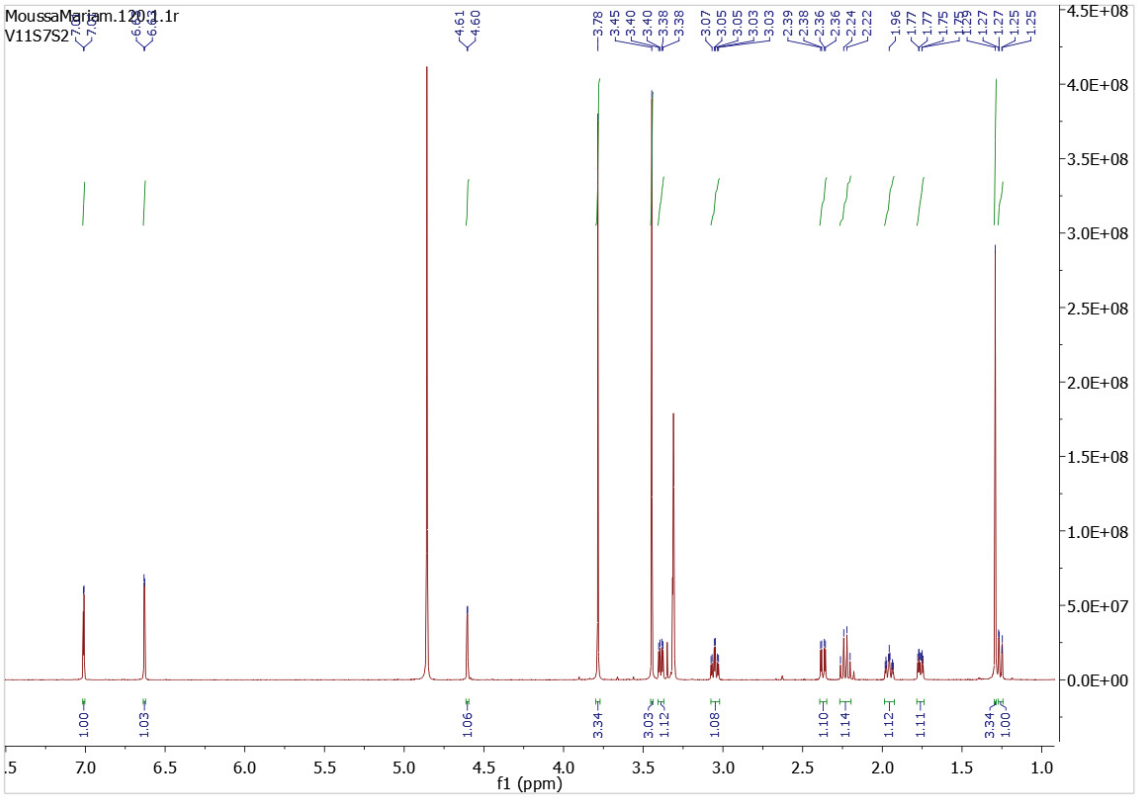

S11. [1]H NMR (600 MHz, MeOD) spectrum of compound **2**.

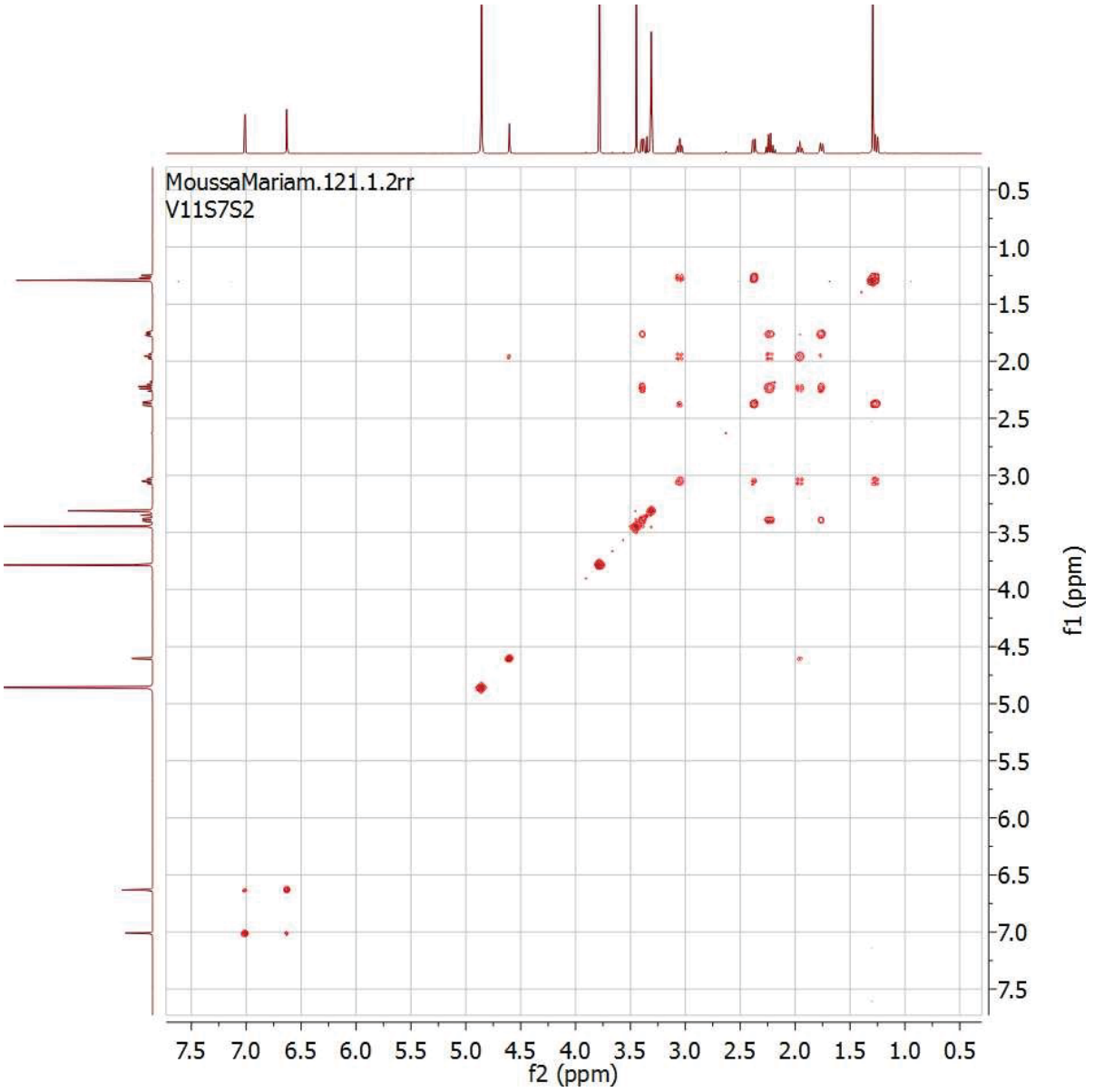

S12. ^{1}H-^{1}H COSY (600 MHz, MeOD) spectrum of compound **2**.

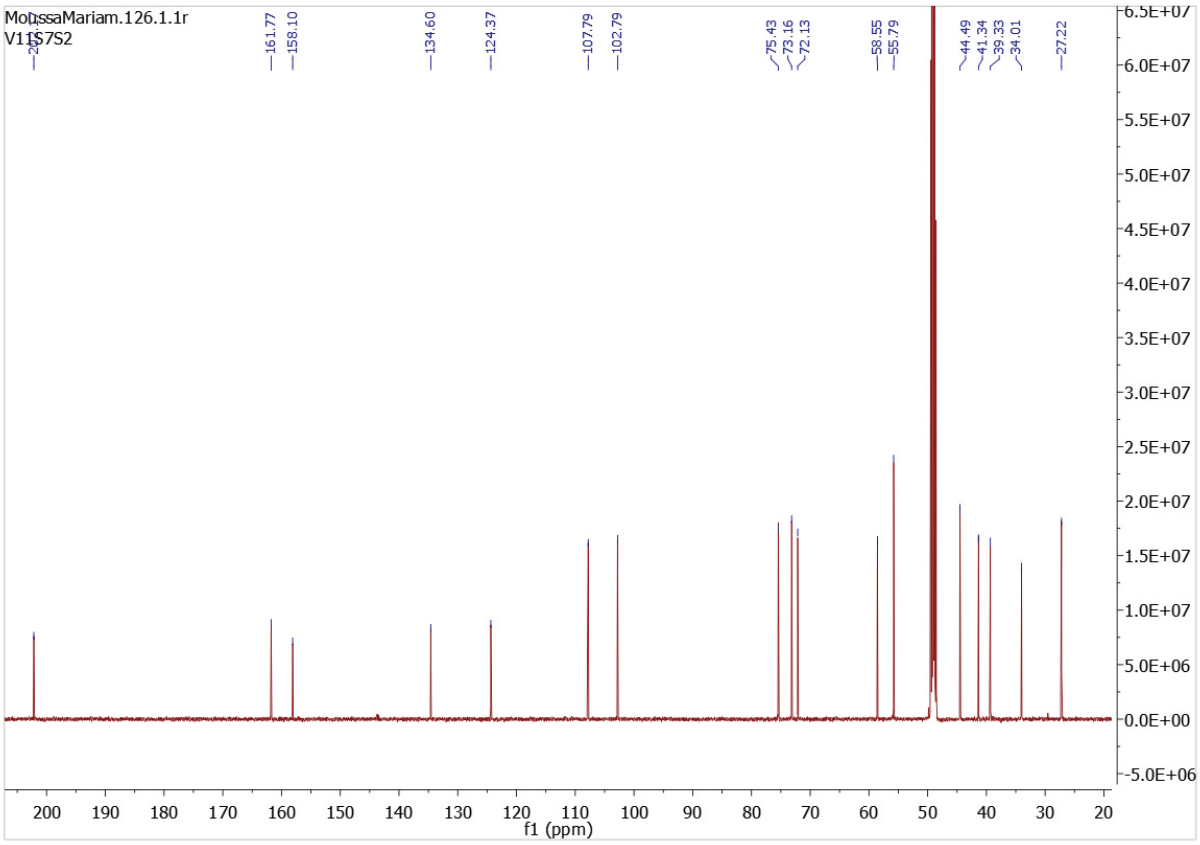

S13. ^{13}C NMR (150 MHz, MeOD) spectrum of compound **2**.

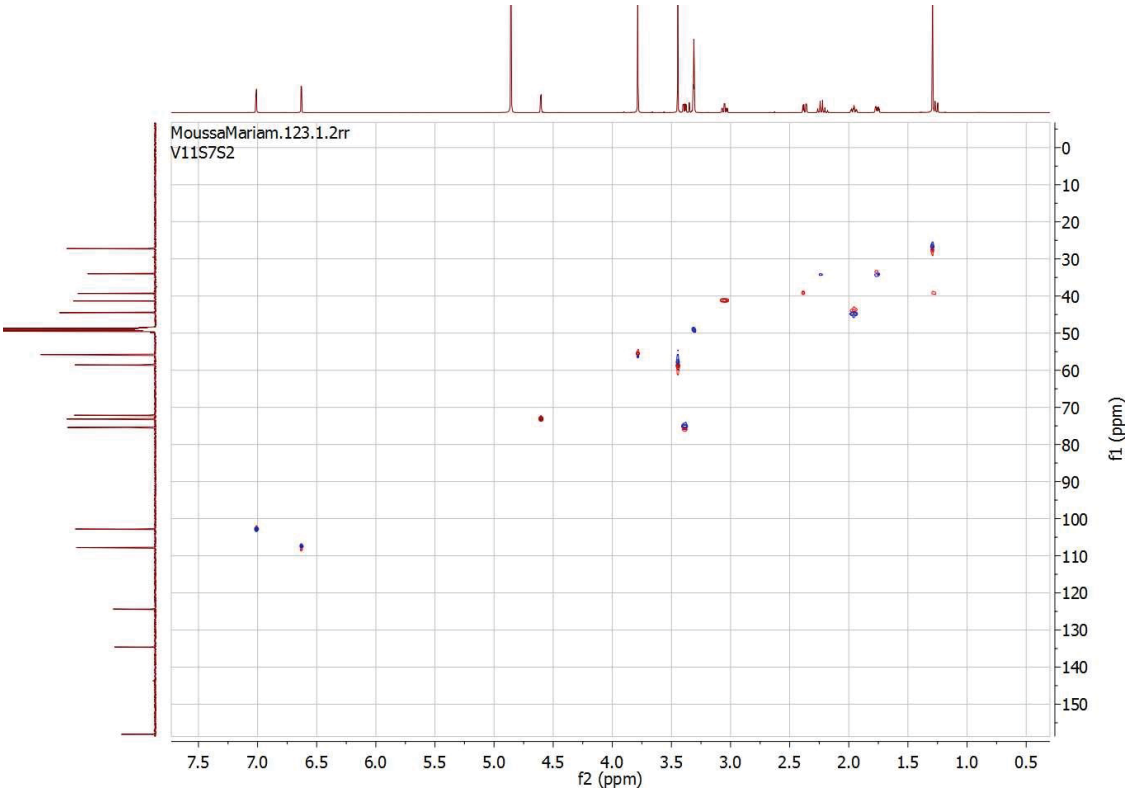

S14. HSQC (600 and 150 MHz, MeOD) spectrum of compound **2**.

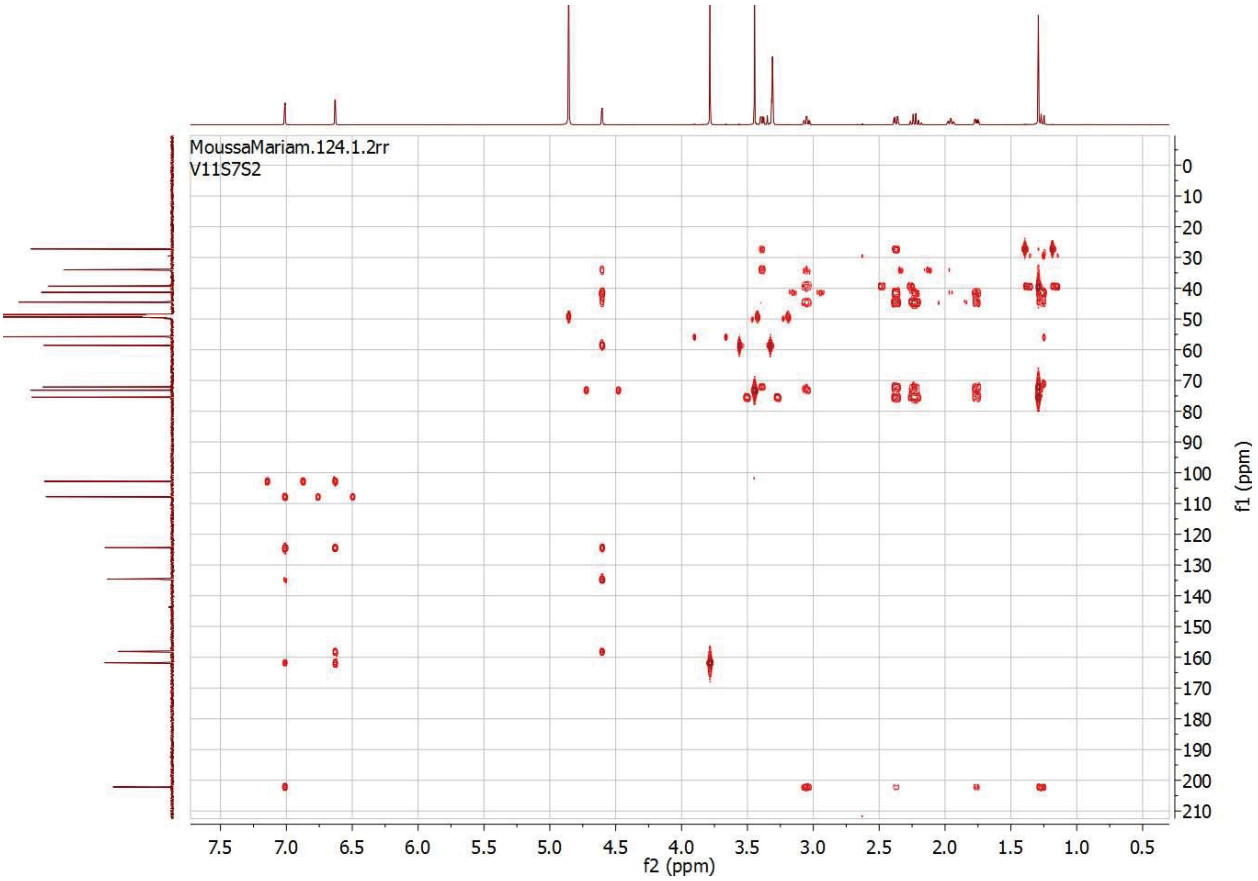

S15. HMBC (600 and 150 MHz, MeOD) spectrum of compound **2**.

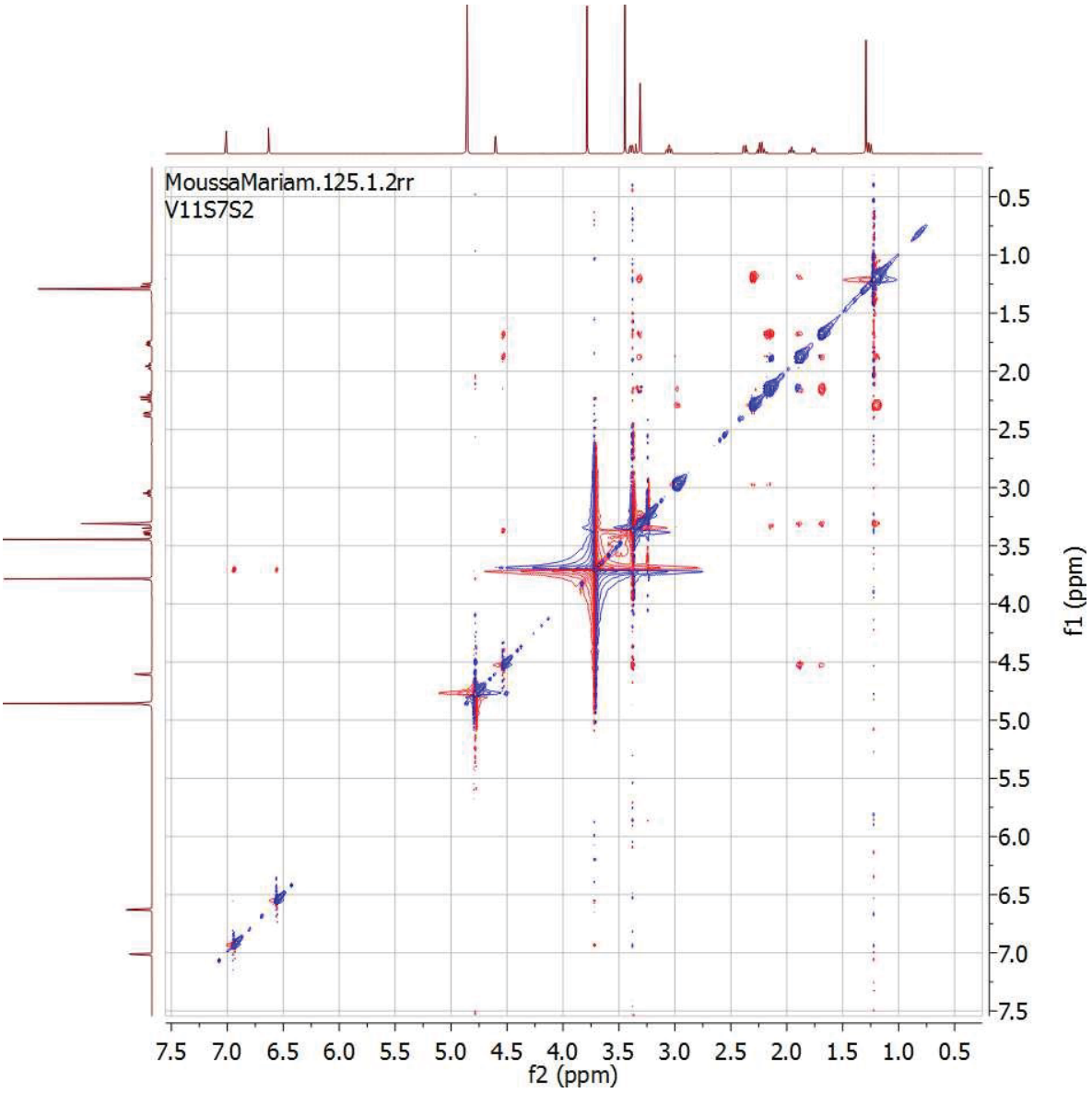

S16. ROESY (600 MHz, MeOD) spectrum of compound **2**.

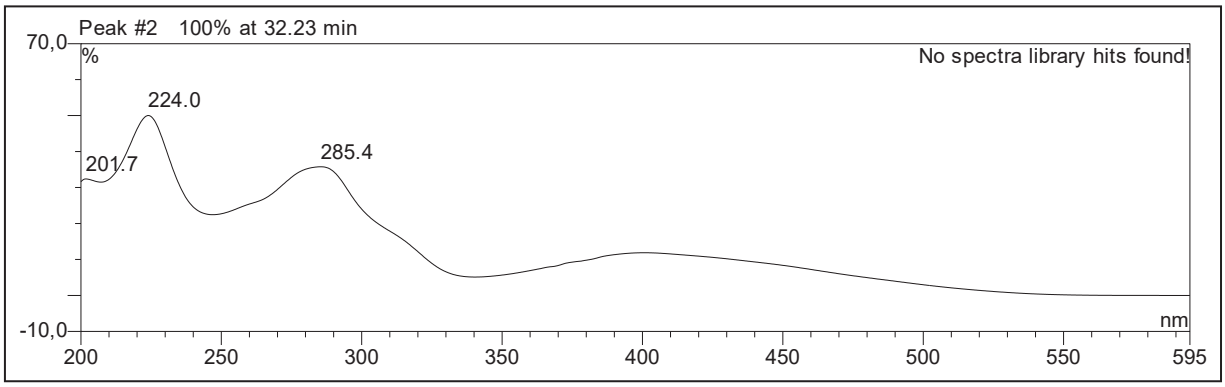

S17. UV spectrum of compound **3**.

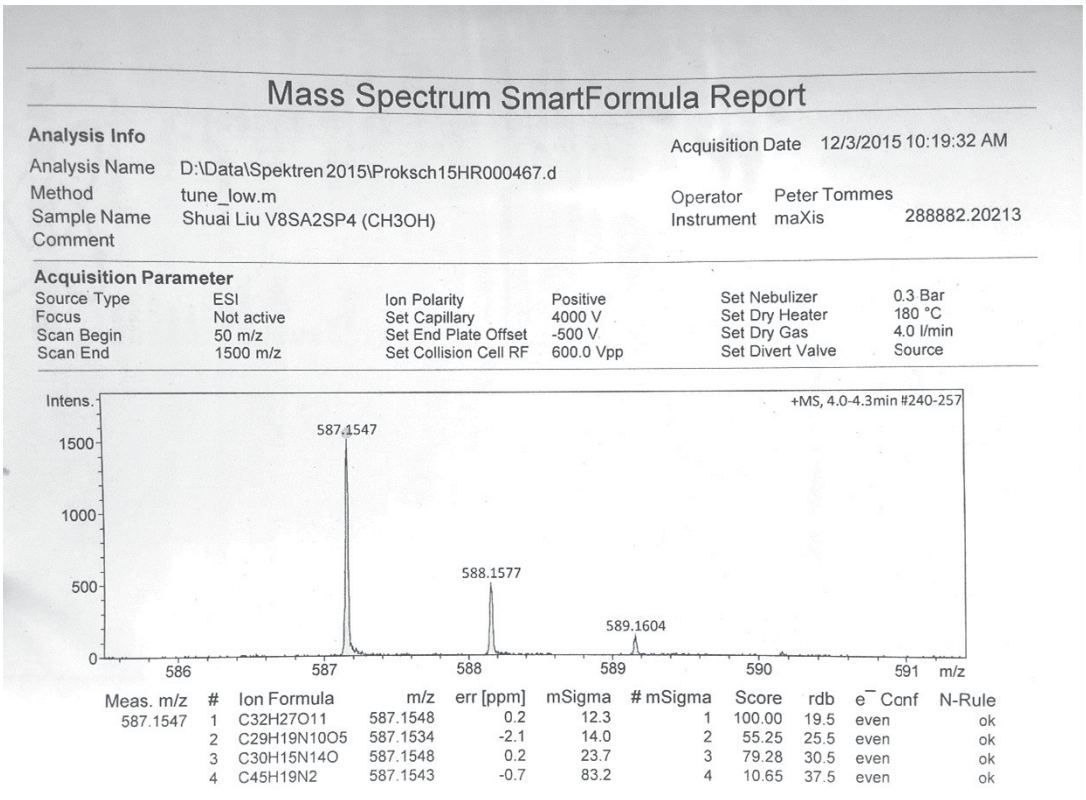

S18. HRESIMS spectrum of compound **3**.

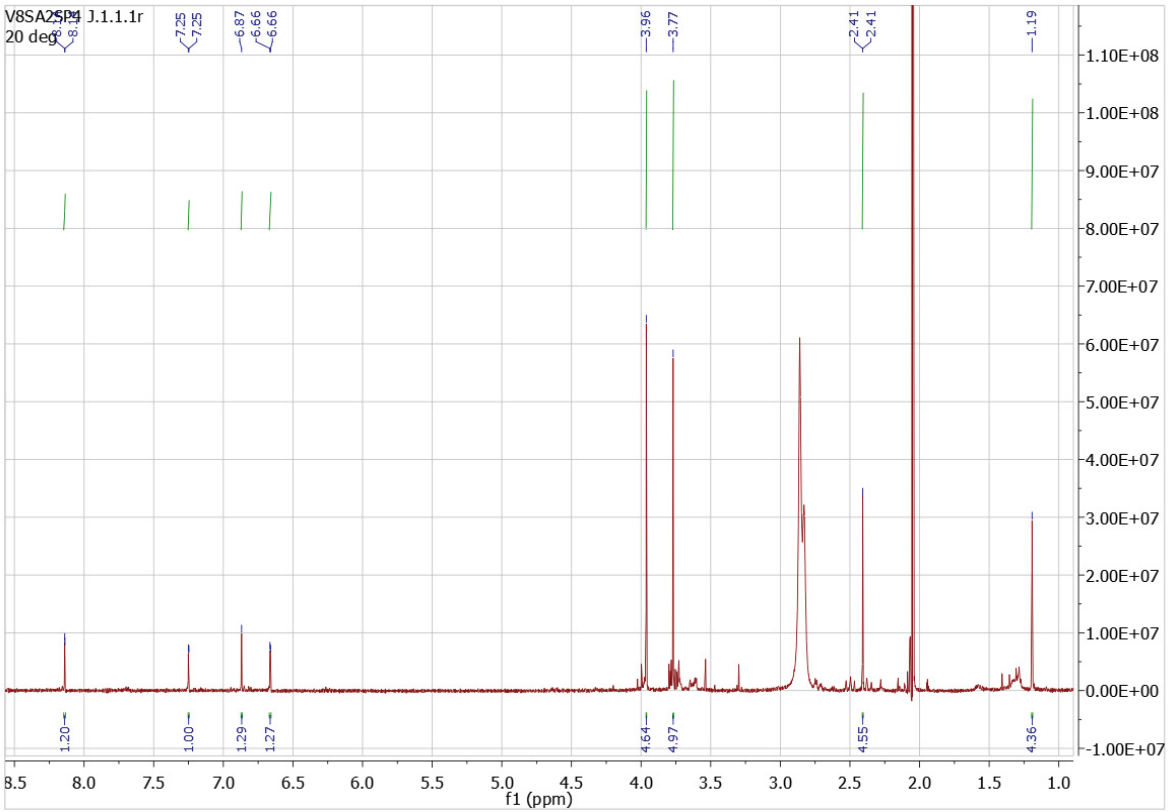

S19. ^{1}H NMR (700 MHz, acetone-d_6) spectrum of compound **3**.

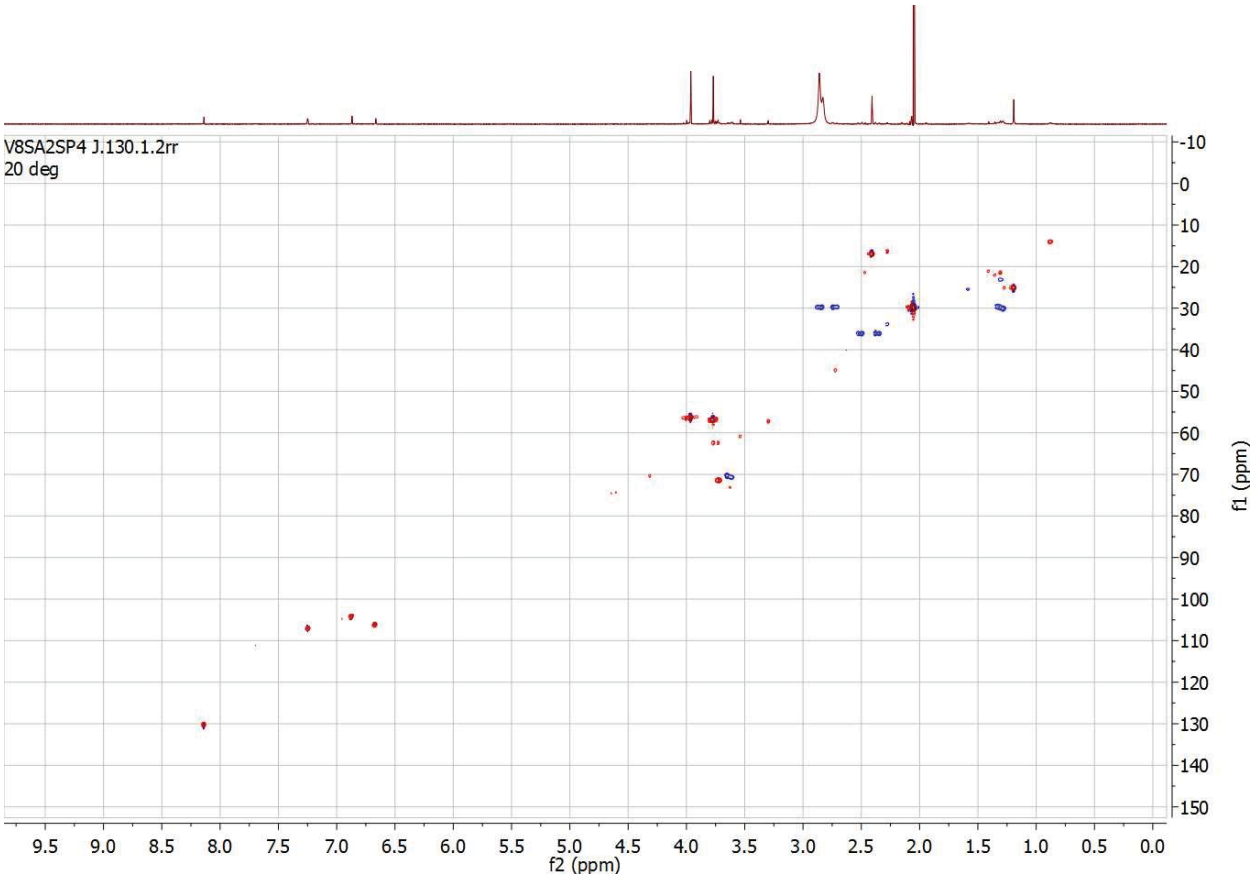

S20. HSQC (700 and 175 MHz, acetone-d_6) spectrum of compound **3**.

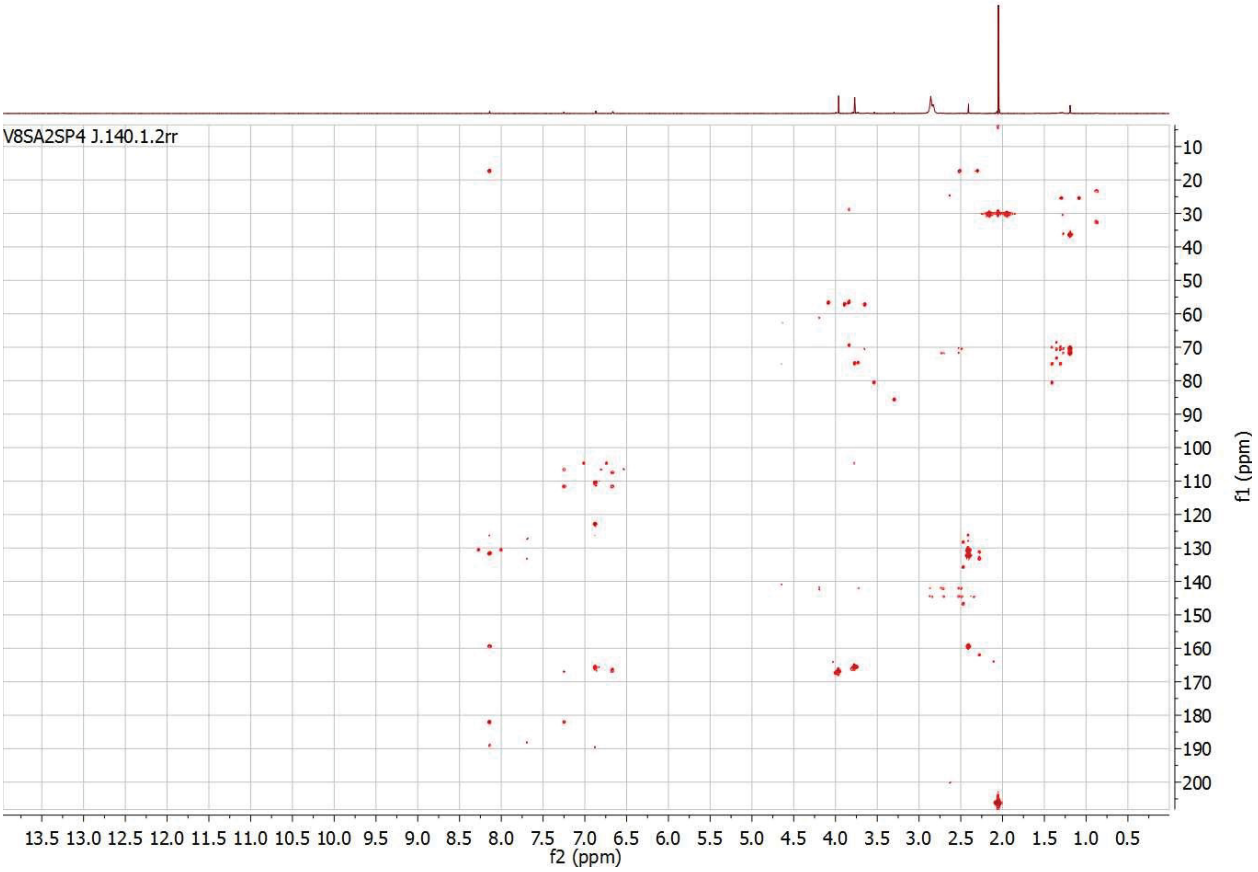

S21. HMBC (700 and 175 MHz, acetone-d_6) spectrum of compound **3**.

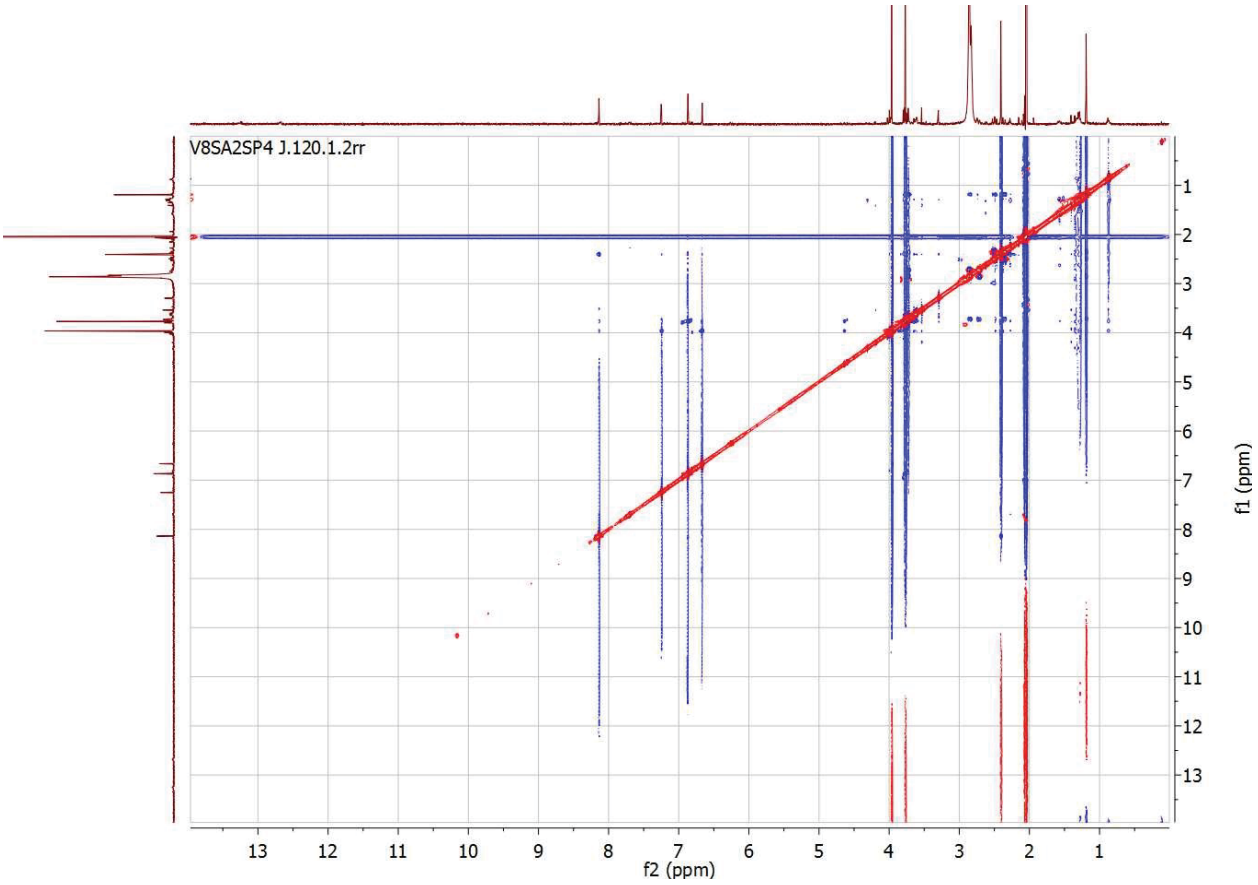

S22. ROESY (700 MHz, acetone-d_6) spectrum of compound **3**.

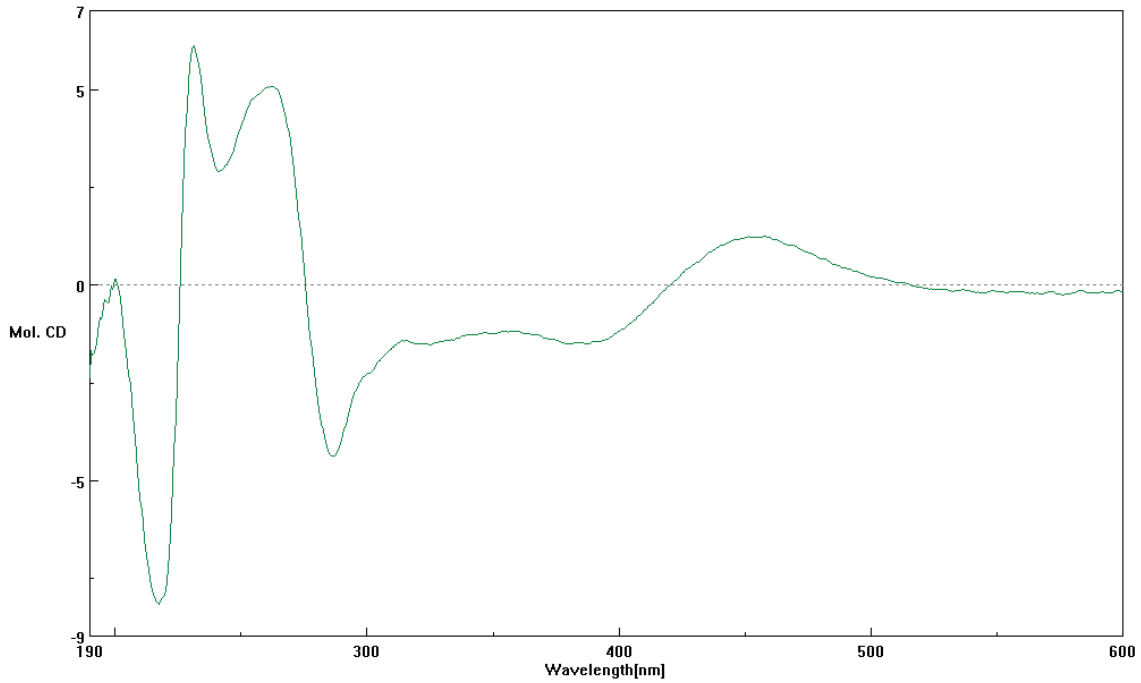

S23. ECD spectrum of compound **3** in acetonitrile.

2.2 Publication II

Title

"*Co-culture of the fungus Fusarium tricinctum with Streptomyces lividans induces production of cryptic naphthoquinone dimers*"

Published in: *RSC (Royal Society of Chemistry) Advances*

Impact factor: 3.049

Personal contribution: 80%, first authorship, performing the laboratorial work, literature research and most of the manuscript writing

.

RSC Advances

PAPER

View Article Online
View Journal | View Issue

Cite this: *RSC Adv.*, 2019, **9**, 1491

Co-culture of the fungus *Fusarium tricinctum* with *Streptomyces lividans* induces production of cryptic naphthoquinone dimers†

Mariam Moussa,[a] Weaam Ebrahim,[ab] Michele Bonus,[c] Holger Gohlke,[cd] Attila Mándi,[e] Tibor Kurtán,[e] Rudolf Hartmann,[f] Rainer Kalscheuer,[a] Wenhan Lin,[g] Zhen Liu[*a] and Peter Proksch[*a]

Co-cultivation of the endophytic fungus *Fusarium tricinctum* with *Streptomyces lividans* on solid rice medium led to the production of four new naphthoquinone dimers, fusatricinones A–D (**1–4**), and a new lateropyrone derivative, dihydrolateropyrone (**5**), that were not detected in axenic fungal controls. In addition, four known cryptic compounds, zearalenone (**7**), (−)-citreoisocoumarin (**8**), macrocarpon C (**9**) and 7-hydroxy-2-(2-hydroxypropyl)-5-methylchromone (**10**), that were likewise undetectable in extracts from fungal controls, were obtained from the co-culture extracts. The known antibiotically active compound lateropyrone (**6**), the depsipeptides enniatins B (**11**), B1 (**12**) and A1 (**13**), and the lipopeptide fusaristatin A (**14**), that were present in axenic fungal controls and in co-culture extracts, were upregulated in the latter. The structures of the new compounds were elucidated by 1D and 2D NMR spectra as well as by HRESIMS data. The relative and absolute configuration of dihydrolateropyrone (**5**) was elucidated by TDDFT-ECD calculations.

Received 1st November 2018
Accepted 2nd January 2019

DOI: 10.1039/c8ra09067j

rsc.li/rsc-advances

Introduction

Cultivating microorganisms under axenic laboratory conditions fails to resemble the natural environment where these microbes are subjected to intense microbial competition. Therefore naturally occurring stimulants and signal molecules that are involved in chemical communication and antagonism between different microbes are absent, which may result in silencing biosynthetic gene clusters and in simplified metabolite patterns.[1,2] The endophytic fungus *Fusarium tricinctum* has already been well investigated with regard to its natural products.[3–5] Applying the OSMAC (One Strain MAny Compounds) approach on cultures of this fungus resulted in the accumulation of new bioactive secondary metabolites such as fusarielin congeners[3] and in an enhanced production of enniatin derivatives.[4] Enniatins are known for their anti-cancer, anti-HIV as well as for their antibacterial activities.[5–7] Enniatins A–C (named fusafungin) were even once available on the drug-market as a local antibiotic for the treatment of respiratory infections. However, due to undesired side effects this approval has meanwhile been withdrawn.[8]

Previous co-cultivation experiments with *F. tricinctum* focused on *Bacillus subtilis* as a prokaryotic antagonist. Co-culture of both microbes on solid rice medium resulted in a dramatically enhanced (up to 80-fold) accumulation of several fungal metabolites including enniatins, the polyketide lateropyrone and the lipopeptide fusaristatin A.[5] Whereas all of the latter compounds were also observed in axenic fungal controls (albeit at much lower concentrations), the co-cultures yielded several additional cryptic metabolites such as macrocarpon C, (−)-citreoisocoumarinol, and (−)-citreoisocoumarin.[5]

Previous experiments also indicated that fungi when co-cultured with different bacteria respond through accumulation of different cryptic metabolites. For example, treatment of the fungus *Chaetomium* sp. with autoclaved cultures of *Pseudomonas aeruginosa* yielded new butenolide derivatives,[9] whereas co-culture of the same fungus with live cultures of *B. subtilis* yielded new shikimic acid derivatives.[10]

[a]*Institute of Pharmaceutical Biology and Biotechnology, Heinrich-Heine-Universität Düsseldorf, Universitätsstrasse 1, 40225 Düsseldorf, Germany. E-mail: zhenfeizi0@sina.com; proksch@uni-duesseldorf.de*

[b]*Department of Pharmacognosy, Faculty of Pharmacy, Mansoura University, Mansoura 35516, Egypt*

[c]*Institute of Pharmaceutical and Medicinal Chemistry, Heinrich-Heine-Universität Düsseldorf, Universitätsstrasse 1, 40225 Düsseldorf, Germany*

[d]*John von Neumann Institute for Computing (NIC), Jülich Supercomputing Centre (JSC), Institute for Complex Systems – Structural Biochemistry (ICS-6), Forschungszentrum Jülich GmbH, Wilhelm-Johnen-Straße, 52425 Jülich, Germany*

[e]*Department of Organic Chemistry, University of Debrecen, Egyetem tér 1, Debrecen 4032, Hungary*

[f]*Institute of Complex Systems – Structural Biochemistry, Forschungszentrum Jülich GmbH, Wilhelm-Johnen-Straße, 52428 Jülich, Germany*

[g]*State Key Laboratory of Natural and Biomimetic Drugs, Peking University, Beijing 100191, China*

† Electronic supplementary information (ESI) available: MS, 1D and 2D NMR spectra of compounds **1–5**. See DOI: 10.1039/c8ra09067j

Here we have studied the influence of *Streptomyces lividans* on accumulation of natural products by *F. tricinctum*. *S. lividans* is known both as a plant-endophyte[11] or as a soil-bacterium.[12,13] Co-cultivation of *F. tricinctum* and *S. lividans* resulted in the accumulation of several new compounds, the dimeric naphthoquinones (**1–4**) and dihydrolateropyrone (**5**), that were not detected in axenic fungal controls (Fig. 1). In addition, several known metabolites such as enniatin derivatives (**11–13**) showed an enhanced accumulation in the co-cultures. Structure elucidation of the new compounds by one- and two-dimensional NMR, HRMS, ECD and quantum chemical calculations is discussed.

Results and discussion

The EtOAc extracts of both axenic fungal cultures and co-cultures resulting from mixed fermentation of *F. tricinctum* and *S. lividans* on solid rice medium were analyzed by HPLC. When fermented axenically on solid rice medium containing liquid YM medium, the fungus accumulates a complex pattern of bioactive metabolites consisting of several enniatines (**11–13**), polyketides (*e.g.* lateropyrone, **6**) and lipopeptides (*e.g.* fusaristatin A, **14**). By comparison of the chromatograms, a dramatic shift in the metabolic profile of the co-cultures compared to the axenic fungal or bacterial controls was obvious. These changes are presented in Table 1 indicating a pronounced (up to 12-fold) upregulation of constitutively present metabolites and induction of several cryptic compounds. Chromatographic workup of the co-culture extracts yielded five new compounds (**1–5**) that were not detected in either fungal or bacterial axenic controls.

Table 1 Yield of induced metabolites per flask of co-culture of *F. tricinctum* and *S. lividans* ($n = 6$) *vs.* axenic controls of *F. tricinctum* ($n = 4$)

Compound	Fungal control (mg)	Co-culture (mg)	Increase (fold)
1	n.d.[a]	7.67 ± 0.1	
2	n.d.	+[c]	
3	n.d.	+	
4	n.d.	+	
5	n.d.	+	
6	1.3 ± n.a.[b]	17.0 ± 0.8	12.5
7	n.d.	+	
8	n.d.	12.5 ± 10.4	
9	n.d.	+	
10	n.d.	+	
11	250.7 ± 50.2	868.9 ± 38.0	3.5
12	203.8 ± 31.8	459.5 ± 25.3	2.3
13	47.6 ± 32.3	95.7 ± 8.9	2.0
14	175.2 ± 54.0	294.8 ± 11.4	1.7

[a] n.d. = not detected. [b] n.a. = not available. [c] Isolated but not detected in all crude extracts.

Compound **1** exhibited distinct UV absorption maxima at λ_{max} 320, 278 and 223 nm. The HRESIMS data of **1** established the molecular formula $C_{31}H_{24}O_{16}$, indicating twenty degrees of unsaturation. The ^{1}H NMR spectrum of **1** (Table 2) showed fewer signals in comparison to the molecular formula, suggesting the possible dimeric nature of **1**. These signals included two singlet aromatic protons at δ_H 7.17 (H-8/8′), two singlet methyl groups at δ_H 1.88 (Me-14) and 1.86 (Me-14′), two singlet methylene groups at δ_H 3.08 (H_2-12′) and 3.03 (H_2-12), in addition to three methoxy groups at δ_H 4.10 (Me-15/15′) and 3.68 (Me-16′). In the HMBC spectrum of **1**, ^3J-HMBC correlations

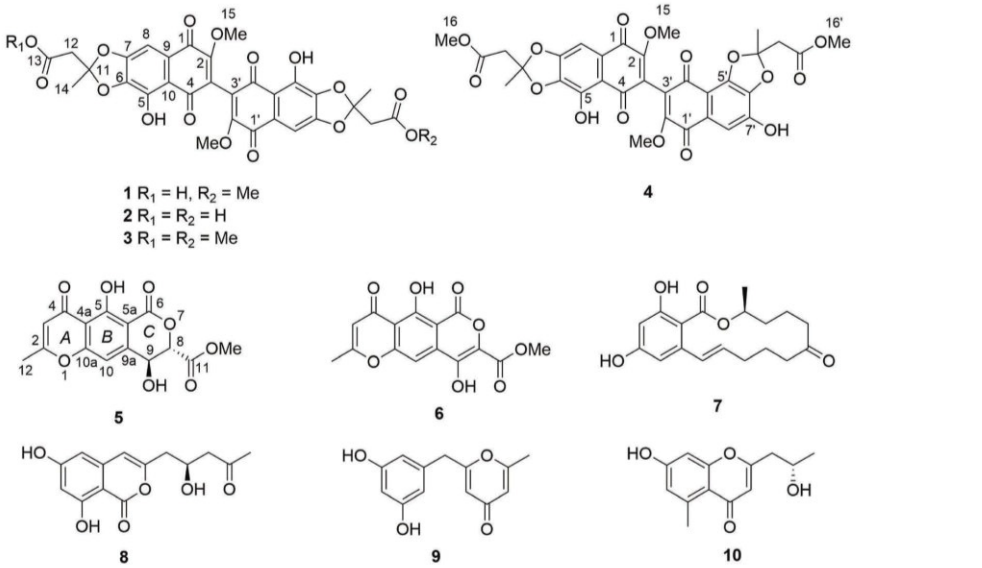

Fig. 1 Structures of compounds **1–10**.

Table 2 NMR data of compound 1[a]

	1a		1b	
Position	δ_C, type	δ_H (J in Hz)	δ_C, type	δ_H (J in Hz)
1/1′	179.5, C		179.5, C	
2/2′	159.0, C		159.0, C	
3/3′	121.2, C		121.2, C	
4/4′	188.3, C		188.3, C	
5/5′	145.4, C		145.4, C	
6/6′	139.8, C		139.8, C	
7/7′	152.8, C		152.8, C	
8/8′	102.5, CH	7.17, s	102.5, CH	7.17, s
9/9′	127.2, C		127.2, C	
10/10′	112.5, C		112.5, C	
11	120.4, C		120.4, C	
12	43.5, CH_2	3.03, s	43.5, CH_2	3.03, s
13	169.9, C		169.9, C	
14	24.8, CH_3	1.88, s	24.8, CH_3	1.88, s
15	61.6, CH_3	4.10, s	61.6, CH_3	4.09, s
11′	120.1, C		120.1, C	
12′	43.3, CH_2	3.08, s	43.3, CH_2	3.08, s
13′	168.5, C		168.5, C	
14′	25.1, CH_3	1.86, s	25.1, CH_3	1.86, s
15′	61.6, CH_3	4.09, s	61.6, CH_3	4.09, s
16′	52.5, CH_3	3.68, s	52.5, CH_3	3.68, s

[a] Measured in $CDCl_3$–CD_3OD (2 : 1) (^1H at 600 MHz and ^{13}C at 150 MHz).

from H-8 to C-1 (δ_C 179.5), C-6 (δ_C 139.8) and C-10 (δ_C 112.5), and from Me-15 to C-2 (δ_C 159.0) as well as weak ^2J-HMBC correlations from H-8 to C-7 (δ_C 152.8) and C-9 (δ_C 127.2) were observed. In addition, H-8 showed long range ^4J-HMBC correlations to C-2, C-4 (δ_C 188.3) and C-5 (δ_C 145.4), while Me-15 exhibited long range HMBC correlations to C-1, C-3 (δ_C 121.2), C-4 and C-9. Furthermore, when the spectra were recorded in $CDCl_3$, an additional signal at δ_H 12.04 assigned for OH-5 was detected which showed HMBC correlations to C-5, C-6 and C-10. These findings confirmed the presence of a dimeric substituted naphthoquinone core structure of **1** through a C-3/3′ linkage (Fig. 1). A methoxy and a hydroxy group were located at C-2/2′ and C-5/5′, respectively. Apart from these, the HMBC correlations from Me-14 to C-11 (δ_C 120.4) and C-12 (δ_C 43.5), and from H_2-12 to C-11, C-13 (δ_C 169.9) and C-14 together with the HMBC correlations from Me-14′ to C-11′ (δ_C 120.1) and C-12′ (δ_C 43.3), from H_2-12′ to C-11′, C-13′ (δ_C 168.5) and C-14′, and from Me-16′ to C-13′, indicated the presence of two side chains from C-14 to C-13 and from C-14′ to C-16′ as shown. Based on the molecular formula and the chemical shifts of **1**, these two side chains are connected to the core structure through two acetonide rings between C-6/6′, C-7/7′ and C-11/11′. Thus, the structure of **1**, to which the trivial name fusatricinone A is given, was established as shown.

The UV pattern and NMR data of compound **2** (Table 3) resembled those of **1**, suggesting their structural similarity. The molecular formula $C_{30}H_{22}O_{16}$ of **2** was determined by the HRESIMS data, differing from that of **1** by the loss of 14 amu, which was due to the absence of the carboxymethyl group of **1** as shown by comparison of the 1D and 2D NMR spectra of both

Table 3 NMR data of compound 2[a]

	2a		2b	
Position	δ_C,[b] type	δ_H (J in Hz)	δ_C,[b] type	δ_H (J in Hz)
1/1′	179.1, C		179.1, C	
2/2′	158.6, C		158.6, C	
3/3′	n.d.[c]		n.d.[c]	
4/4′	188.3, C		188.3, C	
5/5′	145.5, C		145.5, C	
6/6′	139.1, C		139.1, C	
7/7′	152.1, C		152.1, C	
8/8′	102.0, CH	7.21, s	102.0, CH	7.20, s
9/9′	127.1, C		127.1, C	
10/10′	112.2, C		112.2, C	
11/11′	119.2, C		119.2, C	
12/12′	42.9, CH_2	3.12, s	42.9, CH_2	3.10, s
13/13′	171.4, C		171.4, C	
14/14′	24.6, CH_3	1.91, s	24.6, CH_3	1.88, s
15/15′	61.2, CH_3	4.13, s	61.2, CH_3	4.12, s
OH-5/OH-5′		12.06, s	12.06, s	

[a] Measured in $CDCl_3$ (^1H at 600 MHz and ^{13}C at 150 MHz). [b] Data were extracted from the HSQC and HMBC spectra. [c] n.d. = not detected.

compounds. In addition, the 1D NMR of **2** showed the same chemical shifts for related nuclei in both molecule halves, indicating that both molecule halves are constitutionally identical. Thus, **2** was identified as a new natural product and was given the trivial name fusatricinone B.

The molecular formula of compound **3** was determined as $C_{32}H_{26}O_{16}$ based on the HRESIMS data, differing from that of **1** by an additional 14 amu and implying the presence of an additional methyl group in **3**. The UV and NMR (Table 4) data of **3** were similar to those of **2** and likewise exhibited only one set of NMR signals, indicating methylation of both terminal

Table 4 NMR data of compound 3[a]

	3a		3b	
Position	δ_C,[b] type	δ_H (J in Hz)	δ_C,[b] type	δ_H (J in Hz)
1/1′	179.3, C		179.3, C	
2/2′	158.7, C		158.7, C	
3/3′	n.d.[c]		n.d.[c]	
4/4′	n.d.[c]		n.d.[c]	
5/5′	145.4, C		145.4, C	
6/6′	139.3, C		139.3, C	
7/7′	152.6, C		152.6, C	
8/8′	102.0, CH	7.21, s	102.0, CH	7.21, s
9/9′	127.6, C		127.6, C	
10/10′	112.1, C		112.1, C	
11/11′	119.5, C		119.5, C	
12/12′	43.3, CH_2	3.07, s	43.3, CH_2	3.06, s
13/13′	167.6, C		167.6, C	
14/14′	24.7, CH_3	1.90, s	24.7, CH_3	1.89, s
15/15′	61.2, CH_3	4.13, s	61.2, CH_3	4.12, s
16/16′	52.0, CH_3	3.71, s	52.0, CH_3	3.71, s
OH-5/OH-5′		12.05, s		12.05, s

[a] Measured in $CDCl_3$ (^1H at 600 MHz and ^{13}C at 150 MHz). [b] Data were extracted from the HSQC and HMBC spectra. [c] n.d. = not detected.

carboxyl groups to form the respective methyl ester functions. This deduction was further confirmed by the HMBC correlation from Me-16/16′ (δ_H 3.71) to C-13/13′ (δ_C 167.6). The trivial name fusatricinone C was assigned to the new compound **3**.

Compound **4** had the same molecular formula as that of **3** ($C_{32}H_{26}O_{16}$) as established by HRESIMS. The UV spectrum was similar to those of compounds **1–3**, suggesting the presence of the same naphthoquinone core structure. Unlike **3**, however, the ^{1}H and ^{13}C NMR spectra of the monomers of **4** (Table 5) exhibited two sets of signals, one of which (from C-1 to C-16) showed the same pattern as that of the monomer in **3**. The second monomer of **4** showed signals accounting for the aromatic proton at δ_H 7.23 (H-8′) and a hydroxy group at δ_H 11.10 (OH-7′), which are key signals to determine the substitution pattern of the second monomer. The HMBC spectrum of **4** displayed correlations from H-8′ to C-6′ (δ_C 140.2), C-7′ (δ_C 144.3), C-10′ (δ_C 107.6) and C-1′ (δ_C 178.6), and from OH-7′ to C-6′, C-7′ and C-8′ (δ_C 111.4). In addition, a ROESY correlation between H-8′ and OH-7′ was observed. These data indicated that cyclisation of one acetonide moiety of **4** included the oxygens at the C-5′ and C-6′ positions. Thus, the structure of **4** was elucidated as shown and the trivial name fusatricinone D was assigned to this compound.

Table 5 NMR data of compound 4[a]

	4a		4b	
Position	δ_C,[b] type	δ_H (J in Hz)	δ_C,[b] type	δ_H (J in Hz)
1	179.0, C		179.0, C	
2	158.5, C		158.5, C	
3	n.d.[c]		n.d.[c]	
4	n.d.[c]		n.d.[c]	
5	143.8, C		143.8, C	
6	139.3, C		139.3, C	
7	152.4, C		152.4, C	
8	101.1, CH	7.16, s	101.1, CH	7.16, s
9	n.d.[c]		n.d.[c]	
10	111.8, C		111.8, C	
11	120.0, C		120.0, C	
12	42.1, CH_2	3.29, s	42.1, CH_2	3.28, s
13	167.9, C		167.9, C	
14	24.2, CH_3	1.82, s	24.2, CH_3	1.81, s
15	60.4, CH_3	3.96, s	60.4, CH_3	3.95, s
16	52.0, CH_3	3.57, s	52.0, CH_3	3.56, s
OH-5		11.80, s		11.79, s
1′	178.6, C		178.6, C	
2′	157.8, C		157.8, C	
3′	n.d.[c]		n.d.[c]	
4′	n.d.[c]		n.d.[c]	
5′	n.d.[c]		n.d.[c]	
6′	140.2, C		140.2, C	
7′	144.3, C		144.3, C	
8′	111.4, CH	7.23, s	111.4, CH	7.23, s
9′	n.d.[c]		n.d.[c]	
10′	107.6, C		107.6, C	
11′	120.0, C		120.0, C	
12′	41.8, CH_2	3.24, s	41.8, CH_2	3.24, s
13′	167.9, C		167.9, C	
14′	24.6, CH_3	1.80, s	24.6, CH_3	1.80, s
15′	60.7, CH_3	4.01, s	60.7, CH_3	4.00, s
16′	52.0, CH_3	3.59, s	52.0, CH_3	3.59, s
OH-7′		11.10, s		11.10, s

[a] Measured in DMSO-d_6 (^{1}H at 600 MHz and ^{13}C at 150 MHz). [b] Data were extracted from the HSQC and HMBC spectra. [c] n.d. = not detected.

Compounds **1–4** were detected in the original fungal-bacterial co-culture crude EtOAc extract by LC-MS, indicating that they are true natural products and not formed through methylation during chromatographic workup.

The ^{1}H NMR data of dimeric naphthoquinone core structure of **1–3** were comparable to those of synthetic 3,3′-dimethoxy-8,8′-dihydroxy-2,2′-bi-1,4-naphthoquinone, which exhibited signals of methoxy groups at δ_H 4.15 and signals of hydroxy groups at δ_H 12.08.[14,15]

For the isolated dimeric naphthoqinones **1–4**, the 3/3′-biaryl linkage between monomers can lead to axial chirality if the rotational energy barrier is sufficiently high.[16] DFT quantum chemical calculations of the rotation energy barrier for the biaryl axis were performed to check the possibility of atropisomers or interconversion of R_a and S_a conformers, which yielded ~22 kcal mol^{-1} for the inversion (Fig. 2), indicating that the atropisomers interconvert with a half-life of ~1.7×10^3 s = ~28 min at 300 K.[17,18]

Compounds **1–4** gave baseline ECD spectra and zero specific rotation. Each monomer contains one chiral center (C-11 and C-11′), and there is a configurationally labile biaryl axis, which is expected to allow the interconversion of R_a and S_a conformers in solution. Provided that the monomers have identical absolute configuration for the central chirality elements, namely (11*R*,11′*R*) or (11*S*,11′*S*) absolute configuration, distinct ECD spectra would be expected for **1–4** as observed for biaryls with central chirality but low rotational energy barrier exemplified by dicerandrol B,[19] and versixanthone C.[20] Thus the baseline ECD curves suggest stereoisomeric mixtures of **1–4** containing either equimolar amounts of (11*R*,11′*R*) and (11*S*,11′*S*) stereoisomers or four stereoisomers with (11*R*,11′*R*), (11*S*,11′*S*), (11*S*,11′*R*), (11*R*,11′*S*) absolute configuration. If there is a mixture of two quasi-enantiomers [(11*R*,11′*R*) and (11*S*,11′*S*)], the duplication of NMR signals derives from the slowly interconverting R_a and S_a conformers, which represent rotational diastereomers (Fig. 3A). If there is a mixture of four stereoisomers or two racemates [(11*R*,11′*R*), (11*S*,11′*S*), (11*S*,11′*R*), (11*R*,11′*S*)], the duplication can be due to diastereomers that differ in the configuration of the central chirality elements [(11*S**,11′*S**) *versus* (11*S**,11′*R**)], but not due to stereoisomers with enantiomorphic molecule halves [(11*S*,11′*R*) *versus* (11*R*,11′*S*)] (Fig. 3B). However, it is more likely that the slowly interconverting R_a and S_a conformers with homomorphic molecule halves are distinguished by the NMR even in this case, and the remote central chirality elements do not result in duplication of NMR signals.

The related biaryl derivative xanthomegnin, which was isolated from several *Penicillium* and *Aspergillus* species and occurs naturally as a 1 : 1 mixture of atropisomers,[21] has the same naphthoquinone core structure as compounds **1–4** isolated in this study, but the condensed 1,3-dioxolane ring is replaced by a δ-lactone ring. The biogenetic precursor of xanthomegnin is (*R*)-semivioxanthin, and xanthomegnin has a distinct ECD spectrum allowing configurational assignment of analogues.[22]

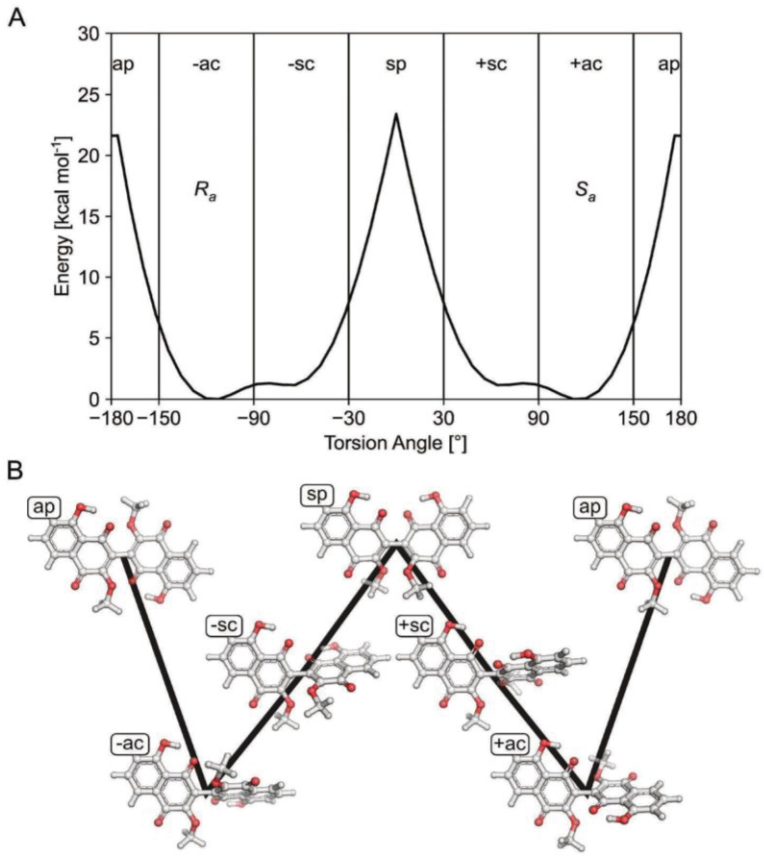

Fig. 2 Calculation of the height of the rotation barrier for compounds **1–4**. (A) Conformational energy profile obtained for the gas phase at the B3LYP/6-31G(d) level of theory for the rotation about the central biaryl bond in the model compound 8,8′-dihydroxy-3,3′-dimethoxy-2,2′-binaphthyl-1,1′,4,4′-tetrone. Vertical lines separate regions of values for the torsion angle that correspond to distinct conformations according to the Klyne–Prelog notation. The structures of the R_a and S_a atropisomers are assigned to the corresponding minimum-energy conformers in the anticlinal conformations. (B) Visualization of the distinct conformers according to the Klyne–Prelog notation. The height of the black line indicates the relative energy of the depicted conformer.

In the biosynthesis of xanthomegnin, the optically active monomers are formed first and are then dimerized by oxidative coupling.[23]

Compound **5** showed UV absorption maxima at 350, 263, 243 and 229 nm and had the molecular formula $C_{15}H_{12}O_8$ based on the HRESIMS data. Compound **5** contains two additional protons compared to the co-isolated structurally related known compound lateropyrone (**6**),[24] suggesting hydrogenation of the olefinic double bond of **6** at C-8 and 9, thus yielding **5**. This was also evident from the ^{1}H NMR spectrum of **5** (Table 6), which exhibited two aromatic protons at δ_H 6.36 (s, H-3) and 7.38 (s, H-10), two oxygenated methines at δ_H 4.92 (br s, H-9) and 6.04 (br s, H-8), an aromatic methyl group at δ_H 2.51 (s, Me-12) in addition to a methoxy group at δ_H 3.73 (s, OMe-11). The HMBC correlations from H-3 to C-2 (δ_C 170.9), C-4 (δ_C 184.4) and C-4a (δ_C 113.1), from Me-12 to C-2 and C-3, and from H-10 to C-10a (δ_C 158.1), C-9a (δ_C 125.6) and C-4a indicated the presence of the same rings A and B in **5**. However, the HMBC correlation from H-8 to C-6 (δ_C 168.6), C-11 (δ_C 170.6), C-9a (δ_C 125.6) and from H-9 to C-11 and C-9a confirmed the disappearance of the double bond of **6** in **5**.

Based on the small $^3J_{H\text{-}8,H\text{-}9}$ coupling constant value, a *cis* relative configuration of **5** was expected, and hence TDDFT-ECD calculations were performed on the arbitrarily chosen *cis*-(8*R*,9*S*) stereoisomer.[25,26] DFT optimization of the 15 initial conformers generated using the Merck Molecular Force Field (MMFF) at various levels of theory (B3LYP/6-31G(d), B97D/TZVP PCM/MeCN and CAM-B3LYP/TZVP PCM/MeCN) resulted in 1, 3 and 5 low-energy DFT conformers (≥1%), respectively. In the lowest-energy CAM-B3LYP/TZVP PCM/MeCN conformer (63.6% population), the C-8 methoxycarbonyl group adopted axial orientation, while the C-9 hydroxy group was axial and formed

View Article Online
RSC Advances Paper

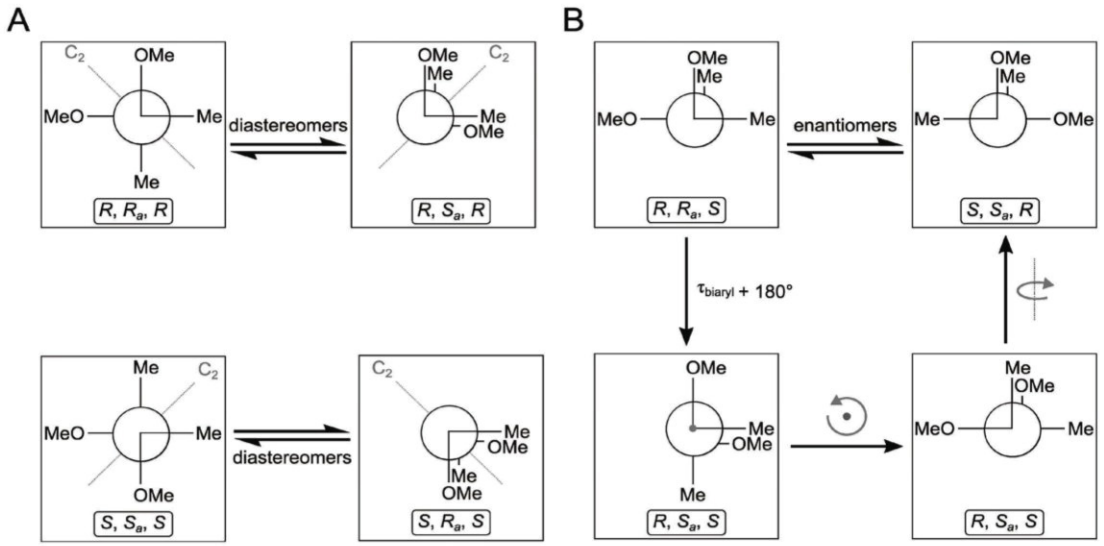

Fig. 3 Stereochemical relationship of atropisomers in the case of the symmetric molecules **2** and **3**. If both molecule halves are homomorph (A), diastereomeric atropisomers result. If both molecule halves are enantiomorph (B), enantiomeric atropisomers result. "Me" and "OMe" relate to C-14 and 15 as well as C-14′ and 15′ in Fig. 1. The grey arrows in the right panel indicate whole-body rotations; the configuration descriptors relate to the central/axial/central chirality elements in the molecules.

Table 6 NMR data of compound **5**[a]

Position	δ_C,[b] type	δ_H (J in Hz)
2	170.9, C	
3	109.6, CH	6.36, s
4	184.4, C	
4a	113.1, C	
5	n.d.[c]	
5a	n.d.	
6	168.6, CH	
8	81.8, CH	6.04, br s
9	70.9, CH	4.92, br s
9a	125.6, C	
10	103.6, CH	7.38, s
10a	158.1, C	
11	170.6, C	
12	20.3, CH_3	2.51, s
OMe-11	52.4, CH_3	3.73, s

[a] Measured in acetone-d_6 (^{1}H at 750 MHz and ^{13}C at 175 MHz). [b] Data were extracted from the HSQC and HMBC spectra. [c] n.d. = not detected.

an intramolecular hydrogen bond to the carbonyl oxygen. Conformers B–D represented geometries with inversed helicity of the α-pyrone ring having equatorial methoxycarbonyl and equatorial hydroxy groups with a total population of 31.4%. Boltzmann-weighted ECD spectra computed for all the sets of conformers of *cis*-(8*R*,9*S*) at various levels (B3LYP/TZVP, BH&HLYP, CAM-B3LYP and PBE0/TZVP) gave a mismatch with the experimental ECD spectrum (Fig. 4). This suggested that the small $^3J_{H\text{-}8,H\text{-}9}$ coupling constant may derive from a *trans*-diequatorial orientation of H-8 and H-9 of the *trans* relative configuration, which, considering the *trans*-diaxial orientation of the large substituents, is less common for 1,2-disubstituted benzene-condensed heterocyclic derivatives. However, we have demonstrated recently by ECD and NMR calculation and X-ray analysis that in benzene-condensed chiral heterocycles the large substituents of contiguous chirality centers preferably adopt *trans*-diaxial orientation both in solution and in the solid-state rendering the protons to *trans*-diequatorial position.[27,28] The same computational ECD protocol was carried out for the arbitrarily chosen *trans*-(8*S*,9*S*) stereoisomer, for which all combinations of the applied levels gave

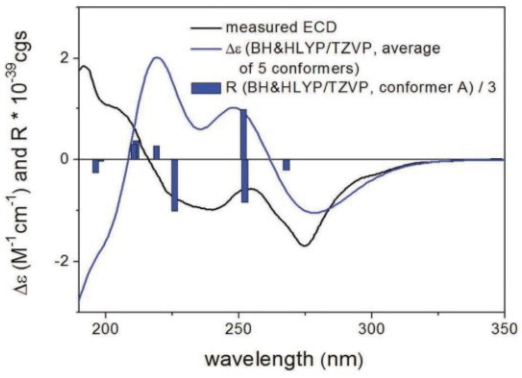

Fig. 4 Experimental ECD spectrum of **5** in MeCN compared with the Boltzmann-weighted BH&HLYP/TZVP PCM/MeCN//CAM-B3LYP/TZVP PCM/MeCN spectrum of the *cis*-(8*R*,9*S*)-**5**.

moderate to good agreement with the experimental ECD spectrum. The diequatorial orientation of the methoxycarbonyl and hydroxy groups was found in conformers A and D with a total population of 46%, while the diaxial geometry was found in conformers B–D and G totaling 53% population. Conformers A and B with opposite helicity of the condensed α-pyrone ring had markedly different computed ECD spectra as demonstrated by their rotatory strengths (Fig. 5). Based on the good ECD agreement, (−)-*trans*-(8*S*,9*S*) absolute configuration was determined for dihydrolateropyrone (**5**).

The five known cryptic compounds that were isolated from the co-culture extracts but were not detected in extracts of the axenic fungal control included lateropyrone (**6**),[24] zearalenone (**7**),[29] (−)-citreoisocoumarin (**8**),[30,31] macrocarpon C (**9**),[5] and 7-hydroxy-2-(2-hydroxypropyl)-5-methylchromone (**10**).[32] In addition, four constitutively present compounds (also detected in axenic fungal controls) including enniatins B, B1 and A1 (**11–13**)[6] and fusaristatin A (**14**)[33] were upregulated in the co-culture extracts.

The new dimeric naphthoquinones **1–4** and the likewise new compound **5** were evaluated for their antibacterial activity against human pathogenic bacterial strains, including *Staphylococcus aureus* and *Pseudomonas aeruginosa* but exhibited no antibacterial activity. For compound **5**, this is in sharp contrast to the structurally closely related known compound lateropyrone (**6**), which had previously been noted for its pronounced activity against Gram positive bacteria.[5] Apparently, hydrogenation of the double bond at C-8 and 9 leads to a complete loss of antibacterial activity.

The observed upregulation of antibiotically active lateropyrone (**6**) and enniatins (**11–13**) during co-cultivation of *F. tricinctum* and *S. lividans* (Table 1) may be interpreted as chemical defense of the fungus.[5] The most interesting finding from this study is, however, the observation that *F. tricinctum* responds to the presence of *S. lividans* in a metabolically different way compared to co-cultures of this fungus with *B. subtilis*, leading to the accumulation of the new compounds **1–4** that are not detected when the fungus is co-cultured with *B. subtilis*. This result mirrors data from a similar study with the fungus *Chaetomium* sp. Co-culture of *Chaetomium* sp. either with *B. subtilis* or with *P. aeruginosa* likewise provoked accumulation of different sets of cryptic fungal compounds.[9,10] Future experiments should aim at unravelling the molecular patterns that underlie these specific fungal metabolic responses.

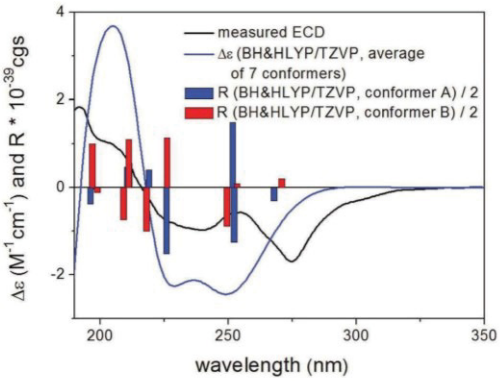

Fig. 5 Experimental ECD spectrum of **5** in MeCN compared with the Boltzmann-weighted BH&HLYP/TZVP PCM/MeCN//CAM-B3LYP/TZVP PCM/MeCN spectrum of the *trans*-(8*S*,9*S*)-**5**.

Experimental section

General experimental procedures

For measuring the optical rotations a Perkin-Elmer-241 MC polarimeter was used. ECD spectra were recorded on a J-810 spectropolarimeter. Solvents used for spectroscopic measurements had spectral grade and for other usage solvents were distilled prior to use. For 1D and 2D NMR spectra, Bruker AVANCE DMX 600 or Bruker ARX 700 NMR spectrometers were used. Mass spectra were recorded with a Finnigan LCQ Deca mass spectrometer, while HRMSESI spectra were acquired with a FTHRMS-Orbitrap (Thermo-Finnigan) mass spectrometer. HPLC chromatograms were obtained with a Dionex P580 system connected to a photodiode array detector (UVD340S). Routine UV lengths for detection were set at 235, 254, 280, and 340 nm. The stationary phase of the analytical column (125 × 4 mm) was Eurosphere-10 C_{18} (Knauer, Germany). The mobile phase was a gradient of acidic nanopure water, set to pH 2 by adding HCOOH and HPLC grade methanol, following the gradient: 0 min, 10% MeOH; 5–35 min, 10–100% MeOH; 35–45 min, 100% MeOH. Semi-preparative HPLC chromatography was performed using the Lachrom–Merck Hitachi semi-preparative HPLC system (UV detector L-7400; pump L-7100; Eurosphere-100 C_{18}, 300 × 8 mm, Knauer, Germany) at a flow rate of 5.0 mL min^{-1}. Column chromatography was carried out using Sephadex LH-20 and Merck MN Silica gel 60 M (0.04–0.063 mm). During the isolation work, precoated silica gel 60 F254 TLC plates (Merck, Darmstadt, Germany) served to control the progress of isolation, under detection at 254 and 365 nm and then sprayed with anisaldehyde reagent.

Microbial material

The endophytic fungus *F. tricinctum* was obtained from healthy fresh rhizomes of *A. paucinervis* (Aristolochiaceae) adapting standard procedures.[34] The fresh plant was collected in January 2006 from the mountains Beni-Mellal, located in Morocco.[6] The bacterial strain *Streptomyces lividans* TK24 (ref. 35) complies to standard laboratory strains.[36]

Identification of fungal material

The fungal microorganism was identified as *F. tricinctum* using the ITS method according to the protocol of molecular biology, by DNA isolation and amplification of the ITS region as previously described.[6] The same strain of the fungus, encoded as F.t., is kept under laboratorial conditions at −80 °C in the Institute of Pharmaceutical Biology and Biotechnology, Heinrich-Heine University, Düsseldorf, Germany.

Co-cultivation of *F. tricinctum* with *S. lividans*

In order to cultivate the fungus and the bacterium under sterile conditions, ten Erlenmeyer flasks (1 L each) were prefilled with solid rice medium (50 g of milk rice, *Oryza*) and Yeast Malt (YM) medium (60 mL), and then autoclaved. Four Erlenmeyer flasks were inoculated with only fungus or bacterium, serving as axenic control cultures. *S. lividans* was precultured using YM medium, which was incubated at 30 °C and shaken at 200 rpm, left overnight to reach exponential mid growth. Since the distribution of the bacterial colonies was not measurable by OD because of agglomeration, the average amount of colonies was estimated visually in order to divide equal amounts of the bacterium to each flask. This has been performed by using a sterilized 5 mL Eppendorf pipette. The bacteria were then added to flasks containing the solid rice medium and left for three days at 30 °C before the fungus was added to the flasks and left at room temperature. This protocol was chosen as the fungus readily killed the bacteria when added simultaneously to the culture flasks. The axenic fungal or bacterial cultures on solid rice media were kept under identical conditions. All flasks were then cultivated at room temperature. Flasks were extracted when the fungus had completely covered the surface of the culture media.

Extraction and isolation

After fermentation, 300 mL EtOAc were added to the fully grown cultures which were then extracted for 8 h under continuous shaking. The EtOAc extracts of the co-cultures of *F. tricinctum* and *S. lividans* following HPLC chromatography were combined, yielding an amount of 3.8 g. This extract was dissolved in a solvent mixture of MeOH–H_2O (9 : 1) followed by partitioning against *n*-hexane. The aqueous MeOH extract was subjected to a Sephadex LH-20 column, using acetone as mobile phase, to obtain 12 fractions (Fr.1–14). The second and third fractions (Fr.2 and 3) were combined due to their similar HPLC profiles followed by separation on a silica column. From the first fraction of this chromatographic separation which was eluted with CH_2Cl_2–MeOH (99 : 1), compound **3** (2.3 mg) was purified using semi-preparative RP-HPLC with 100% MeOH. Fr.4 was further fractionated using a Sephadex LH-20 column with MeOH as mobile phase which yielded compound **1** (10.8 mg) as the subfraction Fr.4–4. Fraction Fr.4–3 was subjected to semi-preparative RP-HPLC to afford compound **4** (2.1 mg). From Fr.5, compounds **5** (0.8 mg), **6** (3.9 mg) and **7** (1.5 mg) were obtained by semi-preparative RP-HPLC with MeOH/H_2O as mobile phase. Compounds **2** and **8** were isolated from Fr.8 by semi-preparative RP-HPLC, where **2** (4.2 mg) was eluted at 100% MeOH and **8** (1.1 mg) at 55% MeOH–H_2O. Furthermore, purification of Fr.10 with semi-preparative HPLC yielded compound **9** (1.1 mg) at 40% MeOH–H_2O and compound **10** (1.2 mg) at 55% MeOH–H_2O elution system.

Fusatricinone A (1). Red solid; $[\alpha]_D^{23}$ 0 (*c* 0.1, DCM); UV (MeOH) λ_{max} 223, 278 and 320 nm; ^1H and ^{13}C NMR data see Table 2; HRESIMS $[M + H]^+$ *m/z* 653.1141 (calcd for $C_{31}H_{25}O_{16}$ 653.1137).

Fusatricinone B (2). Red solid; $[\alpha]_D^{23}$ 0 (*c* 0.1, DCM); UV (MeOH) λ_{max} 223, 277 and 320 nm; ^1H and ^{13}C NMR data see Table 3; HRESIMS $[M + H]^+$ *m/z* 639.0977 (calcd for $C_{30}H_{23}O_{16}$, 639.0981).

Fusatricinone C (3). Red solid; $[\alpha]_D^{23}$ 0 (*c* 0.1, DCM); UV (MeOH) λ_{max} 222, 277 and 319 nm; ^1H and ^{13}C NMR data see Table 4; HRESIMS $[M + H]^+$ *m/z* 667.1289 (calcd for $C_{32}H_{27}O_{16}$, 667.1294).

Fusatricinone D (4). Red solid; $[\alpha]_D^{23}$ 0 (*c* 0.1, DCM); UV (MeOH) λ_{max} 223, 278 and 313 nm; ^1H and ^{13}C NMR data see Table 5; HRESIMS $[M + H]^+$ *m/z* 667.1299 (calcd for $C_{32}H_{27}O_{16}$, 667.1294).

Dihydrolateropyrone (5). Yellow, amorphous powder; $[\alpha]_D^{23}$ −84 (*c* 0.1, EtOH); UV (MeOH) λ_{max} 229, 243, 263 and 350 nm; ECD (MeCN, λ [nm] ($\Delta\varepsilon$), $c = 0.23$ mM): 399 br (−0.09), 301 (−0.30), 275 (−1.74), 239 (−1.01), 202 sh (1.11), 192 (2.25). ^1H and ^{13}C NMR data see Table 6; HRESIMS $[M + H]^+$ *m/z* 321.0604 (calcd for $C_{15}H_{13}O_8$, 321.0605).

Calculation of the rotation barrier for compounds 1–4

To obtain an energy profile for the rotation about the central biaryl bond in compounds **1–4** at reasonable computational expense, 8,8′-dihydroxy-3,3′-dimethoxy-2,2′-binaphthyl-1,1′,4,4′-tetrone (Fig. 2B) was used as model compound. First, structures in which the torsion angle defined by atoms C4–C3–C3′-C4′ (Fig. 1) was varied from −180° to 180° in increments of 8° were constructed in the Maestro GUI of the Schrödinger Suite of programs. A single structure with a torsion angle of 0° was added to the resulting series of conformer structures. For each of the resulting 47 structures, a conformational search with a harmonic restraint of 10^4 kcal mol^{-1} rad^{-2} on the corresponding value of the torsion angle was performed using MacroModel and its default settings except for the truncated Newton conjugate gradient method for energy minimization. The minimum energy conformers for each of the 47 searches were then geometry optimized while freezing the respective value of the torsion angle. Geometry optimization was carried out in the gas phase at the B3LYP/6-31G(d) level using the GAUSSIAN 09 software.

Conformational analysis and TDDFT-ECD calculations of 5

Mixed torsional/low-frequency mode conformational searches were carried out by means of the MacroModel 10.8.011 software by using the Merck Molecular Force Field (MMFF) with an implicit solvent model for $CHCl_3$.[37] Geometry reoptimizations were carried out at the B3LYP/6-31G(d) level *in vacuo*, the B97D/TZVP[38,39] and the CAM-B3LYP/TZVP[40] levels with the PCM solvent model for MeCN. TDDFT-ECD calculations were run with various functionals (B3LYP, BH&HLYP, CAM-B3LYP, and PBE0) and the TZVP basis set as implemented in the Gaussian 09 package with the same or no solvent model as in the preceding DFT optimization step.[41] Electronic circular dichroism spectra were generated as sums of Gaussians with 2700 and 3300 cm^{-1} widths at half-height, using dipole-velocity-computed rotational strength values.[42] Boltzmann distributions were estimated from the ZPVE-corrected B3LYP/6-31G(d)

energies in the gas-phase calculations and from the B97D and CAM-B3LYP energies in the solvated ones. The MOLEKEL software package was used for visualization of the results.[43]

Antibacterial assay

The antibacterial activity was determined by using the micro-dilution method in alignment with the CLSI guidelines.[44] Compounds were prepared using a DMSO stock solution with the highest concentration of 0.64% (64 μg mL^{-1}). This was subjected to a prepared inoculum, in which the direct colony suspension method was applied by using an inoculum of 5 × 105 colony forming units per mL. Simultaneously, antibiotics were serial 2-fold diluted in DMSO with the compounds.

Conflicts of interest

There are no conflicts to declare.

Acknowledgements

Financial support by the DFG (GRK 2158) to H. G., R. K. and P. P. is gratefully acknowledged. P. P. also wants to thank the Manchot Foundation for support. H. G. is grateful for computational support and infrastructure provided by the "Zentrum für Informations-und Medientechnologie" (ZIM) at the Heinrich Heine University Düsseldorf and the computing time provided by the John von Neumann Institute for Computing (NIC) on the supercomputer JURECA at Jülich Supercomputing Centre (JSC) (user ID: HKF7). T. K. and A. M. thank the National Research, Development and Innovation Office (NKFI K120181 and PD121020) for financial support and the Governmental Information-Technology Development Agency (KIFÜ) for CPU time.

References

1 A. Marmann, A. H. Aly, W. Lin, B. Wang and P. Proksch, *Mar. Drugs*, 2014, **12**, 1043–1065.
2 G. Daletos, W. Ebrahim, E. Ancheeva, M. El-Neketi, W. Lin and P. Proksch, in *Chemical Biology of Natural Products*, ed. D. Newman, G. Cragg and P. Grothaus, CRC Press, Boca Raton, 2017, ch. 8, pp. 233–284.
3 C. F. Pérez Hemphill, P. Sureechatchaiyan, M. U. Kassack, R. S. Orfali, W. Lin, G. Daletos and P. Proksch, *J. Antibiot.*, 2017, **70**, 726–732.
4 J. Wang, A. Debbab, C. F. Pérez Hemphill and P. Proksch, *Z. Naturforsch.*, 2013, **68c**, 223–230.
5 A. R. B. Ola, D. Thomy, D. Lai, H. Brötz-Oesterhelt and P. Proksch, *J. Nat. Prod.*, 2013, **76**, 2094–2099.
6 W. Wätjen, A. Debbab, A. Hohlfeld, Y. Chovolou, A. Kampkötter, R. A. Edrada, R. Ebel, A. Hakiki, M. Mosaddak, F. Totzke, M. H. G. Kubbutat and P. Proksch, *Mol. Nutr. Food Res.*, 2009, **53**, 431–440.
7 C. G. Shin, D. G. An, H. H. Song and C. Lee, *J. Antibiot.*, 2009, **62**, 687–690.
8 S. Fraeyman, S. Croubels, M. Devreese and G. Antonissen, *Toxins*, 2017, **9**, 228.
9 E. Ancheeva, L. Küppers, S. H. Akone, W. Ebrahim, Z. Liu, A. Mándi, T. Kurtán, W. Lin, R. Orfali, N. Rehberg, R. Kalscheuer, G. Daletos and P. Proksch, *Eur. J. Org. Chem.*, 2017, 3256–3264.
10 S. H. Akone, A. Mándi, T. Kurtán, R. Hartmann, W. Lin, G. Daletos and P. Proksch, *Tetrahedron*, 2016, **72**, 6340–6347.
11 M. Gulshan, G. Y. Zhao, Z. F. Dong and M. Ghopur, *Shengwu Jishu*, 2009, **19**, 43–46.
12 H. Meschke, S. Walter and H. Schrempf, *Environ. Microbiol.*, 2012, **14**, 940–952.
13 R. P. Mellado, *World J. Microbiol. Biotechnol.*, 2011, **27**, 2231–2237.
14 H. Laatsch, *Z. Naturforsch.*, 1990, **45b**, 393–400.
15 H. Laatsch, *Liebigs Ann. Chem.*, 1983, 1886–1900.
16 S. R. LaPlante, P. J. Edwards, L. D. Fader, A. Jakalian and O. Hucke, *ChemMedChem*, 2011, **6**, 505–513.
17 M. Öki, *Top. Stereochem.*, 1983, **14**, 1–63.
18 I. Alkorta, J. Elguero, C. Roussel, N. Vanthuyne and P. Piras, *Adv. Heterocycl. Chem.*, 2012, **105**, 1–188.
19 D. Rönsberg, A. Debbab, A. Mándi, V. Vasylyeva, P. Böhler, B. Stork, L. Engelke, A. Hamacher, R. Sawadogo, M. Diederich, V. Wray, W. Lin, M. U. Kassack, C. Janiak, S. Scheu, S. Wesselborg, T. Kurtán, A. H. Aly and P. Proksch, *J. Org. Chem.*, 2013, **78**, 12409–12425.
20 G. Wu, G. Yu, T. Kurtán, A. Mándi, J. Peng, X. Mo, M. Liu, H. Li, X. Sun, J. Li, T. Zhu, Q. Gu and D. Li, *J. Nat. Prod.*, 2015, **78**, 2691–2698.
21 G. Höfle and K. Röser, *J. Chem. Soc., Chem. Commun.*, 1978, 611–612.
22 R. C. Durley, J. MacMillan and T. J. Simpson, *J. Chem. Soc., Perkin Trans. 1*, 1975, 163–169.
23 I. M. Romaine and G. A. Sulikowski, *Tetrahedron Lett.*, 2015, **56**, 3617–3619.
24 G. W. Bushnell, Y. L. Li and G. A. Poulton, *Can. J. Chem.*, 1984, **62**, 2101–2106.
25 G. Pescitelli and T. Bruhn, *Chirality*, 2016, **28**, 466–474.
26 A. Mándi, I. W. Mudianta, T. Kurtán and M. J. Garson, *J. Nat. Prod.*, 2015, **78**, 2051–2056.
27 P. Zhang, L. H. Meng, A. Mándi, T. Kurtán, X. M. Li, Y. Liu, X. Li, C. S. Li and B. G. Wang, *Eur. J. Org. Chem.*, 2014, 4029–4036.
28 Y. M. Ren, C. Q. Ke, A. Mándi, T. Kurtán, C. Tang, S. Yao and Y. Ye, *Tetrahedron*, 2017, **73**, 3213–3219.
29 W. H. Urry, H. L. Wehrmeister, E. B. Hodge and P. H. Hidy, *Tetrahedron Lett.*, 1966, **27**, 3109–3114.
30 S. Lai, Y. Shizuri, S. Yamamura, K. Kawai and H. Furukawa, *Heterocycles*, 1991, **32**, 297–305.
31 A. Watanabe, Y. Ono, I. Fujii, U. Sankawa, M. E. Mayorga, W. E. Timberlake and Y. Ebizuka, *Tetrahedron Lett.*, 1998, **39**, 7733–7736.
32 J. Xu, J. Kjer, J. Sendker, V. Wray, H. Guan, R. Edrada, W. Lin, J. Wu and P. Proksch, *J. Nat. Prod.*, 2009, **72**, 662–665.
33 Y. Shiono, M. Tsuchinari, K. Shimanuki, T. Miyajima, T. Murayama, T. Koseki, H. Laatsch, T. Funakoshi, K. Takanami and K. Suzuki, *J. Antibiot.*, 2007, **60**, 309–316.

34 J. Kjer, A. Debbab, A. H. Aly and P. Proksch, *Nat. Protoc.*, 2010, **5**, 479–490.
35 H. Chen, G. Daletos, M. S. Abdel-Aziz, D. Thomy, H. Dai, H. Brötz-Oesterhelt, W. H. Lin and P. Proksch, *Phytochem. Lett.*, 2015, **12**, 35–41.
36 D. A. Hopwood, T. Kieser, H. M. Wright and M. J. Bibb, *J. Gen. Microbiol.*, 1983, **129**, 2257–2269.
37 *MacroModel*, Schrödinger, LLC, 2015, http://www.schrodinger.com/MacroModel.
38 S. Grimme, *J. Comput. Chem.*, 2006, **27**, 1787–1799.
39 P. Sun, D. X. Xu, A. Mándi, T. Kurtán, T. J. Li, B. Schulz and W. Zhang, *J. Org. Chem.*, 2013, **78**, 7030–7047.
40 T. Yanai, D. P. Tew and N. C. Handy, *Chem. Phys. Lett.*, 2004, **393**, 51–57.
41 M. J. T. Frisch, G. W. Trucks, H. B. Schlegel, G. E. Scuseria, M. A. Robb, J. R. Cheeseman, G. Scalmani, V. Barone, B. Mennucci, G. A. Petersson, H. Nakatsuji, M. Caricato, X. Li, H. P. Hratchian, A. F. Izmaylov, J. Bloino, G. Zheng, J. L. Sonnenberg, M. Hada, M. Ehara, K. Toyota, R. Fukuda, J. Hasegawa, M. Ishida, T. Nakajima, Y. Honda, O. Kitao, H. Nakai, T. Vreven, J. A. Montgomery Jr, J. E. Peralta, F. Ogliaro, M. Bearpark, J. J. Heyd, E. Brothers, K. N. Kudin, V. N. Staroverov, R. Kobayashi, J. Normand, K. Raghavachari, A. Rendell, J. C. Burant, S. S. Iyengar, J. Tomasi, M. Cossi, N. Rega, J. M. Millam, M. Klene, J. E. Knox, J. B. Cross, V. Bakken, C. Adamo, J. Jaramillo, R. Gomperts, R. E. Stratmann, O. Yazyev, A. J. Austin, R. Cammi, C. Pomelli, J. W. Ochterski, R. L. Martin, K. Morokuma, V. G. Zakrzewski, G. A. Voth, P. Salvador, J. J. Dannenberg, S. Dapprich, A. D. Daniels, Ö. Farkas, J. B. Foresman, J. V. Ortiz, J. Cioslowski and D. J. Fox, *Gaussian 09 (Revision E.01)*, Gaussian, Inc., Wallingford, CT, 2013.
42 P. J. Stephens and N. Harada, *Chirality*, 2010, **22**, 229–233.
43 U. Varetto, *MOLEKEL 5.4*, Swiss National Supercomputing Centre, Manno, Switzerland, 2009.
44 CLSI, *Methods for Dilution Antimicrobial Susceptibility Tests for Bacteria That Grow Aerobically*, Approved Standard Ninth ed. CLSI document M07-A9, Clinical and Laboratory Standards Institute, Wayne, PA, 2012.

2.2a Supplementary data II

Co-Culture of the Fungus *Fusarium tricinctum* with *Streptomyces lividans* Induces Production of Cryptic Naphthoquinone Dimers

Mariam Moussa,[a] Weaam Ebrahim,[a,b] Michele Bonus,[c] Holger Gohlke,[c,d] Attila Mándi,[e] Tibor Kurtán,[e] Rudolf Hartmann,[f] Rainer Kalscheuer,[a] Wenhan Lin,[g] Zhen Liu,[a,*] and Peter Proksch[a,*]

[a]*Institute of Pharmaceutical Biology and Biotechnology, Heinrich-Heine-Universität Düsseldorf, Universitätsstrasse 1, 40225 Düsseldorf, Germany. E-mail: zhenfeizi0@sina.com(Z.L.), proksch@uni-duesseldorf.de(P. P.)*

[b]*Department of Pharmacognosy, Faculty of Pharmacy, Mansoura University, Mansoura 35516, Egypt*

[c]*Institute of Pharmaceutical and Medicinal Chemistry, Heinrich-Heine-Universität Düsseldorf, Universitätsstrasse 1, 40225 Düsseldorf, Germany*

[d]*John von Neumann Institute for Computing (NIC), Jülich Supercomputing Centre (JSC), and Institute for Complex Systems - Structural Biochemistry (ICS-6), Forschungszentrum Jülich GmbH, Wilhelm-Johnen-Straße, 52425 Jülich, Germany.*

[e]*Department of Organic Chemistry, University of Debrecen, Egyetem tér 1, Debrecen 4032, Hungary*

[f]*Institute of Complex Systems - Structural Biochemistry, Forschungszentrum Jülich GmbH, Wilhelm-Johnen-Straße, 52428 Jülich, Germany*

[g]*State Key Laboratory of Natural and Biomimetic Drugs, Peking University, Beijing 100191, China*

Table of Contents

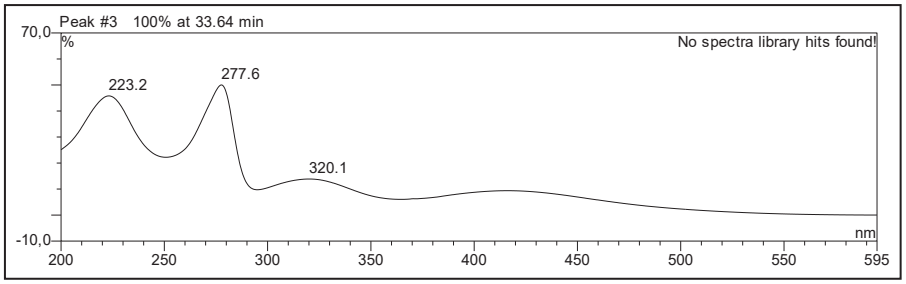

S1. UV spectrum of compound **1**.

Mass Spectrum SmartFormula Report

Analysis Info

Analysis Name	D:\Data\spektren2016\Proksch16HR000151.d	Acquisition Date	6/21/2016 3:26:22 PM
Method	tune_low_new.m	Operator	Peter Tommes
Sample Name	M. Moussa 3M4S4 (CH3OH)	Instrument	maXis 288882.20213
Comment			

Acquisition Parameter

Source Type	ESI	Ion Polarity	Positive	Set Nebulizer	0.3 Bar
Focus	Not active	Set Capillary	4000 V	Set Dry Heater	180 °C
Scan Begin	50 m/z	Set End Plate Offset	-500 V	Set Dry Gas	4.0 l/min
Scan End	1500 m/z	Set Collision Cell RF	600.0 Vpp	Set Divert Valve	Source

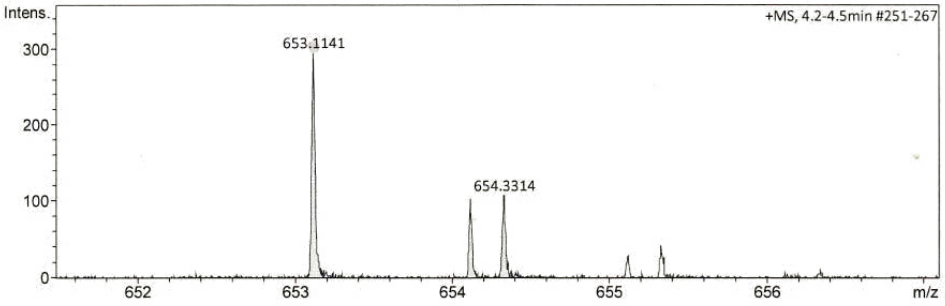

Meas. m/z	#	Ion Formula	m/z	err [ppm]	mSigma	# mSigma	Score	rdb	e¯ Conf	N-Rule
653.1141	1	C29H13N14O6	653.1137	-0.6	40.4	1	100.00	30.5	even	ok
	2	C30H9N18O2	653.1150	1.4	44.4	2	68.59	35.5	even	ok
	3	C31H25O16	653.1137	-0.6	46.2	3	85.29	19.5	even	ok

S2. HRESIMS spectrum of compound **1**.

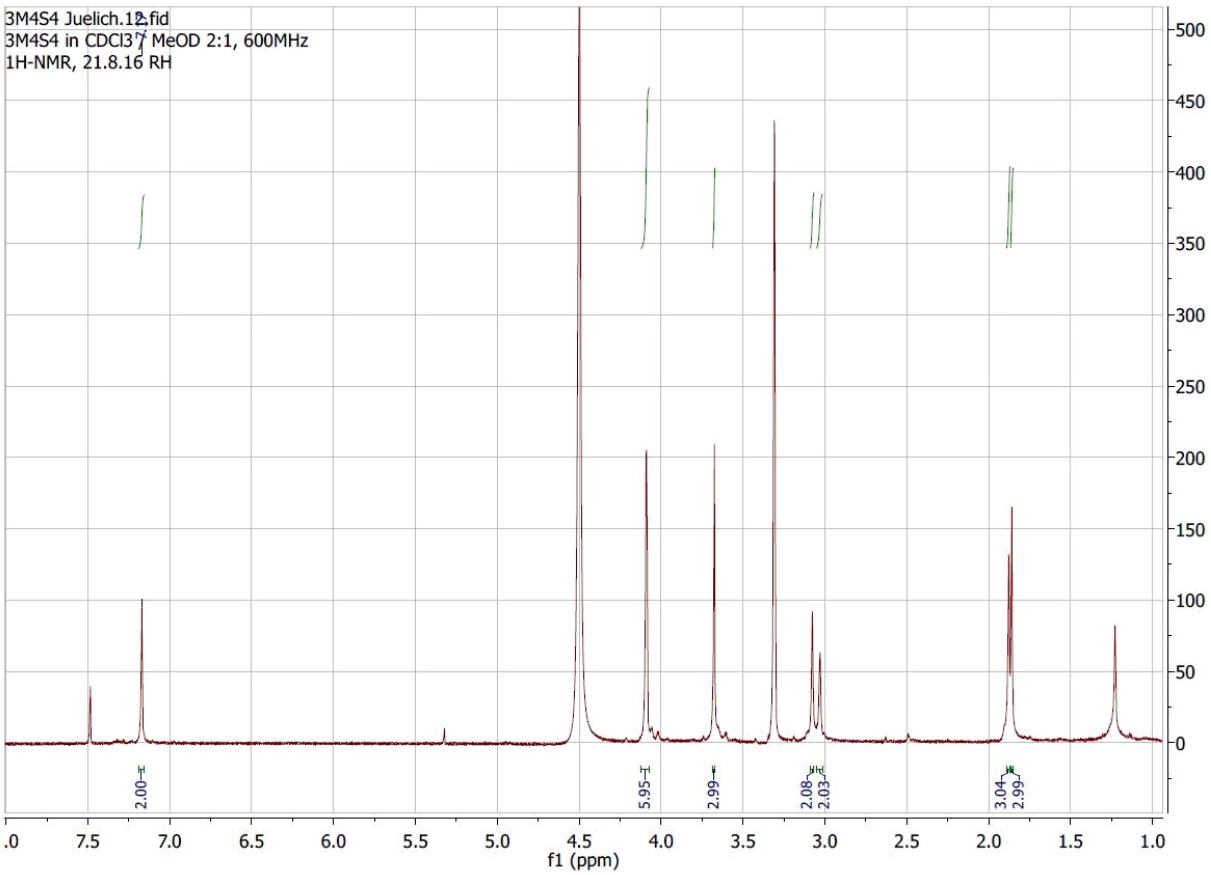

S3. ^{1}H NMR (600 MHz, $CDCl_3$-CD_3OD 2:1) spectrum of compound **1**.

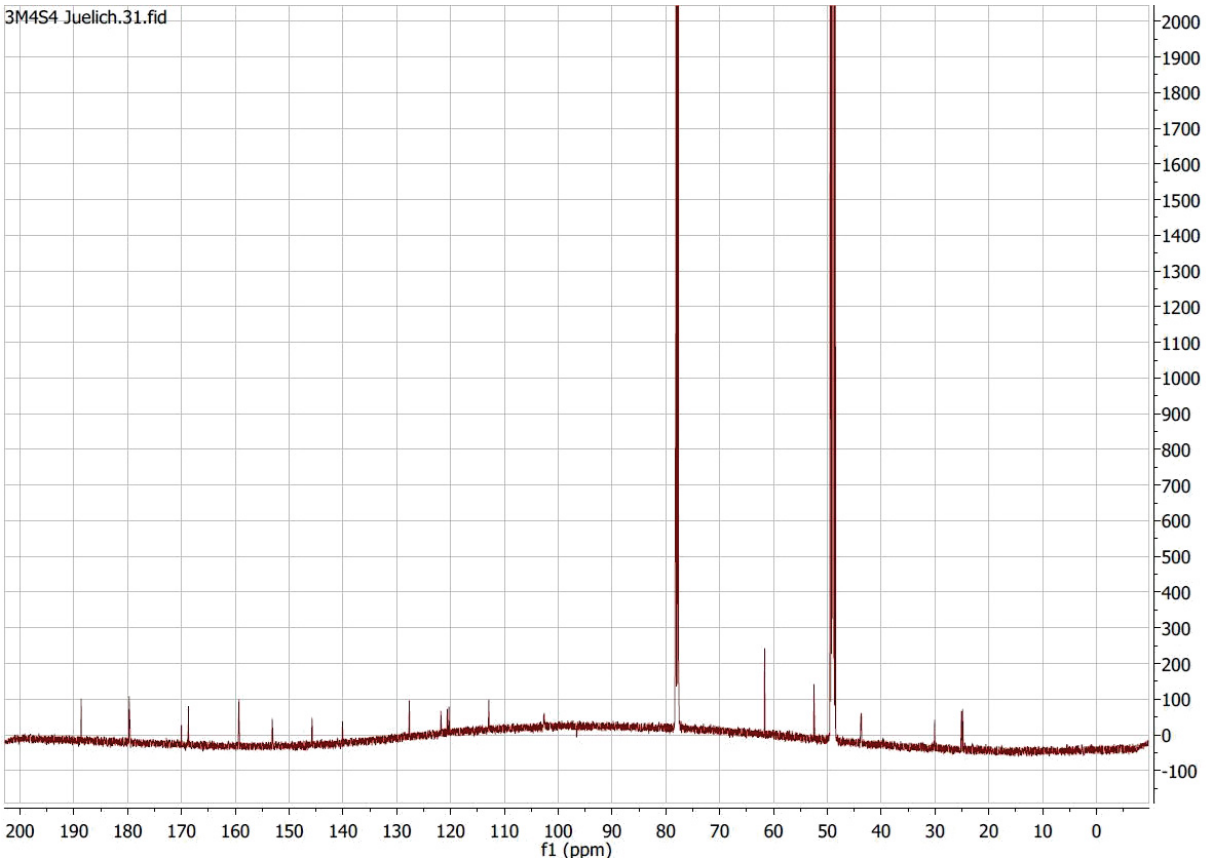

S4. ^{13}C NMR (150 MHz, $CDCl_3$-CD_3OD 2:1) spectrum of compound **1**.

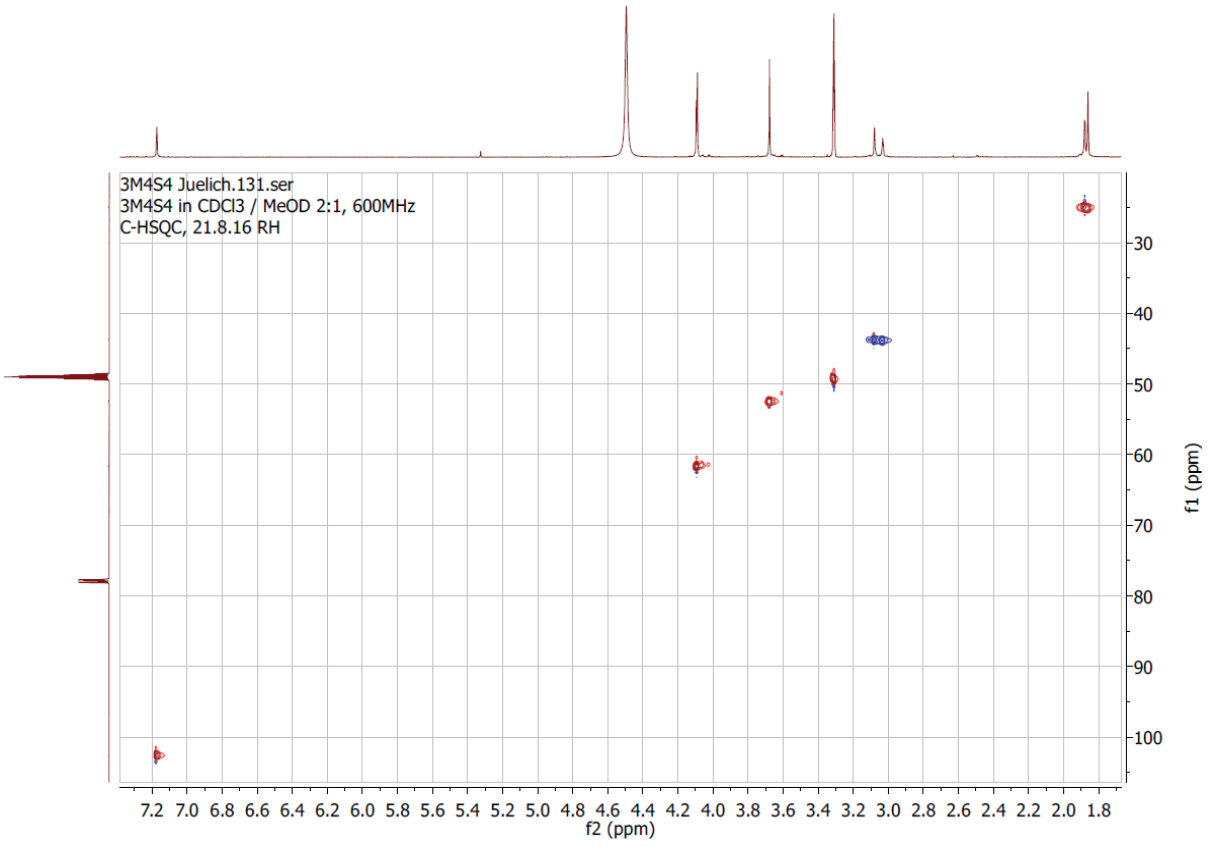

S5. HSQC (600 and 150MHz, $CDCl_3$-CD_3OD 2:1) spectrum of compound **1**.

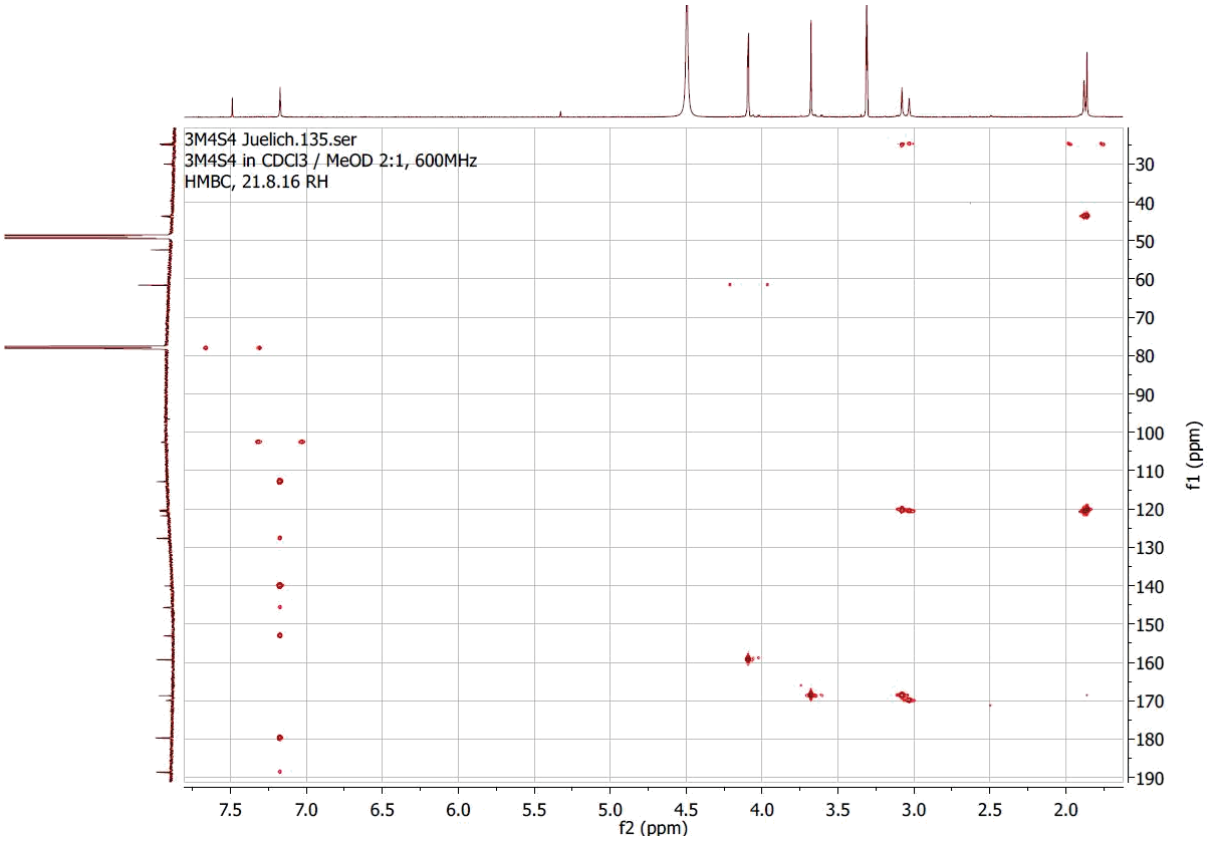

S6. HMBC (600 and 150 MHz, $CDCl_3$-CD_3OD 2:1) spectrum of compound **1**.

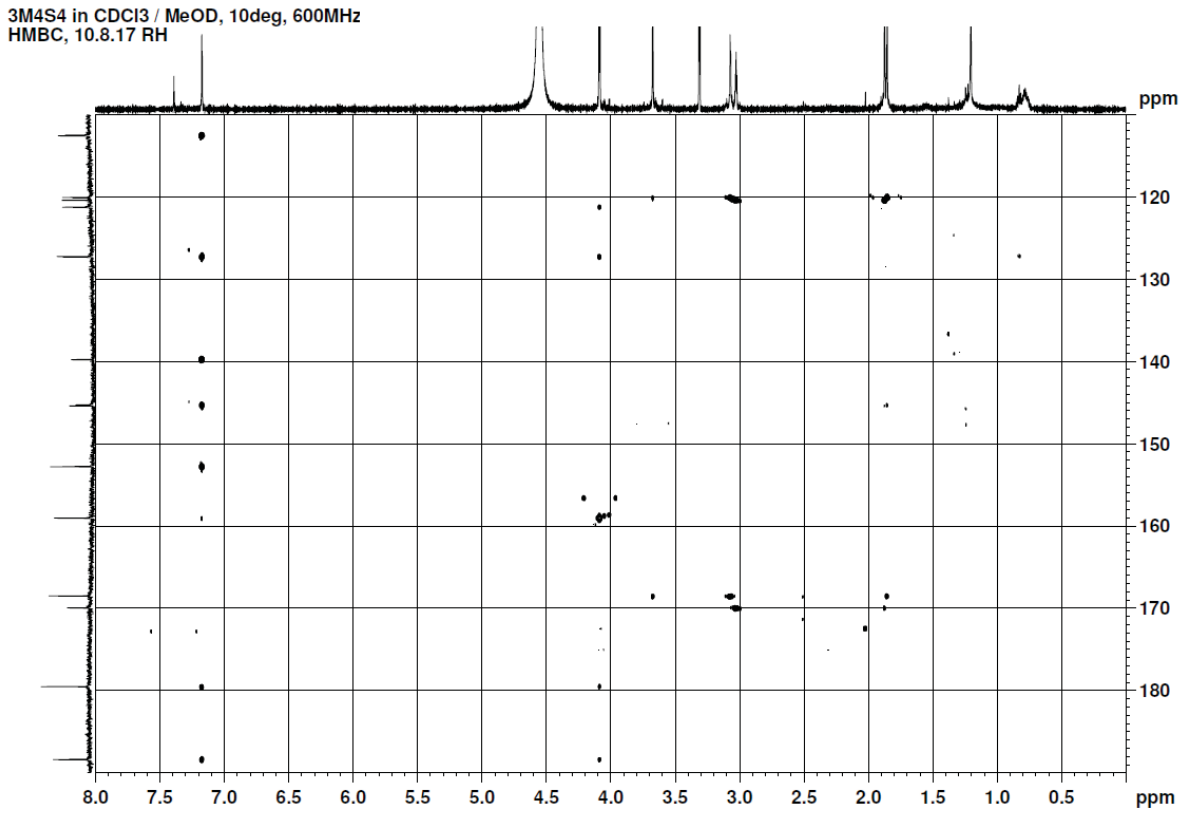

S7. Long-range HMBC (600 and 150 MHz, $CDCl_3$-CD_3OD 2:1) spectrum of compound **1**.

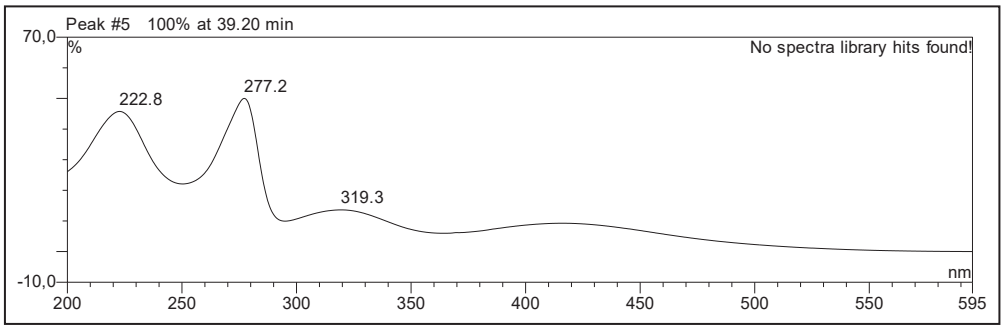

S8. UV spectrum of compound **2**.

Mass Spectrum SmartFormula Report

Analysis Info

Analysis Name	D:\Data\spektren2016\Proksch16HR000294.d	Acquisition Date	12/8/2016 2:36:47 PM
Method	tune_low_new.m	Operator	Peter Tommes
Sample Name	Moussa 3M8SP10 (CH3OH)	Instrument	maXis 288882.20213
Comment			

Acquisition Parameter

Source Type	ESI	Ion Polarity	Positive	Set Nebulizer	0.3 Bar
Focus	Not active	Set Capillary	4000 V	Set Dry Heater	180 °C
Scan Begin	50 m/z	Set End Plate Offset	-500 V	Set Dry Gas	4.0 l/min
Scan End	1500 m/z	Set Collision Cell RF	600.0 Vpp	Set Divert Valve	Source

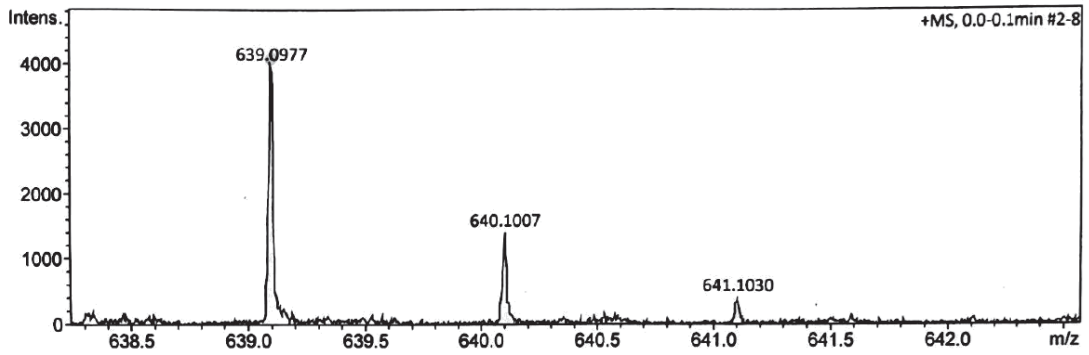

Meas. m/z	#	Ion Formula	m/z	err [ppm]	mSigma	# mSigma	Score	rdb	e⁻ Conf	N-Rule
639.0977	1	C28H11N14O6	639.0981	0.6	16.7	1	100.00	30.5	even	ok
	2	C30H23O16	639.0981	0.6	17.3	2	98.34	19.5	even	ok

S9. HRESIMS spectrum of compound **2**.

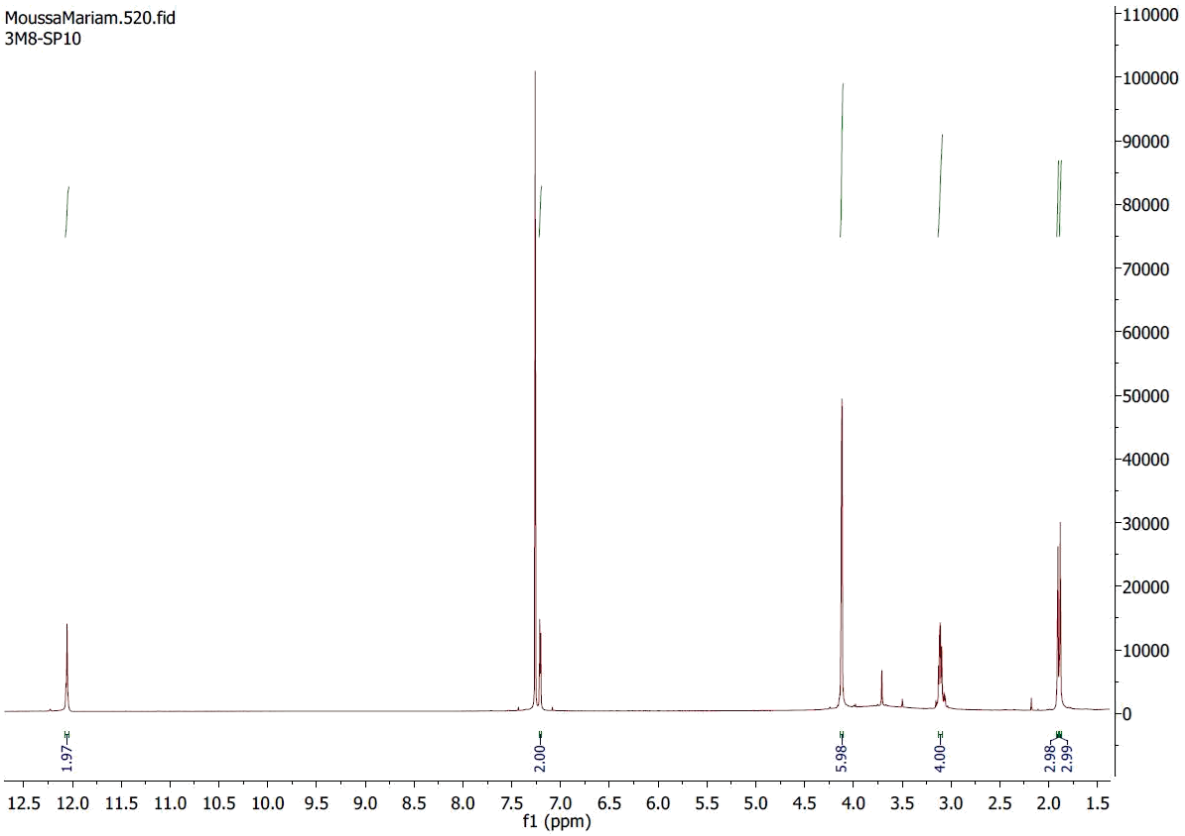

S10. ^{1}H NMR (600 MHz, $CDCl_3$) spectrum of compound **2**.

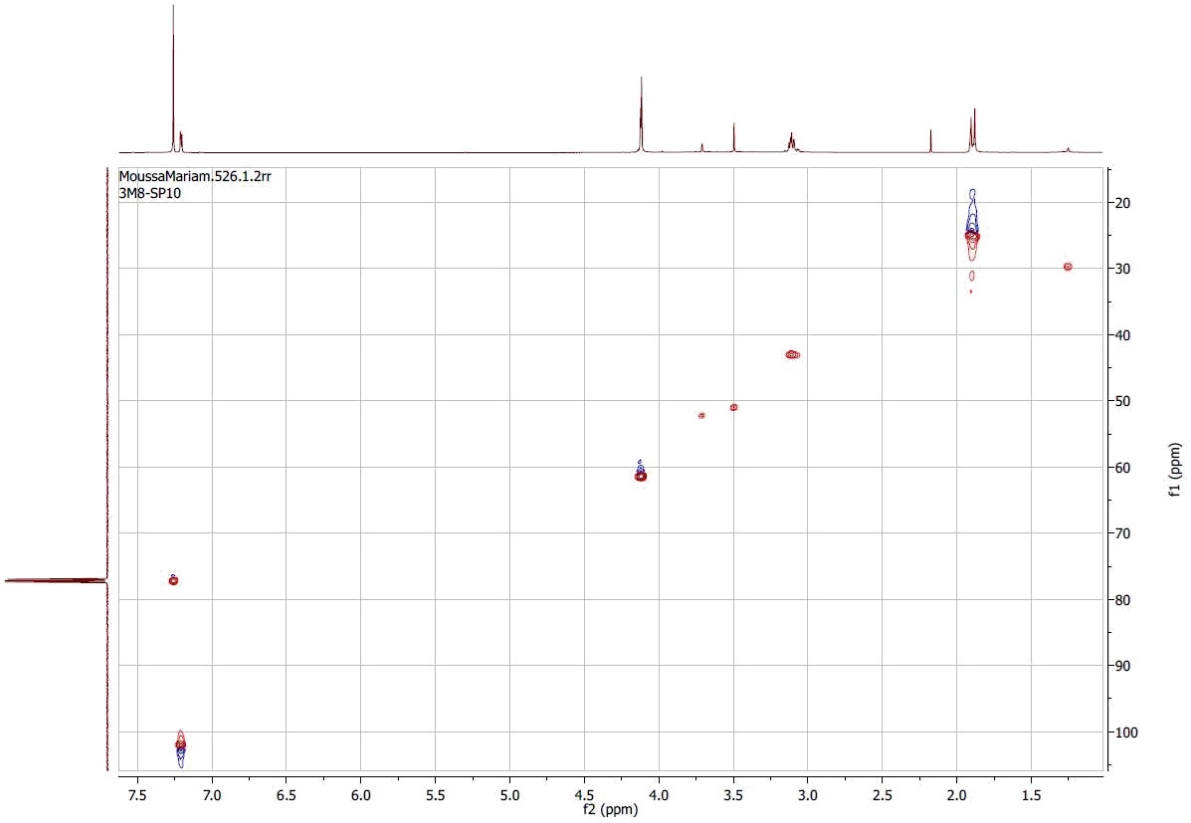

S11. HSQC (600 and 150 MHz, $CDCl_3$) spectrum of compound **2**.

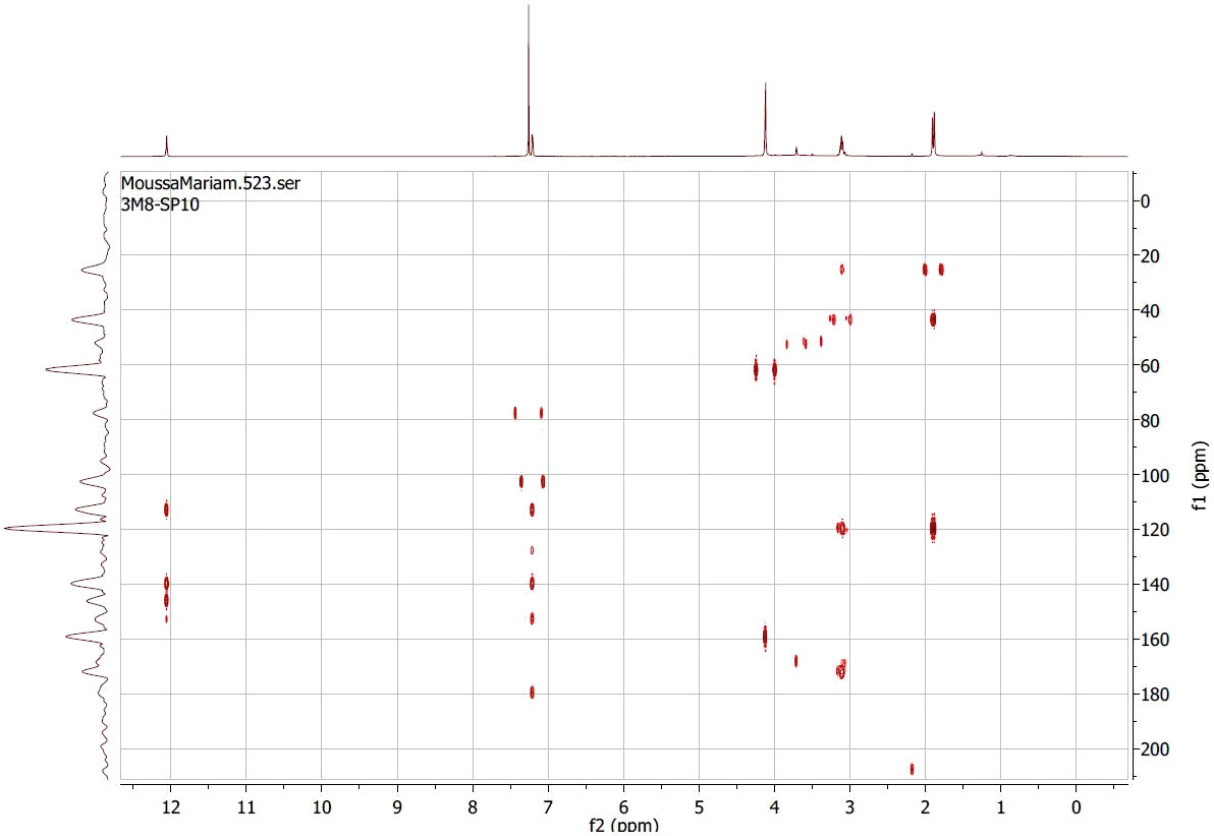

S12. HMBC (600 and 150 MHz, $CDCl_3$) spectrum of compound **2**.

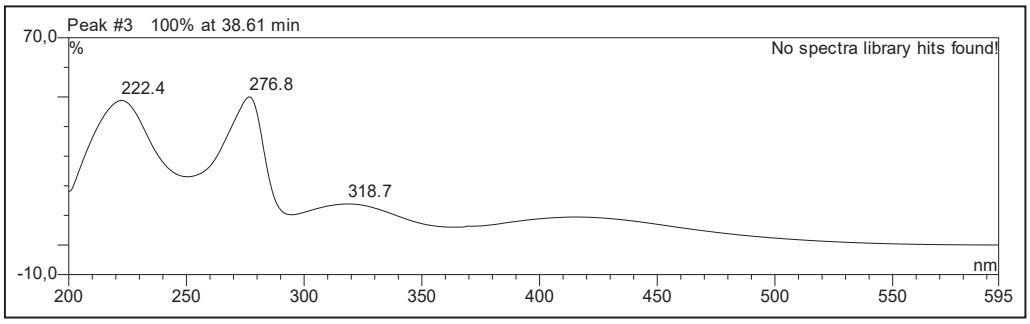

S13. UV spectrum of compound **3**.

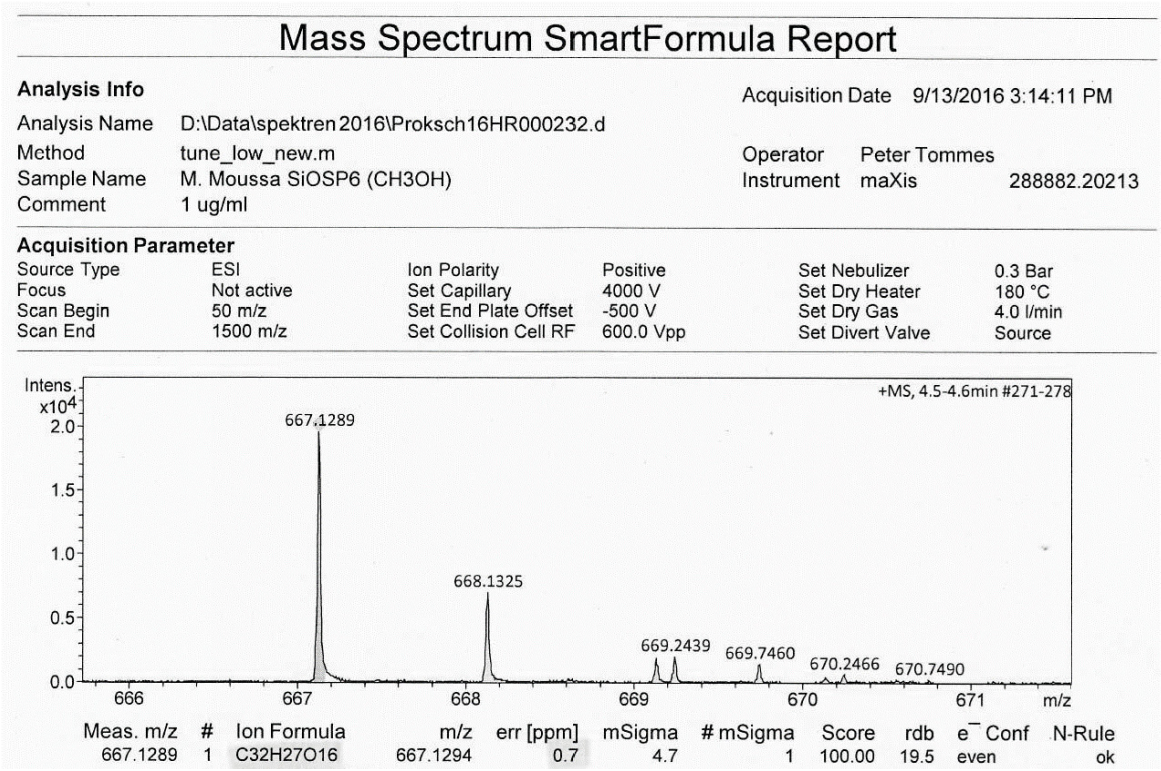

S14. HRESIMS spectrum of compound **3**.

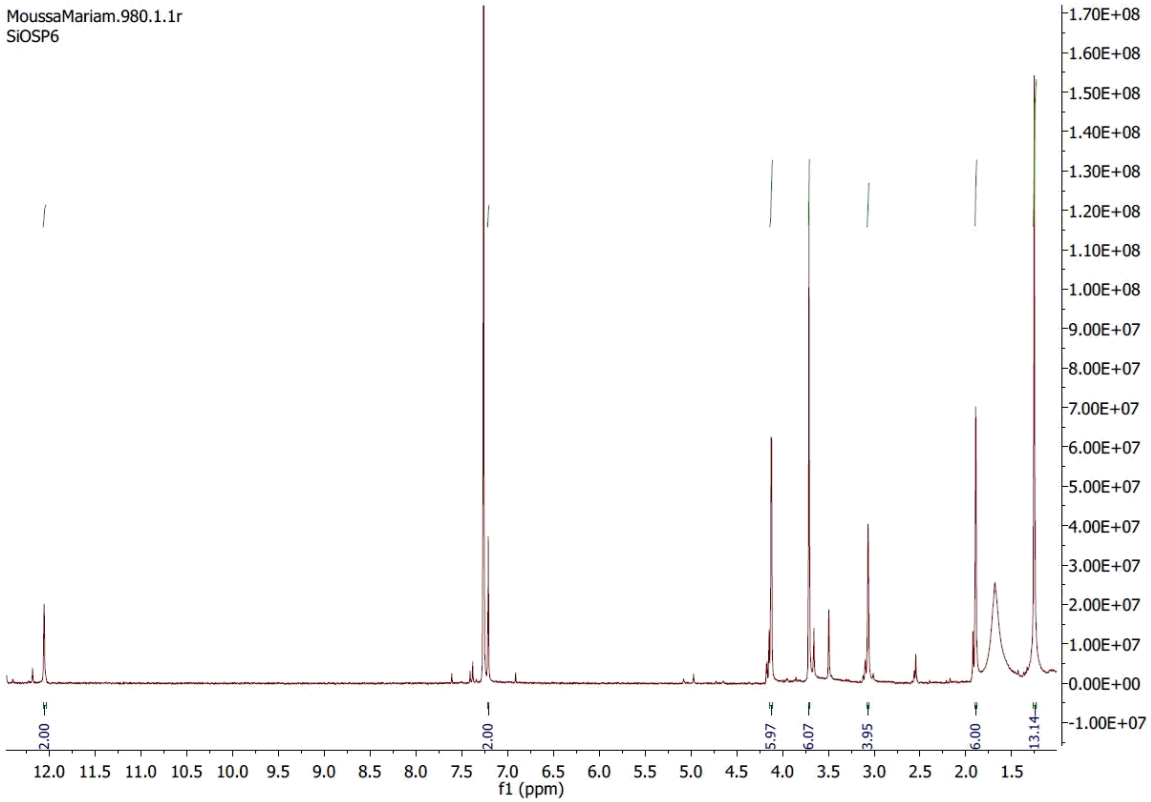

S15. ^{1}H NMR (600 MHz, $CDCl_3$) spectrum of compound **3**.

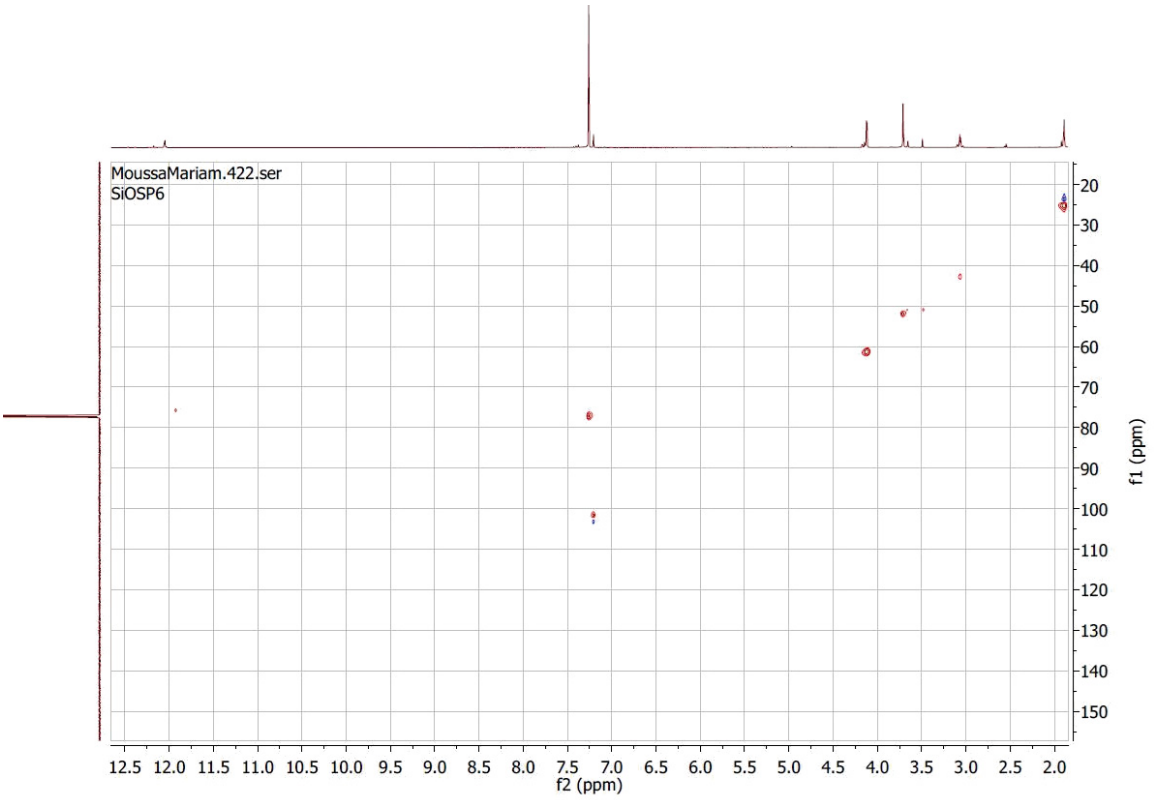

S16. HSQC (600 and 150 MHz, $CDCl_3$) spectrum of compound **3**.

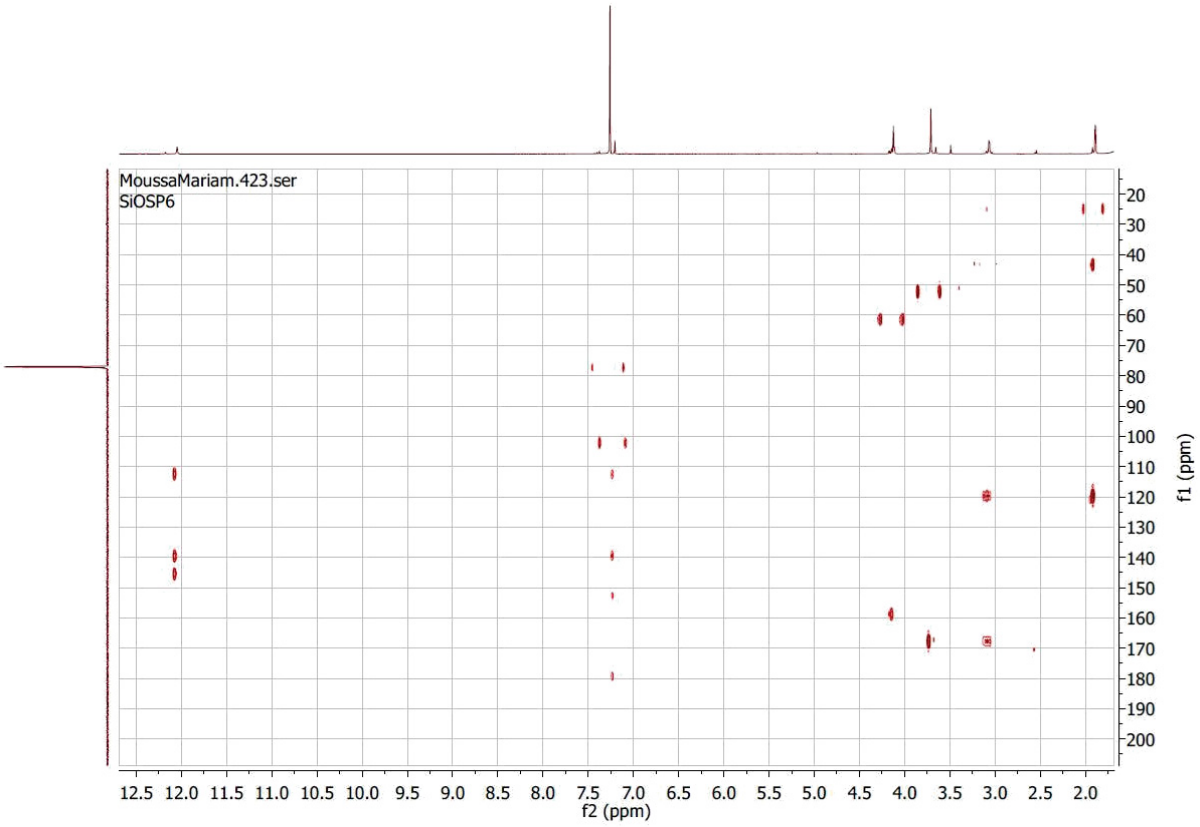

S17. HMBC (600 and 150 MHz, $CDCl_3$) spectrum of compound **3**.

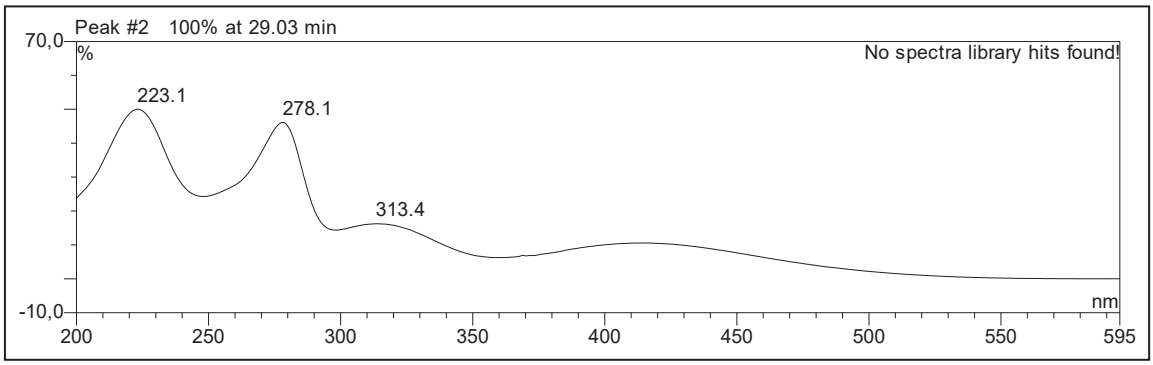

S18. UV spectrum of compound **4**.

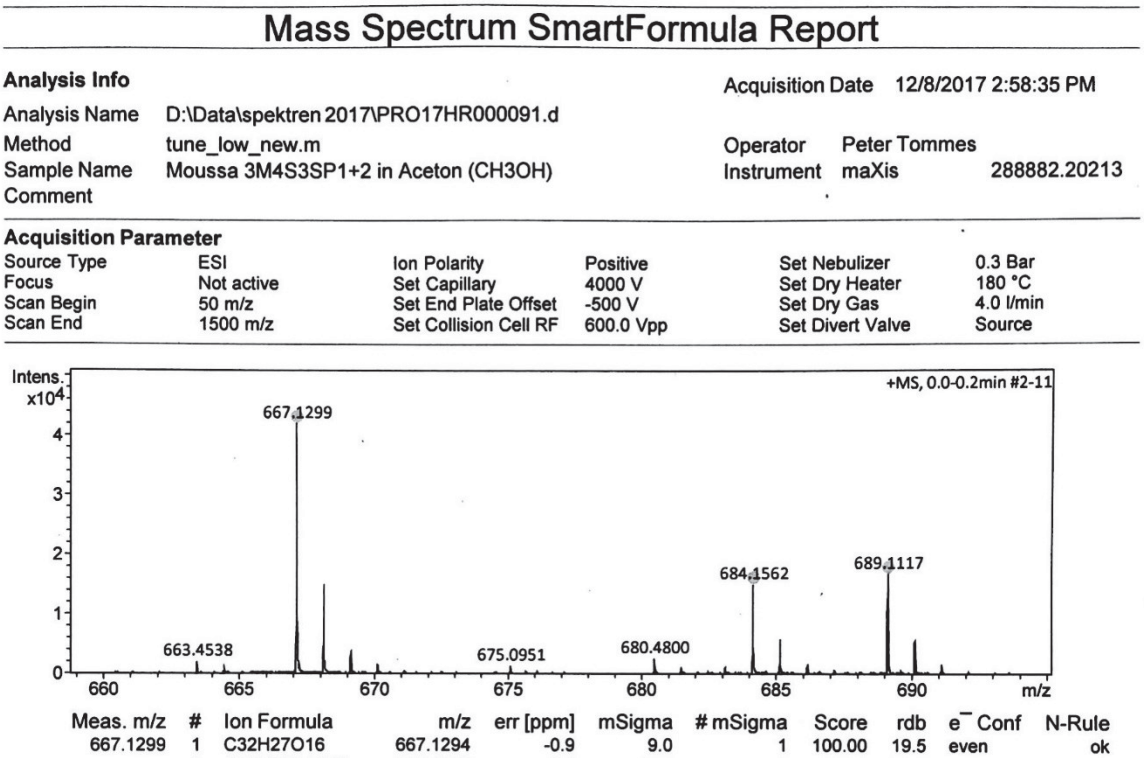

S19. HRESIMS spectrum of compound **4**.

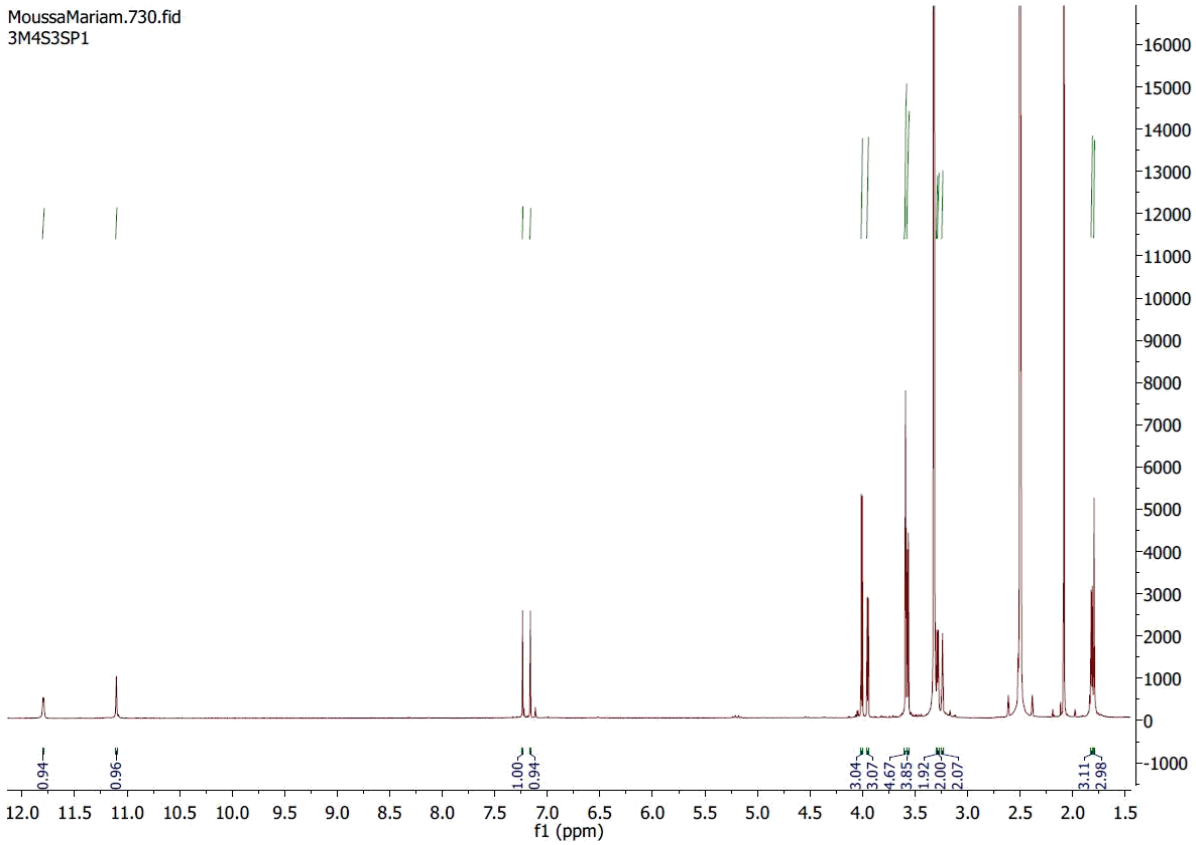

S20. ^{1}H NMR (600 MHz, DMSO-d_6) spectrum of compound **4**.

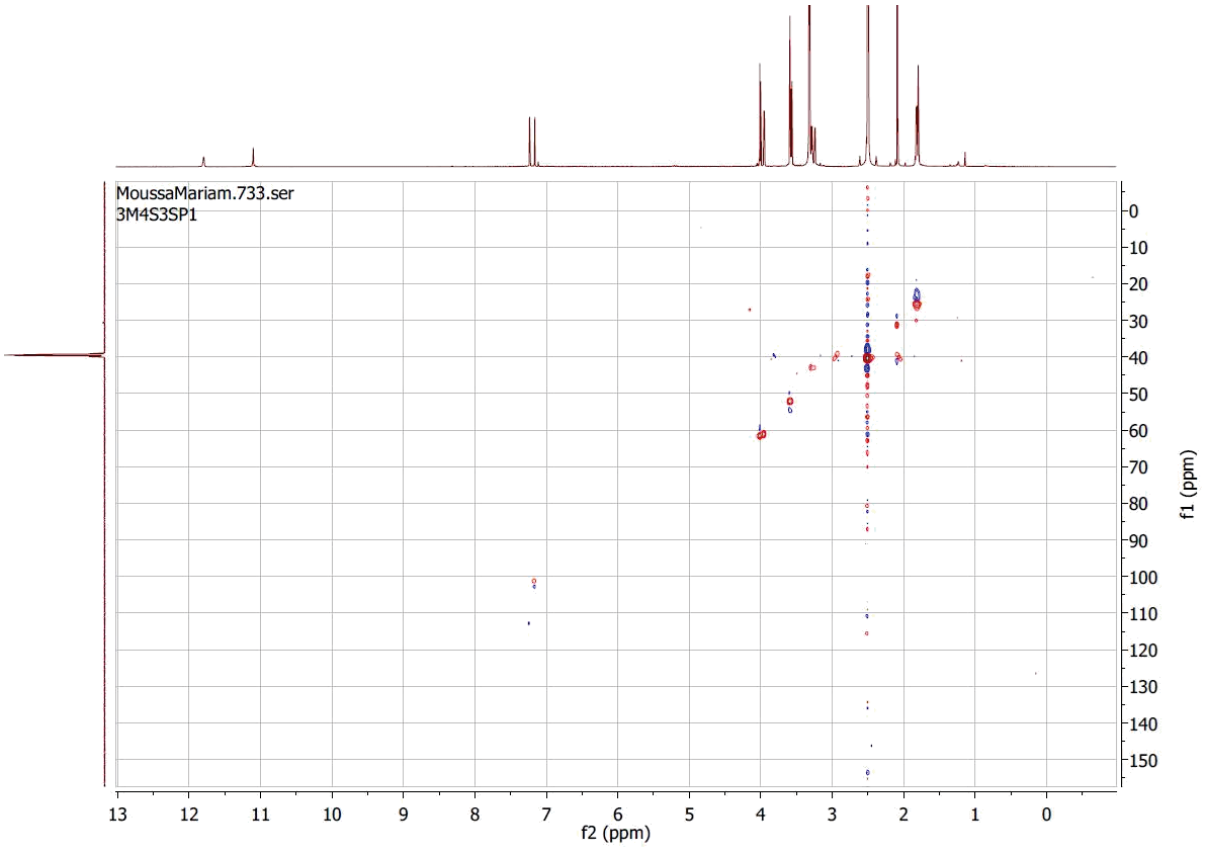

S21. HSQC (600 and 150 MHz, DMSO-d_6) spectrum of compound **4**.

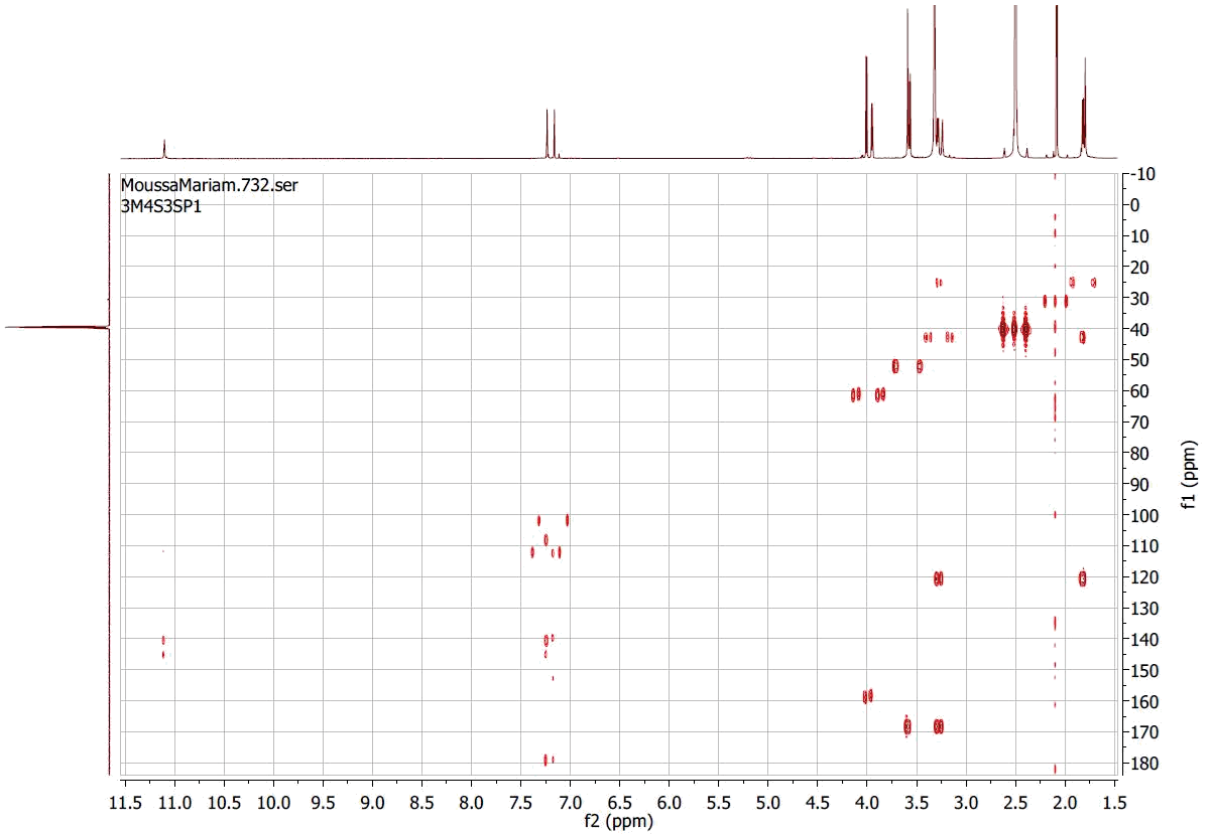

S22. HMBC (600 and 150 MHz, DMSO-d_6) spectrum of compound **4**.

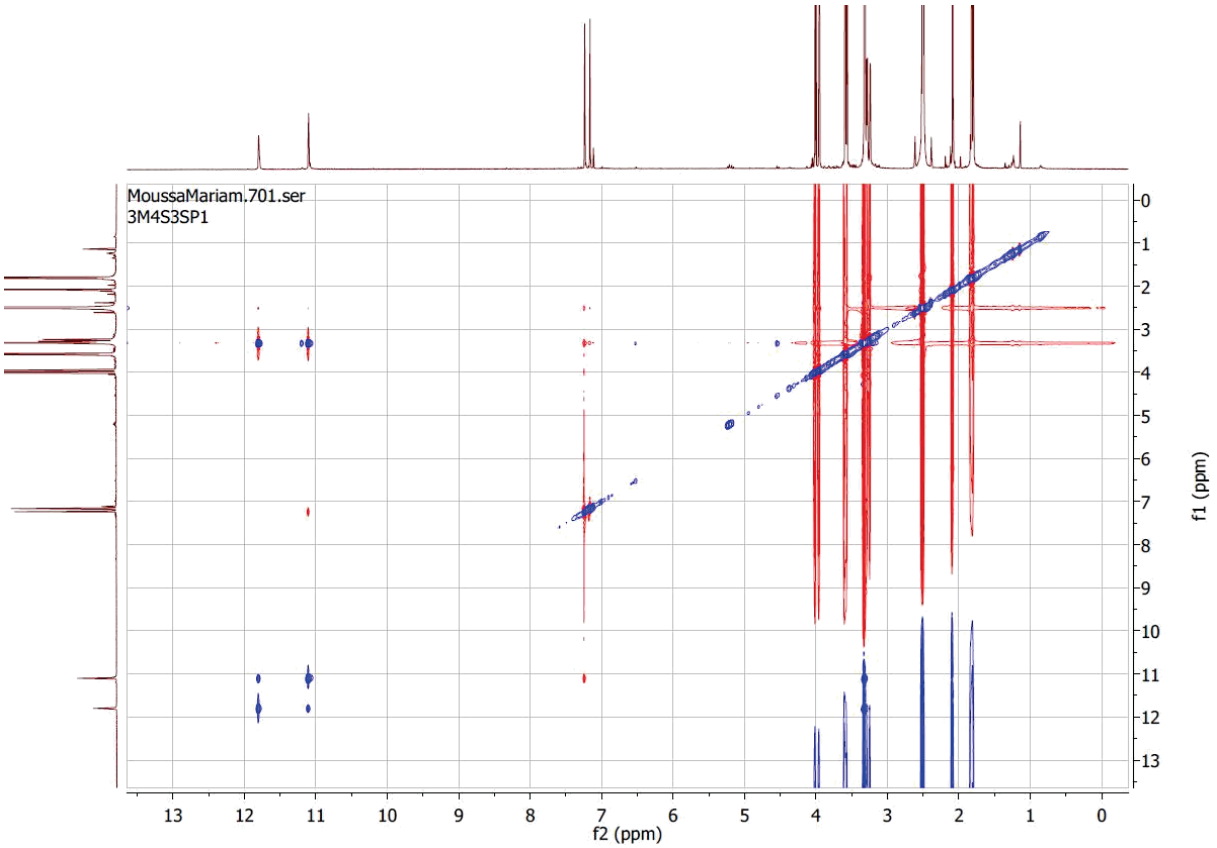

S23. ROESY (600 and 150 MHz, DMSO-d_6) spectrum of compound **4**.

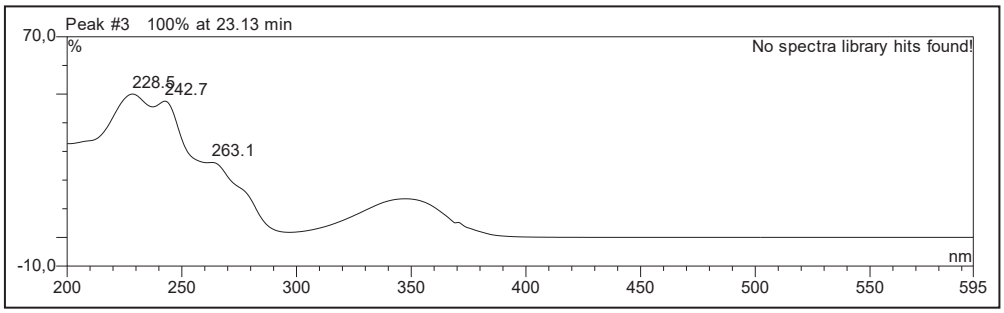

S24. UV spectrum of compound **5**.

Mass Spectrum SmartFormula Report

Analysis Info

Analysis Name	D:\Data\spektren 2016\Proksch16HR000128.d	Acquisition Date	4/28/2016 1:15:53 PM
Method	tune_low_new.m	Operator	Peter Tommes
Sample Name	Moussa 3M5SP1 (CH3OH)	Instrument	maXis 288882.20213
Comment			

Acquisition Parameter

Source Type	ESI	Ion Polarity	Positive	Set Nebulizer	0.3 Bar
Focus	Not active	Set Capillary	4000 V	Set Dry Heater	180 °C
Scan Begin	50 m/z	Set End Plate Offset	-500 V	Set Dry Gas	4.0 l/min
Scan End	1500 m/z	Set Collision Cell RF	600.0 Vpp	Set Divert Valve	Source

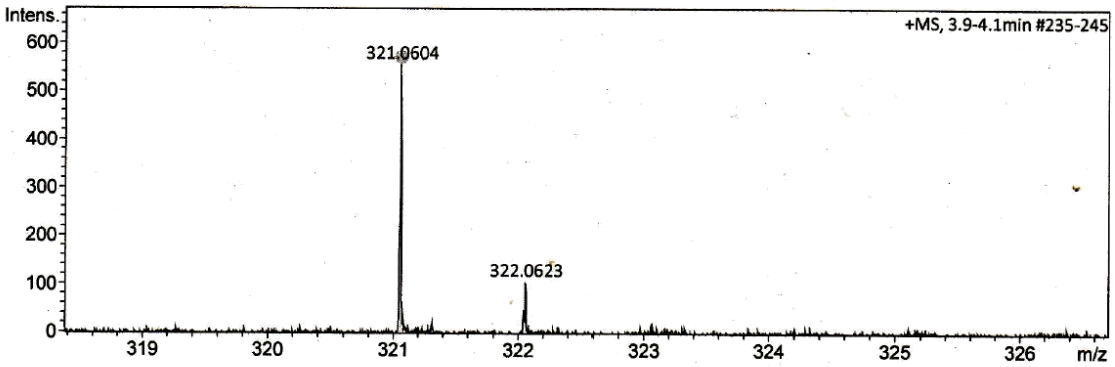

Meas. m/z	#	Ion Formula	m/z	err [ppm]	mSigma	# mSigma	Score	rdb	e⁻ Conf	N-Rule
321.0604	1	C15H13O8	321.0605	0.3	22.1	1	100.00	9.5	even	ok

S25. HRESIMS spectrum of compound **5**.

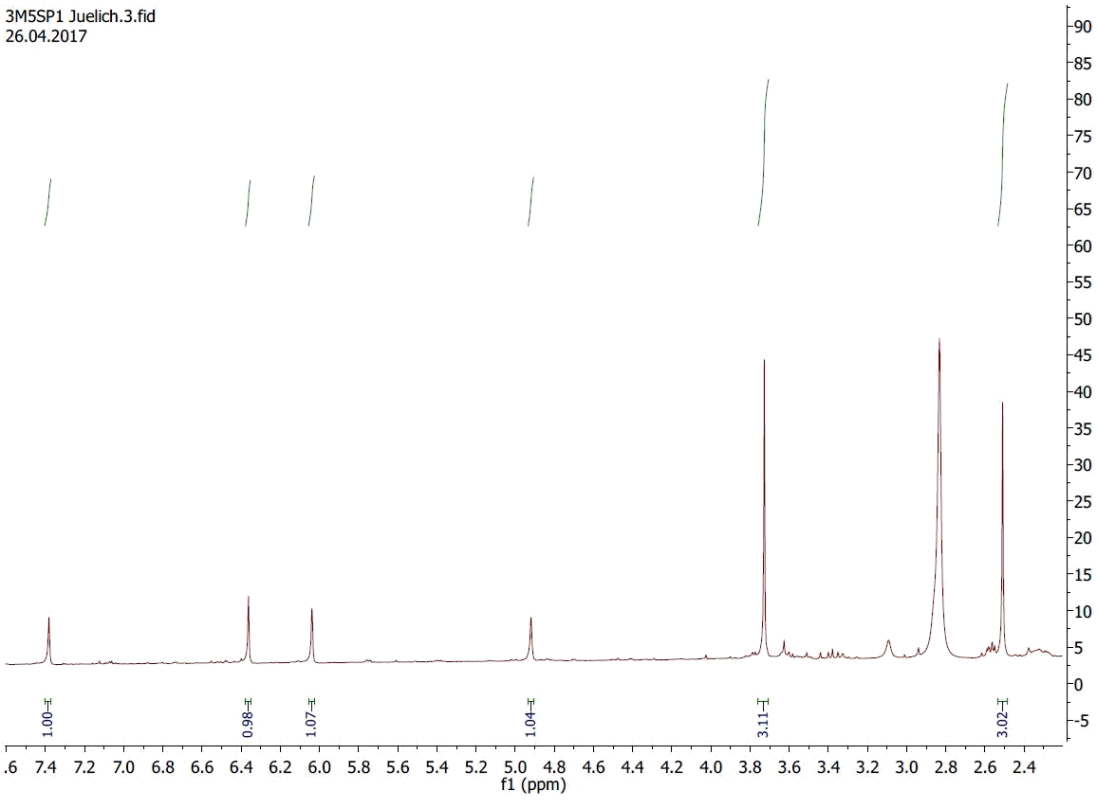

S26. ^{1}H NMR (750 MHz, acetone-d_6) spectrum of compound **5**.

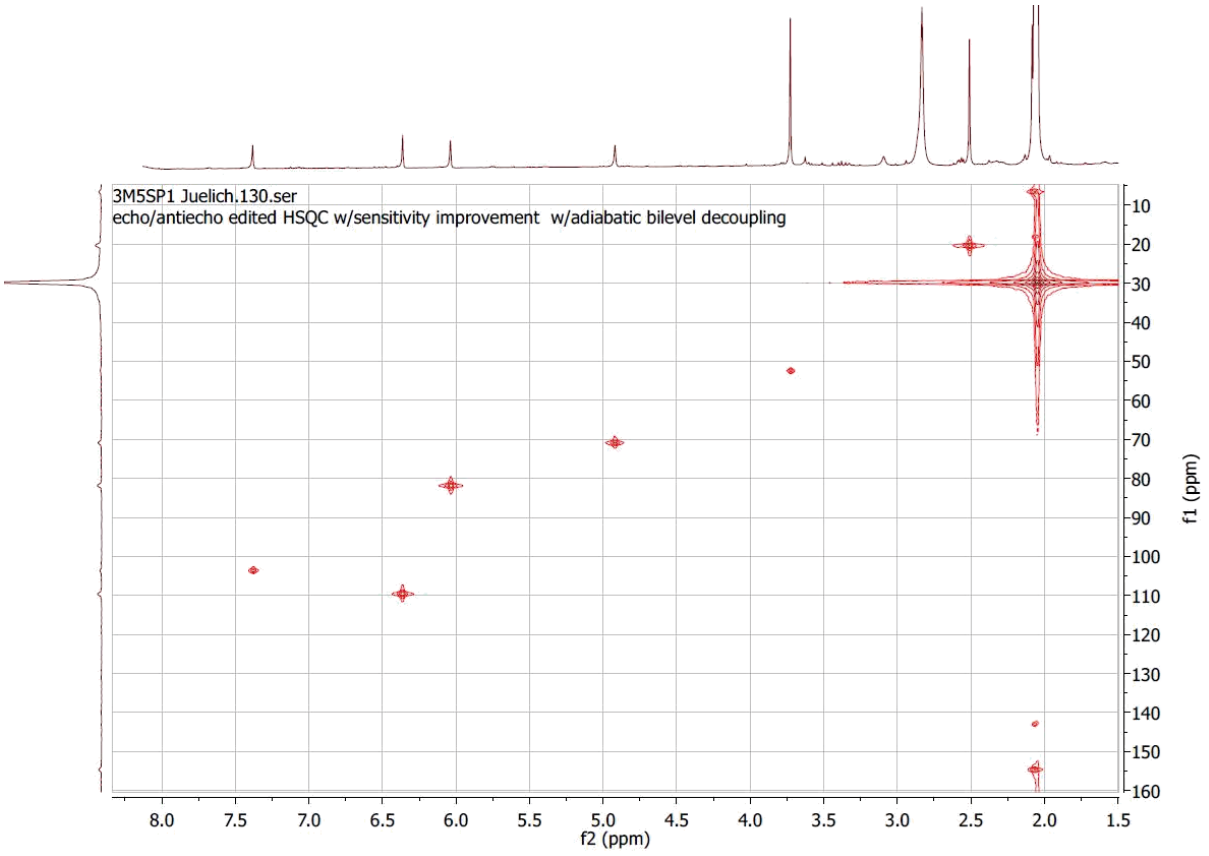

S27. HSQC (750 and 175 MHz, acetone-d_6) spectrum of compound **5**.

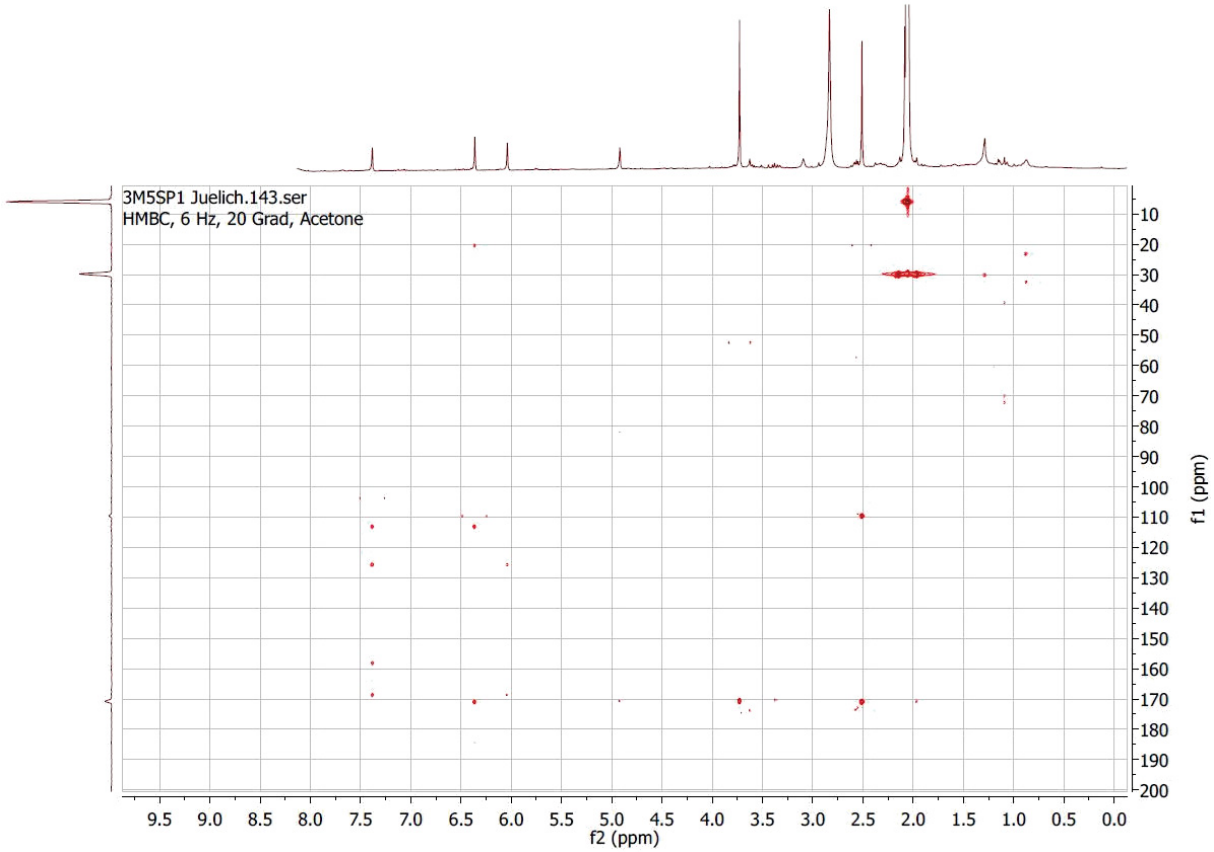

S28. HMBC (750 and 175 MHz, acetone-d_6) spectrum of compound **5**.

2.3 Publication III

Title

"*Co-culture of the Bacterium Pseudomonas aeruginosa with the Fungus Fusarium tricinctum Induces Bacterial Antifungal and Quorum Sensing Signalling Molecules*"

Submitted to: *Phytochemistry Letters*

Impact factor: 1.338

Personal contribution: 95%, first authorship, performing almost all of the laboratorial work, literature research, manuscript writing

Reprint from "Moussa, M.; Ebrahim, W.; Kalscheuer, R.; Liu, Z.; Proksch, P. (2020) Co-culture of the bacterium *Pseudomonas aeruginosa* with the fungus *Fusarium tricinctum* induces bacterial antifungal and quorum sensing signalling molecules. *Phytochemistry Letters*, submitted."

Co-culture of the Bacterium *Pseudomonas aeruginosa* with the Fungus *Fusarium tricinctum* Induces Bacterial Antifungal and Quorum Sensing Signalling Molecules

Mariam Moussa[a], Weaam Ebrahim[a,b], Rainer Kalscheuer[a], Zhen Liu[a,*], Peter Proksch[a,*]

[a] *Institute of Pharmaceutical Biology and Biotechnology, Heinrich-Heine-Universität Düsseldorf, Universitätsstrasse 1, 40225 Düsseldorf, Germany*

[b] *Department of Pharmacognosy, Faculty of Pharmacy, Mansoura University, Mansoura 35516, Egypt*

Corresponding authors:

Tel.: +49 211 81 15979; fax: +49 211 81 11923;

email: zhenfeizi0@sina.com (Z. Liu), proksch@uni-duesseldorf.de (P. Proksch)

ABSTRACT

Co-cultivation of viable cells of the human pathogenic bacterium *Pseudomonas aeruginosa* with the endophytic fungus *Fusarium tricinctum* induced silent bacterial biosynthetic gene clusters. Visual and chemical inspection of the co-cultures by comparison with the axenic cultures showed a clear reaction of *P. aeruginosa* towards its fungal competitor which was reflected by the deep greenish colouration of the co-cultures. Inspection of the HPLC chromatograms of the co-cultures revealed the induction of the pseudomonal quorum sensing molecule 2-heptyl-4-hydroxy-quinolone (HHQ) along with the antifungal phenazine alkaloids, phenazine-1-carboxylic acid (PCA) and phenazine-1-carboxamide (PCN), which are well-known metabolites of *P. aeruginosa*. The latter compounds were not detected in axenic bacterial cultures. In contrast to *P. aeruginosa*, no metabolic responses were detected for *F. tricinctum* which is in sharp contrast to previous co-culture experiments with this fungus using other bacteria.

Keywords: *Pseudomonas aeruginosa*; *Fusarium tricinctum*; co-culture; quorum sensing; antifungal.

1. Introduction

Co-cultivation of bacteria and fungi has been proven a powerful tool to expand the chemical diversity of microorganisms by inducing silent biosynthetic gene clusters thereby leading to the accumulation of non-expressed metabolites, meaning they were not detected in axenic cultures (Pettit et al., 2010; Marmann et al., 2014; Nonaka et al., 2015; Daletos et al., 2017). It is well-known from other studies as well as from our own previous investigations that usually the fungal metabolite pattern is affected in fungal-bacterial mixed fermentations whereas no clear induction of bacterial non-expressed metabolites is observed (Wang et al., 2013; Chen et al., 2015; Abdelwahab et al., 2018). During our previous co-culture experiments with the endophytic fungus *Fusarium tricinctum* employing different bacteria, the fungus was found to be very susceptible to the presence of bacteria, which resulted in the induced accumulation of several new and/or bioactive secondary metabolites. Co-cultivation of *F. tricinctum* with the bacterium *Bacillus subtilis* for example caused a clear enhancement of constitutively present antibiotic fungal compounds such as enniatins (up to 80-fold) and lateropyrone, and moreover induced the production of (−)-citreoisocoumarin and three further new NPs (Ola et al., 2013). In addition, co-culture of *F. tricinctum* with the bacterium *Streptomyces lividans* induced production of non-expressed fungal naphthoquinone dimers and of dihydrolateropyrone, that were not detected in axenic fungal controls (Moussa et al., 2019). For some non-expressed metabolites, however, that are produced during fungal-bacterial mixed cultures it is not obvious whether they are of fungal or bacterial origin. Prominent examples of the latter type are anthranilic acid derivatives (Wiklund et al., 2003 and Kamdem et al., 2018), which may be produced by fungi and by bacteria alike (Larentis et al., 2011; Li et al., 2013).

In the present study we report on metabolic responses of the gram-negative human pathogenic bacterium *Pseudomonas aeruginosa* in mixed fermentation with the fungus *F. tricinctum* which resulted in an induced accumulation of the bacterial metabolites 2-heptyl-4-hydroxy-quinolone (HHQ), which is known as chemical clue for bacterial quorum sensing

(Diggle et al., 2007; McGlacken et al., 2010). Along with this compound, the metabolic production of the antifungal phenazine alkaloids, phenazine-1-carboxylic acid (PCA) and phenazine-1-carboxamide (PCN) was highly enhanced, which are known for their antifungal properties and have been reported to play a role in quorum sensing, aswell (Jayatilake et al., 1996; Price-Whelan et al., 2006).

2. Results and discussion

Performing a preliminary co-culture experiment of *F. tricinctum* with viable cells of *P. aeruginosa* resulted in the detection of new peaks in the HPLC chromatograms of the co-cultures when compared to the axenic fungal or bacterial cultures, thereby indicating the induction of non-expressed compounds. Based on this preliminary result, a second co-culture experiment under the exact same conditions as the first set up co-culture of *F. tricinctum* and *P. aeruginosa*, involving several culture flasks, was conducted (**Fig. 1**). Interestingly, the fungal and bacterial growth areas on the solid rice medium were macroscopically clearly distinct from each other. The deep greenish colour of the bacterium *P. aeruginosa* highlights the induced production of secondary metabolites as a metabolic response to the presence of the fungus.

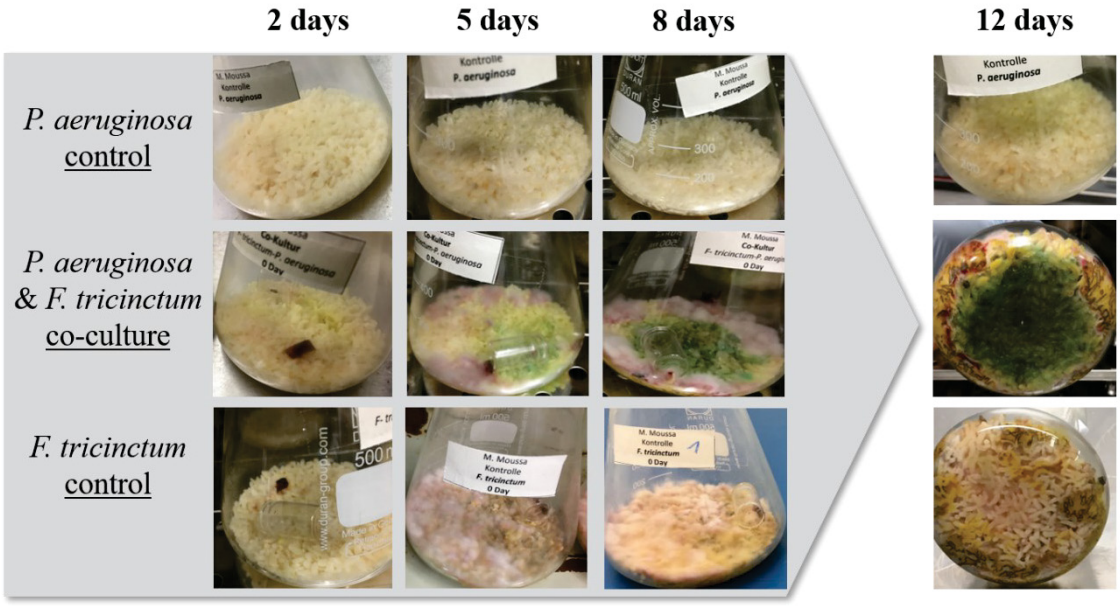

Fig. 1. Comparison of the growth behaviour and colouration of *P. aeruginosa* and *F. tricinctum* in axenic culture and as co-cultures after 2, 5, 8 and 12 days.

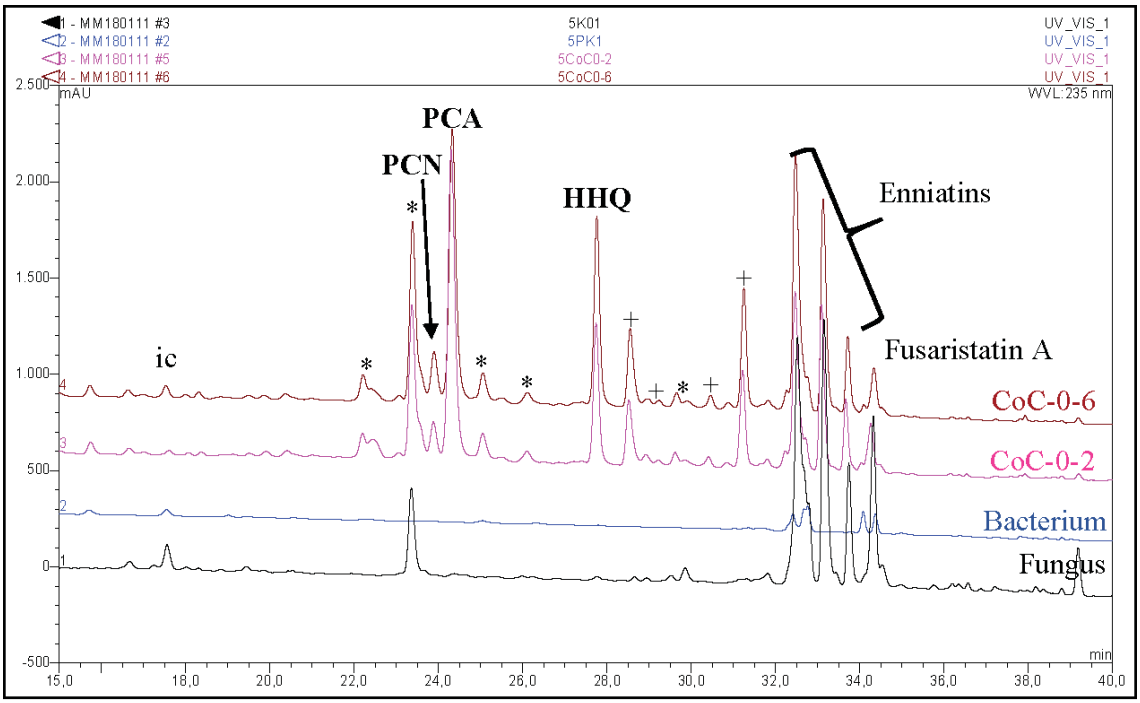

Fig. 2. HPLC overlay of extracts from axenic and from co-cultures of *F. tricinctum* and *P. aeruginosa*; ic: isocoumarine-derivative; *: further unknown induced compounds; +: further unknown HHQ derivatives.

The HPLC chromatograms of the axenic bacterial and fungal cultures and of the co-cultures give a clear insight into the interaction of the two microbes. The chromatograms of the axenic fungal cultures along with the co-cultures showed almost no changes in the chemical pattern of the fungus, which mainly consists of several enniatins and of fusaristatin A, in contrast to that of the bacterium (**Fig. 2**). The individual fungal compounds, enniatins and fusaristatin A were identified by comparison with the same metabolites, which have been re-isolated from the same fungus by our group, using HPLC and UV data comparison (Ola et al., 2013, Hemphill et al., 2017, Moussa et al., 2019). **Table 1** indicates that the amounts of the enniatins along with that of fusaristatin A remain almost unchanged in both the axenic fungal culture and in fungal-bacterial mixed cultures. At the same time prominent induced peaks were noticed in the chromatograms of the co-cultures (**Fig. 2**). The subsequent targeted chromatographic isolation of these compounds resulted in their identification as 2-heptyl-4-hydroxy-quinolone (HHQ) along with phenazine-1-carboxylic acid (PCA) and phenazine-1-

carboxamide (PCN) (**Fig. 3**) (Jayatilake et al., 1996, Pritchard, 2008). These alkaloids represent typical bacterial metabolites of *P. aeruginosa* which are accumulated at different amounts per culture flask in the co-cultures but are below detection limit in the axenic bacterial cultures. HHQ was found to be produced up to 26 mg, PCN up to 7.5 mg and PCA, showing the highest amounts, up to 85 mg per flask (**Table 2**). In previous studies devoted to co-culture experiments of *F. tricinctum* with other bacteria such as *B. subtilis* or *S. lividans*, metabolic reactions were largely confined to the fungus which responded to the presence of bacteria by an enhanced accumulation of constitutively present compounds or by production of non-expressed metabolites induced by activation of silent biosynthetic gene clusters. For example, a co-culture of *F. tricinctum* with *B. subtilis* resulted in an up to 78-fold enhanced production of bioactive compounds such as the polyketide lateropyrone, the cyclic depsipeptides enniatins A, B and B1 and the lipopeptide fusaristatin A and in the accumulation of three new non-expressed compounds (macrocarpon C, *N*-(carboxymethyl)anthranilic acid, (-)-citreoisocoumarinol) (Ola et al., 2013), whereas the co-culture of *F. tricinctum* with *S. lividans* caused an up to 12-fold increase of the latter *Fusarium* metabolites in addition to the accumulation of four new naphthoquinone dimers (fusatricinones A−D), a new lateropyrone derivative (dihydrolateropyrone) and the production of four non-expressed compounds (zearalenone, macrocarpon C, (-)-citreoisocoumarin, 7-hydroxy-2-(2-hydroxypropyl)-5-methylchromone) (Moussa et al., 2019).

In all cases, no clear induction of bacterial metabolites was observed. Combined with the results of the present study it appears that the metabolic responses of fungi (in this case *F. tricinctum*) and bacteria during a co-culture situation depend highly on the specific bacteria chosen.

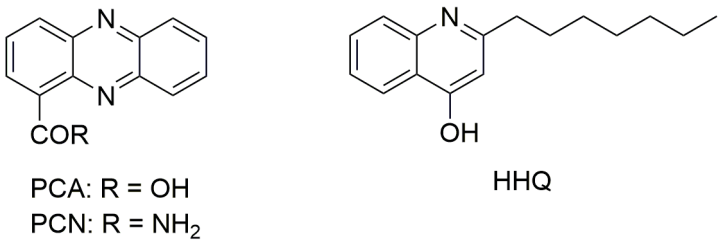

Fig. 3. Structures of identified non-expressed compounds from the co-culture of *F. tricinctum* with viable *P. aeruginosa*.

Table 1. Yields of induced fungal metabolites per flask of co-culture of *F. tricinctum* and *P. aeruginosa*; flasks of co-cultures (*n*=7) vs. axenic controls of *F. tricinctum* (*n*=3).

compound	Fungal control (mg)	Co-cultures (mg)
Enniatin B	169.7 ± 110.7	161.9 ± 149.4
Enniatin B1	107.1 ± 72.9	136.1 ± 125.7
Enniatin A1	49.9 ± 25.0	48.7 ± 46.3
Fusaristatin A	74.2 ± 37.7	36.5 ± 47.9

Table 2. Yield of induced bacterial metabolites per flask of co-cultures of *F. tricinctum* and *P. aeruginosa*; flasks of co-cultures (*n*=7) vs. axenic controls of *P. aeruginosa* (*n*=2).

compound	Bacterial control (mg)	Co-cultures (mg)
PCA	n.d.	85.1 ± 75.1
PCN	n.d.	7.5 ± 8.5
HHQ	n.d.	26.1 ± 11.4

n.d.= not detected.

Similar results were reported for the fungus *Chaetomium* sp. During co-cultivation of this fungus with *B. subtilis*, five new fungal products (shikimeran, bipherin A, chorismeron, quinomeran, serkydayn) and two non-expressed compounds (isosulochrin, protocatechuic acid methyl ester), which are lacking in axenic fungal cultures, were accumulated (Akone et al., 2016). Treatment of *Chaetomium* sp. with autoclaved cultures of *P. aeruginosa,* however, resulted in an enhanced accumulation (up to 33-fold) of constitutively present new fungal butenolides (chaetobutenolides A−C, WF-3681) and of further shikimic acid derivatives (chaetoisochorismin, shikimeran B) (Ancheeva et al., 2017).

The gram-negative bacterium *P. aeruginosa* is known for its resistance towards many antibiotic drugs, thereby causing acute and chronic infections (Rasamirakava et al., 2015). *P.*

aeruginosa was found to protect itself against antibiotic treatment and the host immune defence system by quorum sensing and biofilm formation (Wagner et al., 2016). Members of the genus *Pseudomonas* are also known for their antifungal phenazines, which can be interpreted as a metabolic response of *P. aeruginosa* to the presence of *F. tricinctum* as described in this study. The quorum sensing molecule HHQ was first reported in 1998 as a metabolite of a marine *Pseudomonas* species, which was isolated from the sponge *Suberea creba* (Debitus et al., 1998). HHQ has been identified as the direct precursor of the quorum sensing molecule 2-heptyl-3-hydroxy-4(1*H*)-quinolone, also known as pseudomonal quinolone signal (PQS) (Diggle et al., 2007; McGlacken et al., 2010). It was found to be produced by *P. aeruginosa* cells and then is taken up by neighbouring cells, which convert it into PQS – cell-to-cell communication (Diggle et al., 2007). One of the virulence factors of this microbe is MvfR, which regulates transcriptional pathways, and HHQ can bind to a specific ligand-binding domain of this protein. Researchers are focusing on this pathway, in order to inhibit this protein-based gene expression of pathogenicity by creating similar molecules to HHQ (Xiao et al., 2006).

The present study describes the fungal effect on silent bacterial gene clusters of *P. aeruginosa*, leading to the activation of the bacterial defence system by producing antifungal and quorum sensing molecules. A similar experiment was recently reported for the marine derived fungus *Aspergillus fumigatus* and two different *Streptomyces leeuwenhoekii* strains, which induced the accumulation of the bacterial natural product chaxapeptin. The latter was only detectable in co-cultures. The authors stated that this was the first time of bacterial secondary metabolites induction in a co-culture experiment (Wakefield et al., 2017). Our study is the second example that shows a fungal activation of silent bacterial biosynthetic gene clusters.

3. Experimental section

3.1.General experimental procedures

In order to assess the metabolic profile of crude extracts or subfractions and the purity of

isolated natural products, a Dionex P580 system connected with the UVD340S detector was utilized. Standard operation system started with 10% MeOH and increased to 100% MeOH within 30 min, and then keeping the 100% MeOH gradient for another 30 min. UV detection was set up at 235, 254, 280, and 340 nm. The analytical column (125 × 4 mm, L × i.d.) was packed with Eurosphere-10 C_{18} (Knauer, Germany). Elution was carried out with a flow rate of 1.0 mL/min. TLC was performed on sheets of aluminium foil, coated with a thin layer of silica gel 60 F254 (Merck).

3.2.Microbial material

The endophytic fungus *F. tricinctum* was isolated from fresh and healthy rhizomes of *Aristolochia paucinervis*. The plant material was gathered in January 2006 from the mountains of Beni-Mellal in Morocco. A voucher sample is kept in the Laboratoire des Substances Naturelles et Thermolyse Éclair, University Mohammad V-Agdal, Faculty of Sciences, Rabat, Morocco. The fungal competitor was identified as *F. tricinctum* applying the biological protocol of DNA isolation and amplification using ITS method that has been described before (Moussa et al., 2019). A voucher strain of the fungus *F. tricinctum* is stored at -80 °C in the Institute of Pharmaceutical Biology and Biotechnology, Heinrich-Heine University Düsseldorf, Germany. The bacterium *Pseudomonas aeruginosa* ATCC27853 was obtained from LGC Standards GmbH, Germany.

3.3.Co-cultivation procedure

The bacterium *P. aeruginosa* was pre-cultured on Müller-Hinton (MH) solid medium at 37°C. Afterwards, colonies of the bacterium were transferred to an Erlenmeyer flask (200 mL), prefilled with MH broth and left on a shaker at 37°C and 80 rpm, until the culture density reached 0.235 $OD_{600\ nm}$ (approximate value 0.15-0.4 OD). The fungus was also pre-cultured. Pure cultures of the fungus were pre-cultivated on agar plates containing purification agar. Additional steps were necessary to keep the contamination risk to a minimum, by cutting equal amounts of fungal agar with a sterile razor blade and transferring them into small autoclaved

Eppendorf vials, that were consecutively added to the culture flasks that already had been inoculated with *P. aeruginosa*. Twelve Erlenmeyer flasks (500 mL) were prefilled with rice medium (25 g) and 50 mL water followed by autoclavation. Nine flasks were incubated with 5 mL of the bacterium in MH broth using a sterile 5 mL Eppendorf pipette. Seven flasks were simultaneously incubated with the fungus, whereas another two flasks were left as axenic bacterial controls (bacterial axenic culture showed no significant metabolic profile, so two flasks were sufficient references, since no quantification would be underdone with the axenic bacterial cultures). Fungal axenic controls (three flasks for quantification purposes) were set up under the same conditions and prepared accordingly on the first day of addition of the fungus to the bacterial cultures. In each step of fungal incubation, the vials with the fungal agar were sterilized with 70 % EtOH. The cultures were stored at 37°C.

The preliminary co-culture of *F. tricinctum* with *P. aeruginosa* was done by using six Erlenmeyer flasks (500 mL) prepared like described above (500 ml Erlenmeyer flasks, prefillied with 25 g rice and 50 ml water and afterwards autoclaved), from which two served for the co-culture, and the other four for the axenic bacterial and fungal cultures. The bacterial strain *P. aeruginosa* was pre-cultured (0.18 $OD_{600\ nm}$, approximate value 0.15-0.4 OD) and added to four flasks (co-culture and axenic bacterial control), as described before. Afterwards, the bacterial cultures were autoclaved. Next, the fungus was inoculated into four flasks (axenic fungal controls and co-culture) and the flasks stored in the fungi room at room temperature.

The fermentations of the preliminary and main co-cultures were stopped after 12 days, respectively, by adding 150 mL MeOH through the cellulose plugs of the flasks via 50 mL syringe holding a specific cannula (Erhardt SUPRA 2.00 × 120 mm). All incubation and fermentation steps were performed under the laminar airflow and sterile conditions. After adding MeOH, the plug was removed to slice the rice into pieces. The sterile flasks where next put on a shaker for 5 h. The MeOH extract was subjected to liquid-liquid partitioning by adding 10 % distilled H_2O and shaking against *n*-hexane. The MeOH fraction was then evaporated and

dissolved in EtOAc, followed by liquid-liquid partitioning against distilled H_2O. The obtained EtOAc fraction was then subjected to HPLC analysis. After removing EtOAc, 50 mL HPLC grade MeOH was added to the resulting residue followed by injection into the HPLC system.

Acknowledgements

This work was supported by the Deutsche Forschungsgemeinschaft (DFG, German Research Foundation) – project number 270650915/GRK2158 (to P.P. and R.K.). P.P. is further indebted to the Manchot Foundation for support. Also, we thank H. Goldbach-Gecke for technical assistance.

References

Abdelwahab, M.F., Kurtán, T., Mándi, A., Müller, W.E.G., Fouad, M.A., Kamel, M.S., Liu, Z., Ebrahim, W., Daletos, G., Proksch, P., 2018. Induced secondary metabolites from the endophytic fungus *Aspergillus versicolor* through bacterial co-culture and OSMAC approaches. Tetrahedron Lett. 59, 2647−2652.

Akone, S.H., Mándi, A., Kurtán, T., Hartmann, R., Lin, W.H., Daletos, G., Proksch, P., 2016. Inducing secondary metabolite production by the endophytic fungus *Chaetomium* sp. through fungal-bacterial co-culture and epigenetic modification. Tetrahedron 72, 6340−6347.

Ancheeva, E., Küppers, L., Akone, S.H., Ebrahim, W., Liu, Z., Mándi, A., Kurtán, T., Lin, W.H., Orfali, R., Rehberg, N., Kalscheuer, R., Daletos, G., Proksch, P., 2017. Expanding the metabolic profile of the fungus *Chaetomium* sp. through co-culture with autoclaved *Pseudomonas aeruginosa*. Eur. J. Org. Chem. 2017, 3256−3264.

Chen, H., Daletos, G., Abdel-Aziz, M.S., Thomy, D., Dai, H., Brötz-Oesterhelt, H., Lin, W.H., Proksch, P., 2015. Inducing secondary metabolite production by the soil-dwelling fungus *Aspergillus terreus* through bacterial co-culture. Phytochem. Lett. 12, 35−41.

Daletos, G., Ebrahim, W., Ancheeva, E., El-Neketi, M., Lin, W.H., Proksch, P., 2017. Microbial co-culture and OSMAC approach as strategies to induce cryptic fungal biogenetic gene

clusters. Chem. Biol. Nat. Prod., Grothaus, P., Cragg, G.M., Newman, D.J., Eds, 233−284.

Debitus, C., Guella, G., Mancini, I.I., Waikedre, J., Guemas, J.P., Nicolas, J.L., Pietra, F., 1998. Quinolones from a bacterium and tyrosine metabolites from its host sponge, *Suberea creba* from the Coral Sea. J. Mar. Biotechnol. 6, 136−141.

Diggle, S.P., Matthijs, S., Wright, V.J., Fletcher, M.P., Chhabra, S.R., Lamont, I.L., Kong, X., Hider, R.C., Cornelis, P., Cámara, M., Williams, P., 2007. The *Pseudomonas aeruginosa* 4-quinolone signal molecules HHQ and PQS play multifunctional roles in quorum sensing and iron entrapment. Chem. Biol. 14, 87−96.

Hemphill, C.F.P., Sureechatchaiyan, P., Kassack, M.U., Orfali, R.S., Lin, W.H., Daletos, G., Proksch, P., 2017. OSMAC approach leads to new fusarielin metabolites from *Fusarium tricinctum*. J. Antibiot. 70, 726-732.

Jayatilake, G.S., Thornton, M.P., Leonard, A.C., Grimwade, J.E., Baker, B.J., 1996. Metabolites from an Antarctic sponge-associated bacterium, *Pseudomonas aeruginosa*. J. Nat. Prod. 59, 293−296.

Kamdem, R.S.T., Wang, H., Wafo, P., Ebrahim, W., Özkaya, F.C., Makhloufi, G., Janiak, C., Sureechatchaiyan, P., Kassack, M.U., Lin, W.H., Liu, Z., Proksch, P., 2018. Induction of new metabolites from the endophytic fungus *Bionectria* sp. through bacterial co-culture. Fitoterapia. 124, 132−136.

Larentis, A.L., Sampaio, H.C.C., Carneiro, C.C., Martins, O.B., Alves, T.L.M., 2011. Evaluation of growth, carbazole biodegradation and anthranilic acid production by *Pseudomonas stutzeri*. Braz. J. Chem. Eng. 28, 37−44.

Li, C.S., Li, X.M., Gao, S.S., Lu, Y.H., Wang, B.G., 2013. Cytotoxic anthranilic acid derivatives from deep sea sediment-derived fungus *Penicillium paneum* SD-44. Mar. Drugs 11, 3068−3076.

Marmann, A., Aly, A.H., Lin, W., Wang, B., Proksch, P., 2014. Co-cultivation - a powerful emerging tool for enhancing the chemical diversity of microorganisms. Mar. Drugs 12,

1043−1065.

McGlacken, G.P., McSweeney, C.M., O'Brien, T., Lawrence, S.E., Elcoate, C.J., Reen, F.J., O'Gara, F., 2010. Synthesis of 3-halo-analogues of HHQ, subsequent cross-coupling and first crystal structure of *Pseudomonas* quinolone signal (PQS). Tetrahedron Lett. 51, 5919−5921.

Moussa, M., Ebrahim, W., Bonus, M., Gohlke, H., Mándi, A., Kurtán, T., Hartmann, R., Kalscheuer, R., Lin, W.H., Liu, Z., Proksch, P., 2019. Co-culture of the fungus *Fusarium tricinctum* with *Streptomyces lividans* induces production of cryptic naphthoquinone dimers. RSC Adv. 9, 1491−1500.

Nonaka, K., Chiba, T., Suga, T., Asami, Y., Iwatsuki, M., Masuma, R., Ōmura, S., Shiomi, K., 2015. Coculnol, a new penicillic acid produced by a coculture of *Fusarium solani* FKI-6853 and *Talaromyces* sp. FKA-65. J. Antibiot. 68, 530−532.

Ola, A.R., Thomy, D., Lai, D., Brötz-Oesterhelt, H., Proksch, P., 2013. Inducing secondary metabolite production by the endophytic fungus *Fusarium tricinctum* through coculture with *Bacillus subtilis*. J. Nat. Prod. 76, 2094−2099.

Pettit, R.K., Pettit, G.R., Xu, J.P., Weber, C.A., Richert, L.A., 2010. Isolation of human cancer cell growth inhibitory, antimicrobial lateritin from a mixed fungal culture. Planta Med. 76, 500−501.

Price-Whelan, A., Dietrich, L.E., Newman, D.K., 2006. Rethinking 'secondary' metabolism: physiological roles for phenazine antibiotics. Nat. Chem. Bio. 2, 71−78.

Pritchard, D.I., 2008. U.S. Patent No. 7,371,779. Washington, DC: U.S. Patent and Trademark Office.

Rasamiravaka, T., Labtani, Q., Duez, P., El Jaziri, M., 2015. The formation of biofilms by *Pseudomonas aeruginosa*: a review of the natural and synthetic compounds interfering with control mechanisms. BioMed Res. Int. 2015, 1−17.

Wagner, S., Sommer, R., Hinsberger, S., Lu, C., Hartmann, R.W., Empting, M., Titz, A., 2016.

Novel strategies for the treatment of *Pseudomonas aeruginosa* infections. J. Med. Chem. 59, 5929−5969.

Wakefield, J., Hassan, H.M., Jaspars, M., Ebel, R., Rateb, M.E., 2017. Dual induction of new microbial secondary metabolites by fungal bacterial co-cultivation. Front. Microbiol. 8, 1−10.

Wang, J.P., Lin, W.H., Wray, V., Lai, D., Proksch, P., 2013. Induced production of depsipeptides by co-culturing *Fusarium tricinctum* and *Fusarium begoniae*. Tetrahedron Lett. 54, 2492−2496.

Wiklund, P., Romero, I., Bergman, J., 2003. Products from dehydration of dicarboxylic acids derived from anthranilic acid. Org. Biomol. Chem. 1, 3396−3403.

Xiao, G., Déziel, E., He, J., Lépine, F., Lesic, B., Castonguay, M.H., Milot, S., Tampakaki, A. P., Stachel, S.E., Rahme, L.G., 2006. MvfR, a key *Pseudomonas aeruginosa* pathogenicity LTTR-class regulatory protein, has dual ligands. Mol. Microbiol. 62, 1689−1699.

2.3a Supplementary data III

Co-culture of the Bacterium *Pseudomonas aeruginosa* with the Fungus *Fusarium tricinctum* Induces Bacterial Antifungal and Quorum Sensing Signalling Molecules

Mariam Moussa[a], Weaam Ebrahim[b], Rainer Kalscheuer[a], Zhen Liu[a,*], Peter Proksch[a,*]

[a]Institute of Pharmaceutical Biology and Biotechnology, Heinrich-Heine-Universität Düsseldorf, Universitätsstrasse 1, 40225 Düsseldorf, Germany

[b]Department of Pharmacognosy, Faculty of Pharmacy, Mansoura University, Mansoura 35516, Egypt

Corresponding authors:

Tel.: +49 211 81 15979; fax: +49 211 81 11923;

email: zhen.liu@uni-duesseldorf.de (Z. Liu),

proksch@uni-duesseldorf.de (P. Proksch)

Table of Contents

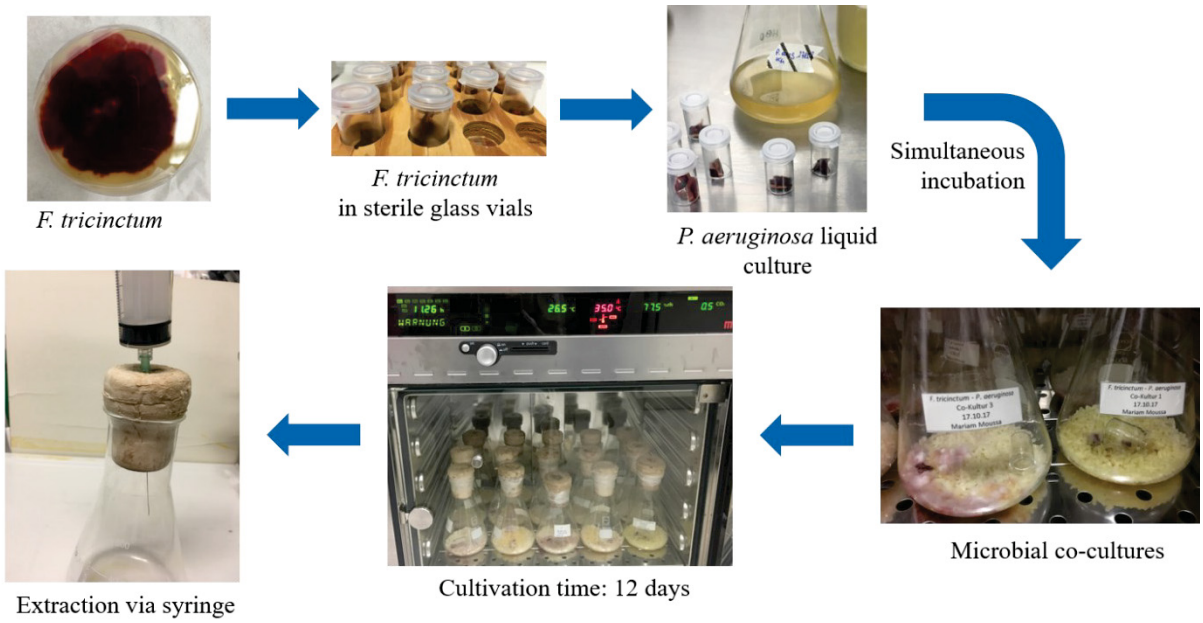

S1. Experimental procedure of co-culture experiment between *F. tricinctum* and *P. aeruginosa*.

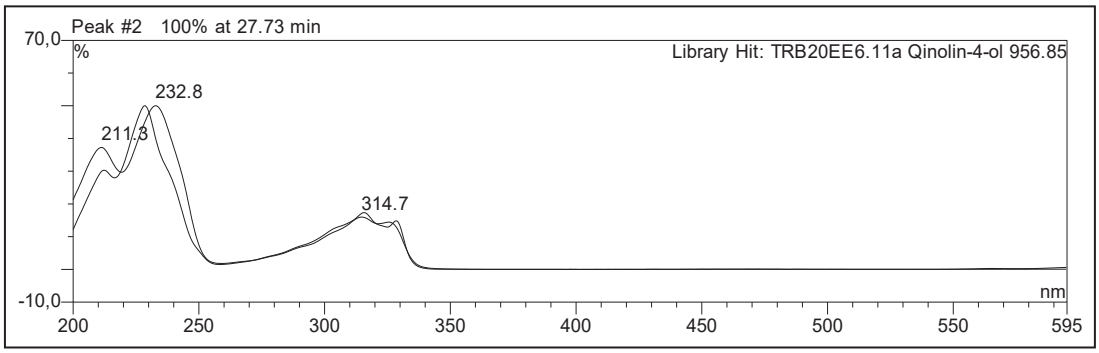

S2. UV spectrum of 2-heptyl-4-hydroxy-quinolone (HHQ).

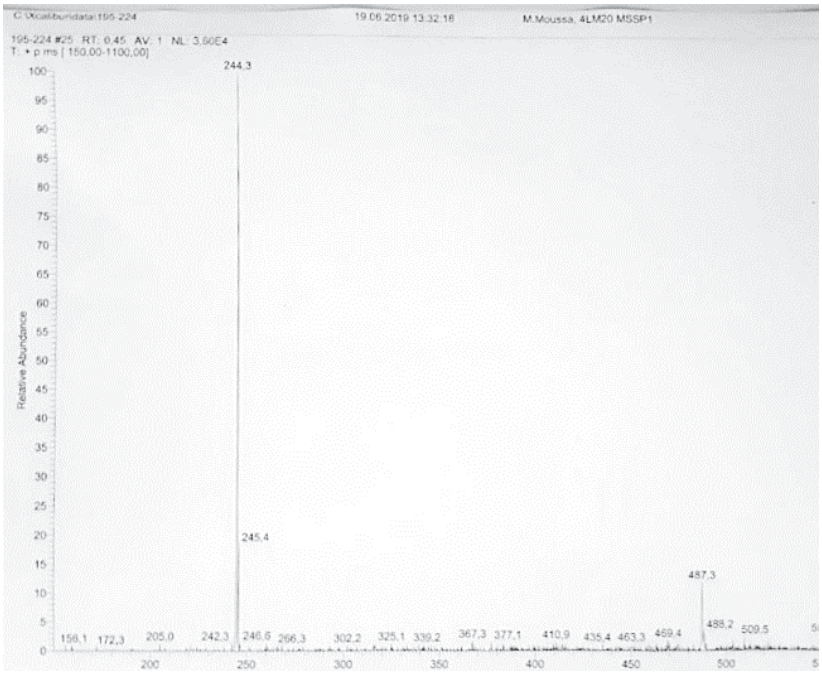

S3. ESIMS spectrum of HHQ.

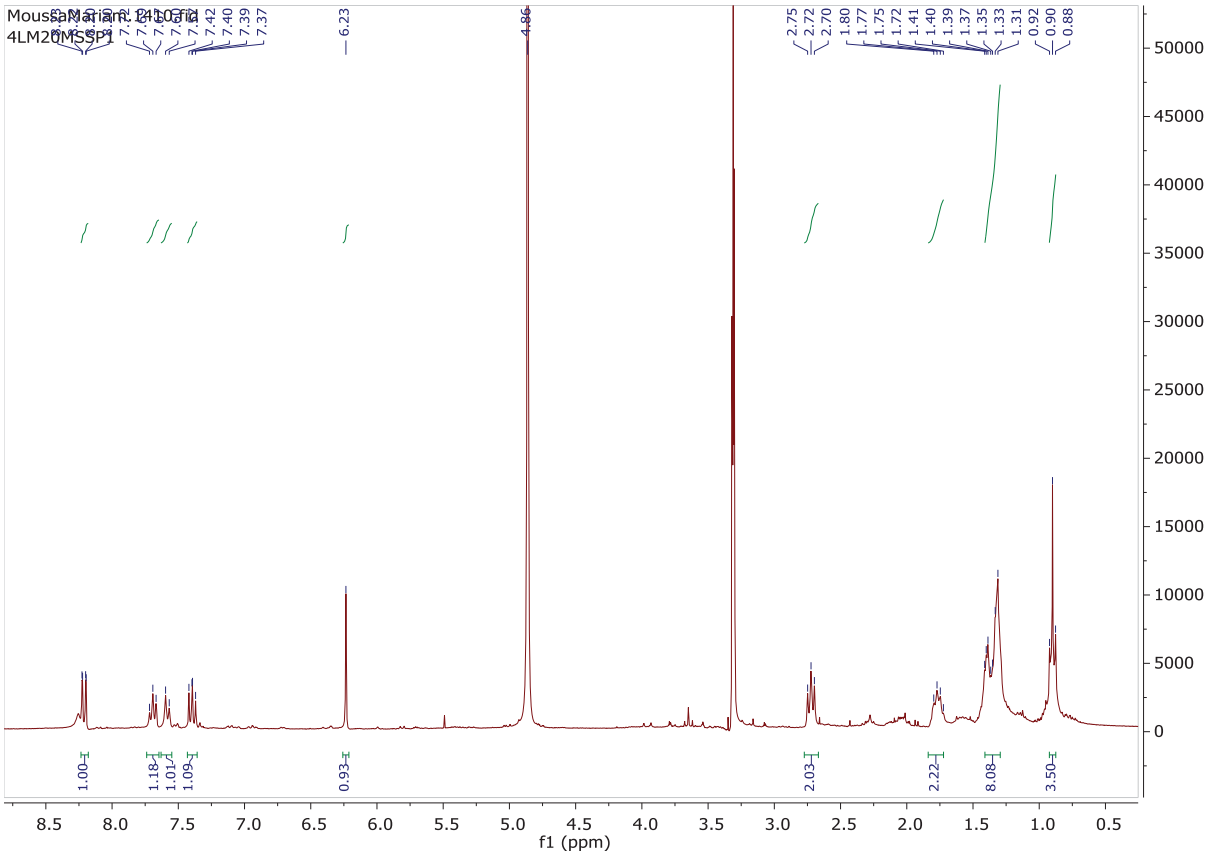

S4. ^{1}H NMR (300 MHz, CD_3OD-d_4) spectrum of HHQ.

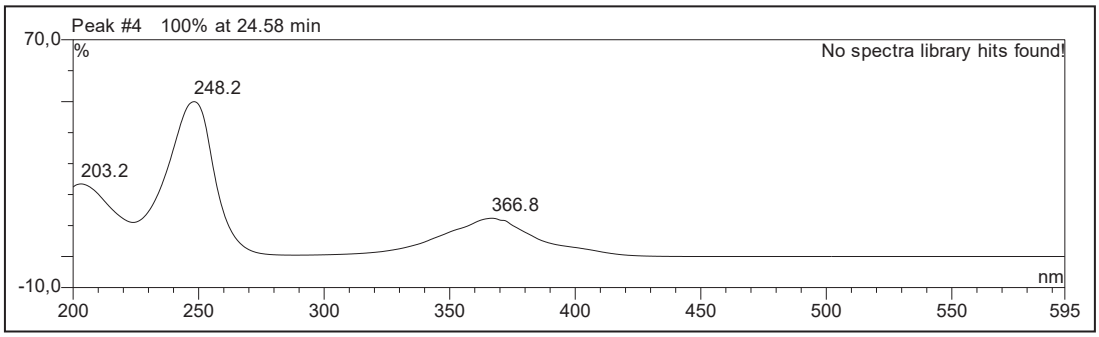

S5. UV spectrum of phenazine-1-carboxylic acid (PCA).

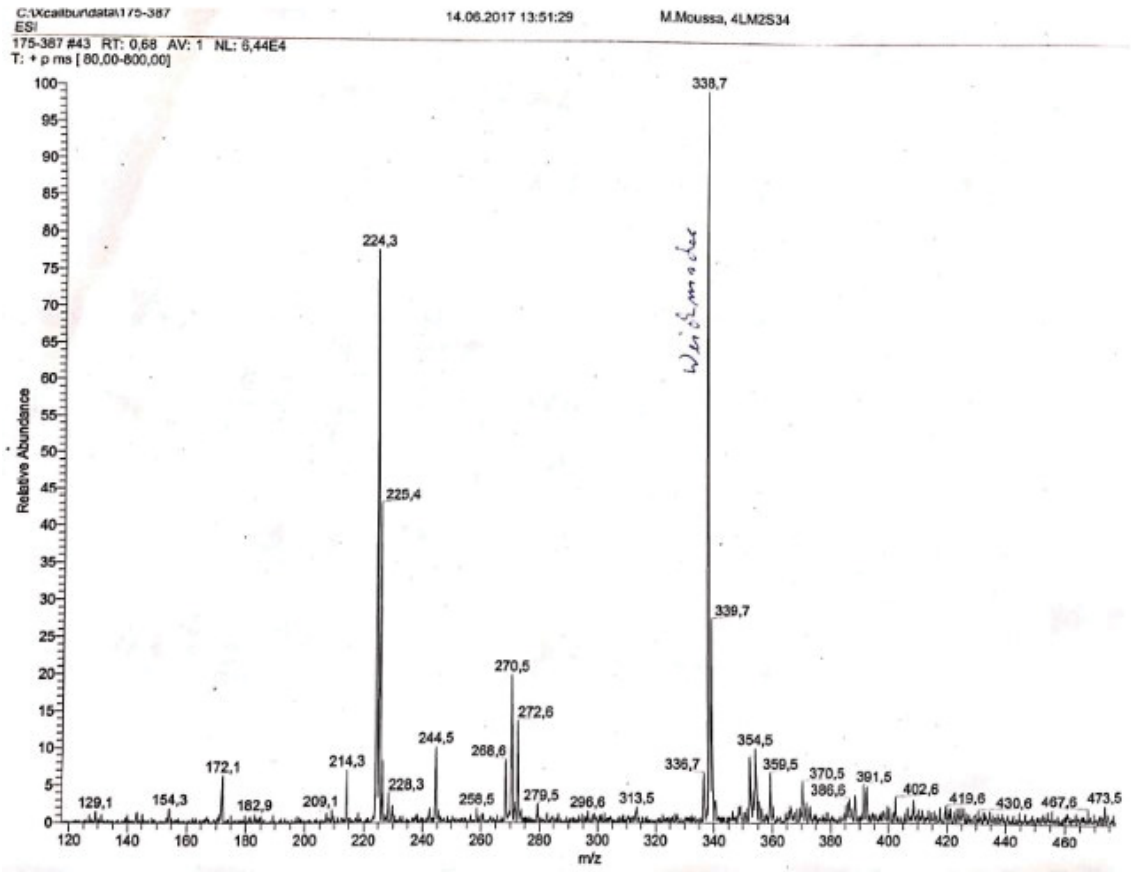

S6. ESIMS spectrum of PCA.

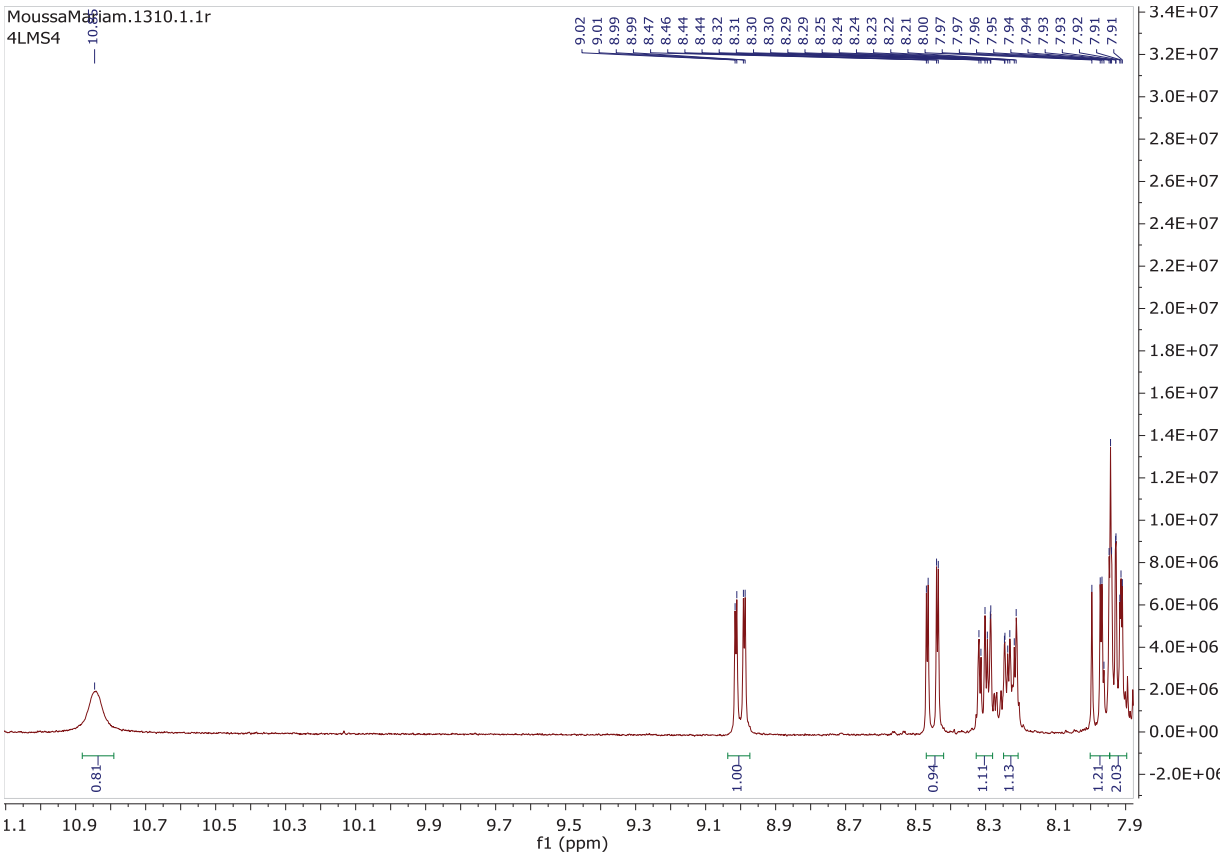

S7. ^{1}H NMR (300 MHz, acetone-d_6) spectrum of PCA

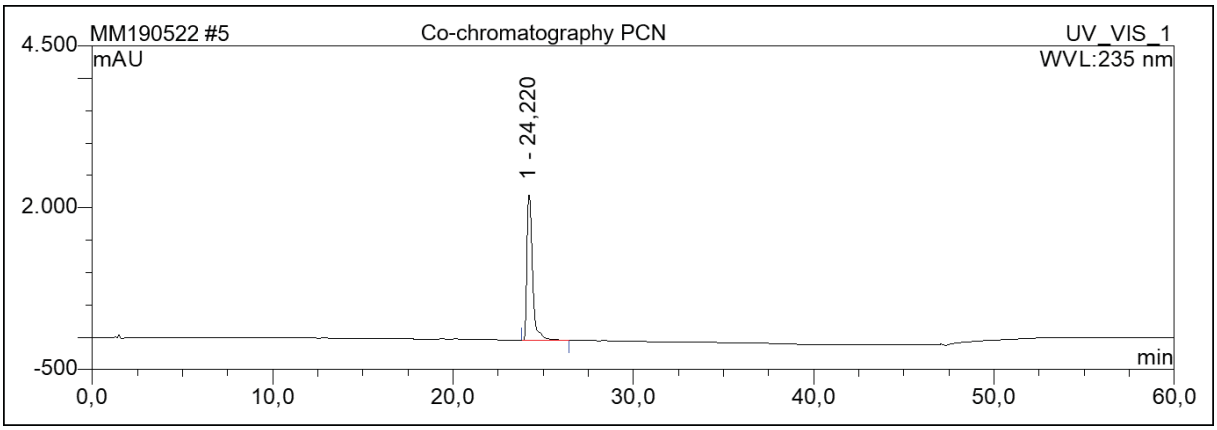

S8. HPLC chromatogram of phenazine-1-carboxamide (PCN).

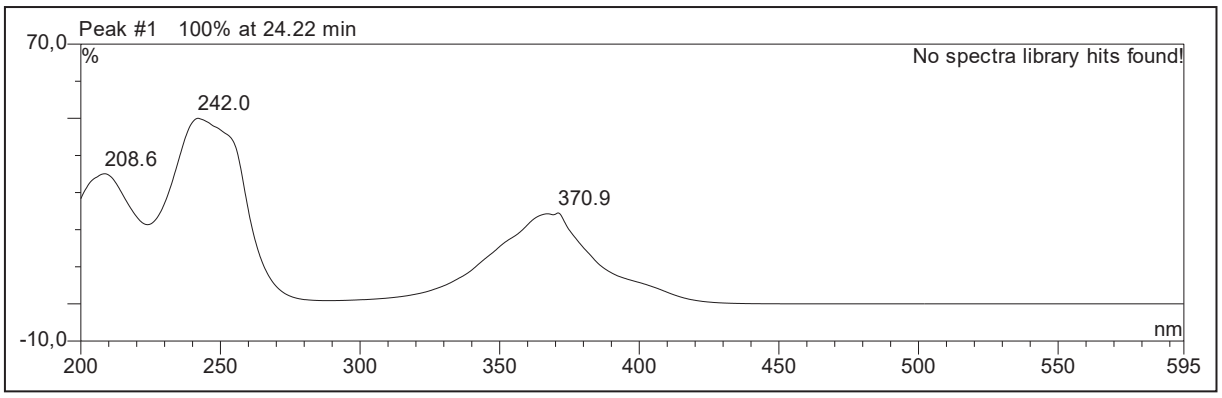

S9. UV spectrum of PCN.

3 Discussion

3.1 The role of microbial secondary metabolites (MSM) in drug discovery

The FDA approved in 2017 a peak of New Chemical Entities, from which several are derived structurally from NPs. Their structural features vary in their complexity and pharmaceutical applications (De la Torre and Albericio, 2018; De la Torre and Albericio, 2019). Despite the yearly approval of new drugs by the FDA, researchers draw the attention to the efficiency of drug discovery. As shown in **Figure 3.1.A**, the present chemical space is underexplored, containing a larger number of discovered NPs and constructed synthetics being beyond comparison to the chemicals with drug potential (Deng *et al.*, 2013). Nevertheless, a quarter of FDA-approved drugs are from fungal origin (**Figure 3.1.B**). Microbial secondary metabolites are undisputable essential for drug discovery, since nature provides the most complex structures which can at least inspire new drugs, as stated above (De la Torre and Albericio, 2018; De la Torre and Albericio, 2019). Especially in antibiotic research, microbes still take 100 % credit for the natural derived drugs that were approved since 2010 (Partridge *et al.*, 2016). As already mentioned in 1.2.1, antibiotic resistance is striking and the investigation of bacteria and fungi demand a more efficient monitoring (Deng *et al.*, 2013; Partridge *et al.*, 2016). Many factors that could increase the possibility of exploring new microbial chemistry have been tackled in this study. Host plants were collected from unusual and exotic niches, to give a rise to the chemical diversity of the isolated endophytes, as listed in **Table 3.1** (Moussa *et al*., 2016; Moussa *et al*., 2019). The aim of this study was first and foremost to contribute to drug discovery from microbial, e.g. fungal origin and to provide further insight to the chemistry of underexplored fungi, i.e. *Stemphylium globuliferum*, or expand the well investigated chemistry of well-known fungal metabolism, i.e. *F. tricinctum*. Higher efficiency during the projects was achieved by applying unconventional methods during cultivating the microbial objects of interest. For this purpose, mainly the OSMAC approach and microbial co-cultivation were

performed, as presented in the parts before. The contribution of each project will be discussed in the following section.

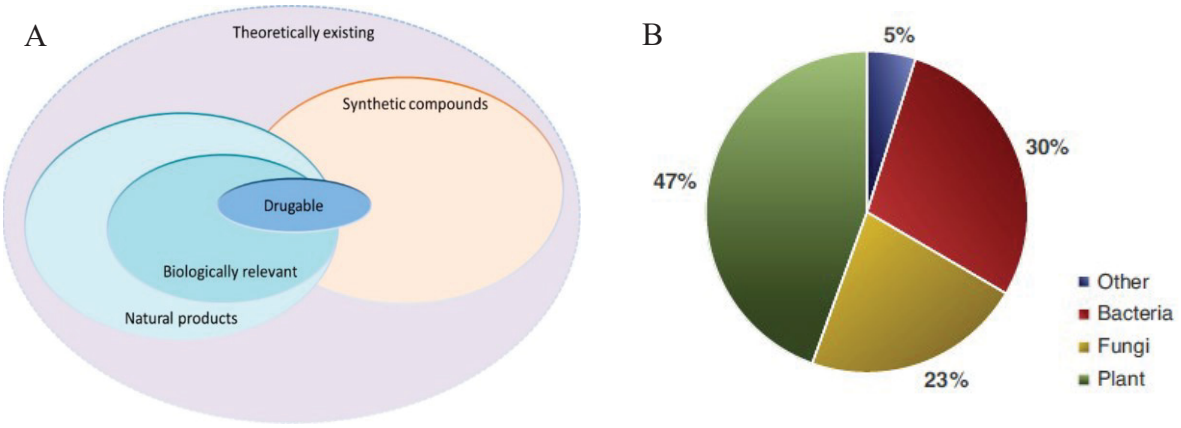

Figure 3.1 Estimation of NPs relevance in drug discovery; A: Venn diagram of finite chemical space and quantitative relation between known NPs and their potential drug development (Deng *et al.*, 2013) B: Circular chart of FDA-approved NPs divided into their biological source (Partridge *et al.*, 2016)

Table 3.1 Host plants' physiological environment and features

Hostplant	Isolated endophyte	Geological origin	Features
Avicennia marina	*S. globuliferum*	Red Sea coast in Hurghada, Egypt	tropical marine habitat (Mohamed, 2005)
Aristolochia paucinervis	*F. tricinctum*	Mountains of Beni-Mellal in Morocco	alternate dry and humid seasons (Brahim *et al.*, 2016)

3.2 OSMAC applied on endophytic fungi

The researcher's investment on studying endophytic fungi should focus on increased biological relevance (Deng *et al.*, 2013). Avoiding time consuming re-isolation of known compounds, or fungal cultivation under standard laboratory conditions, which only leads to the same chemistry and keeps biosynthetic pathways silent, represents an underlying expectation to today's drug discovery. The one strategy that was characterized as the simplest tool to activate silent biosynthetic pathways is the OSMAC approach (Pan *et al*., 2019).

3.2.1 OSMAC approach applied on *Stemphylium globuliferum*

Stemphylium globuliferum has been already investigated for its secondary metabolites (Moussa *et al.*, 2016). The chemistry is strongly dominated by polyketides, which the fungus produces in monomeric, dimeric and even trimeric structures (Liu *et al*., 2014; Liu *et al*., 2015; Olsen *et al.*, 2018). The fungus was repeatedly grown on solid rice medium and still managed to produce a wide range of structurally related anthraquinone derivatives with biological relevant activities (Debbab *et al.*, 2009; Liu *et al.*, 2015; Moussa *et al.*, 2016). In this study, *S. globuliferum* was subjected to an OSMAC experiment. Here, the changed cultivating factor would be the nutrition source. Instead of the standard rice medium, the protein-rich white beans (*Phaseolus vulgaris*) medium was chosen (Moussa *et al.*, 2016). It afforded the shortly before this project published dihydroaltersolanols B and C (Liu *et al.*, 2015). Furthermore, this experiment expanded the endophytes chemistry by the isolation and unambiguous elucidation of two new monomeric tetrahydroanthraquinone derivatives (altersolanol Q and 10-methyl-altersolanol Q) and a new anthraquinone dimer of the alterporriols (alterporriol X) (Moussa *et al.*, 2016). The striking point about altersolanol Q is the reversed stereochemistry of the hydroxyl group at C-10 having *S*-configuration. The before known NP, altersolanol J, has the same structure but *R*-configuration at C-10 (Höller *et al.*, 2002). As for the dimer alterporriol X, the new structure is constructed from macrosporin and altersolanol B monomers, with the carbon linkage established between C-4 and C-8'. Besides the chiral centres in the aliphatic ring system, the structure features axial chirality, being a*R* (Moussa *et al.*, 2016). Biosynthetically, these compounds origin from the acetate-mevalonate pathway. The core structure is constructed by the condensation of eight acetate units. By condensation reaction in a head to tail manner, an octaketide chain is formed. During this process, decarboxylation of the terminal ends forms the macrosporin-like compounds (Suemitsu *et al.*, 1988; Suemitsu *et al.*, 1989). **Figure 3.2** shows the suggested biosynthesis of monomeric and dimeric anthraquinones, which is postulated for

the new compounds. The formation of altersolanol Q to 10-methyl-altersolanol Q is postulated to happen under S-adenosylmethionine (SAM)-dependant methylation (Bauerle *et al.*, 2015). It is worth mentioning that altersolanol A can be metabolized into macrosporin and altersolanol B, from which the new dimer alterporriol X arises by oxidative coupling (Stoessl *et al.*, 1979; Ohnishi *et al.*, 1991; Ohnishi *et al.*, 1992).

3.2.1.1 SAR of tetrahydroanthraquinones obtained from *Stemphylium globuliferum*

Another aspect to cover is the assessment of the structure-activity relations of the new obtained NPs from this project in comparison with known data from the literature. **Table 3.2** summarizes all published data from relevant bioactivities that were reported about the isolated compounds from the *S. globuliferum* beans medium. The profound biologically active altersolanol A exhibits strong cytotoxic activities against 34 cancer cell lines with angiogenetic properties and antibiotic effects (Zhou *et al.*, 2014; Liu *et al.*, 2015; Pompeng *et al.*, 2013; Mishra *et al.*, 2015). Altersolanol A features a tetrahydroanthraquinone core structure with four hydroxyl groups attached to the aliphatic ring system. The loss of the hydroxyl groups at C-1 and C-4 yields altersolanol B. It shows as well strong cytotoxic effects against the murine cancer cell line L5178Y, but a decreased antibiotic activity against *B. subtilis*, *E. coli* and *S. aureus* (Zhou *et al.*, 2014; Liu *et al.*, 2015). Whereas the acetylation of the altersolanol A structure of the hydroxyl group at C-2, forming altersolanol N, maintains the strong cytotoxic inhibition against the murine cell line L5178Y with 100 % growth inhibition (Debbab *et al.*, 2012a), dehydration at positions C-4a and C-9a leads to the compound dihydroaltersolanol B with one missing hydroxyl group at C-1, and dihydroaltersolanol C with two remaining hydroxyl groups at C-2 and C-3. The strong cytotoxic activity of dihydroaltersolanol C against the murine cell line L5178Y and the loss of activity of dihydroaltersolanol B against the same cell line shows the significance of the hydroxyl group at C-4 (Liu *et al.*, 2015). Since both compounds are inactive against bacterial microbes, it is arguable that the aromatic character of the middle ring system

is crucial for the antibiotic effect of these compounds. The alterporriol homodimers D and E, composed of two altersolanol A monomers, only differ in their axial chirality (Kanamaru *et al.*, 2012). Still, this dimerization process results in a loss of the bioactivity against cancer cell lines and a decreased activity against the bacterial strains *B. subtilis*, *E. coli* and *S. aureus* (Zhou *et al.*, 2014; Liu *et al.*, 2015). Nonetheless, the axial chirality of alterporriol E still maintains moderate cytotoxicity against L5178Y (Liu *et al.*, 2015). The new monomeric NPs, altersolanol Q and 10-methyl-altersolanol Q, share the same structure as dihydroaltersolanol C, with an exchange of the carbonyl group at C-10 with either a hydroxyl or a methoxy group. These features also lead to the loss of cytotoxicity and antibacterial activity, when compared to altersolanol A (Moussa *et al.*, 2016). Proceeding with the anthraquinone macrosporin, it has been characterized as being inactive as a cytotoxic agent (Liu *et al.*, 2014; Moussa *et al.*, 2016). Nevertheless, it has moderate antibiotic activity against *E. coli* and the meningitis causing gram-positive bacterium *Micrococcus tetragenus* (Zhou *et al.*, 2014; Fosse *et al.*, 1985). The different combinations of constructing dimers from macrosporin are reflected in the isolation of alterporriol R and V. These compounds differ in the carbon linkages of the monomeric subunits. Since alterporriol R shows neither cytotoxic, nor antibacterial activities, it is arguable that the linkage between C-4 and C-8' results in a total loss of activity. But the linkage between C-5 and C-5', as seen in alterporriol V, maintains a moderate activity against the gram-positive bacterium *B. cereus* (Zhou *et al.*, 2014). It is therefore logical to assume that the presence of the hydroxy group at C-8' is crucial for the exhibited activity. As for the new dimer isolated in this study, alterporriol X, it is already mentioned that the two monomeric subunits are macrosporin and altersolanol B. This combination has shown to give no activity results (Moussa *et al.*, 2016). Summarized, it can be stated that the tetriol ring with quinone function and in monomeric structure are responsible for the cytotoxic and antibacterial activities, whereas dimerization or dihydroxylation cause the loss of cytotoxicity and decreases antibacterial activity. Dimerization will cause moderate cytotoxic and antibiotic activity, whereas full

aromatization leads to moderate antibacterial activity, but dimerization of the latter will make the compound inactive. The structurally closest fungal NP is emodin, which is being investigated for its antibacterial activity in the treatment of Glässer's disease, caused by *Haemophilus parasius* (Li *et al.*, 2016). Emodin and other naturally occurring anthraquinones are also known for their laxative effects, whereas emodin is excelling in cytotoxic activities, i.e. by inducing apoptosis (Srinivas *et al.*, 2007). It is noteworthy to mention that all anthranoids available on the drug market have the 1,8-dihydroxyanthron core structure.

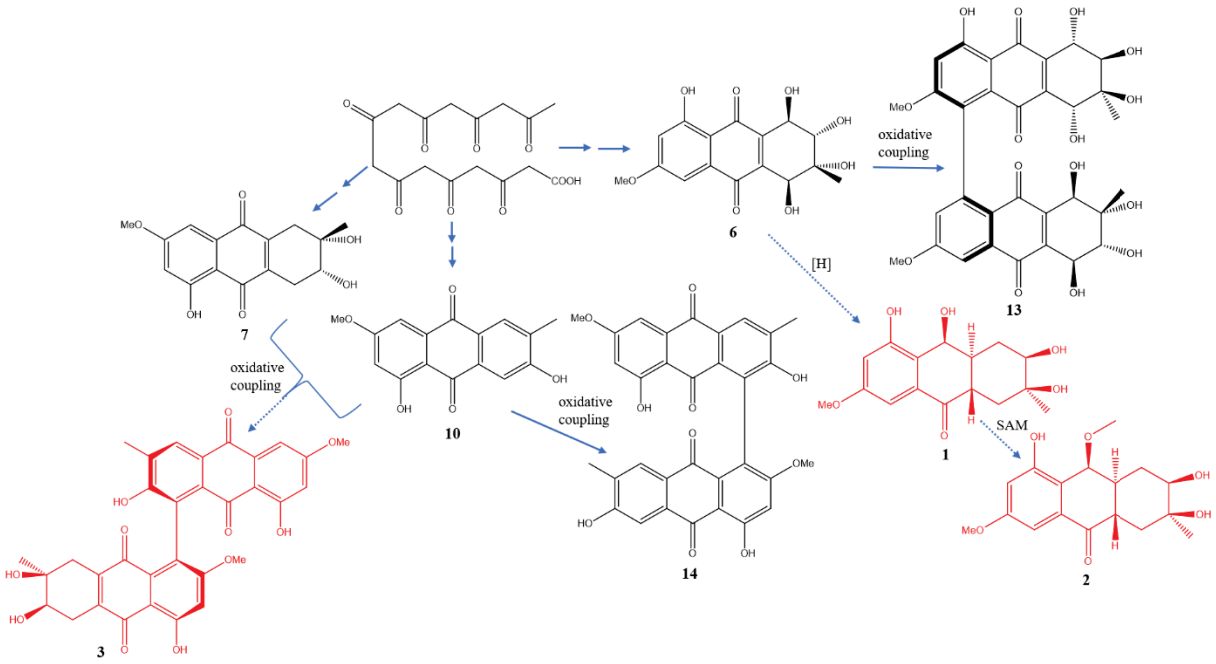

Figure 3.2 Plausible biosynthesis for new NPs (altersolanol Q, 10-methyl-altersolanol Q and alterporriol X) and related derivatives; eight acetyl-CoA units form anthraquinone core structures, building altersolanol B (**7**), macrosporin (**10**) and altersolanol A (**6**); oxidative coupling of **6** and **10** lead to the new dimer alterporriol X (**3**); reduction of **6** leads to new monomer altersolanol Q (**1**) and after enzymatic methylation via SAM to 10-methyl-altersolanol Q (**2**); oxidative coupling of two macrosporin units form alterporriol R (**14**); oxidative coupling of two altersolanol A units form alterporriol E (**13**) (Suemitsu *et al.*, 1988; Suemitsu *et al.*, 1989; Bauerle *et al.*, 2015; Moussa *et al.*, 2016)

Table 3.2 *Stemphylium globuliferum* summarized bioactivities for SAR

	Anti-Cancer IC_{50} [µM]							Antibiotic MIC [µg/mL]; [µM]																
Name	Anti-angiogenic	L5178Y	HSP90	HCT116	K562	A2780CisR	A2780sens	*B. subtilis*	*E. coli*	*A. niger*	*P. fluorescens*	*S. aureus*	*T. rubrum*	*C. albicans*	*M. tetragenus*	*S. albus*	*B. cereus*	*K. rhizophila*	*P. aeruginosa*	*MRSA*	*S. pneumoniae*	*E. faecalis*	*E. cloacae*	*A. fumigatus*	*A. faecalis*	*C. albicans*
Altersolanol A[1,2,4]	ac	2.5	n.d.	1,4	3.6	4.0	1.4	4.1	4.1			2.1			8.2	>10	>10	>10								
Altersolanol B[1,2]		3.8	-	-	-	-	-	7.8	7.8			7.8			>10	>10	>10	7.8								
Altersolanol N[3]		ac																		n.d.	n.d.	n.d.	n.d.	>62	>62	>62
Alterporriol D[1,2]		-	-	-	-	-	-	>10	7.5			5.0			>10	>10	10.0	>10								
Alterporriol E[1,2]		6.9	-	-	-	-	-	>10	5.0			>10			>10	>10	2.5	>10								
Alterporriol R[1]								ia	ia			ia			ia	ia	ia	ia								
Alterporriol V[1]								>10	>10			>10			>10	>10	8.1	>10								
Dihydroaltersolanol B[2]		-							>64			>64							>64							
Dihydroaltersolanol C[2]		3.4							>64			49.7							>64							
Macrosporin[1,2,3,4]	-	-	-	-	-	-	-	>10	4.6			9.2			4.6	>10	>10	>10		>62	n.d.	n.d.	n.d.	n.d.	n.d.	n.d.
Altersolanol Q[5]		ia																								
10-Methyl-altersolanol Q[5]		ia																								
Alterporriol X[5]		ia																								

[1] Zhou *et al.*, 2014; [2] Liu *et al.*, 2015; [3] Debbab *et al.*, 2012a; [4] Pompeng *et al.*, 2013; [5]Moussa *et al.*, 2016; n.d.: not detected; ia: inactive; ac: active

3.3. Microbial co-cultivation

Simultaneous cultivation of at least two microbes of fungal or bacterial origin can lead to a dramatic shift in the metabolic pattern (Ola *et al.*, 2013; Wang *et al.*, 2013b; Daletos 2017). In the strive against re-isolation and expansion of a microbe's chemistry, co-culture has been established as a proven methodology (Marfori *et al.*, 2002; Pettit *et al.*, 2010; Nonaka *et al.*, 2015; Marmann *et al.*, 2014). Deeper investigation of this method evolves around three key points: identification of activated genes, responsible producer of cryptic compounds and physical condition for the microbial response.

Transcriptome profiling helps identifying the activated gene clusters, which are responsible for the production of cryptic compounds (Hontecillas *et al.*, 2019; Tognon *et al.*, 2019; Yao *et al.*, 2019). As in the case of the mould fungus *Aspergillus nidulans* in co-culture with 58 *Actinomyces* species, cryptic compounds have been identified, i.e. orsellinic acid and cathepsin K inhibitors (F-9775A, F-9775B). Transcriptome profiling was performed by using knockout organisms. It determined the activation of *orsA*-gene clusters associated with the polyketide synthase (Schroeckh *et al.*, 2009).

The same workgroup performed further co-cultivation experiments to determine the needed physical interaction to obtain the same fungal response. Using sterile filtered bacterial fermentation or inserting a semi-permeable membrane left the desired gene clusters silenced. These experiments revealed the necessity of direct contact between the two microbial competitors. Microscopic observation displayed bacterial colonization of the fungal mycelia during the uninhibited co-culture (Schroeckh *et al.*, 2009).

Further investigation of the underlying mechanism pointed at the chromatin modulation by histone modification. In order to understand the effect of the direct contact between fungal mycelia and bacterial colonies, experiments of small molecules that interfere with HAT and HDAC were performed. In use were the HDAC inhibitor SAHA, the HAT inhibitor anacardic

acid, in addition to knockout organisms of the fungal HAT. On the one hand, the results showed that the activation of the silent biosynthetic *orsA*gene clusters depends on histone acetylation via the SAGA/ADA coactivator complex mediation. On the other hand, bacterial colonies within fungal mycelia can interfere with the chromatin modelling and histone modification enzymes, leading to the production of cryptic MSM (Nützmann *et al.*, 2011).

The following co-culturing projects, performed in this study, will be analysed by focusing on the scientific accomplishments mentioned before.

3.3.1 Co-cultivation applied on *F. tricinctum*

The scientific achievement with co-culturing *F. tricinctum* has already been mentioned in 1.4.2.1. Ola *et al.* set up this fungus against *B. subtilis* and achieved a high accumulation of antibacterial compounds, e.g. enniatins (EB, EB1, EA1) and lateropyrone. New cryptic compounds isolated from the co-culture (macrocarpon C, N-(carboxymethyl)anthranilic acid, (-)-citreoisocoumarinol) were attributed to the fungus (Ola *et al.*, 2013).

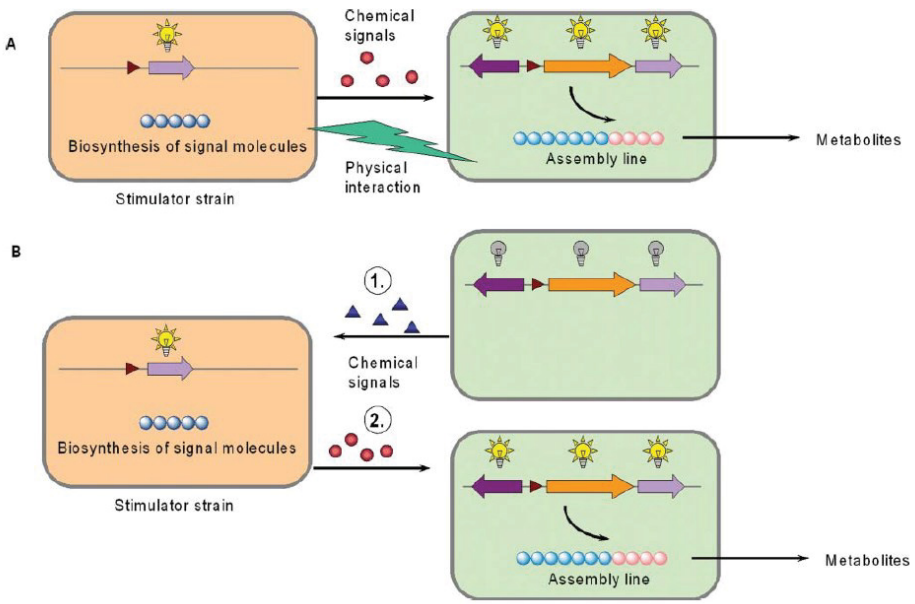

Figure 3.3 Scheme of interspecies association during co-cultivation. A. Physical contact with another microbe and its NPs as chemical signals induce cryptic NP production in another

microbe. B. Chemical signals produced by one microbe induce biosynthesis of NPs and vice versa (Scherlach and Hertweck, 2009).

The mechanism of action may fit the scheme of **Figure 3.3.A**. In the figurative sense, the bacterium affected the fungus by physical interaction and maybe chemical signals, leading to the enhanced accumulation of antibacterial compounds (Scherlach and Hertweck, 2009). In logical terms, the *B. subtilis* strain triggered a self-defensive response system within *F. tricinctum* on a genetic level.

3.3.1.1 Co-culture of *F. tricinctum* and *S. lividans*

Next is to transfer the above-mentioned scientific insight to the co-culture between *F. tricinctum* and *S. lividans*. Common features between the two co-culture experiments are the non-pathogenicity and the 4-day ahead start of the bacteria (Ola *et al.*, 2013; Moussa *et al.*, 2019). Common results are the accumulation of constitutively present compounds (EB, EA1, EB1, lateropyrone, fusaristatin A) and induction of macrocarpon C and another isocoumarin derivative ((-)-citreoisocoumarin). Moussa *et al.* from 2019 demonstrated the dramatic shift in the metabolic profile of the fungus, caused by co-culturing. Illustrated in **Figure 3.4** is the HPLC chromatogram of the co-culture experiment. The striking differences between the axenic and mixed cultures are shown: the red arrows indicate the raised production of the constitutively present compounds lateropyrone up to 12-fold and enniatins up to 4-fold. The induced cryptic compounds were not detectable in any of the axenic cultures. The framed areas show their induction in comparison. Additional known cryptic compounds were the resorcylic acid lactone zearalenone and the chromone derivative 7-hydroxy-2-(2-hydroxy-propyl)-5-methylchromone. New compounds that were obtained through this co-culture are the cryptic naphthoquinone dimers fusatricinones A-D and the lateropyrone derivative dihydrolateropyrone (Moussa *et al.*, 2019).

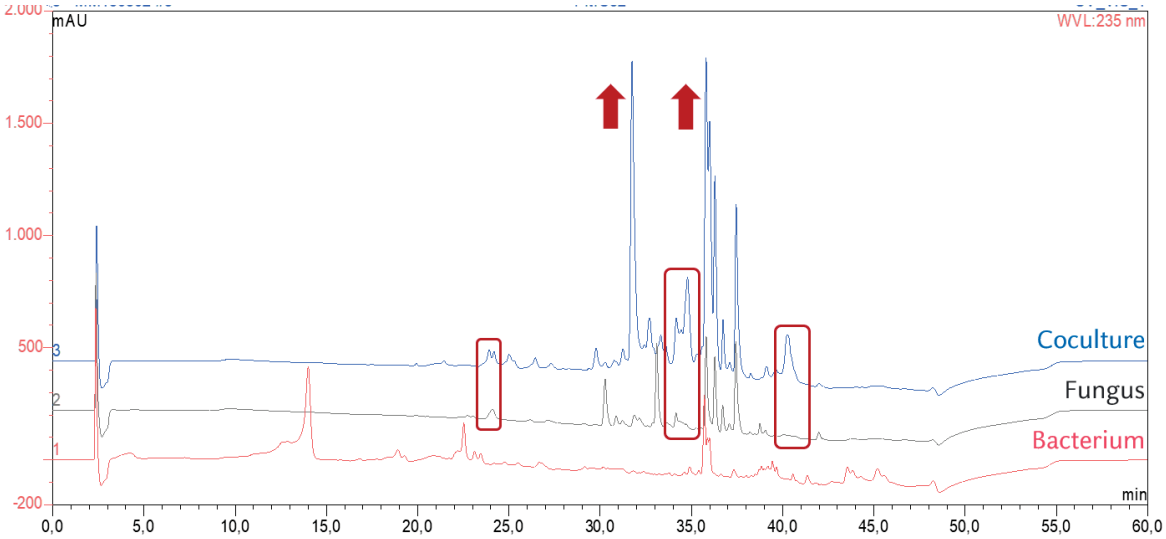

Figure 3.4 Comparison of HPLC data between axenic bacterial and fungal controls with the co-culture; arrows: increased production, frames: induced cryptic compounds

Lateropyrone was first isolated from *F. lateritium* and showed inhibitory effects against the gram-positive bacterium *S. aureus* and the yeast *C. albicans* (Bushnell *et al*., 1984). It is a known antibiotic from the genus *Fusarium* and displayed significant antibacterial activities against *B. subtilis*, *S. aureus*, *S. pneumonia* and *E. faecalis* (Singh *et al.*, 2003). It was also upregulated up to 78-fold during the co-culture of *F. tricinctum* with *B. subtilis* (Ola *et al.*, 2013), maybe as a defence mechanism of the fungus against its opponent. Exact the same effect was noticed during the co-culture of *F. tricinctum* and *S. lividans*, with 12-fold higher production of the compound, compared to fungal axenic cultures. Another cryptic new compound isolated from this co-culture was identified as a lateropyrone derivative (dihydrolateropyrone). Translated structurally, this new compound has a hydrogenated double bond in positions C-8 and C-9. When tested against human pathogenic bacterial strains, e.g. *Pseudomonas aeruginosa* and *Staphylococcus aureus*, dihydrolateropyrone remained inactive. This leads to the assumption that the loss of the double bond and thus the conjugated aromatic character of the whole structure leads to a loss of bioactivity (Moussa *et al.*, 2019).

The resorcylic acid lactone trans-zearalenone is also named F-2 toxin (Kuiper-Goodman *et al.*, 1987). It is a mycotoxin mainly produced by the genus *Fusarium* and detected in cereal crops and their processed food products. It shows estrogenic effects, which can threaten human and animal health if the dietary intake happens at high dosages over a long period of time (Zinedine *et al.*, 2007).

(-)-Citreoisocoumarin, which was previously reported as an NP of *Penicillium citreo-viride* B and *Aspergillus nidulans*, is an isocoumarin (Watanabe *et al.*, 1998). This NP was described as the biosynthetic precursor of naturally occurring spiro-dihydroisocoumarins (Lai *et al.*, 1991).

Macrocarpon C was isolated from the previous mentioned co-culture of *F. tricinctum* with the bacterium *B. subtilis*. It was introduced as a cryptic NP that was only detectable in the co-culture but not in the axenic cultures of the microbes (Ola *et al.*, 2013). In the same publication it was stated that this NP was not duplicated when the fungus was co-cultured with *S. lividans*. This statement has been now corrected by its isolation in this experiment (Moussa *et al.*, 2019; Ola *et al.*, 2013) This statement was maybe based on the detectable UV spectra of the crude extracts. For example, compound dihydrolateropyrone proves the fact that the presence of a compound cannot be absolutely excluded by interpretation of the crude extract. Since this HPLC chromatogram mirrors the relative quantity of the metabolic patterns, it is dominated by those compounds that are produced in a relatively high amount by the microbe. Their quantity supresses the appearance of molecules that are only produced in relatively low amount by the microbe, thus making them undetectable in crude extract HPLCs.

7-hydroxy-2-(2-hydroxy-propyl)-5-methylchromone has the molecular formula $C_{13}H_{14}O_4$ and is known as a plant and fungal metabolite. It has been isolated from the mangrove-derived endophyte *Pestalotiopsis* sp. and from rhizomes of the medicinal rhubarb *Rheum officinale* (Xu *et al.*, 2009). Here it has been reported from *F. tricinctum* for the first time.

3.3.1.2 Naphthoquinone dimers obtained from co-culture of *F. tricinctum*

The metabolic response of the fungus reveals the activation of silent PKS gene clusters. It resulted in the formation of naphthoquinone dimers, which have never been reported from this well investigated fungus before (Moussa *et al.*, 2019). A genetically and structurally close NP is the red pigment aurofusarin, isolated from several *Fusarium* species (Frandsen *et al.*, 2006). It is found to be built through PKS12 gene dependant biosynthesis (Malz *et al.*, 2005). As shown in **Figure 3.5.A**, the microbial biosynthesis of aurofusarin requires a five-step reaction, which is catalysed enzymatically. A prominent intermediate NP of this biosynthesis is the pigment rubrofusarin, which can be found in many biosynthetic pathways that lead up to bioactive NPs or natural pigments (Rugbjerg *et al.*, 2013). It is reported to express antibiotic activity against *Lactobacillus* strains (Sondergaard *et al.*, 2016). Transferring this biosynthesis scheme to the obtained new naphthoquinone dimers of the fusatricinone type, leads to the proposed biosynthesis shown in **Figure 3.5.B**. The proposed pathways suggest enzymatic construction of the naphthoquinone core structure from acetyl-CoA and manolyl-CoA subunits, followed by enzymatic dimerization. Biosynthetic determination of building the 1,3-dioxolane ring was based on a synthetical approach. Galy *et al.* described the reaction between catechol and methyl acetoacetate to form methyl (2-methyl-1,3-benzodioxol-2-yl) acetate, as shown in **Figure 3.5.B** (Galy *et al.*, 2011). The synthetic products resemble the terminal 1,3-dioxolane ring of the dimers. Transferring this reaction to the level of microbial biosynthesis, it would match the reaction of additional acteoacetyl-CoA subunits with the intermediate dimer. This would represent the last step in the proposed biosynthesis, cyclization for building the 1,3- dioxolane ring with terminal acid and ester groups, respectively (**Figure 3.5.B**). These findings prove already that the dimeric naphthoquinone fusatricinones are from fungal origin. Moreover, this discovery is important for analysing the success and the microbial abilities and influences towards one another, respectively.

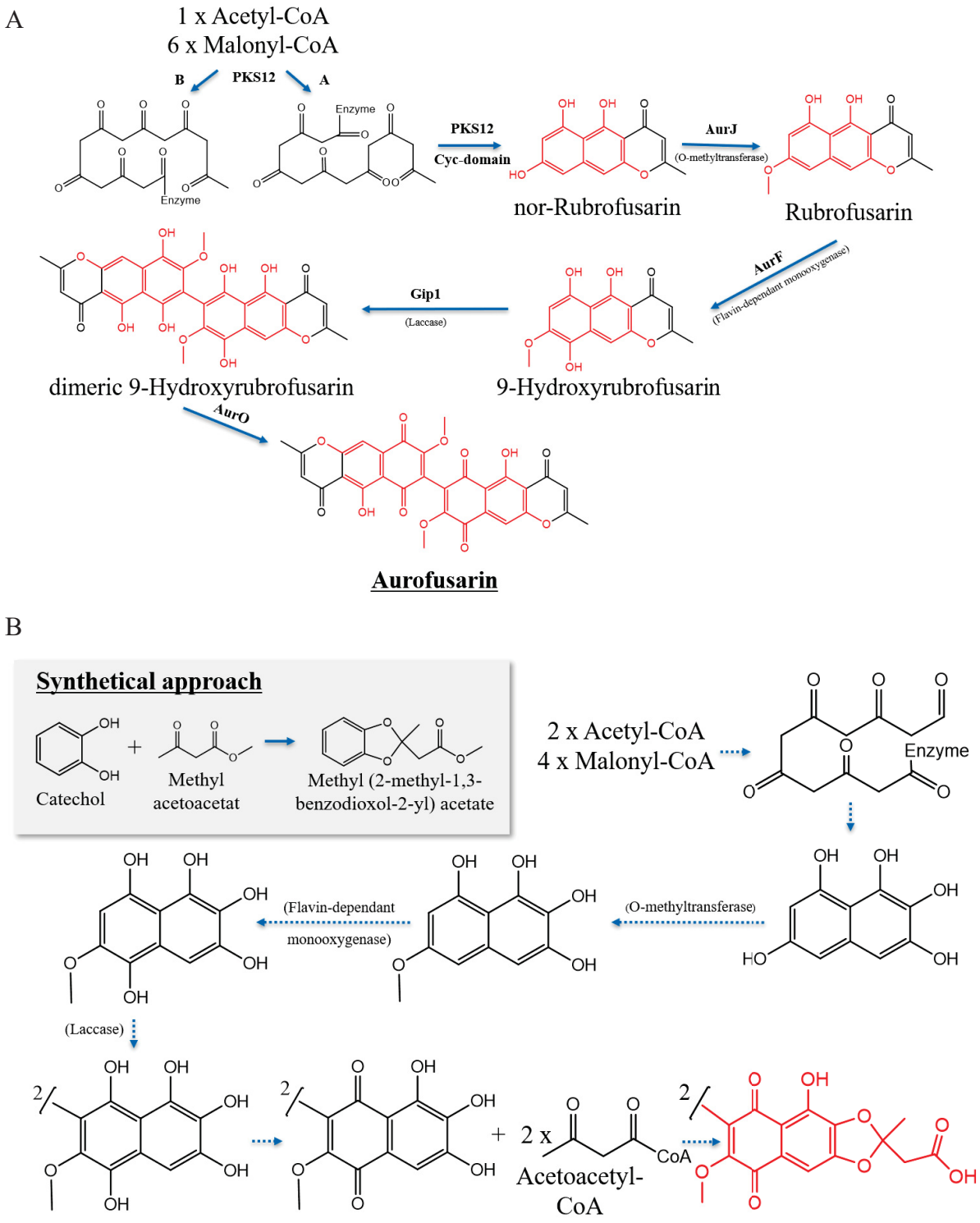

Figure 3.5 A. Reported biosynthesis for naphthoquinone dimer aurofusarin (Frandsen *et al.*, 2006). B. Proposed biosynthesis for new naphthoquinone dimers (fusatricinones A-D) induced by co-cultivation of *F. tricinctum* with *S. lividans* (Galy *et al.*, 2011)

Additional literature findings showed another previously reported NP with identical dimeric features of naphthoquinone core structure and biaryl linkage. It has the identical molecule halves as fusatricinones A-D and is named xanthomegnin. The dimer was obtained from several *Aspergilli* and *Penicilli* endophytes, being described as an inseparable 1:1 mixture of atropisomers (Höfle *et al.*, 1978). The structural difference between the dimers isolated in this study and xanthomegnin is the third ring formation. Xanthomegnin has an additional *δ*-lactone ring, instead of the 1,3-dioxolane ring in the fusatricinone structures. This striking difference allows the determination of xanthomegnins absolute configuration via ECD, since it gives distinct spectral curves. This enables the determination of xanthomegnin analogues, concerning their absolute configurations (Durley *et al.*, 1975). It is constructed biosynthetically from semivioxanthin, where the formation of the optically active monomers precedes their oxidative coupling to lead to the dimerization of the molecules (Romaine *et al.*, 2015; Moussa *et al.*, 2019). In this study the monomers of the fusatricinone dimers were not found. Several subfractions displaying the same UV pattern were repeatedly isolated and reidentified as the already obtained dimers.

The fungus reacted in producing a type of complex structures, which have so far not been reported from this fungal species. The dimeric naphthoquinones might be defence chemicals, which nevertheless cannot be explained with the obtained data. Since none of the new compounds showed significant antibacterial or cytotoxic activity, the response may perhaps be interpreted as a more chemical response. In this case the silent biosynthetic pathways of the fungus seem to be triggered by the bacterial chemistry and its microbial substance. The real trigger for the activation of the naphthoquinone biosynthesis is not clear. But it was only activated through the co-culture of this fungus with *S. lividans*. None of the OSMAC or co-culturing experiments, which were already successful in triggering the production of new NPs from this fungus, led to the presented dimeric structures (Ola *et al.*, 2013; Hemphill *et al.*, 2017).

The workgroup of AK Proksch demonstrated a history of successful experiments with this fungus in avoiding re-isolation and progressing in exploring the metabolic profile of the *F. tricinctum* (Ola *et al.*, 2013; Hemphill *et al.*, 2017; Moussa *et al.*, 2019).

3.3.2 Co-culture of *F. tricinctum* and *P. aeruginosa*

Setting up the same fungus *F. tricinctum* against another living bacterium, helped expanding the knowledge about the behaviour of *F. tricinctum* towards other microbes. The bacterium *P. aeruginosa* is a new type of competitor, because of its human pathogenicity, QS and biofilm formation to accumulate virulence factors (Wagner *et al.*, 2016). This experiment showed different results already on a macroscopic level, when compared to the co-cultivation experiments of this fungus with *B. subtilis* and *S. lividans.* Before, the fungus was noticed to grow throughout the culture. But in this experiment distance inhibition between the two microbes during fermentation was observed (Ola *et al.*, 2013; Moussa *et al.*, 2019; Moussa *et al.*, 2020). Using solid rice medium for the co-cultures gave an advantage in macroscopic analysis, that liquid media could not provide. Also, solid medium has close similarity to the natural conditions these microbes grow in. In this experiment the whole culture was harvested. But since there is a visual confrontation zone, the experiment could be repeated with excising this area and investigating its chemical composition (Bohni *et al.*, 2016).

Another striking difference was the strong effect the co-culture had on the bacterial chemistry, instead on the fungal, as reported before (Ola *et al.*, 2013; Moussa *et al.*, 2019). The induction of the silent biosynthetic pathways and strong accumulation of bacterial NPs was shown via HPLC analysis. Identification of HHQ, PCA and PCN showed the bacterial QS activation by co-culture. The production of these metabolites can be described as a defence response, since the pseudomonad phenazines are known for their antifungal activity (Chin-A-Woeng *et al.*, 2005). These compounds were also described in a process of biocontrol to be plant-protective against bacteria and fungi (Chin-A-Woeng *et al.*, 2003). Since co-culture is a

fermentation method that tries to resemble nature under laboratory conditions, it seems that *P. aeruginosa* can repel a *F. tricinctum* infection of its hostplant. *P. aeruginosa* produces biofilms for protection against antibiotic treatment, as shown with piperacillin. The antibiotic drug was unable to diffuse through the biofilm and could not serve its purpose, hence leading to the survival of the bacterium (Hoyle *et al.*, 1992). One theory is that the bacterium reacted to the fungal antibiotic enniatins, which led to biofilm formation (Hoffman *et al.*, 2005; Kaplan, 2011). Despite reported inactivity of several enniatins towards *P. aeruginosa*, the mechanism of resistance has not been described yet (Ola *et al.*, 2013; Sebastià *et al.*, 2011). Thus, the bacterium may have developed a resistance towards the fungus by creating a diffusion barrier. Mah *et al.* proposed a biofilm-linked resistance mechanism on a molecular basis. They identified periplasmic glucans, which are constituents of the bacterial biofilm, as binding and trapping agents of antibacterial compounds (Mah *et al.*, 2003). Biofilms are characterized as surface-attached sessile communities (Davey and O'toole, 2000). They develop one thousand times stronger high levels of antibiotic resistance than free living planktonic organisms (Hoyle and Costerton, 1991). Therefore, bacterial biofilms are seen as a new target of antibacterial therapy. A new approach for the usage of anticancer drugs is the treatment of resistant biofilm-based microbial infections (Wakharde *et al.*, 2018) Another point to investigate is the link between QS and biofilm formation. As we can see in this experiment, QS molecules accumulated, and a biofilm was formed by *P. aeruginosa*. It was already stated that QS and PCA play roles in biofilm formation (Davies *et al.*, 1998; Maddula *et al.*, 2006). Biofilms develop in five stages. QS controls the rhamnolipid and Pel polysaccharid production, respectively, and the release of DNA. This, in conclusion, effects the mature biofilm formation, i.e. mushroom cap formation and open-channel maintenance (de Kievit, 2009). Influencing the biofilm formation has also been ascribed to PCA (Maddula *et al.*, 2008).

In conclusion, the continuation of *F. tricinctum* co-cultivation experiments gave more insight to microbial reactions. *S. lividans* triggered the fungus to produce new naphthoquinone dimers (fusatricinones A-D) and a new lateropyrone derivative (dihydrolateropyrone). *P. aeruginosa* reacted to the fungus by biofilm formation and antifungal phenazine production whereas no metabolic response of the fungus was observed in this case (Moussa *et al.*, 2019; Moussa *et al.*, 2020). Further studies are required to understand the trigger for the activation of the accumulation of naphthoquinone dimers. Another point would be to identify the chemical trigger for the pseudomonad biofilm formation, which may be the antibacterial metabolites of *F. tricinctum*.

4 Reference List

Abdelwahab, M. F.; Kurtán, T.; Mándi, A.; Müller, W. E. G.; Fouad, M. A.; Kamel, M. S.; Liu, Z.; Ebrahim, W.; Daletos, G.; Proksch, P. (2018) Induced secondary metabolites from the endophytic fungus *Aspergillus versicolor* through bacterial co-culture and OSMAC approaches. *Tetrahedron Letters*, **59**, 2647-2652.

Abraham, E. P.; Newton, G. G. F.; Crawford, K., Burton, H. S.; Hale, C. W. (1953) Cephalosporin N: a new type of penicillin. *Nature*, **171**, 343-343.

Acharya, D.; Miller, I.; Cui, Y.; Braun, D. R.; Berres, M. E.; Styles, M. J.; Li, L.; Kwan, J.; Rajski, S. R.; Blackwell, H. E.; Bugni, T. S. (2019) Omics technologies to understand activation of a biosynthetic gene cluster in *Micromonospora* sp. WMMB235: deciphering keyicin biosynthesis. *ACS Chemical Biology*, **14**, 1260-1270.

Adachi, K.; Kohara, T.; Nakao, N.; Arita, M.; Chiba, K.; Mishina, T.; Sasaki, S.; Fujita, T. (1995) Design, synthesis, and structure-activity relationships of 2-substituted-2-amino-1,3-propanediols: discovery of a novel immunosuppressant, FTY720. *Bioorganic & Medicinal Chemistry Letters*, **5**, 853-856.

Adnani, N.; Chevrette, M. G.; Adibhatla, S. N.; Zhang, F.; Yu, Q.; Braun, D. R.; Nelson, J.; Simpkins, S. W.; McDonald, B. R.; Myers, C. L.; Piotrowski, J. S.; Thompson, C. J.; Currie, C. R.; Li, L.; Rajski, S. R.; Bugni, T. S. (2017) Coculture of marine invertebrate-associated bacteria and interdisciplinary technologies enable biosynthesis and discovery of a new antibiotic, keyicin. *ACS Chemical Biology*, **12**, 3093-3102.

Akone, S. H.; Mándi, A.; Kurtán, T.; Hartmann, R.; Lin, W. H.; Daletos, G.; Proksch, P. (2016) Inducing secondary metabolite production by the endophytic fungus *Chaetomium* sp. through fungal-bacterial co-culture and epigenetic modification. *Tetrahedron*, **72**, 6340- 6347.

Alberts, A. W.; Chen, J.; Kuron, G.; Hunt, V.; Huff, J.; Hoffman, C.; Rothrock, J.; Lopez, M.; Joshua, H.; Harris, E.; Patchett, A.; Monaghan, R.; Currie, S.; Stapley, E.; Albers-

Schonberg, G.; Hensens, O.; Hirshfield, J.; Hoogsteen, K.; Liesch, J.; Springer, J. (1980) Mevinolin: a highly potent competitive inhibitor of hydroxymethylglutaryl-coenzyme A reductase and a cholesterol-lowering agent. *Proceedings of the National Academy of Sciences of the United States of America*, **77**, 3957-3961.

Alberts, A. W. (1988) Discovery, biochemistry and biology of lovastatin. *The American Journal of Cardiology*, **62**, J10-J15.

Allison, A. C.; Eugui, E. M. (2000) Mycophenolate mofetil and its mechanisms of action. *Immunopharmacology*, **47**, 85-118.

Aly, A. H.; Debbab, A.; Kjer, J.; Proksch, P. (2010) Fungal endophytes from higher plants: a prolific source of phytochemicals and other bioactive natural products. *Fungal Diversity*, **4**, 1-16.

Aly, A. H.; Debbab, A.; Proksch, P. (2011a) Fifty years of drug discovery from fungi. *Fungal Diversity*, **50**, 3-19.

Aly, A. H.; Debbab, A.; Proksch, P. (2011b) Fungal endophytes: unique plant inhabitants with great promises. *Applied Microbiology and Biotechnology*, **90**, 1829-1845.

Aly, A. H.; Debbab, A.; Proksch, P. (2013) Fungal endophytes–secret producers of bioactive plant metabolites. *Die Pharmazie-An International Journal of Pharmaceutical Sciences*, **68**, 499-505.

Amakhin, D. V.; Soboleva, E. B.; Zaitsev, A. V. (2018) Cephalosporin antibiotics are weak blockers of GABAa receptor-mediated synaptic transmission in rat brain slices. *Biochemical and Biophysical Research Communications*, **499**, 868-874.

Ancheeva, E.; Küppers, L.; Akone, S.H.; Ebrahim, W.; Liu, Z.; Mándi, A.; Kurtán, T.; Lin, W.H.; Orfali, R.; Rehberg, N.; Kalscheuer, R.; Daletos, G.; Proksch, P. (2017) Expanding the metabolic profile of the fungus *Chaetomium* sp. through co-culture with autoclaved *Pseudomonas aeruginosa*. *European Journal of Organic Chemistry*, **2017**, 3256−3264.

Ashour, M.; Yehia, H. M.; Proksch, P. (2011) Utilization of agro-industrial by-products for production of bioactive natural products from endophytic fungi. *Journal of Natural Products*, **4**, 108-114.

Awasthi, N.; Manickam, N.; Kumar, A. (1997) Biodegradation of endosulfan by a bacterial coculture. *Bulletin of Environmental Contamination and Toxicology*, **59**, 928-934.

Bader, J.; Mast-Gerlach, E.; Popović, M. K.; Bajpai, R.; Stahl, U. (2010) Relevance of microbial coculture fermentations in biotechnology. *Journal of Applied Microbiology*, **109**, 371-387.

Baldwin, E. L.; Osheroff, N. (2005) Etoposide, topoisomerase II and cancer. *Current Medicinal Chemistry-Anti-Cancer Agents*, **5**, 363-372.

Barefoot, S. F.; Chen, Y. R.; Hughes, T. A.; Bodine, A. B.; Shearer, M. Y.; Hughes, M. D. (1994) Identification and purification of a protein that induces production of the *Lactobacillus acidophilus* bacteriocin lactacin B. *Applied Environmental Microbiology*, **60**, 3522-3528.

Bauerle, M. R.; Schwalm, E. L.; Booker, S. J. (2015) Mechanistic diversity of radical S-adenosylmethionine (SAM)-dependent methylation. *Journal of Biological Chemistry*, **290**, 3995-4002.

Benitez, L.; Correa, A.; Daroit, D.; Brandelli, A. (2011) Antimicrobial activity of *Bacillus amyloliquefaciens* LBM 5006 is enhanced in the presence of *Escherichia coli*. *Current Microbiology*, **62**, 1017-1022.

Benz, F.; Knüsel, F.; Nüesch, J.; Treichler, H.; Voser, W.; Nyfeler, R.; Keller-Schierlein, W. (1974) Stoffwechselprodukte von Mikroorganismen 143. Mitteilung. Echinocandin B, ein neuartiges Polypeptid-Antibioticum aus *Aspergillus nidulans var. echinulatus*: Isolierung und Bausteine. *Helvetica Chimica Acta*, **57**, 2459-2477.

Bertrand, S.; Bohni, N.; Schnee, S.; Schumpp, O.; Gindro, K.; Wolfender, J. L. (2014) Metabolite induction via microorganism co-culture: a potential way to enhance

chemical diversity for drug discovery. *Biotechnology Advances*, **32**, 1180-1204.

Blayney, D.; Ogenstad, S.; Shi, Y.; Zhang, Q.; Du, L.; Huang, L.; Mohanlal, R. (2018) P1. 01-06 Plinabulin, a novel immuno-oncology agent mitigates docetaxel chemotherapy-induced-neutropenia and thrombocytopenia in NSCLC patients. *Journal of Thoracic Oncology*, **13**, 461.

Blumenthal, K. G.; Lu, N.; Zhang, Y.; Li, Y.; Walensky, R. P.; Choi, H. K. (2018) Risk of meticillin resistant *Staphylococcus aureus* and *Clostridium difficile* in patients with a documented penicillin allergy: population based matched cohort study. *British Medical Journal*, **361**, k2400.

Bode, H. B.; Bethe, B.; Höfs, R.; Zeeck, A. (2002) Big effects from small changes: possible ways to explore nature's chemical diversity. *ChemBioChem*, **3**, 619-627.

Bohni, N.; Hofstetter, V.; Gindro, K.; Buyck, B.; Schumpp, O.; Bertrand, S.; Monond, M.; Wolfender, J. L. (2016) Production of fusaric acid by *Fusarium* spp. in pure culture and in solid medium co-cultures. *Molecules*, **21**, 370.

Böhler, P.; Stuhldreier, F.; Anand, R.; Kondadi, A. K.; Schlütermann, D.; Berleth, N.; Deitersen, J.; Wallot-Hieke, N.; Wu, W.; Frank, M.; Niemann, H.; Wesbuer, E.; Barbian, A.; Luyten, T.; Parys, J. B.; Weidtkamp-Peters, S.; Borchardt, A.; Reichert, A. S.; Peña-Blanco, A.; García-Sáez, A. J.; Itskanov, S.; van der Bilek, A. M.; Proksch, P.; Wesselborg, S.; Stork, B. (2018) The mycotoxin phomoxanthone A disturbs the form and function of the inner mitochondrial membrane. *Cell Death & Disease*, **9**, 286.

Boonchan, S.; Britz, M. L.; Stanley, G. A. (2000) Degradation and mineralization of high-molecular-weight polycyclic aromatic hydrocarbons by defined fungal-bacterial cocultures. *Applied Environmental Microbiology*, **66**, 1007-1019.

Brahim, Y. A.; Bouchaou, L.; Sifeddine, A.; Khodri, M.; Reichert, B.; Cruz, F. W. (2016) Elucidating the climate and topographic controls on stable isotope composition of meteoric waters in Morocco, using station-based and spatially-interpolated data. *Journal of Hydrology*, **543**, 305-315.

Brakhage, A. A. (1998) Molecular regulation of β-lactam biosynthesis in filamentous fungi. *Microbiology and Molecular Biology Reviews,* **62**, 547-585.

Brakhage, A. A.; Spröte, P.; Al-Abdallah, Q.; Gehrke, A.; Plattner, H.; Tüncher, A. (2004) Regulation of penicillin biosynthesis in filamentous fungi. *Advances in Biochemical Engineering/Biotechnology*, **88**, 45-90.

Brinkmann, V.; Billich, A.; Baumruker, T.; Heining, P.; Schmouder, R.; Francis, G.; Aradhye, S.; Burtin, P. (2010) Fingolimod (FTY720): discovery and development of an oral drug to treat multiple sclerosis. *Nature Reviews Drug Discovery*, **9**, 883-897.

Brinkmann, V.; Davis, M. D.; Heise, C. E.; Albert, R.; Cottens, S.; Hof, R.; Bruns, C.; Prieschl, E.; Baumruker, T.; Hiestand, P.; Foster, C. A.; Zollinger, M.; Lynch, K. R. (2002) The immune modulator FTY720 targets sphingosine 1-phosphate receptors. *Journal of Biological Chemistry*, **277**, 21453-21457.

Brotzu, G. (1948) Research on a new antibiotic. *Publications of the Cagliari Institute of Hygiene,* 5-19.

Buckland, B. (1989) Production of lovastatin, an inhibitor of cholesterol accumulation in humans. *Novel Microbials for Medicine and Agriculture*, 161-169.

Bushnell, G. W.; Li, Y. L.; Poulton, G. A. (1984) Pyrones. X. Lateropyrone, a new antibiotic from the fungus *Fusarium lateritium* Nees. *Canadian Journal of Chemistry*, **62**, 2101-2106.

Butler, M. S. (2004) The role of natural product chemistry in drug discovery. *Journal of Natural Products*, **67**, 2141-2153.

Camacho-Zaragoza, J. M.; Hernandez-Chavez, G.; Moreno-Avitia, F.; Ramírez-Iñiguez, R.; Martínez, A.; Bolívar, F.; Gosset, G. (2016) Engineering of a microbial coculture of *Escherichia coli* strains for the biosynthesis of resveratrol. *Microbial Cell Factories*, **15**, 163.

Chadwick, A. J.; Jackson, B. (1969) Intraocular penetration of the antibiotic fucidin. *The British Journal of Ophthalmology*, **53**, 26-29.

Chandra, S. (2012) Endophytic fungi: novel sources of anticancer lead molecules. *Applied Microbiology and Biotechnology*, **95**, 47-59.

Chanos, P.; Mygind, T. (2016) Co-culture-inducible bacteriocin production in lactic acid bacteria. *Applied Microbiology and Biotechnology*, **100**, 4297-4308.

Chen, H.; Daletos, G.; Abdel-Aziz, M. S.; Thomy, D.; Dai, H.; Brötz-Oesterhelt, H.; Lin, W. H.; Proksch, P. (2015) Inducing secondary metabolite production by the soil-dwelling fungus *Aspergillus terreus* through bacterial co-culture. *Phytochemistry Letters*, **12**, 35-41.

Chin, Y. W.; Balunas, M. J.; Chai, H. B.; Kinghorn, A. D. (2006) Drug discovery from natural sources. *The AAPS Journal*, **8**, E239-E253.

Chin-A-Woeng, T. F.; Bloemberg, G. V.; Lugtenberg, B. J. (2003) Phenazines and their role in biocontrol by *Pseudomonas* bacteria. *New Phytologist*, **157**, 503-523.

Chin-A-Woeng, T. F.; van den Broek, D.; Lugtenberg, B. J.; Bloemberg, G. V. (2005) The *Pseudomonas chlororaphis* PCL1391 sigma regulator psrA represses the production of the antifungal metabolite phenazine-1-carboxamide. *Molecular Plant-Microbe Interactions*, **18**, 244-253.

Chintalapally, S.; Rao, D. M. (2016) Origin, evolution and milestones in the field of natural product research. *International Journal of Current Microbiology and Applied Sciences*, **5**, 89-92.

Chun, J.; Hartung, H. P. (2010) Mechanism of action of oral fingolimod (FTY720) in multiple sclerosis. *Clinical Neuropharmacology*, **33**, 91-101.

Cimino, P. J.; Huang, L.; Du, L.; Wu, Y.; Bishop, J.; Dalsing-Hernandez, J.; Kotlarczyk, K.; Gonzales, P.; Carew, J.; Nawrocki, S.; Jordan, M. A.; Wilson, L.; Lloyd, G. K.; Wirsching, H. G. (2019) Plinabulin, an inhibitor of tubulin polymerization, targets

KRAS signaling through disruption of endosomal recycling. *Biomedical Reports*, **10**, 218-224.

Cragg, G. M.; Newman, D. J. (2013) Natural products: a continuing source of novel drug leads. *Biochimica et Biophysica Acta (BBA)-General Subjects*, **1830**, 3670-3695.

Crosbie, R. B. (1963) Treatment of staphylococcal infections with "fucidin". *British Medical Journal*, **1**, 788-794.

Cundliffe, E. (1972) The mode of action of fusidic acid. *Biochemical and Biophysical Research Communications*, **46**, 1794-1801.

Daletos, G.; Ebrahim, W.; Ancheeva, E.; El-Neketi, M.; Lin, W. H.; Proksch, P. (2017) Microbial co-culture and OSMAC approach as strategies to induce cryptic fungal biogenetic gene clusters. *Chemical Biology of Natural Products*, **8**, 233-284. Dangmann, E.; Stolz, A.; Kuhm, A. E.; Hammer, A.; Feigel, B.; Noisommit-Rizzi, N.; Rizzi, M.; Reuß, M.; Knackmuss, H. J. (1996) Degradation of 4-aminobenzenesulfonate by a two-species bacterial coculture. *Biodegradation*, **7**, 223-229. Davey, M. E.; O'toole, G. A. (2000) Microbial biofilms: from ecology to molecular genetics. *Microbiology and Molecular Biology Reviews*, **64**, 847–867.

Davies, D. G.; Parsek, M. R.; Pearson, J. P.; Iglewski, B. H.; Costerton, J. W.; Greenberg, E. P. (1998) The involvement of cell-to-cell signals in the development of a bacterial biofilm. *Science*, **280**, 295–298.

Debbab, A.; Aly, A. H.; Edrada-Ebel, R.; Wray, V.; Müller, W. E. G.; Totzke, F.; Zirrgiebel, U.; Schächtele, C.; Kubbutat, M. H. G.; Lin, W. H.; Mosaddak, M.; Hakiki, A.; Proksch, P.; Ebel, R. (2009) Bioactive metabolites from the endophytic fungus *Stemphylium globuliferum* isolated from *Mentha pulegium*. *Journal of Natural Products*, **72**, 626-631.

Debbab, A.; Aly, A. H.; Edrada-Ebel, R.; Wray, V.; Pretsch, A.; Pescitelli, G.; Kurtán, T.; Proksch, P. (2012a) New anthracene derivatives – structure elucidation and

antimicrobial activity. *European Journal of Organic Chemistry*, **2012**, 1351-1359.

Debbab, A.; Aly, A. H.; Proksch, P. (2012b) Endophytes and associated marine derived fungi-ecological and chemical perspectives. *Fungal Diversity*, **57**, 45-83.

Debbab, A.; Aly, A. H.; Proksch, P. (2013) Mangrove derived fungal endophytes–a chemical and biological perception. *Fungal Diversity*, **61**, 1-27.

Debono, M.; Turner, W. W.; LaGrandeur, L.; Burkhardt, F. J.; Nissen, J. S.; Nichols, K. K.; Rodriguez, M. J.; Zweifel, M. J.; Zeckner, D. J.; Gordee, R. S.; Tang, J.; Parr, T. R. Jr. (1995) Semisynthetic chemical modification of the antifungal lipopeptide echinocandin B (ECB): structure-activity studies of the lipophilic and geometric parameters of polyarylated acyl analogs of ECB. *Journal of Medicinal Chemistry*, **38**, 3271-3281.

De Kievit, T. R. (2009) Quorum sensing in *Pseudomonas aeruginosa* biofilms. *Environmental microbiology*, **11**, 279-288.

De la Torre, B. G.; Albericio, F. (2018) The pharmaceutical industry in 2017. An analysis of FDA drug approvals from the perspective of molecules. *Molecules*, **23**, 533.

De la Torre, B. G.; Albericio, F. (2019) The pharmaceutical industry in 2018. An analysis of FDA drug approvals from the perspective of molecules. *Molecules*, **24**, 809.

Deng, Z. L.; Du, C. X.; Li, X.; Hu, B.; Kuang, Z. K.; Wang, R.; Feng, S. Y.; Zhang, H. Y.; Kong, D. X. (2013) Exploring the biologically relevant chemical space for drug discovery. *Journal of Chemical Information and Modeling*, **53**, 2820-2828.

Denning, D. W. (1997) Echinocandins and pneumocandins - a new antifungal class with a novel mode of action. *The Journal of Antimicrobial Chemotherapy*, **40**, 611-614.

Di Cagno, R.; De Angelis, M.; Coda, R.; Minervini, F.; Gobbetti, M. (2009) Molecular adaptation of sourdough *Lactobacillus plantarum* DC400 under co-cultivation with other lactobacilli. *Research in Microbiology*, **160**, 358-366.

Dornetshuber, R.; Heffeter, P.; Kamyar, M. R.; Peterbauer, T.; Berger, W.; Lemmens-Gruber, R. (2007) Enniatin exerts p53-dependent cytostatic and p53-independent cytotoxic

activities against human cancer cells. *Chemical Research in Toxicology*, **20**, 465-473.

Doyle, D. (2014) Thomas MacLagan's 1876 demonstration of the dramatic effects of salicin in rheumatic fever. *Journal of the Royal Society of Medicine*, **107**, 287-289.

Durley, R. C.; MacMillan, J.; Simpson, T. J.; Glen, A. T.; Turner, W. B. (1975) Fungal products. Part XIII. Xanthomegnin, viomellin, rubrosulphin, and viopurpurin, pigments from *Aspergillus sulphureus* and *Aspergillus melleus. Journal of the Chemical Society, Perkin Transactions 1*, **1975**, 163-169.

Ebrahim, W.; Kjer, J.; El Amrani, M.; Wray, V.; Lin, W. H.; Ebel, R.; Lai, D.; Proksch, P. (2012) Pullularins E and F, two new peptides from the endophytic fungus *Bionectria ochroleuca* isolated from the mangrove plant *Sonneratia caseolaris*. *Marine Drugs*, **10**, 1081-1091.

El-Sayed, A. S.; Safan, S.; Mohamed, N. Z.; Shaban, L.; Ali, G. S.; Sitohy, M. Z. (2018) Induction of taxol biosynthesis by *Aspergillus terreus*, endophyte of *Podocarpus gracilior* Pilger, upon intimate interaction with the plant endogenous microbes. *Process Biochemistry*, **71**, 31-40.

Emri, T.; Majoros, L.; Tóth, V.; Pócsi, I. (2013) Echinocandins: production and applications. *Applied Microbiology and Biotechnology*, **97**, 3267-3284.

Endo, A.; Kuroda, M.; Tsujita, Y. (1976) ML-236A, ML-236B, and ML-236C, new inhibitors of cholesterogenesis produced by *Penicillium citrinum*. *The Journal of Antibiotics*, **29**, 1346-1348.

European Mycophenolate Mofetil Cooperative Study Group. (1995) Placebo-controlled study of mycophenolate mofetil combined with cyclosporin and corticosteroids for prevention of acute rejection. *The Lancet*, **345**, 1321-1325.

Eyberger, A. L.; Dondapati, R.; Porter, J. R. (2006) Endophyte fungal isolates from *Podophyllum peltatum* produce podophyllotoxin. *Journal of Natural Products*, **69**, 1121-1124.

Fenical, W.; Jensen, P. R.; Cheng, X. C. (2000) Halimide, a cytotoxic marine natural product, and derivatives thereof. U.S. Patent No. 6,069,146. *Washington, DC: U.S. Patent and Trademark Office*.

Fosse, T.; Toga, B.; Peloux, Y.; Granthil, C.; Bertrando, J.; Sethian, M. (1985) Meningitis due to *Micrococcus luteus*. *Infection*, **13**, 280-281.

Frandsen, R. J.; Nielsen, N. J.; Maolanon, N.; Sørensen, J. C.; Olsson, S.; Nielsen, J.; Giese, H. (2006) The biosynthetic pathway for aurofusarin in *Fusarium graminearum* reveals a close link between the naphthoquinones and naphthopyrones. *Molecular Microbiology*, **61**, 1069-1080.

Frank, M.; Niemann, H.; Böhler, P.; Stork, B.; Wesselborg, S.; Lin, W. H.; Proksch, P. (2015) Phomoxanthone A-from mangrove forests to anticancer therapy. *Current Medicinal Chemistry*, **22**, 3523-3532.

Galy, N.; Moraleda, D.; Santelli, M. (2011) Allylsilane and diallylsilane reactions with functionalized ethylene ketals or benzodioxoles. *Tetrahedron*, **67**, 1448-1455. Ge, J.; Fang, B.; Wang, Y.; Song, G.; Ping, W. (2014) *Bacillus subtilis* enhances production of Paracin1. 7, a bacteriocin produced by *Lactobacillus paracasei* HD1-7, isolated from Chinese fermented cabbage. *Annals of Microbiology*, **64**, 1735-1743.

German-Fattal, M. (2001) Fusafungine, an antimicrobial with anti-inflammatory properties in respiratory tract infections. *Clinical Drug Investigation*, **21**, 653-670.

Godtfredsen, W. O.; Roholt, K.; Tybring, L. (1962) Fucidin. A new orally active antibiotic. *Lancet*, 928-931.

Grove, J. F.; MacMillan, J.; Mulholland, T. P. C.; Thorold Rogers, M. A. (1952) 762. Griseofulvin. Part IV. Structure. *Journal of the Chemical Society (Resumed)*, 3977-3987.

Hande, K. R. (1998) Etoposide: four decades of development of a topoisomerase II inhibitor. *European Journal of Cancer*, **34**, 1514-1521.

Hemphill, C. F. P.; Sureechatchaiyan, P.; Kassack, M. U.; Orfali, R. S.; Lin, W. H.; Daletos, G.; Proksch, P. (2017) OSMAC approach leads to new fusarielin metabolites from *Fusarium tricinctum*. *The Journal of Antibiotics*, **70**, 726-732.

Höfle, G.; Röser, K. (1978) Structure of xanthomegnin and related pigments: reinvestigation by ^{13}C nuclear magnetic resonance spectroscopy. *Journal of the Chemical Society, Chemical Communications*, **14**, 611-612.

Höller, U.; Gloer, J. B.; Wicklow, D. T. (2002) Biologically active polyketide metabolites from an undetermined fungicolous hyphomycete resembling *Cladosporium*. *Journal of Natural Products*, **65**, 876-882.

Hoffman, L. R.; D'Argenio, D. A.; MacCoss, M. J.; Zhang, Z.; Jones, R. A.; Miller, S. I. (2005) Aminoglycoside antibiotics induce bacterial biofilm formation. *Nature*, **436**, 1171-1175.

Hontecillas, R.; Tubau-Juni, N.; Bassaganya-Riera, J.; Leber, A.; Zoccoli-Rodriguez, V.; Kronsteiner, B.; Viladomiu, M.; Abedi, V. (2019) Identification of regulatory genes through global gene expression analysis of a *Helicobacter pylori* co-culture system. *BioRxiv - the Preprint Server for Biology*, **523274**.

Hoshino, S.; Okada, M.; Wakimoto, T.; Zhang, H.; Hayashi, F.; Onaka, H.; Abe, I. (2015a) Niizalactams A–C, multicyclic macrolactams isolated from combined culture of *Streptomyces* with mycolic acid-containing bacterium. *Journal of Natural Products*, **78**, 3011-3017.

Hoshino, S.; Onaka, H.; Abe, I. (2019) Activation of silent biosynthetic pathways and discovery of novel secondary metabolites in actinomycetes by co-culture with mycolic acid-containing bacteria. *Journal of Industrial Microbiology & Biotechnology*, **46**, 363-374.

Hoshino, S.; Wakimoto, T.; Onaka, H.; Abe, I. (2015b) Chojalactones A–C, cytotoxic butanolides isolated from *Streptomyces* sp. cultivated with mycolic acid-containing

bacterium. *Organic Letters*, **17**, 1501-1504.

Hoshino, S.; Wong, C. P.; Ozeki, M.; Zhang, H.; Hayashi, F.; Awakawa, T.; Asamizu, S.; Onaka, H.; Abe, I. (2018) Umezawamides, new bioactive polycyclic tetramate macrolactams isolated from a combined-culture of *Umezawaea* sp. and mycolic acid-containing bacterium. *The Journal of Antibiotics*, **71**, 653-657.

Hoshino, S.; Zhang, L.; Awakawa, T.; Wakimoto, T.; Onaka, H.; Abe, I. (2015c) Arcyriaflavin E, a new cytotoxic indolocarbazole alkaloid isolated by combined-culture of mycolic acid-containing bacteria and *Streptomyces cinnamoneus* NBRC 13823. *The Journal of Antibiotics*, **68**, 342-344.

Hoyle, B. D.; Alcantara, J.; Costerton, J. W. (1992) *Pseudomonas aeruginosa* biofilm as a diffusion barrier to piperacillin. *Antimicrobial Agents and Chemotherapy*, **36**, 2054-2056.

Hoyle, B. D.; Costerton, J. W. (1991) Bacterial resistance to antibiotics: the role of biofilms. *Progress in Drug Research/Fortschritte der Arzneimittelforschung/Progrès des recherches pharmaceutiques*, **37**, 91–105.

Huber, F. M.; Gottlieb, D. (1968) The mechanism of action of griseofulvin. *Canadian Journal of Microbiology*, **14**, 111-118.

Ishikawa, H. (1999) Mizoribine and mycophenolate mofetil. *Current Medicinal Chemistry*, **6**, 575-598.

Jalgaonwala, R. E.; Mohite, B. V.; Mahajan, R. T. (2011) A review: natural products from plant associated endophytic fungi. *Journal of Microbiology and Biotechnology Research*, **1**, 21-32.

Kadkade, P. G. (1982) Growth and podophyllotoxin production in callus tissues of *Podophyllum peltatum*. *Plant Science Letters*, **25**, 107-115.

Kanamaru, S.; Honma, M.; Murakami, T.; Tsushima, T.; Kudo, S.; Tanaka, K.; Nihei, K. I.;

Nehira, T.; Hashimoto, M. (2012) Absolute stereochemistry of altersolanol A and alterporriols. *Chirality*, **24**, 137-146.

Kanoh, K.; Kohno, S.; Asari, T.; Harada, T.; Katada, J.; Muramatsu, M.; Kawashima, H.; Sekiya, H.; Uno, I. (1997) (−)-Phenylahistin: a new mammalian cell cycle inhibitor produced by *Aspergillus ustus*. *Bioorganic & Medicinal Chemistry Letters*, **7**, 2847-2852.

Kanski, J. J. (1974) Treatment of late endophthalmitis associated with filtering blebs. *Archives of Ophthalmology*, **91**, 339-343.

Kaplan, J. B. (2011) Antibiotic-induced biofilm formation. *The International Journal of Artificial Organs*, **34**, 737-751.

Kaul, S.; Gupta, S.; Ahmed, M.; Dhar, M. K. (2012) Endophytic fungi from medicinal plants: a treasure hunt for bioactive metabolites. *Phytochemistry Reviews*, **11**, 487-505.

Keller-Juslén, C.; Kuhn, M.; Loosli, H. R.; Pechter, T. J.; von Weber, H. P.; Von Wartburg, A. (1976) Struktur des Cyclopeptid-Antibiotikums SL 7810 (= Echinocandin B). *Tetrahedron Letters*, **17**, 4147-4150.

Kharwar, R. N.; Mishra, A.; Gond, S. K.; Stierle, A.; Stierle, D. (2011) Anticancer compounds derived from fungal endophytes: their importance and future challenges. *Natural Product Reports*, **28**, 1208-1228.

Kingston, D. G.; Chaudhary, A. G.; Gunatilaka, A. L.; Middleton, M. L. (1994) Synthesis of taxol from baccatin III via an oxazoline intermediate. *Tetrahedron Letters*, **35**, 4483-4484.

Kluepfel, D.; Bagli, J.; Baker, H.; Charest, M. P.; Kudelski, A.; Sehgal, S. N.; Vézina, C. (1972) Myriocin, a new antifungal antibiotic from *Myriococcum albomyces*. *The Journal of Antibiotics*, **25**, 109-115.

Kos, B.; Beganović, J.; Jurašić, L.; Švađumović, M.; Leboš Pavunc, A.; Uroić, K.; Šušković, J. (2011) Coculture-inducible bacteriocin biosynthesis of different probiotic strains by

dairy starter culture *Lactococcus lactis*. *Mljekarstvo: časopis za unaprjeđenje proizvodnje i prerade mlijeka*, **61**, 273-282.

Kuhnert, N. (2000) Hundert Jahre Aspirin®-Die Geschichte des wohl erfolgreichsten Medikaments des letzten Jahrhunderts. *Pharmazie in unserer Zeit*, **29**, 32-39.

Kuiper-Goodman, T.; Scott, P.; Watanabe, H. (1987) Risk assessment of the mycotoxin zearalenone. *Regulatory Toxicology and Pharmacology*, **7**, 253-306.

Kumar, A.; Patil, D.; Rajamohanan, P. R.; Ahmad, A. (2013) Isolation, purification and characterization of vinblastine and vincristine from endophytic fungus *Fusarium oxysporum* isolated from *Catharanthus roseus*. *PloS One*, **8**, e71805.

Lai, S.; Shizuri, Y.; Yamamura, S.; Kawai, K.; Furukawa, H. (1991) Three new phenolic metabolites from *Penicillium* species. *Heterocycles*, **32**, 297-305.

Li, B. J.; Wang, H.; Gong, T.; Chen, J. J.; Chen, T. J.; Yang, J. L.; Zhu, P. (2017) Improving 10-deacetylbaccatin III-10-β-O-acetyltransferase catalytic fitness for Taxol production. *Nature Communications*, **8**, 15544.

Li, L.; Song, X.; Yin, Z.; Jia, R.; Li, Z.; Zhou, X.; Zou, Y.; Li, L.; Yin, L.; Yue, G.; Ye, G.; Lv, C.; Shi, W.; Fu, Y. (2016) The antibacterial activity and action mechanism of emodin from *Polygonum cuspidatum* against *Haemophilus parasuis* in vitro. *Microbiological Research*, **186**, 139-145.

Liebner, D. A. (2015). The indications and efficacy of conventional chemotherapy in primary and recurrent sarcoma. *Journal of Surgical Oncology*, **111**, 622-631.

Liu, Y.; Marmann, A.; Abdel-Aziz, M. S.; Wang, C. Y.; Müller, W. E. G.; Lin, W. H.; Mándi, A.; Kurtán, T.; Daletos, G.; Proksch, P. (2015) Tetrahydroanthraquinone derivatives from the endophytic fungus *Stemphylium globuliferum*. *European Journal of Organic Chemistry*, **2015**, 2646-2653.

Liu, Y.; Wray, V.; Abdel-Aziz, M. S.; Wang, C. Y.; Lai, D.; Proksch, P. (2014) Trimeric anthracenes from the endophytic fungus *Stemphylium globuliferum*. *Journal of Natural*

Products, **77**, 1734-1738.

Maddula, V. S. R. K.; Pierson, E. A.; Pierson, L. S. (2008) Altering the ratio of phenazines in *Pseudomonas chlororaphis* (*aureofaciens*) strain 30-84: effects on biofilm formation and pathogen inhibition. *Journal of Bacteriology*, **190**, 2759–2766.

Maddula, V. S. R. K.; Zhang, Z.; Pierson, E. A.; Pierson, L. S. (2006) Quorum sensing and phenazines are involved in biofilm formation by *Pseudomonas chlororaphis* (*aureofaciens*) strain 30-84. *Microbial Ecology*, **52**, 289–301.

Mah, T. F.; Pitts, B.; Pellock, B.; Walker, G. C.; Stewart, P. S.; O'Toole, G. A. (2003) A genetic basis for *Pseudomonas aeruginosa* biofilm antibiotic resistance. *Nature*, **426**, 306-310.

Maldonado, A.; Jiménez-Díaz, R.; Ruiz-Barba, J. L. (2004) Induction of plantaricin production in *Lactobacillus plantarum* NC8 after coculture with specific gram-positive bacteria is mediated by an autoinduction mechanism. *Journal of Bacteriology*, **186**, 1556-1564.

Malz, S.; Grell, M. N.; Thrane, C.; Maier, F. J.; Rosager, P.; Felk, A.; Albertsen, K. S.; Salomon, S.; Bohn, L.; Schäfer, W.; Giese, H. (2005) Identification of a gene cluster responsible for the biosynthesis of aurofusarin in the *Fusarium graminearum* species complex. *Fungal Genetics and Biology*, **42**, 420-433.

Man, L. L.; Meng, X. C.; Zhao, R. H. (2012) Induction of plantaricin MG under co-culture with certain lactic acid bacterial strains and identification of LuxS mediated quorum sensing system in *Lactobacillus plantarum* KLDS1. 0391. *Food Control*, **23**, 462-469.

Marfori, E. C.; Kajiyama, S. I.; Fukusaki, E. I.; Kobayashi, A. (2002) Trichosetin, a novel tetramic acid antibiotic produced in dual culture of *Trichoderma harzianum* and *Catharanthus roseus callus*. *Zeitschrift für Naturforschung C*, **57**, 465-470.

Marmann, A.; Aly, A. H.; Lin, W. H.; Wang, B.; Proksch, P. (2014) Co-cultivation—a powerful emerging tool for enhancing the chemical diversity of microorganisms. *Marine Drugs*, **12**, 1043-1065.

Mathijssen, R. H.; Loos, W. J.; Verweij, J.; Sparreboom, A. (2002) Pharmacology of topoisomerase I inhibitors irinotecan (CPT-11) and topotecan. *Current Cancer Drug Targets*, **2**, 103-123.

McCarty, T. P.; Lockhart, S. R.; Moser, S. A.; Whiddon, J.; Zurko, J.; Pham, C. D.; Pappas, P. G. (2018) Echinocandin resistance among *Candida* isolates at an academic medical centre 2005–15: analysis of trends and outcomes. *Journal of Antimicrobial Chemotherapy*, **73**, 1677-1680.

Millward, M.; Mainwaring, P.; Mita, A.; Federico, K.; Lloyd, G. K.; Reddinger, N.; Nawrocki, S.; Mita, M.; Spear, M.A. (2012) Phase 1 study of the novel vascular disrupting agent plinabulin (NPI-2358) and docetaxel. *Investigational New Drugs*, **30**, 1065-1073.

Mishra, P. D.; Verekar, S. A.; Deshmukh, S. K.; Joshi, K. S.; Fiebig, H. H.; Kelter, G. (2015) Altersolanol A: a selective cytotoxic anthraquinone from a *Phomopsis* sp. *Letters in Applied Microbiology*, **60**, 387-391.

Mohamed, A. W. (2005). Geochemistry and sedimentology of core sediments and the influence of human activities; Qusier, Safaga and Hurghada harbors, Red Sea Coast, Egypt. *Egyptian Journal of Aquatic Research*, **31**, 92-103.

Montecucco, A.; Biamonti, G. (2007) Cellular response to etoposide treatment. *Cancer Letters*, **252**, 9-18.

Moussa, M.; Ebrahim, W.; Bonus, M.; Gohlke, H.; Mándi, A.; Kurtán, T.; Hartmann, R.; Kalscheuer, R.; Lin, W. H.; Liu, Z.; Proksch, P. (2019) Co-culture of the fungus *Fusarium tricinctum* with *Streptomyces lividans* induces production of cryptic naphthoquinone dimers. *RSC Advances*, **9**, 1491-1500.

Moussa, M.; Ebrahim, W.; El-Neketi, M.; Mándi, A.; Kurtán, T.; Hartmann, R.; Lin, W. H.; Liu, Z.; Proksch, P. (2016) Tetrahydroanthraquinone derivatives from the mangrove-derived endophytic fungus *Stemphylium globuliferum*. *Tetrahedron Letters*, **57**, 4074-4078.

Moussa, M.; Ebrahim, W.; Kalscheuer, R.; Liu, Z.; Proksch, P. (2020) Co-culture of the bacterium *Pseudomonas aeruginosa* with the fungus *Fusarium tricinctum* induces bacterial antifungal and quorum sensing signalling molecules. *Phytochemistry Letters*, submitted.

Negishi, S.; Huang, Z. C.; Hasumi, K.; Murakawa, S.; Endo, A. (1986) Productivity of monacolin K (mevinolin) in the genus *Monascus*. *Hakko Kogaku Kaishi*, **64**, 509–512.

Newman, D. J.; Cragg, G. M. (2016) Natural products as sources of new drugs from 1981 to 2014. *Journal of Natural Products*, **79**, 629-661.

Newman, D. J.; Cragg, G. M.; Snader, K. M. (2000) The influence of natural products upon drug discovery. *Natural Product Reports*, **17**, 215-234.

Newton, G. G. F.; Abraham, E. P. (1956) Isolation of cephalosporin C, a penicillin-like antibiotic containing D-α-aminoadipic acid. *Biochemical Journal*, **62**, 651-658.

Nonaka, K.; Chiba, T.; Suga, T.; Asami, Y.; Iwatsuki, M.; Masuma, R.; Ōmura, S.; Shiomi, K. (2015) Coculnol, a new penicillic acid produced by a coculture of *Fusarium solani* FKI-6853 and *Talaromyces* sp. FKA-65. *The Journal of Antibiotics*, **68**, 530-532.

Nützmann, H. W.; Reyes-Dominguez, Y.; Scherlach, K.; Schroeckh, V.; Horn, F.; Gacek, A.; Schümann, J.; Hertweck, C.; Strauss, J.; Brakhage, A. A. (2011) Bacteria-induced natural product formation in the fungus *Aspergillus nidulans* requires Saga/Ada-mediated histone acetylation. *Proceedings of the National Academy of Sciences*, **108**, 14282-14287.

Oberlies, N. H.; Kroll, D. J. (2004) Camptothecin and taxol: historic achievements in natural products research. *Journal of Natural Products*, **67**, 129-135.

Ohnishi, K.; Suemitsu, R.; Kubota, M.; Matano, H.; Yamada, Y. (1991) Biosyntheses of alterporriol D and E by *Alternaria porri*. *Phytochemistry*, **30**, 2593-2595.

Ohnishi, K.; Tanabe, H.; Hayashi, S.; Suemitsu, R. (1992) Biosynthesis of alterporriol A by *Alternaria porri*. *Bioscience, Biotechnology, and Biochemistry*, **56**, 42-43.

Ola, A. R.; Thomy, D.; Lai, D.; Brötz-Oesterhelt, H.; Proksch, P. (2013) Inducing secondary metabolite production by the endophytic fungus *Fusarium tricinctum* through coculture with *Bacillus subtilis*. *Journal of Natural Products*, **76**, 2094-2099.

Olsen, K. J. K.; Rossman, A.; Andersen, B. (2018) Metabolite production by species of *Stemphylium*. *Fungal Biology*, **122**, 172-181.

Onaka, H.; Mori, Y.; Igarashi, Y.; Furumai, T. (2011) Mycolic acid-containing bacteria induce natural-product biosynthesis in *Streptomyces* species. *Applied Environmental Microbiology*, **77**, 400-406.

Onaka, H.; Ozaki, T.; Mori, Y.; Izawa, M.; Hayashi, S.; Asamizu, S. (2015) Mycolic acid-containing bacteria activate heterologous secondary metabolite expression in *Streptomyces lividans*. *The Journal of Antibiotics*, **68**, 594-597.

Oxford, A. E., Raistrick, H.; Simonart, P. (1939) Studies in the biochemistry of micro-organisms: griseofulvin, $C_{17}H_{17}O_6Cl$, a metabolic product of *Penicillium griseo-fulvum* Dierckx. *Biochemical Journal*, **33**, 240-248.

Pan, R.; Bai, X.; Chen, J.; Zhang, H.; Wang, H. (2019) Exploring structural diversity of microbe secondary metabolites using OSMAC strategy: A literature review. *Frontiers in Microbiology*, **10**, 294.

Panda, D.; Rathinasamy, K.; Santra, M. K.; Wilson, L. (2005) Kinetic suppression of microtubule dynamic instability by griseofulvin: implications for its possible use in the treatment of cancer. *Proceedings of the National Academy of Sciences*, **102**, 9878-9883.

Park, H. B.; Park, J. S.; Lee, S. I.; Shin, B.; Oh, D. C.; Kwon, H. C. (2017) Gordonic acid, a polyketide glycoside derived from bacterial coculture of *Streptomyces* and *Gordonia* species. *Journal of Natural Products*, **80**, 2542-2546.

Parrales, A.; Thoenen, E.; Iwakuma, T. (2018) The interplay between mutant p53 and the mevalonate pathway. *Cell Death & Differentiation*, **25**, 460-467.

Partridge, E.; Gareiss, P.; Kinch, M. S.; Hoyer, D. (2016) An analysis of FDA-approved drugs:

natural products and their derivatives. *Drug Discovery Today*, **21**, 204-207.

Penman, R. (1962) Fusidic acid in bacterial endocarditis. *The Lancet*, **280**, 1277–1278.

Pettit, R. K.; Pettit, G. R.; Xu, J. P.; Weber, C. A.; Richert, L. A. (2010) Isolation of human cancer cell growth inhibitory, antimicrobial lateritin from a mixed fungal culture. *Planta Medica*, **76**, 500-501.

Pfaller, M. A.; Marco, F.; Messer, S. A.; Jones, R. N. (1998) In vitro activity of two echinocandin derivatives, LY303366 and MK-0991 (L-743,792), against clinical isolates of *Aspergillus*, *Fusarium*, *Rhizopus*, and other filamentous fungi. *Diagnostic Microbiology and Infectious Disease*, **30**, 251-255.

Pompeng, P.; Sommit, D.; Sriubolmas, N.; Ngamrojanavanich, N.; Matsubara, K.; Pudhom, K. (2013) Antiangiogenetic effects of anthranoids from *Alternaria* sp., an endophytic fungus in a Thai medicinal plant *Erythrina variegata*. *Phytomedicine*, **20**, 918-922.

Pritchard, D. I. (2005) Sourcing a chemical succession for cyclosporine from parasites and human pathogens. *Drug Discovery Today*, **10**, 688-691.

Proksch, P.; Putz, A.; Ortlepp, S.; Kjer, J.; Bayer, M. (2010) Bioactive natural products from marine sponges and fungal endophytes. *Phytochemistry Reviews*, **9**, 475-489. Rajabalian, S. (2008) Methanolic extract of *Teucrium polium L*. potentiates the cytotoxic and apoptotic effects of anticancer drugs of vincristine, vinblastine and doxorubicin against a panel of cancerous cell lines. *Experimental Oncology*, **30**, 133-138.

Ribeiro, A. R.; Sures, B.; Schmidt, T. C. (2018) Cephalosporin antibiotics in the aquatic environment: a critical review of occurrence, fate, ecotoxicity and removal technologies. *Environmental Pollution*, **241**, 1153-1166.

Richardson, M. D.; Warnock, D. W. (2003) Fungal infection: diagnosis and management, 3rd edn. *Blackwell Publishing Ltd*, 70-72.

Rishton, G. M. (2008) Natural products as a robust source of new drugs and drug leads: past successes and present day issues. *The American Journal of Cardiology*, **101**, 43-49.

Rönsberg, D.; Debbab, A.; Mándi, A.; Vasylyeva, V.; Böhler, P.; Stork, B.; Engelke, L.; Hamacher, A.; Sawadogo, R.; Diedrich, M.; Wray, V.; Lin, W. H.; Kassack, M. U.; Janiak, C.; Scheu, S.; Wesselborg, S.; Kurtán, T.; Aly, A. H.; Proksch, P. (2013) Pro-apoptotic and immunostimulatory tetrahydroxanthone dimers from the endophytic fungus *Phomopsis longicolla*. *The Journal of Organic Chemistry*, **78**, 12409-12425.

Rojo-Bezares, B.; Saenz, Y., Navarro, L.; Zarazaga, M.; Ruiz-Larrea, F.; Torres, C. (2007) Coculture-inducible bacteriocin activity of *Lactobacillus plantarum* strain J23 isolated from grape must. *Food Microbiology*, **24**, 482-491.

Romaine, I. M.; Sulikowski, G. A. (2015) Studies on a biomimetic oxidative dimerization approach to the hibarimicins. *Tetrahedron Letters*, **56**, 3617-3619.

Rugbjerg, P.; Naesby, M.; Mortensen, U. H.; Frandsen, R. J. (2013) Reconstruction of the biosynthetic pathway for the core fungal polyketide scaffold rubrofusarin in *Saccharomyces cerevisiae*. *Microbial Cell Factories*, **12**, 31.

Sauvage, E.; Kerff, F.; Terrak, M.; Ayala, J. A.; Charlier, P. (2008) The penicillin-binding proteins: structure and role in peptidoglycan biosynthesis. *FEMS Microbiology Reviews*, **32**, 234-258.

Scherlach, K.; Hertweck, C. (2009) Triggering cryptic natural product biosynthesis in microorganisms. *Organic & Biomolecular Chemistry*, **7**, 1753-1760.

Schiewe, H. J.; Zeeck, A. (1999) Cineromycins, γ-butyrolactones and ansamycins by analysis of the secondary metabolite pattern created by a single strain of *Streptomyces*. *The Journal of Antibiotics*, **52**, 635-642.

Schroeckh, V.; Scherlach, K.; Nützmann, H. W.; Shelest, E.; Schmidt-Heck, W.; Schuemann, J.; Martin, K.; Hertweck, C.; Brakhage, A. A. (2009) Intimate bacterial–fungal interaction triggers biosynthesis of archetypal polyketides in *Aspergillus nidulans*. *Proceedings of the National Academy of Sciences*, **106**, 14558-14563.

Schwartz, R. E.; Giacobbe, R. A.; Bland, J. A.; Monaghan, R. L. (1989) L-671, 329, a new

antifungal agent. *The Journal of Antibiotics*, **42**, 163-167.

Sebastià, N.; Meca, G.; Soriano, J. M.; Mañes, J. (2011) Antibacterial effects of enniatins J1 and J3 on pathogenic and lactic acid bacteria. *Food and Chemical Toxicology*, **49**, 2710-2717.

Shaw, L. M. (1989) Advances in cyclosporine pharmacology, measurement, and therapeutic monitoring. *Clinical Chemistry*, **35**, 1299-1308.

Sheehan, J. C.; Henery-Logan, K. R. (1959) The total synthesis of penicillin V. *Journal of the American Chemical Society*, **81**, 3089-3094.

Shi, Q.; Meroueh, S. O.; Fisher, J. F.; Mobashery, S. (2011) A computational evaluation of the mechanism of penicillin-binding protein-catalyzed cross-linking of the bacterial cell wall. *Journal of the American Chemical Society*, **133**, 5274-5283.

Shin, C. G.; An, D. G.; Song, H. H.; Lee, C. (2009) Beauvericin and enniatins H, I and MK1688 are new potent inhibitors of human immunodeficiency virus type-1 integrase. *The Journal of Antibiotics*, **62**, 687-690.

Singh, S. B.; Jayasuriya, H.; Dewey, R.; Polishook, J. D.; Dombrowski, A. W.; Zink, D. L.; Guan, Z.; Collado, J.; Platas, G.; Pelaez, F.; Felock, P. J.; Hazuda, D. J. (2003) Isolation, structure, and HIV-1- integrase inhibitory activity of structurally diverse fungal metabolites. *Journal of Industrial Microbiology and Biotechnology*, **30**, 721-731.

Sneader, W. (2005) Drug discovery. A history. *John Wiley & Sons, Ltd*.

Soliman, S. S.; Raizada, M. N. (2018) Darkness: a crucial factor in fungal taxol production. *Frontiers in Microbiology*, **9**, 353.

Sollinger, H. W. (1995) Mycophenolate mofetil for the prevention of acute rejection in primary cadaveric renal allograft recipients. U.S. Renal Transplant Mycophenolate Mofetil Study Group. *Transplantation*, **60**, 225-232.

Sondergaard, T.; Fredborg, M.; Oppenhagen Christensen, A. M.; Damsgaard, S.; Kramer, N.;

Giese, H.; Sørensen, J. (2016) Fast screening of antibacterial compounds from fusaria. *Toxins*, **8**, 355.

Spratt, B. G.; Cromie, K. D. (1988) Penicillin-binding proteins of gram-negative bacteria. *Clinical Infectious Diseases*, **10**, 699-711.

Srinivas, G.; Babykutty, S.; Sathiadevan, P. P.; Srinivas, P. (2007) Molecular mechanism of emodin action: transition from laxative ingredient to an antitumor agent. *Medicinal Research Reviews*, **27**, 591-608.

Stierle, A.; Strobel, G.; Stierle, D. (1993) Taxol and taxane production by *Taxomyces andreanae*, an endophytic fungus of Pacific yew. *Science*, **260**, 214-216. Stierle, A.; Strobel, G.; Stierle, D.; Grothaus, P.; Bignami, G. (1995) The search for a taxol-producing microorganism among the endophytic fungi of the Pacific yew, *Taxus brevifolia*. *Journal of Natural Products*, **58**, 1315-1324.

Stoessl, A.; Unwin, C. H.; Stothers, J. B. (1979) Metabolites of *Alternaria solani* part V. Biosynthesis of altersolanol A and incorporation of altersolanol A-$^{13}C_x$ into altersolanol B and macrosporin. *Tetrahedron Letters*, **20**, 2481-2484.

Strobel, G.; Daisy, B.; Castillo, U.; Harper, J. (2004) Natural products from endophytic microorganisms. *Journal of Natural products*, **67**, 257-268.

Stull, D. P.; Scales, T. A.; Daughenbaugh, R.; Jans, N. A.; Bailey, D. T. (1995) Taxol® (Paclitaxel). *Applied Biochemistry and Biotechnology*, **54**, 133-140.

Suemitsu, R.; Ohnishi, K.; Yanagawase, S.; Yamamoto, K.; Yamada, Y. (1989) Biosynthesis of macrosporin by *Alternaria porri*. *Phytochemistry*, **28**, 1621-1622.

Suemitsu, R.; Ueshima, T.; Yamamoto, T.; Yanagawase, S. (1988) Alterporriol C: a modified bianthraquinone from *Alternaria porri*. *Phytochemistry*, **27**, 3251-3254.

Tabasco, R.; García-Cayuela, T.; Peláez, C.; Requena, T. (2009) *Lactobacillus acidophilus* La-5 increases lactacin B production when it senses live target bacteria. *International Journal of Food Microbiology*, **132**, 109-116.

Tanaka, N.; Kinoshita, T.; Masukawa, H. (1968) Mechanism of protein synthesis inhibition by fusidic acid and related antibiotics. *Biochemical and Biophysical Research Communications*, **30**, 278-283.

Taylor, G.; Bloor, K. (1962) Antistaphylococcal activity of fucidin. *Lancet*, **279**, 935–937.

Tognon, M.; Köhler, T.; Luscher, A.; Van Delden, C. (2019) Transcriptional profiling of *Pseudomonas aeruginosa* and *Staphylococcus aureus* during in vitro co-culture. *BMC Genomics*, **20**, 30.

Van Leeuwen, J.; Pandyra, A.; Goard, C.; Mullen, P. J.; Yu, R.; Penn, L. Z. (2017) Targeting the metabolic mevalonate pathway with statins as anti-breast cancer agents. *Cancer Research*, **77**, 3543.

Wagner, S.; Sommer, R.; Hinsberger, S.; Lu, C.; Hartmann, R. W.; Empting, M.; Titz, A. (2016) Novel strategies for the treatment of *Pseudomonas aeruginosa* infections. *Journal of Medicinal Chemistry*, **59**, 5929-5969.

Wakharde, A. A.; Halbandge, S. D.; Phule, D. B.; Karuppayil, S. M. (2018) Anticancer drugs as antibiofilm agents in *Candida albicans*: potential targets. *Assay and Drug Development Technologies*, **16**, 232-246.

Waller, D.; Gazda, G.; Minden, Z.; Barton, L.; Leigh, C. (2018) Synthesis of cephalosporin compounds. U.S. Patent No. 10,125,149. *Washington, DC: U.S. Patent and Trademark Office.*

Wang, J. P.; Debbab, A.; Hemphill, C. F. P.; Proksch, P. (2013a) Optimization of enniatin production by solid-phase fermentation of *Fusarium tricinctum*. *Zeitschrift für Naturforschung C*, **68**, 223-230.

Wang, J. P.; Lin, W. H.; Wray, V.; Lai, D.; Proksch, P. (2013b) Induced production of depsipeptides by co-culturing *Fusarium tricinctum* and *Fusarium begoniae*. *Tetrahedron Letters*, **54**, 2492-2496.

Watanabe, A.; Ono, Y.; Fujii, I.; Sankawa, U.; Mayorga, M. E.; Timberlake, W. E.; Ebizuka,

Y. (1998) Product identification of polyketide synthase coded by *Aspergillus nidulans* wA gene. *Tetrahedron letters*, **39**, 7733-7736.

Weber, D. (2009) Endophytic fungi, occurrence and metabolites. *Physiology and Genetics, Springer, Berlin, Heidelberg*, **15**, 153-195.

Whitby, M. (1999) Fusidic acid in septicaemia and endocarditis. *International Journal of Antimicrobial Agents*, **12**, 17-22.

Williamson, J.; Russell, F.; Doig, W. M.; Paterson, R. W. (1970) Estimation of sodium fusidate levels in human serum, aqueous humour, and vitreous body. *British Journal of Ophthalmology*, **54**, 126-130.

Xia, Z. Q.; Costa, M. A.; Proctor, J.; Davin, L. B.; Lewis, N. G. (2000) Dirigent-mediated podophyllotoxin biosynthesis in *Linum flavum* and *Podophyllum peltatum*. *Phytochemistry*, **55**, 537-549.

Xu, J.; Kjer, J.; Sendker, J.; Wray, V.; Guan, H.; Edrada, R.; Lin W. H.; Wu, J.; Proksch, P. (2009) Chromones from the endophytic fungus *Pestalotiopsis* sp. isolated from the Chinese mangrove plant *Rhizophora mucronata*. *Journal of Natural Products*, **72**, 662-665.

Yamazaki, Y.; Sumikura, M.; Hidaka, K.; Yasui, H.; Kiso, Y.; Yakushiji, F.; Hayashi, Y. (2010) Anti-microtubule ‘plinabulin’chemical probe KPU-244-B3 labeled both α-and β-tubulin. *Bioorganic & Medicinal Chemistry*, **18**, 3169-3174.

Yao, S.; Zhou, R.; Jin, Y.; Huang, J.; Wu, C. (2019) Effect of co-culture with *Tetragenococcus halophilus* on the physiological characterization and transcription profiling of *Zygosaccharomyces rouxii*. *Food Research International*, **121**, 348-358.

Yu, X.; Che, Z.; Xu, H. (2017) Recent advances in the chemistry and biology of podophyllotoxins. *Chemistry–A European Journal*, **23**, 4467-4526.

Zhang, H.; Pereira, B.; Li, Z.; Stephanopoulos, G. (2015) Engineering *Escherichia coli* coculture systems for the production of biochemical products. *Proceedings of the*

National Academy of Sciences, **112**, 8266-8271.

Zhou, X. M.; Zheng, C. J.; Chen, G. Y.; Song, X. P.; Han, C. R.; Li, G. N.; Fu, Y. H.; Chen W. H.; Niu, Z. G. (2014) Bioactive anthraquinone derivatives from the mangrove-derived fungus *Stemphylium* sp. 33231. *Journal of Natural Products*, **77**, 2021–2028.

Zhou, X.; Zhu, H.; Liu, L.; Lin, J.; Tang, K. (2010) A review: recent advances and future prospects of taxol-producing endophytic fungi. *Applied Microbiology and Biotechnology*, **86**, 1707-1717.

Zinedine, A.; Soriano, J. M.; Molto, J. C.; Mañes, J. (2007) Review on the toxicity, occurrence, metabolism, detoxification, regulations and intake of zearalenone: an oestrogenic mycotoxin. *Food and Chemical Toxicology*, **45**, 1-18.

5 Abbreviations

A. faecalis	*Alcaligenes faecalis*
A. fumigatus	*Aspergillus fumigatus*
A. niger	*Aspergillus niger*
A2780CisR	human ovarian cancer cell line, Cisplatin resistance
A2780sens	humane ovarian cancer cell line, Cisplatin sensitive
ADA	adenosine deaminase
B. cereus	*Bacillus cereus*
BC	before Christ
br	broad signal
C. albicans	*Candida albicans*
calcd	calculated
$CDCl_3$	deuterated chloroform
CH_2Cl_2	dichlormethane
$CHCl_3$	chloroform
cm	centimetre
COSY	correlation spectroscopy
d	doublet
DCM	dichlormethane
dd	doublet of doublets
DMSO	dimethyl sulfoxide
DNA	deoxyribonucleic acid
E. cloacae	*Enterobacter cloacae*
E. coli	*Escherichia coli*
E. faecalis	*Enterococcus faecalis*

e.g.	exempli gratia
EA1	enniatin A1
EB	enniatin B
EB1	enniatin B1
ECD	electronic circular dichroism
ESIMS	electrospray ionization mass spectrometry
et. al.	et altera
EtOAc	ethyl acetate
FDA	U.S. Food and Drug Administration
g	gram
GABA	gamma aminobutyric acid
GTP	guanosine triphosphate
H_2O	water
HAT	histone acetyltransferase
HCT116	human colon cancer cell line
HDAC	histone deacetylase
HMBC	heteronuclear multiple bond connectivity
HMQC	heteronuclear multiple quantum coherence
HPLC	high performance liquid chromatography
HRESIMS	high resolution electrospray ionization mass spectrometry
HSP90	heat shock protein 90
HSQC	heteronuclear single quantum correlation
Hz	Hertz
IC_{50}	half maximal inhibitory concentration
i.e.	id est

ITS	internal transcribed spacer
J	coupling constant
K562	human leukaemia cell line
K. rhizophila	*Kocuria rhizophila*
kcal	kilocalorie
L	liter
LDL	low density lipoprotein
Ltd.	limited
M	molar
M. tetragenus	*Micrococcus tetragenus*
m/z	mass per charge
MeCN	acetonitrile
MeOD or CD_3OD	deuterated methanole
Me/MeOH	methanole
mg	milligram
MHz	mega Hertz
MIC	minimal inhibitory concentration
min	minute
mL	milliliter
mm	millimetre
mol	mole, amount of substance
MRSA	methicillin-resistent *Staphylococcus aureus*
MTT	microculture tetrazolium assay
nm	nanometre
NMR	nuclear magnetic resonance

NP	natural product
NSCLC	non-small-cell lung carcinoma
OD	optical density
OSMAC	One Strain MAny Compounds
P. fluorescens	*Pseudomonas fluorescens*
PCM	polarizable continuum model
PCR	polymerase chain reaction
PKS	polyketide synthase
ppm	parts per million
q	quartet
ROESY	rotating frame Overhauser enhancement spectroscopy
RP 18	reversed phase C 18
s	singlet
S. albus	*Staphylococcus albus*
S. aureus	*Staphylococcus aureus*
S. pneumoniae	*Streptococcus pneumoniae*
SAHA	suberoylanilide hydroxamic acid
sp.	species (singular)
SAGA	Spt-*Ada*-Gcn5 acetyltransferase
t	triplet
T. rubrum	*Trichophyton rubrum*
TDDFT-ECD	time-dependent density functional theory electronic circular dichroism
TFA	trifluoroacetic acid
THF	tetrahydrofuran
TLC	thin layer chromatography

TNF-α	tumor necrosis factor α
UV	ultra-violet
VLC	vacuum liquid chromatography
ZPVE	zero-point vibrational energy
1D/2D	1-/2-dimensional
µg	microgram
µM	micromolar
$[\alpha]_D^{20}$	specific rotation at the sodium D-line
°C	degree Celsius

6 List of publications

Mariam Moussa, Weaam Ebrahim, Rainer Kalscheuer, Zhen Liu and Peter Proksch. Co-culture of the bacterium *Pseudomonas aeruginosa* with the fungus *Fusarium tricinctum* induces bacterial antifungal and quorum sensing signalling molecules. *Phytochemistry Letters*, 2020, submitted.

Mariam Moussa, Weaam Ebrahim, Michele Bonus, Holger Gohlke, Attila Mándi, Tibor Kurtán, Rudolf Hartmann, Rainer Kalscheuer, Wenhan Lin, Zhen Liu and Peter Proksch. Co-culture of the fungus *Fusarium tricinctum* with *Streptomyces lividans* induces production of cryptic naphthoquinone dimers. *Royal Society of Chemistry Advances*, 2019, 9, 1491-1500.

Mariam Moussa, Weaam Ebrahim, Mona El-Neketi, Attila Mándi, Tibor Kurtán, Rudolf Hartmann, Wenhan Lin, Zhen Liu and Peter Proksch. Tetrahydroanthraquinone derivatives from the mangrove-derived endophytic fungus *Stemphylium globuliferum*. *Tetrahedron Letters*, 2016, 57, 4074-4078.

Haiqian Yu, Simon-Patrick Höfert, **Mariam Moussa**, Christoph Janiak, Werner E. G. Müller, Blessing O. Umeokoli, Haofu Dai, Zhen Liu and Peter Proksch. Polyketides and nitrogenous metabolites from the endophytic fungus *Phomopsis* sp. D15a2a. *Tetrahedron Letters*, 2019, 151325, 1-16.

7 Acknowledgement

I would like to take this opportunity to express my deepest appreciation to Prof. Dr. Dr. h.c. Proksch for making this work possible with his generously offered opportunity to me, to pursue science in drug discovery in his workgroup. I am deeply grateful for your continuous guidance and support throughout my work, which helped me accomplish my goals and grow in this profession. Your continuous strive towards scientific excellence is something I will always look up to, learn from and get inspired by. Thank you, dear Prof. Proksch, for giving me the honour of you being my doctoral supervisor. Thank you also for your patience with me. Here I also want to thank Ms. Dr. Proksch for her support. It was always a pleasure meeting you and having nice conversations at our dinnertimes.

Prof. Dr. Matthias Kassack, from the Institute for Pharmaceutical and Medicinal Chemistry, I want to thank for giving me the honour to be my second supervisor. I also want to thank for the great collaboration on providing insights about the cytotoxic profile of my obtained compounds.

Prof. Dr. Rainer Kalscheuer, from the Institute of Pharmaceutical Biology and Biotechnology, I want to thank deeply for the great cooperation on providing the bacterial samples to conduct co-cultivation experiments, as well as antibacterial tests.

Prof. Dr. Wenhan Lin, from the Marine Medicine Research Laboratory at the School of Pharmaceutical Sciences Peking University (China), I want to thank for sharing his expertise in structure elucidation and discussing my compounds with him.

Prof. Dr. Holger Gohlke, from the Institute for Pharmaceutical and Medicinal Chemistry, I want to thank for his great collaboration and investment on my new compounds, to provide more insight to their structural facilities by contributing rotational barrier calculations. Here I also want to thank Michele Bonus from the RG of Prof. Gohlke, for his participation and effort into this experiment.

Prof. Dr. Tibor Kurtán, from the Department of Organic Chemistry at the University of Debrecen (Hungary), I am indebted for the ECD measurements and calculations. Here I also want to thank Dr. Attila Mándi, from the Department of Organic Chemistry at the University of Debrecen (Hungary), for his participation and effort he put into these experiments.

Dr. Rudolf Hartmann, from the Institute of Complex Systems at the Forschungszentrum Jülich, I want to thank for the great collaboration and allowing me to have my compounds measured at his high technology NMR facilities and the insightful discussions on my compounds.

Dr. Martina Holz, coordinator of the GRK 2158 at the Institute of Pharmaceutical Biology and Biotechnology, I want to thank for the great organizational work for our GRK graduate school. It was an honour for me to be part of the symposium and actively participate in it.

My deep appreciation goes to Assoc. Prof. Dr. Weaam Ebrahim, from the Department of Pharmacognosy, Faculty of Pharmacy at the Mansoura University (Egypt), for his guidance throughout my PhD with his professional expertise. I am very grateful for your contribution to my work with valuable suggestions, thesis and manuscript revisions. I also want to express my gratitude to Dr. Mona El-Neketi, from the Department of Pharmacognosy, Faculty of Pharmacy at the Mansoura University (Egypt), for her support and contribution to my first manuscript.

My deep appreciation goes to Dr. Zhen Liu for sharing his amazing skills in the discussions on NMR for structure elucidations, manuscript revisions and valuable suggestions.

A great thank you to Claudia Eckelskemper and the technicians, Simone Miljanovic, Katja Friedrich, Waltraud Schlag, Linda Wiegand, Eva Müller, Heike Goldbach-Gecke, Simone Mönninghoff-Pützer, for their great support and assistance during my PhD time.

In honourable mention, I want to thank Imke Form for being my friend and first laboratorial partner. I will always treasure our wonderful memories. May you rest in peace.

Dr. Marian Frank I want to thank for giving me a great time as my second laboratorial partner. Thank you for your support and the great time working with you. I am grateful for our discussions and you sharing your ideas and knowledge with me.

Dr. Huiqin Chen I want to thank dearly for introducing me to microbial co-culturing.

Dr. Nam Michael Tranc-Cong I want to thank for his support during my thesis writing and submission, and for the abstract revision. Dr. Haiqian Yu I want to thank for the valuable discussions. I am grateful for the happy times we shared together, especially in the GRK group.

I´m very thankful to Kim Thao Le for her support and consistent connection with me after my lab work and during my thesis writing.

My appreciation goes to my former colleagues for the happy times, the warm and supportive atmosphere at the institute and the valuable friendships that developed during this time: Lisa

Anne Küppers, Dina El-Kashef, Dr. Peter Eze, Nihal Aktas, Dr. Mohammad Said El-Naggar, Dr. Blessing Umeokoli, Dr. Annika Frank, Dr. Yang Liu, Arta Kuci, Laura Lewald, Lisa Ennulat, Sebastian Scharf, Nada Abdel-Wahab, Dr. Hervé Sergi Akone, Dr. Mousa Al-Tarabeen, Katrin Papadopoulos, Ni Putu Ariantari, Dr. Catherine Bogner, Dr. Miada Fouad Abdelwahab Sakr, , Mi-Young Chung, Ying Gao, Dr. Lena Hammerschmidt, Harowoko, Dr. Hajar Heydari, Dr. Ramsay Kamdem, Dr. Shuai Liu, Dr. Andreas Marmann, Dr. Amin Mokhlesi, Dr. Rini Muharini, Dr. Hendrik Niemann, Dr. Raha Orfali, Dr. Ferhat Can Özkaya, Dr. Catalina Peréz Hemphill, Dr. Sherif Sayed Ebada, Dr. Festus Okoye, Dr. Feng Pan, Dr. Georgios Daletos, Dr. Elena Ancheeva, Dr. Hao Wang, Dr. Rudi Yansiah, , Xiaoqin Yu, Dr. Yanbo Zeng, my colleagues from the RG Prof. Kalscheuer, RG Prof. Gohlke and the GRK group.

My special thanks I want to express to my friends and family for their love and supporting words. And of course, my dearest parents, Sami and Basna Moussa, who supported me with their love, blessings and prayers. This work is especially dedicated to you.

و آخر دعوانا أن الحمد لله ربّ العالمين